UNIVERSITÉ LILLE 2

ÉCOLE DOCTORALE BIOLOGIE SANTÉ

INSTITUT DE BIOLOGIE DE LILLE

THÈSE

Pour obtenir le grade de

DOCTEUR DE L'UNIVERSITÉ LILLE 2

Discipline : Biologie moléculaire et structurale, biochimie

Spécialité : Biochimie et biologie moléculaire

Présentée et soutenue publiquement par :

Jia Jieshuang

Le 1er Avril 2015

Study of molecules with nonsense mutation correction capacity

Jury:

Pr. Yves LEMOINE – Professeur, Université Lille1	Président
Dr. Alex DUVAL – Directeur de recherche, Inserm	Rapporteur
Dr. Alexandra MARTINS – Chargée de recherche, Inserm	Rapporteur
Dr. Fabrice LEJEUNE – Chargé de recherche, Inserm	Directeur de thèse

ACKNOWLEDGEMENTS

First I would like to thank from the bottom of my heart Professor Yves Lemoine for agreeing to be the president of my thesis committee, and Professors Alex Duval and Alexandra Martins for being the reporters of my thesis.

I also would like to thank one more time Pr. Yves Lemoine who always supported our AVENIR team as a director of the IFR142. I am also very grateful to Pr Yvan de Launoit to welcome me in his unit and to agree to let me go on my projects even though they are not immediate close to the other projects that are developed in the UMR8161.

I want to thank the funding Vaincre La Mucoviscidose. Under the support of this patient care association, I finished my project and lived in France for three years. During these three years I was so lucky to be selected several times to present my results and exchange the ideas in the meeting 'European CF Young Investigator Meeting' organized by Vaincre La Mucoviscidose.

I am also very grateful to every member of the signal team. The team leader David Tulasne who is very kind, enthusiastic gave me a lot of constructive suggestions on my project and helped me to finish my thesis. Catherine Leroy is a very competent person and gave me a lot of help on my experiments. Alessandro Furlan is very cordial and like a brother for me. He helped me to do some experiments to finish my thesis. Nadège Debreuck is warmhearted and she explained to me a lot of things to let me quickly used to the life in the lab and in France when I came to the lab in the first year. Rémi Montagne was also PHD student like me and he is like my comrade-in-arms.

I would love to thank Zoulika Kherrouche, Anne Baranzelli, Hana Benhabiles, Simon Baldacci, Claire Simonneau, Louis Doublet, Luc Stoven, Isabelle Damour and Melanie Berbon because they were very kind to me and let me live in a big warm family.

I also would like to thank Madame Laurence Fofana, Madame Céline Delohen

and Monsieur François Delcroix because they are so kind and responsible. They helped me a lot about all the administrative issues such as the information for thesis registration, titre de séjour, etc.

During these three years the best outcome is my daughter. My daughter was born in 2014 and she gave me a lot of happiness. I also thank my husband, my parents, my sister and my brother in-law who very supports my work, help me to take care of our daughter and do a lot of favors for my life in France.

CATALOGUE

The list of abbreviations

CTD:	Carboxyl-terminal domain
CBC:	Cap binding complex
CBP:	Cap binding protein
CPSF:	Cleavage and polyadenylation specificity factor
CStF:	Cleavage stimulation factor
CFI and CFII:	Cleavage factors I and II
CH domain:	Cysteine- and histidine-rich domain
CF:	Cystic fibrosis
CFTR:	Cystic fibrosis transmembrane conductance regulator
DSE:	Downstream sequence element
DMD:	Duchenne muscular dystrophy
DsRNA:	Double-stranded RNA
ESE:	Exonic splicing enhancers
ESS:	Exonic splicing silencer
EJC:	Exon junction complex
Edc:	Enhancer of decapping
eIF4G:	Eukaryotic translation initiation factor 4G
eRF1:	Eukaryotic release factor 1
eIF4E:	Eukaryotic translation initiation factor 4E
Fluc:	Firefly luciferase
GPx1:	Glutathione peroxidase 1
HnRNP:	Heterogeneous nuclear ribonucleoproteins
ISE:	Intronic splicing enhancer
ISS:	Intronic splicing silencer
L-AHA:	L-azidohomoalanine
MIF4G:	Middle portion of eIF4G
Mdx mouse :	X-linked muscular dystrophy mouse
NMD:	Nonsense-mediated mRNA decay
NMDI 1:	NMD inhibitor 1
NES:	Nuclear export signal
NLS:	Nuclear localization signal
NPCs:	Nuclear pore complexes
NGD:	No-go mRNA decay
NSD:	Non-stop mRNA decay
Pre-mRNA :	precursor messenger RNA
PTC :	Premature termination codon
PABPC1:	Poly (A) binding protein cytoplasmic 1
PABPN1:	Poly (A) binding protein nuclear 1
PTB:	Polypyrimidine tract binding protein
PP2A:	Protein phosphatase 2A
rRNA:	Ribosomal RNAs

RRM:	RNA recognition motif
SnRNAs:	Small nuclear RNAs
SF1:	Splicing factor
SR proteins:	Serine/arginine rich proteins
SMD:	Staufen 1 (STAU1)-mediated mRNA decay
SMG proteins :	Suppressor with morphological effect on genitalia proteins
SURF:	SMG1 kinase complex-UPF1 -eRF1-eRF3 complex
TCR:	T-cell receptor
tRNA:	Transfer RNAs
U2AF:	U2 snRNP associated factor
3'UTR:	3' untranslated region
UPF protein:	Up-frameshift proteins
uORF:	Upstream open reading frame

The list of figure

Introduction

Project 1

Project 2

Project 3

RÉSUMÉ EN FRANÇAIS

1. Introduction

L'expression des gènes nécessite une transmission parfaite de l'information codée par la molécule d'ADN. A chaque étape de cette expression, depuis la transcription jusqu'à la traduction en une protéine, des systèmes de surveillance contrôlent que le produit généré est fidèle à l'information portée par le gène. Parmi ces mécanismes de surveillance, le mécanisme de nonsense-mediated mRNA decay (NMD) recherche et dégrade les ARNm porteurs d'un codon stop prématuré (PTC en anglais pour premature termination codon) (Lejeune and Maquat 2005; Rebbapragada and Lykke-Andersen 2009; Popp and Maquat 2014).

Le NMD prévient la synthèse de protéine tronquée qui pourrait être non fonctionnelle voire même délétère pour la cellule dû à un effet dominant négatif. C'est aussi un mécanisme de régulation d'environ 5% des gènes humains (Mendell, Sharifi et al. 2004). Malheureusement, le NMD prévient aussi la synthèse de protéine tronquée qui conserverait une partie ou la totalité de la fonction de la protéine sauvage. Il est donc devenu évident que l'inhibition du NMD pourrait représenter une nouvelle approche thérapeutique de maladies génétiques liées à l'apparition d'une mutation non sens (Keeling, Du et al. 2006). L'inhibition du NMD pourrait aussi être utilisée en complément d'autres approches thérapeutiques de maladies génétiques causées par une mutation non sens (Linde, Boelz et al. 2007). La translecture serait notamment une très bonne candidate puisque l'inhibition du

NMD permettrait d'augmenter la quantité d'ARNm porteurs de la mutation non sens et la translecture conduirait à la synthèse d'une protéine vraisemblablement fonctionnelle. En effet, ce processus qui consiste à forcer la machinerie traductionnelle à incorporer un acide aminé à la position du codon stop pour poursuivre la traduction de la phase ouverte de lecture sauvage et ainsi synthétiser une protéine de taille sauvage. Cette protéine générée par translecture possède au maximum un acide aminé différent par rapport à la protéine sauvage. Cet acide aminé est celui incorporé au niveau de la mutation non sens car la translecture n'incorpore pas forcément l'acide aminé original. Cependant, la protéine générée par translecture est très souvent fonctionnelle sauf dans les cas où l'acide aminé incorporé à la position du PTC est incompatible avec la fonction de la protéine.

La correction des mutations non sens soit par inhibition du NMD, soit par translecture couplée à l'inhibition du NMD représente une nouvelle stratégie de développement d'approches thérapeutiques de maladies génétiques. Ces maladies génétiques sont soit des maladies rares comme la mucoviscidose ou la myopathie de Duchenne pour ne citer que les plus connues mais aussi des maladies génétiques fréquentes comme le cancer ou des maladies métaboliques (Perez, Rodriguez-Pombo et al. 2012). On estime à environ 10% les cas de patients atteints de maladies génétiques qui pourraient être soignés par une correction de mutation non sens (Mort, Ivanov et al. 2008). Il s'agit donc d'un problème de santé public significatif.

Depuis plusieurs années, nous nous intéressons au laboratoire à rechercher des inhibiteurs du NMD et/ou des activateurs de la translecture. Pour cela, nous

avons développé un système de criblage permettant de tester de nombreuses molécules chimiques pour leur capacité à inhiber le NMD. Plusieurs campagnes de criblage ont été achevées à partir de différentes banques de molécules comme une banque de molécules approuvées par la Food and Drug Administration (FDA), des molécules issues de la médecine traditionnelle chinoise, des extraits de plantes ou des extraits d'organismes marins. Suite à ces campagnes de criblage, plusieurs molécules ont été identifiées et nécessitaient d'être caractérisées. Ma thèse à portée sur la caractérisation de plusieurs de ces molécules potentiellement inhibitrices du NMD. Ces caractérisations m'ont amenée durant ma thèse à explorer des domaines très différents comme celui du cytosquelette ou le processus d'apoptose.

2. Résultats

2.1. Caractérisation d'un médicament déjà présent sur le marché comme inhibiteur du NMD et activateur de la translecture

Lors de mon arrivée au laboratoire, l'équipe travaillait sur une molécule qui avait été identifiée par criblage à partir d'une banque de médicaments déjà présents sur le marché. La stratégie en criblant ce genre de banques était de pouvoir repositionner un médicament afin d'aller plus vite dans les phases des essais cliniques et aussi de partir de molécules dont on avait déjà des données de toxicité et de pharmacologie.

La molécule qui avait été identifiée est l'amlexanox, un médicament qui est utilisé dans le traitement des aphtes et de certaines formes d'asthme au Japon et aux

Etats-Unis. J'ai donc participé à la caractérisation de cette molécule qui a consisté à montrer une augmentation spécifique des ARNm porteurs d'une mutation non sens afin de mettre en évidence la propriété inhibitrice du NMD et valider le résultat du criblage. Nous avons pour cela incubé trois lignées cellulaires différentes porteuses d'une mutation non sens dans le gène P53, CFTR ou dystrophine, avec des quantités croissantes d'amlexanox. Après extraction des ARN totaux et RT-PCR en conditions quantitatives, nous avons montré que la quantité des ARNm porteurs d'une mutation non sens augmente avec la quantité d'amlexanox dans le milieu de culture des cellules.

Nous voulions ensuite savoir si ces ARNm pouvaient être traduits en protéine tronquée. Nous avons incubé les trois lignées cellulaires précédentes avec des quantités croissantes d'amlexanox avant d'extraire les protéines pour une analyse par western-blot. Cette analyse a montré que nous étions non seulement capables d'observer la protéine tronquée mais aussi la protéine de taille sauvage suggérant que l'amlexanox puisse aussi activer la translecture. Le fait qu'il y ait production d'une protéine entière nous a conduits à déterminer si cette protéine était fonctionnelle. Nous avons pour cela établit 3 systèmes expérimentaux différents pour étudier la fonctionnalité des protéines P53, dystrophine et CFTR. Dans le cas de P53, nous avons mesuré le niveau d'expression du gène P21 en mesurant son ARNm puisque P53 est un facteur de transcription dont une des cibles est le gène P21. Dans le cas de la dystrophine, nous avons observé sa localisation à la membrane cellulaire ce qui sous-entend qu'elle est fonctionnelle. Enfin, la fonctionnalité de la protéine

CFTR a été mesurée par un protocole expérimental qui relie la fluorescence d'une molécule appelé SPQ (6-methoxy-*N*-39 -sulfopropylquino linium) à la fonctionnalité du canal CFTR (Mansoura, Biwersi et al. 1999). Ce dernier système est extrêmement intéressant puisqu'il permet de quantifier la correction de la mutation non sens dans le gène CFTR. Toutes ces analyses ont permis de mettre en évidence que l'amlexanox conduisait dans les 3 systèmes cellulaires à la synthèse d'une protéine fonctionnelle à partir d'un ARNm porteur d'une mutation non sens. Ces travaux ont été publiés en 2012 dans le journal Orphanet Journal of Rare diseases (Gonzalez-Hilarion, Beghyn et al. 2012).

Le travail sur l'amlexanox m'a permis de me familiariser avec les différentes techniques et outils utilisés au laboratoire pour étudier et caractériser des molécules correctrices des mutations non sens. Je me suis donc concentrée ensuite sur la caractérisation de 2 autres familles de molécules.

2.2. Le NMD est inhibé durant l'apoptose

Au cours d'une des campagnes de criblage, la doxorubicine a été identifiée comme un inhibiteur potentiel du NMD. La doxorubicine est un inducteur de l'apoptose très utilisé. Nous avons dans un premier temps validé les résultats du criblage en mesurant l'efficacité du NMD sur des cellules HeLa transfectées avec des vecteurs d'expression exprimant des ARNm substrats du NMD ou sur des cellules exprimant un ARNm CFTR porteur d'une mutation non sens. Puisque la doxorubicine est un inducteur de l'apoptose, j'ai en même temps testé d'autres inducteurs

d'apoptose afin de déterminer si la capacité à inhiber le NMD était spécifique à la doxorubicine ou généralisable aux inducteurs d'apoptose. C'est ainsi que j'ai observé une inhibition du NMD avec la doxorubicine validant ainsi les résultats du crible mais aussi avec la staurosporine, l'etoposide, le cis-platine, l'anisomycine et l'apoptosis activator 2. De manière intéressante, l'inhibition du NMD obtenue avec les inducteurs d'apoptose est plus importante que celle observée avec l'amlexanox et contrairement à l'amlexanox, les substrats naturels du NMD sont aussi stabilisés en présence des inducteurs d'apoptose. Ces résultats montrent clairement que le NMD est inhibé durant l'apoptose.

J'ai ensuite cherché à comprendre comment les inducteurs d'apoptose inhibent le NMD. De manière intéressante, une analyse de la séquence protéique des facteurs principaux du NMD tels qu'UPF1, UPF2 ou UPF3X révèle la présence de sites de coupures par les caspases. Les caspases sont des protéines qui interviennent notamment au début de l'apoptose afin d'activer certaines protéines impliquées dans le processus d'apoptose et afin d'inactiver d'autres protéines pour progresser dans la voie de la mort cellulaire par apoptose. La présence de sites de coupure par les caspases suggérait la possibilité que les facteurs de NMD soient coupés durant l'apoptose. J'ai donc vérifié cette hypothèse et montré qu'effectivement UPF1 et UPF2 mais pas UPF3X sont coupés durant l'apoptose. J'ai démontré que ces coupures impliquaient les caspases les bloquant au moyen d'un inhibiteur de caspases appelé zVAD (benzyloxycarbonyl-Val-Ala-DL-Asp-fluoromethylketone). J'ai ensuite, recherché les sites de coupures et identifié la position exacte grâce à des mutations faux sens

sur les sites prédits *in silico*. Il semblait évident que la conséquence fonctionnelle de la dégradation spécifique des facteurs UPF1 et UPF2 est une inhibition du NMD mais je voulais savoir si les fragments générés pouvaient avoir une fonction ce qui justifierait pourquoi UPF1 et UPF2 sont dégradés mais pas UPF3X par exemple. J'ai donc construit des versions étiquetées de chaque fragment généré par les coupures caspases (N et C terminaux) et mesuré le taux d'apoptose lorsqu'ils sont produits au sein d'une cellule. Le résultat a montré que les fragments N terminaux issus des coupures dans les protéines UPF1 et UPF2 sont apoptotiques contrairement aux fragments C-terminaux qui n'ont aucun effet sur l'apoptose. Je voulais aussi savoir si ces fragments pouvaient agir sur le NMD. Pour cela, j'ai mesuré l'efficacité du NMD sur des transgènes substrats du NMD en présence de chacun des fragments UPF générés par coupure caspase. Les résultats ont montré que le fragment C-terminal issu de la coupure de UPF1 et le fragment N-terminal issu de la coupure de UPF2 jouent le rôle d'inhibiteur du NMD. Ce résultat est très important pour la compréhension du mécanisme de NMD car s'il avait déjà été montré que la partie C-terminale de UPF1 rentre en compétition avec la protéine sauvage et inhibe le NMD, le rôle des domaines de UPF2 reste encore très peu connu. La dernière étape de ce travail a consisté à montrer que l'inhibition du NMD observée en culture cellulaire se produit aussi *in vivo*. Pour cela, nous avons injecté des anticorps anti-fas à des souris et analysé les niveaux d'expression des protéines UPF1 et UPF3X car nos anticorps ne peuvent pas reconnaitre la protéine UPF2 murine. Nous avons observé une diminution du niveau de la protéine UPF1 mais pas de la protéine UPF3X validant

ainsi les résultats obtenus en culture cellulaire. Nous avons aussi montré l'inhibition du NMD dans ces conditions apoptotiques en mesurant le niveau d'un ARNm soumis au NMD. L'ensemble de ce travail a été accepté récemment pour publication dans le journal Cell Death and Differentiation.

2.3. Le cytosquelette est nécessaire au NMD

Le taxol a été identifié dans une campagne de criblage faite au laboratoire comme une molécule capable d'inhiber le NMD. Le taxol est connu pour perturber le cytosquelette en stabilisant les microtubules qui perdent ainsi leur dynamique de polymérisation et dépolymérisation. Nous voulions donc savoir si les microtubules pouvaient avoir un rôle dans le mécanisme de NMD en permettant par exemple une localisation spécifique des mRNP soumises au NMD. En effet, il y a quelques années, l'équipe avait montré que les facteurs de NMD et les substrats soumis au NMD transitent par des foyers cytoplasmiques appelés P-bodies (Durand, Cougot et al. 2007). Jusqu'à présent les P-bodies sont considérés comme des zones de stockage des enzymes impliquées dans la dégradation des ARN ou comme le lieu de dégradation des ARN. Néanmoins, ces résultats suggèrent que les mRNP soumises au NMD doivent être adressées aux P-bodies. Il est donc fort probable que cet adressage soit pris en charge par des structures du type cytosquelette.

Le cytosquelette est composé de 3 structures principales que sont les filaments d'actine, les microtubules et les filaments intermédiaires. Le rôle de ces derniers reste encore assez obscur et peu caractérisé ce qui nous a conduits à nous concentrer sur les 2 autres structures. Le cytosquelette intervient dans des processus

très variés tels que la morphologie des cellules, le transport moléculaire intracellulaire ou la division cellulaire.

Dans un premier temps, j'ai mesuré l'efficacité du NMD dans des cellules traitées avec des molécules affectant le cytosquelette : la cytochalasine D qui interfère avec la polymérisation des filaments d'actine, le jasplakinolide qui stabilise les filaments d'actine en inhibant leur dépolymérisation, la colchicine qui inhibe la polymérisation des microtubules et le taxol. Chacune de ces molécules a montré une capacité à inhiber le NMD d'une manière similaire ou plus efficace que l'amlexanox indiquant que ces molécules sont des inhibiteurs du NMD au moins aussi efficaces que l'amlexanox. Comme dans l'étude sur l'amlexanox, j'ai ensuite déterminé si les ARNm qui échappent au NMD sont traduits en une protéine tronquée. Les protéines tronquées issues d'ARNm porteurs d'une mutation non sens ont été observées avec chacune des molécules testées. De manière surprenante, la protéine de taille sauvage a aussi été observée mais uniquement avec la cytochalasine D et le jasplakinolide. Ce dernier résultat suggère que les microtubules sont nécessaires à la translecture puisque les drogues affectant les microtubules ne conduisent pas à la synthèse d'une protéine translue à partir d'ARNm qui ont la capacité à être translus.

J'ai ensuite étudié l'impact des différentes perturbations du cytosquelette sur la localisation cellulaires des facteurs et substrats du NMD. J'ai tout d'abord observé la concentration des facteurs du NMD dans des foyers cytoplasmiques en présence des inhibiteurs du cytosquelette. Ces foyers cytoplasmiques ne colocalisent pas avec les agrégats formés par les protéines du cytosquelette lorsque celui-ci est désorganisé.

Puisque nous savons que les facteurs du NMD peuvent se concentrer dans les P-bodies, nous avons recherché une éventuelle colocalisation entre les facteurs du NMD et des marqueurs de P-bodies en présence des inhibiteurs du cytosquelette. Lorsque les perturbateurs des microtubules (colchicine ou taxol) sont utilisés, j'observe une colocalisation des facteurs du NMD et des P-bodies. Par contre, lorsque la cytochalasine D ou le jasplakinolide est utilisés, cette colocalisation est seulement partielle indiquant que certains foyers cytoplasmiques contenant les facteurs de NMD ne sont pas des P-bodies. L'étude de la localisation des substrats du NMD dans les mêmes conditions a révélé des résultats similaires c'est-à-dire la présence de ces substrats du NMD dans les P-bodies en présence de taxol ou colchicine et la présence partielle dans les P-bodies et dans d'autres foyers cytoplasmiques en présence de cytochalasine D ou de jasplakinolide.

J'ai donc cherché à identifier l'autre type de foyers cytoplasmiques observés en présence des inhibiteurs des filaments d'actine. Pour cela, j'ai étudié la localisation cellulaire de facteurs de NMD et de marqueurs d'autres foyers cytoplasmiques connus lorsque les filaments d'actine sont désorganisés. J'ai ainsi montré que ces foyers cytoplasmiques ne sont ni des granules de stress, ni des autophagosomes. Il est intéressant de faire le rapprochement entre ces structures cytoplasmiques qui ne sont pas encore identifiées et la détection de translecture lorsque les filaments d'actine sont perturbés. Dans la poursuite de ce projet, je m'employerai à déterminer si ces foyers cytoplasmiques sont le lieu où la translecture se produit.

Afin de montrer un lien encore plus direct entre le cytosquelette et le

mécanisme de NMD, j'ai recherché d'éventuelles interactions entre des protéines du cytosquelette et des facteurs du NMD. Pour cela, j'ai immunoprécipité l'actine ou la tubuline et analysé la présence de facteurs de NMD dans ces immunprécipitations à partir d'extraits cellulaires traités ou non avec des inhibiteurs du cytosquelette. Le résultat de ces immunoprécipitations montrent une interaction entre l'actine ou la tubuline avec les facteurs de NMD UPF1, UPF2 et UPF3X lorsque les cellules ont été traitées avec du DMSO démontrant l'existence d'une interaction entre le cytosquelette et les protéines du NMD. En revanche, ces interactions sont perdues lorsque les cellules sont traitées avec un inhibiteur du cytosquelette indiquant que lorsque le cytosquelette est désorganisé, les monomères d'actine ou de tubuline ne sont pas capables d'interagir avec les facteurs du NMD. Ces résultats suggèrent fortement que les protéines du NMD sont transportées par le cytosquelette.

L'ensemble des résultats de ce projet a permis de montrer pour la première fois que le mécanisme de NMD nécessite la présence d'un cytosquelette fonctionnel. J'ai aussi montré qu'une interaction physique existe entre les protéines du cytosquelette et les protéines du NMD. Mes travaux ont enfin permis d'identifier une nouvelle structure cytoplasmique qu'il reste encore à caractériser et qui pourrait peut-être représenter un environnement particulier où se déroulerait la translecture.

Pour ce projet, je dois encore poursuivre l'identification et la caractérisation de ces nouveaux foyers cytoplasmiques afin de pouvoir valider mon hypothèse. Pour cela, je rechercherai la présence de protéines impliquées dans la traduction et dans la translecture telles que la protéine eIF5A notamment (Saini, Eyler et al. 2009).

J'envisage aussi d'acquérir du G418 (une molécule activant la translecture et qui interagit avec le site A du ribosome) porteur d'un fluorophore afin d'étudier sa distribution cellulaire et sa colocalisation éventuelle avec les protéines UPF lorsque les cellules sont traitées avec de la colchicine ou du taxol. Un article sera alors préparé et soumis pour publication au cours de l'année 2015.

3. Discussion

Notre équipe se concentre sur la recherche de molécules capables d'inhiber le processus de NMD et/ou d'activer la translecture pour deux raisons principales. La première est l'identification et la caractérisation de nouvelles approches thérapeutiques pour des maladies génétiques causées par une mutation non sens. La seconde est l'utilisation de ces molécules pour étudier le mécanisme de reconnaissance des codons stop prématurés et approfondir nos connaissances sur le mécanisme de NMD.

Mon projet de thèse s'inscrit parfaitement dans cette démarche. Ainsi, concernant le premier axe, mes travaux ont pu mettre en évidence l'existence de molécules inhibitrices du NMD plus efficaces que l'amlexanox par exemple. Sachant que par exemple la colchicine ou le taxol sont déjà des médicaments utilisés pour le traitement de la goutte dans le cas de la colchicine ou du cancer pour le taxol, leur intérêt thérapeutique semble évident en tout cas pour certaines pathologies. En effet, toutes deux conduisent à perturber le cytosquelette ce qui est une stratégie

anti-cancéreuse. Il serait intéressant d'étudier l'efficacité de ces 2 molécules dans des cas de cancers impliquant notamment des mutations non sens dans des gènes suppresseurs de tumeurs. L'idée serait la suivante : les molécules ciblant le cytosquelette vont perturber la division cellulaire et les cellules cancéreuses sont par définition des cellules qui se répliquent constamment. Ces cellules seront donc directement affectées par les molécules inhibitrices du cytosquelette. Dans le cas de cellules cancéreuses porteuses d'une mutation non sens dans un gène suppresseur de tumeur, l'effet sera double puisque ces cellules n'ont plus la capacité à rentrer en apoptose du fait de l'absence d'expression du gène suppresseur de tumeur. L'action de la cytochalasine D ou du jasplakinolide conduira donc non seulement à bloquer la dynamique du cytosquelette mais aussi à induire l'inhibition du NMD et l'activation de la translecture donc à la réexpression du gène suppresseur de tumeur. Les cellules retrouvant la capacité à rentrer en apoptose pourront donc être plus sensibles aux agents apoptotiques ainsi qu'au blocage de la dynamique du cytosquelette.

Concernant le second axe, mes travaux ont apporté de nouvelles connaissances dans le domaine du NMD. Mon premier projet a permis de mettre en évidence une nouvelle régulation du NMD. En effet, il a déjà été montré que le NMD est régulé par miRNA, épissage alternatif et par NMD. Par contre, rien n'était connu sur l'efficacité du NMD au cours de l'apoptose. La question qu'on se posait était de savoir si lors d'un processus de mort cellulaire impliquant des synthèses protéiques spécifiques, un mécanisme de contrôle qualité tel que le NMD était maintenu ou pas. Mes résultats montrent clairement que le NMD est inhibé et que certains facteurs UPF

sont des cibles des caspases. A ma connaissance, il s'agit du premier cas d'inhibition d'un mécanisme de contrôle qualité des ARNm au cours de l'apoptose qui est rapporté. En allant un peu plus dans le détail, ces travaux ont apporté aussi des indications sur la fonction des domaines protéiques des facteurs UPF1 et UPF2. Ainsi, j'ai montré que les séquences peptidiques allant des acides aminés 1 à 37 de la protéine UPF1 et la séquence peptidique allant des acides aminés 1 à 741 de la protéine UPF2 sont apoptotiques lorsqu'ils sont générés. Ce résultat suggère que l'inhibition du NMD n'est pas une inhibition par défaut mais plus une inhibition ayant un rôle à jouer dans le processus de mort cellulaire par apoptose. Le fait que la protéine UPF2 mais pas la protéine UPF3X soit ciblée par les caspases semble aussi révéler une fonction de UPF2 plus importante dans le mécanisme de NMD et/ou dans le processus d'apoptose qu'initialement imaginé car UPF2 n'a pas de fonction très claire même au sein du complexe NMD. Mes travaux permettront certainement d'améliorer notre connaissance sur le rôle joué par UPF2 que ce soit dans le NMD ou dans l'apoptose.

Le second projet exposé dans ma thèse a permis de mettre en évidence un lien physique entre le cytosquelette et les facteurs de NMD. J'ai aussi montré qu'un cytosquelette fonctionnel est nécessaire pour assurer l'élimination des ARNm porteurs d'un codon stop prématuré par NMD. Ces résultats suggèrent donc qu'il y a nécessité d'un transport actif des facteurs et substrats du NMD par le cytosquelette. Ces travaux ont aussi permis de mettre en évidence une nouvelle catégorie de foyers cytoplasmiques qui peuvent contenir des facteurs et des substrats du NMD mais pas

l'enzyme de décoiffage DCP1 par exemple qui est un marqueur de P-body. Sachant que ces structures apparaissent lorsque de la translecture est détectée, il pourrait s'agir soit d'un lieu de préparation des mRNP à la translecture soit du lieu où se produit la translecture. Cette dernière hypothèse ouvrirait la possibilité que la translecture se fasse dans un environnement bien particulier et différent de la traduction normale. Il est clair que la poursuite de la caractérisation de ces foyers cytoplasmiques est importante et pourrait permettre de faire progresser notre connaissance du mécanisme de translecture dont on commence à réaliser qu'il touche aussi des codons normaux de terminaison de la traduction de manière naturelle et régulée (Yamaguchi, Hayashi et al. 2012; Loughran, Chou et al. 2014).

Comme illustré par ma thèse, l'étude de molécules capables d'inhiber le NMD et/ou d'activer la translecture constituent un moyen original d'étudier les mécanismes en lien avec la reconnaissance des codons stop prématurés et présentent aussi un intérêt pour le développement d'approches thérapeutiques de pathologies associées à des mutations non sens. Ces pathologies comprennent notamment les maladies génétiques rares telles que la mucoviscidose ou la myopathie de Duchenne. On comprend dans ce cas que l'idée est de ré-exprimer le gène mutant pour retrouver la fonction manquante dans la cellule. Les mutations non sens touchent aussi les maladies génétiques fréquentes comme le cancer. Dans ce cas, la stratégie thérapeutique est un peu différente puisqu'elle va consister soit à permettre la réexpression d'un gène suppresseur de tumeur porteur d'une mutation non sens afin de redonner la capacité à la cellule à rentrer en apoptose. Il est donc

attendu que des traitements apoptotiques soient plus efficaces lorsque la mutation non sens est corrigée. L'inhibition du NMD peut aussi devenir en soi une méthode anti-cancéreuse en permettant l'expression d'isoformes d'ARNm qui normalement ne sont pas exprimées car dégradées par le NMD. Ces isoformes pourraient coder pour des peptides toxiques pour la cellule. Il a aussi été montré que ces isoformes génèrent de nouveaux peptides antigéniques dans les cellules cancéreuses qui expriment un grand nombre de gènes mutants. L'inhibition du NMD pourrait donc apparaitre comme un moyen de cibler les cellules cancéreuses grâce à la présentation en surface cellulaire de ces peptides antigéniques pour lesquels on pourrait produire des anticorps spécifiques (Pastor, Kolonias et al. 2010). L'approche thérapeutique visant à inhiber le NMD et/ou activer la translecture rentre dans le développement de médecine personnalisée ou ciblée. Ce type d'approche n'en est qu'à ces débuts mais semble très prometteuse vue le nombre croissant d'essais cliniques entrepris dans ce domaine.

INTRODUCTION

During gene expression, gene first is transcribed to a precursor messenger RNA (pre-mRNA) and this pre-mRNA goes through several processes to become a mature messenger RNA (mRNA). This mRNA is subject to several quality controls which can eliminate aberrant mRNAs. Among these quality controls one of them is called nonsense-mediated mRNA decay (NMD) which can distinguish and degrade the mRNAs containing premature termination codons (PTCs) to prevent the synthesis of toxic or no functional truncated proteins.

It has been shown that about one-third of inherited genetic diseases are caused by PTCs and among PTCs found on the pathogenic genes of inherited disease, nonsense mutations account for 10% (Frischmeyer and Dietz 1999; Mort, Ivanov et al. 2008). My project is to find and characterize molecules to correct nonsense mutations. Several strategies for correction of nonsense mutations have been developed. In our lab, we mainly study two of them: one is NMD inhibition, the other is PTC-readthrough. We use a screening system to identify molecules which can inhibit NMD and then validate the screening results in different cell lines containing nonsense mutation. We determine whether these molecules can also activate PTC-readthrough by analyzing the proteins synthesized from PTC-containing mRNAs. In my study, I found several molecules either inhibit NMD only or inhibit NMD and activate readthrough.

To understand my projects clearly, I will make some introductions for the processing of pre-mRNAs, mRNAs degradation pathway and mRNA surveillance system.

1. The processing of pre-mRNAs

Genes encoding a protein start their expression with the transcription of the

gene into a pre-mRNA by the RNA polymerase II. Before becoming a functional and mature mRNA, the pre-mRNA will be subjected to three major processes: the addition of a methyl 7 guanosine cap structure at the 5' end, a cleavage and a polyadenylation at the 3' end and the removing of intronic sequences by RNA splicing **(Figure 1)**. The maturation of the 5'- and the 3'-ends prevent the decay of the RNA by exoribonucleases present in cells (Wahl, Will et al. 2009). The 5' cap and 3' poly (A) tail are also a characteristic of mRNA that is not found in other types of RNAs such as non coding RNAs, transfer RNAs (tRNAs) or ribosomal RNAs (rRNAs) (Gunnery and Mathews 1995). Once mRNA is generated, it is exported to the cytoplasm to be translated into a protein. Because RNA metabolism is mechanistically different among bacteria, plants, inferior and superior eukaryotes (Darmon and Lutz 2012) and since my project focuses on human cells, I am going to describe in detail all the maturation processes that generate a mature mRNA in mammalian cells otherwise I will indicate the species that is considered.

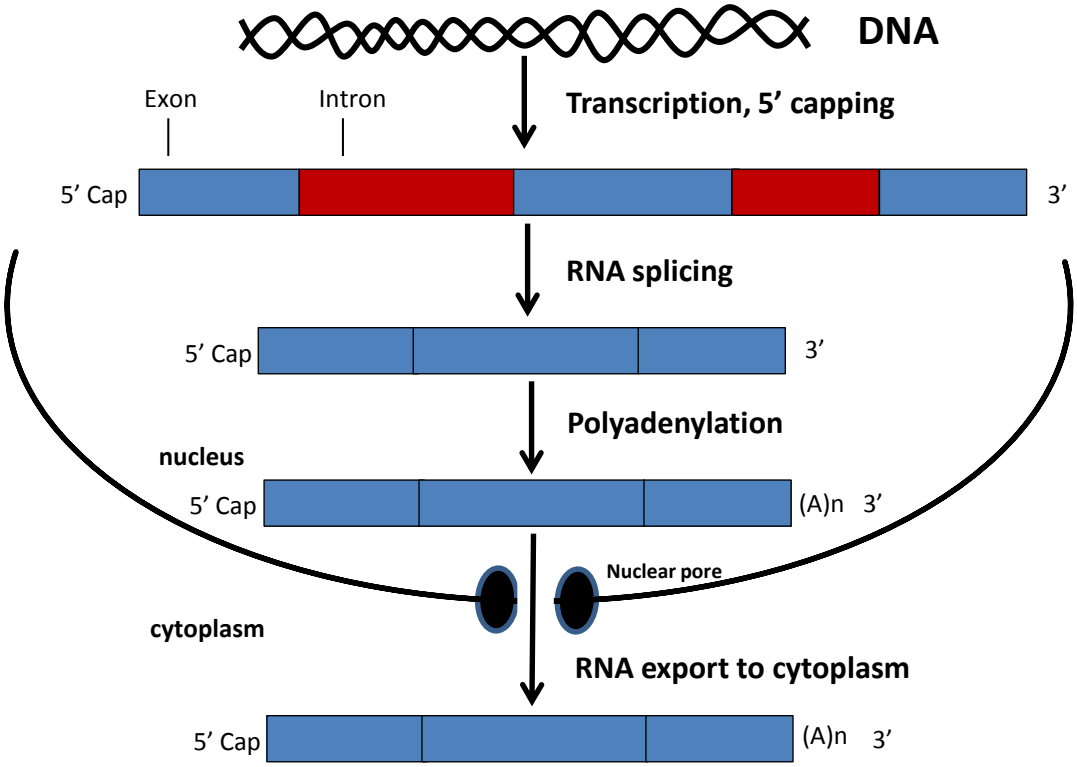

Figure 1: From the pre-mRNA to the mRNA

Blue rectangles represent exons and red rectangles represent introns. Shortly after RNA polymerase II starts transcription, the 5' end of the nascent RNA is capped, then introns are splicing, and 3'end is cleaved at poly (A) site and is polyadenylated to add adenosine (A) residues (poly(A) tail). Finally the mature mRNA is exported to cytoplasm.

1.1. The cap structure

1.1.1. The 5' capping processing

When the transcription of the pre-mRNA reaches a length of about 25 nucleotides, a 7-methylguanosine is added to the 5'-end with an opposite polarity to form a cap structure. The cap structure protects the pre-mRNA from 5' to 3' exoribonucleolytic degradation. And the 5' cap plays an important role in some processes such as pre-mRNA splicing, mRNA export from nucleus to cytoplasm, translation, etc (Ghosh and Lima 2010; Li and Kiledjian 2010). The carboxyl-terminal domain (CTD) of the RNA polymerase II is involved in the cap formation by recruiting the capping enzymes (triphosphatase, guanylyltransferase and methyltransferase). First the triphosphatase cleaves the 5'-terminal phosphate of the nascent pre-mRNA, then the guanylyltransferase catalyses the addition of a guanosine (G) mono-phosphate to the 5' end of the pre-mRNA to form a G(5')ppp(5')structure and finally the methyltransferase adds a methyl group to the N-7 position of the guanosine to create a 7mG G(5')ppp(5') structure **(Figure 2)** (Bentley 2005; Bentley 2014; Gonatopoulos-Pournatzis and Cowling 2014).

1.1.2. Cap-binding proteins

As soon as the cap structure of the mRNA is completed, a protein complex called cap binding complex (CBC) binds it in the nucleus. The CBC is composed by a protein of 20 kDa (Cap binding protein (CBP) 20) and a protein of 80 kDa (CBP80). CBP20 and CBP80 localize in the nucleus and bind to the 7mG of the cap structure. They function synergistically and can be recruited to the cap structure soon after the beginning of the transcription. CBP80 binds to CBP20 that directly interact with the

cap structure with high affinity (Calero, Wilson et al. 2002). Neither CBP20 nor CBP80 alone has considerable affinity for the cap structure (Calero, Wilson et al. 2002). Once the CBC binds the cap structure in the nucleus, it can recruit several transcription factors to promote an efficient transcription elongation (Lenasi, Peterlin et al. 2011; Hossain, Chung et al. 2013). CBC is also involved in pre-mRNA splicing in the pre-mRNA 3' end processing and in the export of mRNAs from the nucleus to the cytoplasm through the nuclear pore complex (Flaherty, Fortes et al. 1997; McCracken, Fong et al. 1997; Lenasi, Peterlin et al. 2011; Gonatopoulos-Pournatzis and Cowling 2014). Finally, CBC has been shown to play a role in the first round or pioneer round of translation and in an mRNA surveillance pathway called nonsense-mediated mRNA decay (NMD) (Gonatopoulos-Pournatzis and Cowling 2014).

Beside of CBP20/80, another cap-binding complex called eIF4F is present in cells. The protein complex eIF4F consists of three subunits: eIF4E which is the protein binding the cap structure; eIF4A, a DEAD-box RNA helicase and ATPase unwinding the secondary structure of the 5' untranslated region (UTR); and eIF4G, a scaffolding protein that makes a bridge between eIF4E and eIF4A. The protein complex eIF4F is the cytoplasmic CBC, replaces CBP20/80 complex in cytoplasm (Sato and Maquat 2009) and supports the bulk of translation (Topisirovic, Svitkin et al. 2011; Gonatopoulos-Pournatzis and Cowling 2014)

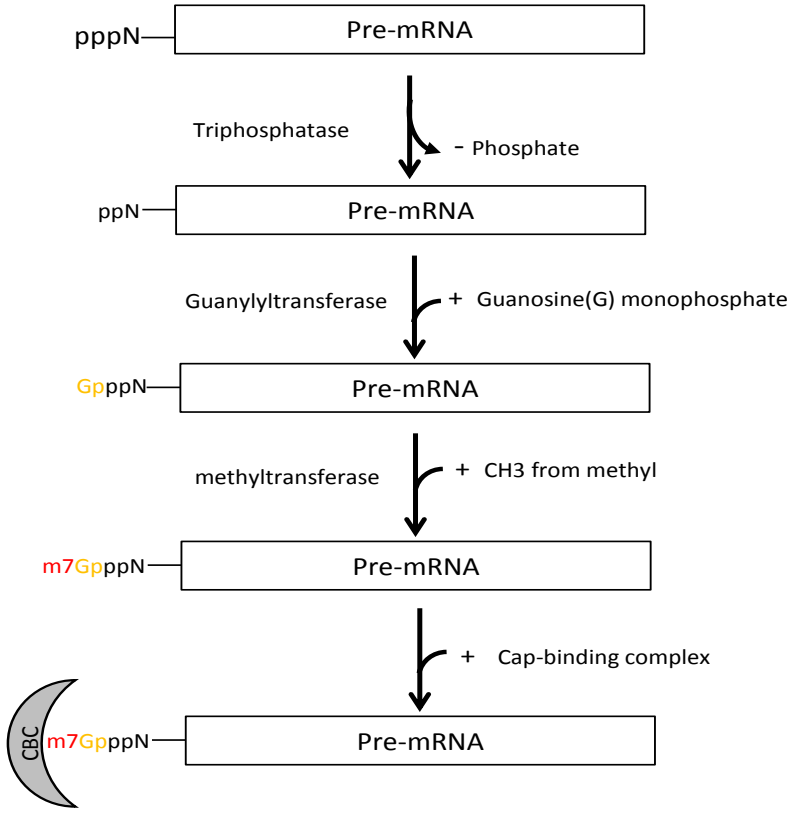

Figure 2: Addition of the cap structure at the 5’ end of the pre-mRNA

During the formation of the cap structure, a triphosphate is present at the 5' end of the pre-mRNA. A triphosphatase cleaves the 5’ terminal phosphate of the RNA then a guanosine (G) monophosphate is added to the terminal phosphate of the RNA to form a G(5’)ppp(5’) structure thanks to a guanylyltransferase catalysis; next a methyl group is added at the N-7 position of the guanosine by a methyltransferase to create a 7mG G(5’)ppp(5’); Finally the cap-binding complex is loaded to the 5’ cap structure.

1.2. Maturation of the 3’ end of the pre-mRNA

In eukaryotic cells, all mRNAs except histone mRNAs possess a 3’ poly (A) tail (Adesnik and Darnell 1972; Adesnik, Salditt et al. 1972). Poly (A) tail protects mRNA from decay by 3’-to-5’ exoribonucleases, helps mRNA to be exported from the nucleus to the cytoplasm (A, van der Loo et al. 2008), and promotes mRNA translation (Kerekatte, Keiper et al. 1999; Macdonald 2001). Poly (A) tail is also bound by two different poly (A) binding proteins (one is PABPC1 present in the cytoplasm and PABPN1 loaded on the polyA tail in the nucleus and removed from the mRNA in the cytoplasm; these proteins can shuttle from cytoplasm to nucleus)(Kumar and Glaunsinger 2010; Kumar, Shum et al. 2011) PABPC1 is involved in the initiation of translation and can regulate the mRNA decay; PABPN1 functions in the synthesis of poly (A) tails (Gallie 1991; Colgan and Manley 1997; Kuhn and Wahle 2004).

In mammalian cells, there are two sequence elements that play the core role in the 3’ end processing: one element is the AAUAAA hexamer or a variant AUUAAA. This sequence called poly (A) signal is located 10-35nt upstream of the cleavage site (also called poly (A) site). This sequence is bound by the cleavage and polyadenylation specificity factor (CPSF) complex; the second element is the U/GU-rich region which is located ~30nt downstream of the cleavage site and serves as the binding site for the CStF (cleavage stimulation factor) complex. During the processing of the 3’ end, CPSF recognizes and binds to the poly (A) signal sequence; and CStF interacts with a U/GU-rich sequence. Then CPSF and CStF proteins can interact with

each other to form a loop with the 3’ end of the pre-mRNA. Then CStF recruits the cleavage factors I and II (CFI and CFII) to form the pre-mRNA-CPSF-CStF-CFI-CFII complex. Subsequently, the poly (A) polymerase (PAP) is recruited by this complex to stimulate the 3’-end cleavage at the cleavage site. The cleavage factors are then released and the downstream RNA cleavage product is degraded (Perez Canadillas and Varani 2003; Millevoi and Vagner 2010; Elkon, Ugalde et al. 2013).

At the newly generated 3’ end, the PAP first adds few adenosine (A) residues to form the short poly (A) tail that induces the recruitment of PABPN1. The presence of the PABPN1 to the initial short poly (A) tail increases the processivity of the PAP. After 200 – 300 A residues in the majority of mammalian mRNAs, PABPN1 forces the PAP to stop the poly (A) polymerization (Eckmann, Rammelt et al. 2011) (Figure 3). In a study, Darmon et al compared the sequence of the protein factors that join in the 3’ end processing in the different eukaryotic species ranging from human to plants, and they found that the majority of these protein factors are conserved, which demonstrated that the processing of the 3’ end of pre-mRNAs is an ancient mechanism (Darmon and Lutz 2012).

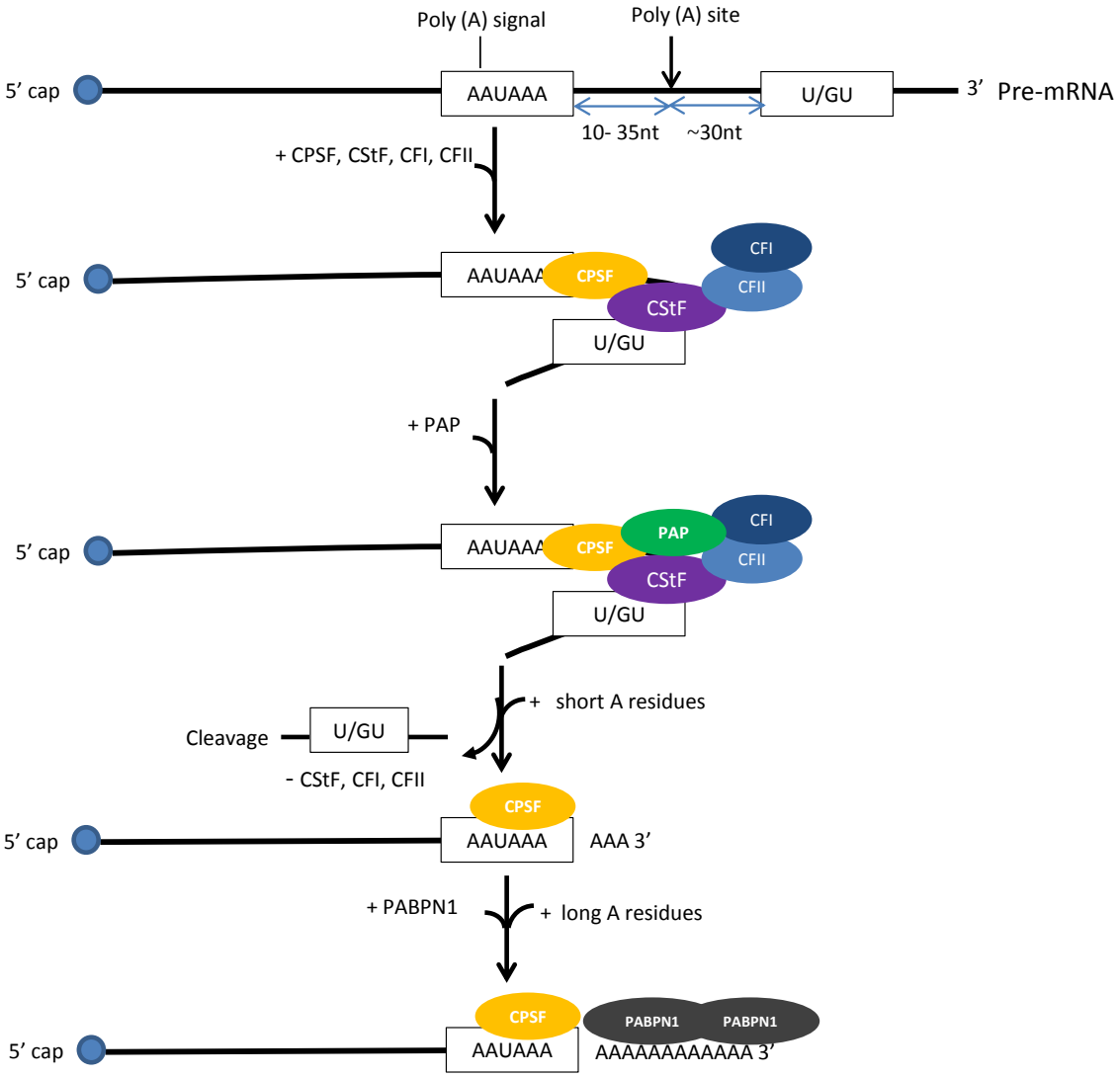

Figure 3: The 3' end processing.

At the 3' end of pre-mRNAs, there are two sequences which are a AAUAAA hexamer (poly (A) signal) located 10-35nt upstream of the cleavage site (poly (A) site) and a U/GU-rich region located ~30nt downstream of poly (A) site. The cleavage and polyadenylation specificity factor (CPSF) recognizes the AAUAAA poly (A) signal, and the cleavage stimulation factor (CStF) recognizes the U/GU-rich sequence; CPSF and CStF interact with each other to form a loop in the RNA. In addition, CStF recruits the cleavage factors I and II (CFI and CFII) to help stabilizing the RNA-protein complex. Then the poly (A) polymerase (PAP) binds this complex stimulating the cleavage at the poly (A) site, the release of the cleavage factors and the degradation of the downstream RNA cleavage product. The PAP first adds few adenosine residues to allow the recruitment of the poly (A)-binding protein nuclear 1 (PABPN1). The PABPN1 then stimulates the PAP to complete the synthesis of the poly (A) tail. After the polymerization of about 200-300 adenosine residues, the PABPN1 promotes the arrest of the poly (A) tail synthesis by the PAP.

1.3. Pre-mRNA splicing

1.3.1. The processing of pre-mRNA splicing

To produce a mature and functional mRNA, pre-mRNAs have to support splicing in order to remove intronic sequences and keep exonic sequences (Matera and Wang 2014). The splicing machinery is conserved from yeast to human (Kaufer and Potashkin 2000). The key element for the splicing machinery is to identify the splicing sites made of few bases in a long polyribonucleotide sequence. In vertebrate, there are four main consensus splice sites: (1) the 5' splice site (5'ss) with a consensus sequence GURAGU (in which R is for purine), (2) the 3' splice site (3'ss) with a consensus sequence of CAG, (3) a pyrimidine-rich region (10-12 bases) located near 3' end of the intron and (4) the branch point with a degenerate consensus sequence with an adenosine (A) as an almost exclusive branched nucleotide, situated 20-50 bases upstream of the 3' ss. Pre-mRNAs are spliced by a large complex called spliceosome which is composed of five small nuclear ribonucleoproteins (snRNPs) consisting of the U-rich small nuclear RNAs (snRNAs) designated U1, U2, U4, U5 and U6 and about 170 associated proteins (Hastings and Krainer 2001). During the process of splicing, first U1 snRNP binds to the 5'ss by base pairing, simultaneously the splicing factor (SF1) bund to the branch point A and U2 snRNP associated factor (U2AF) linked to the pyrimidine-rich region and 3' ss respectively by its large and small subunits, which induces U2 snRNP binds to the branch point A and the release of SF1. Then a trimeric U4-U6-U5 complex joins the complex formed by U1/U2 snRNP to generate the spliceosome. After RNA/RNA and RNA-protein rearrangements, pre-mRNAs undergo two sequential transesterification reactions, remove intron sequences as lariats and ligate the exons **(Figure 4)**. This type of splicing is called constitutive splicing (Hastings and Krainer 2001; Sanford and Caceres 2004; Keren, Lev-Maor et al. 2010).

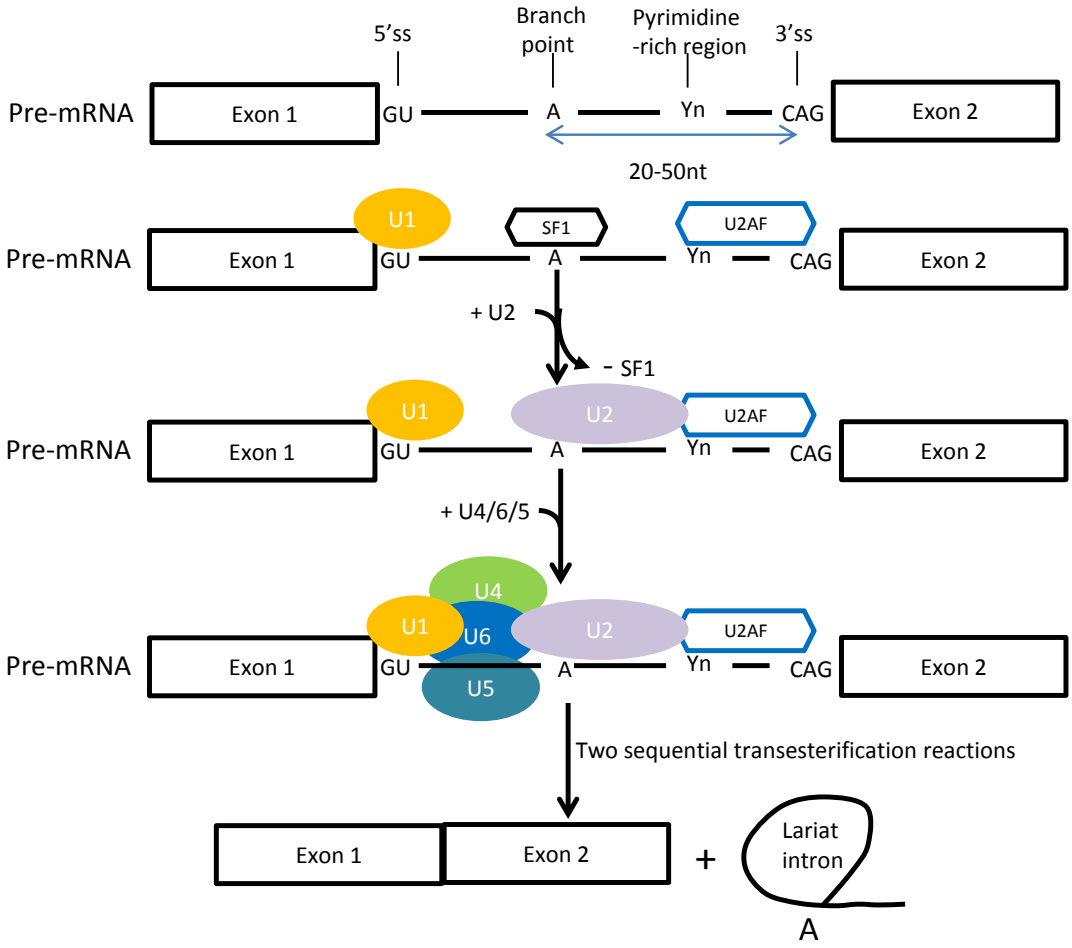

Figure 4: The processing of spliceosome-mediated splicing.

In vertebrate, introns contain four consensus splice sites: (1) the 5' GU splice site (5'ss), (2) the 3' CAG splice site (3'ss), (3) a pyrimidine-rich region containing 10-12 bases (4) the branch point adenosine (A) located 20-50 bases upstream of the 3' ss. At the beginning, 5'ss and the branch point A are separately recognized by U1 snRNP and SF1 (splicing factor 1), at the same time the pyrimidine-rich region and 3'ss are associated with U2AF (U2 snRNP associated factor); then U2 snRNP interacts with the branch point A displacing SF1, which recruits the trimeric snRNP complex of U4, U5, and U6 to bind to U1/U2 snRNP complex to form the spliceosome; Finally pre-mRNAs are subjected to two sequential transesterification reactions resulting in the removing of introns as lariats and the ligation of exons.

In some cases the splicing signal becomes suboptimal. We saw that the consensus sequences of each splice site are highly degenerated making some splice sites highly recognized by the spliceosome and some others ignored by the splicing machinery. Sometimes, intronic mutations can occur at the splice site transforming a strong splice site into a weak splice site (Ram and Ast 2007; Semlow and Staley 2012).

In order to help the spliceosome to recognize the splice sites, numerous additional proteins are involved in splicing mechanism such as the members of the serine/arginine rich (SR) proteins family and of the heterogenous nuclear ribonucleoproteins (hnRNP) family (see below) (Martinez-Contreras, Cloutier et al. 2007; Ram and Ast 2007). These proteins and the strength of splice sites are the key components to allow alternative splicing (Keren, Lev-Maor et al. 2010). Alternative splicing is more abundant in higher eukaryotic and in vertebrates in particular as highlighted by studies based on deep sequencing methodologies that have found that more than 90% of human genes undergo alternative splicing (Keren, Lev-Maor et al. 2010). Alternative splicing plays an important role in gene expression and evolution and can increase the diversification of protein from the same mRNA precursor (Keren, Lev-Maor et al. 2010).

Alternative splicing can be categorized into four main types (Black 2003; Labrador and Corces 2003; Horiuchi and Aigaki 2006; Keren, Lev-Maor et al. 2010) (Figure 5). (1) The exon skipping (cassette exon) in which an exon can be spliced out of the transcript with its flanking introns. The exon skipping is the most frequent event among alternative splicing reactions and is found in about 40% of alternative splicing reactions in the higher eukaryotes; (2) the alternative 5'ss or (3) 3'ss selection in which two or more 5' or 3' splice sites are in a competition for the same splicing reaction leading to shorten an exon. Alternative 5'ss and 3'ss selection account for 7.9% and 18.4% of alternative splicing in higher eukaryotes, respectively. (4) The intron retention, where an intron remains in the mature mRNA. Intron retention is more frequent in lower metazoan, fungi and protozoa than in vertebrates. Other studies have found additional less frequent alternative splicing categories (Edwalds-Gilbert, Veraldi et al. 1997; Horiuchi and Aigaki 2006; Pohl, Bortfeldt et al. 2013): (1) the mutually exclusive exons in which two exons are in a competition to be included in the mRNA and the presence of one preclude the incorporation of the other one; (2) the alternative promoters and (3) alternative poly (A) which can modify the 5'- or 3'-most exon of a transcript; (4) The trans-splicing that is a splicing reaction between two different RNA molecules to form a mRNA.

1.3.2. The regulation of splicing

Constitutive and alternative splicings are both regulated and dependent of the recognition of the splice sites by the spliceosome. The splice site sequences are necessary but not sufficient for spliceosome to recognize the correct splice sites, and auxiliary elements (cis-acting sequence elements and trans-acting splicing factors) help to the recognition of exon and intron borders. According to their location and effects on promoting or inhibiting the recognition of splice sites, cis-acting sequence elements are classified into four classes: the exonic splicing enhancers (ESE), the exonic splicing silencer (ESS), the intronic splicing enhancer (ISE) and the intronic splicing silencer (ISS) **(Figure 6)**. Alternative splicing is tightly controlled according to the cell type, the tissue or some external stimuli (Faustino and Cooper 2003).

The SR proteins are a family of RNA-binding proteins that contain at their N-terminal end, one or more RNA recognition motif (RRM) which determine the binding specificity of SR proteins. In addition, SR proteins have at their C-terminal part one protein-protein interaction domain rich in arginine (R) and serine (S) residues called RS domains. This domain can be phosphorylated to activate SR proteins and this phosphorylation has been shown to modify their cellular distribution and to modify the protein-protein interaction properties (Caceres, Misteli et al. 1997). The SR proteins were divided into twelve proteins: SRSF1 (ASF/SF2, SRp30a), SRSF2 (SC35, PR264, SRp30b), SRSF3 (SRp20), SRSF4 (SRp75), SRSF5 (SRp40, HRS), SRSF6 (SRp55, B52), SRSF7 (9G8), SRSF8 (SRp46), SRSF9 (SRp30c), SRSF10 (TASR1, SRp38, SRrp40), SRSF11 (p54, SRp54), SRSF12 (SRrp35). They interact with different RNA by recognizing different degenerate consensus sequences. The role of SR proteins by binding ESEs, is to help the recognition of the 5'ss by U1snRNP, the 3'ss by U2AF, SF1 and U2snRNP and also to recruit U4-U6-U5 complex to the spliceosome to activate splicing (Kohtz, Jamison et al. 1994; Roscigno and Garcia-Blanco 1995).

The exon silencers are often bound by heterogeneous nuclear ribonucleoproteins (hnRNPs) that inhibit splicing by preventing the recognition of a

splice site by the spliceosome. Among the different hnRNPs, one of them is called hnRNP I (also named as PTB (polypyrimidine tract binding protein)). PTB can compete with U2AF for the binding of the polypyrimidine tract located at the 3'ss. PTB also can bind ESSs to inhibit splicing (Llorian, Schwartz et al. 2010). Among the members of hnRNP, hnRNP A1 and H have been also shown to inhibit splicing by binding ESSs and then preventing the local binding of SR proteins to an ESE for example (Fisette, Toutant et al. 2010).

Intron splicing enhancers (ISEs) and the proteins regulating their effects are less well characterized. Some studies have identified one ISE element which is the hexanucleotide UGCAUG (Huh and Hynes 1994; Hedjran, Yeakley et al. 1997). The sequence UGCAUG can be bound to the Fox-1 family of RNA-binding proteins which regulates the tissue-specific alternative splicing in metazoans(Kuroyanagi 2009). Forch *et al* have showed that the T cell-restricted intracellular antigen 1 (TIA-1) binds a U-rich sequence (intronic splicing enchancers) downstream of some 5' ss to help the recruitment of the U1 snRNP at the 5'ss (Forch, Puig et al. 2002). CUGBP and ETR-like factors (CELF) can activate splicing through intronic splicing enhancers (Forch, Puig et al. 2002) (Charlet, Logan et al. 2002). But the mechanism of these factors on splicing and the proteins bound to the intronic splicing enhancers need to be further determined.

There are also intronic splicing silencers (ISSs) which are bound by some proteins in order to inhibit splicing. Among the proteins that bind to ISS, SR proteins have been found to bind an intronic splicing silencer located near a branch point in the adenovirus L1 mRNA and to prevent the recruitment of U2 snRNP to the branch point A (Kanopka, Muhlemann et al. 1996). PTB can also bind to ISS of fibroblast growth factor receptor 2 (FGF-R2) and inhibit splicing and the mechanism should be characterized (Carstens, Wagner et al. 2000; Wagner, Baraniak et al. 2005). Hua et al have found hnRNP A1/A2 can bind two ISSs on survival of motor neuron 2, centrometric (SMN2) gene and inhibit the recognition of the splice site of exon 7 (Hua, Vickers et al. 2008). Wang et al used a cell-based screen system to identify ten group of ISSs, and they demonstrated that many factors could bind different ISS and

one ISS could also be recognized by different factors (for examples hnRNP A1 can bind five different groups of ISSs and the ISS AGATATT can be recognized by 10 different proteins) (Wang, Xiao et al. 2013). The mode of action of ISSs and their binding factors remain poorly understood and are still under investigations.

Although all splice sites do not have the same sequence demonstrating flexibility around a consensus sequence, a simple point mutation can be sufficient to strongly affect the recognition of an intron or an exon by silencing a splice site or a splicing regulator sequence. Indeed, it has been shown that sequence variants which result from point mutation or frameshift mutation can affect RNA splicing by changing 5' or 3' splicing site sequences or modifying cis-acting sequence elements (Cartegni, Chew et al. 2002; Spurdle, Couch et al. 2008). Krawczak et al have shown that about 15% of point mutations can cause defects of RNA splicing (Krawczak, Reiss et al. 1992). For example, it has been found that on BRCA (breast cancer) 1 or 2 gene which are human tumor suppressor genes and the breast and ovarian cancer susceptibility genes, there are some point mutations which can affect RNA splicing (Gaildrat, Krieger et al. 2010; Gaildrat, Krieger et al. 2012). Authors found that on BRCA1 5434 C→G mutation can destroy the function of the splicing enhancer element localized from position 5420 to 5449 and this mutation also creates a new splicing silencer element bound by the hnRNPA1. On BRCA2 gene, the point mutation 517 G→T affects the first nucleotide of the exon 7 decreasing the recognition of the 3' splice site by the spliceaosome.

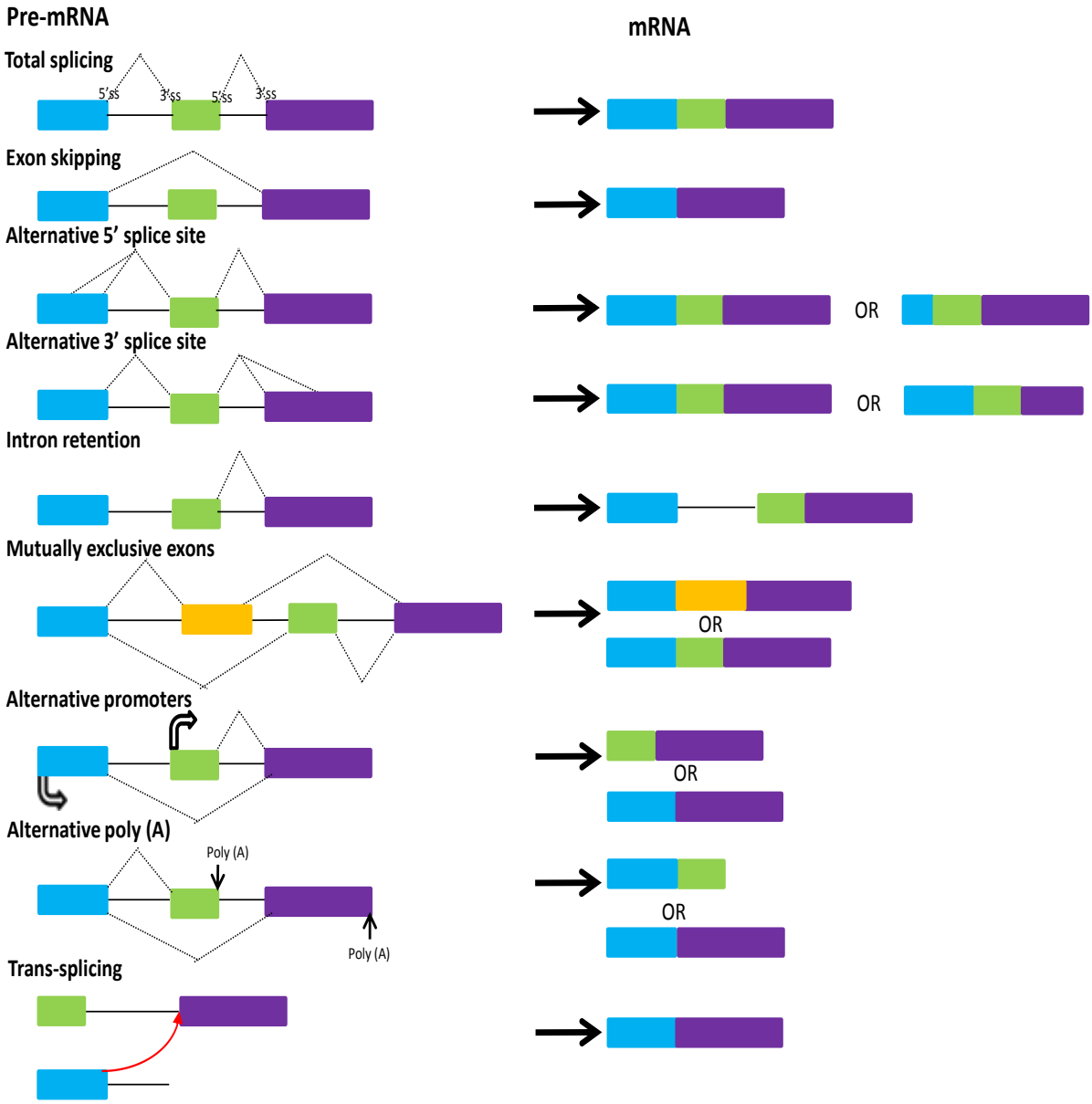

Figure 5: The categories of alternative splicing.

Exons are presented by colored rectangles and introns are represented by solid lines

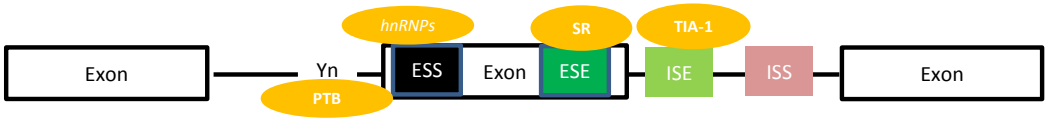

Figure 6: Cis and trans regulatory elements required for splicing.

Exons and introns contain some cis-acting sequence elements bound by splicing regulatory proteins. These sites are exonic splicing enhancers (ESEs), exonic splicing silencers (ESSs), intronic splicing enhancers (ISEs), or intronic splicing silencers (ISSs). Splice site recognition is regulated by proteins binding these specific sequences, such as the serine/arginine (SR) proteins, heterogeneous nuclear ribonucleoproteins (hnRNPs), or other splicing factors.

1.4. The export of mRNA from nucleus to cytoplasm

Because incompletely spliced pre-mRNAs would be translated into defective proteins that might be not functional or deleterious to the cells, only mature mRNAs which are processed by 5'capping, 3'cleavage/ polyadenylation and RNA splicing can be exported to cytoplasm. The nuclear envelope is a double membrane consisting of a water-impermeable phospholipid bilayer and many associated proteins. mRNPs and other molecules go to cytoplasm through holes called nuclear pores thanks to proteins called the nuclear pore complexes (NPCs). NPC is comprised of multiple copies of about 30 different proteins called nucleoporins and the structure formed by NPC consists of two functional regions: (1) the NPC central structure formed an eight-fold symmetrical cylindrical structure and is embedded in the nuclear membrane; (2) the peripheral NPC extensions which anchor the peripheral structure (for example cytoskeleton filaments) to the NPC central structure (Strambio-De-Castillia, Niepel et al. 2010; Bonnet and Palancade 2014). One group of nucleoporins called FG-nucleoporins is rich in hydrophobic phenylalanine(F) and glycine (G) and forms a semi-permeable barrier that allows water, ions, metabolites and small proteins less than 40-60 kDa to pass freely, but restricts the diffusion of the larger molecules containing nuclear localization or export signals (Bonnet and Palancade 2014).

mRNPs are macromolecules and are transported through nuclear membrane thanks to soluble transporter proteins called mRNA export receptors. mRNA export receptors are loaded on mRNPs by export adaptors (such as ALY or REF in mammals), The mRNA export receptors directly interact with the FG-nucleoporins at the NPCs and transport mRNPs to cytoplasm through NPCs (Kohler and Hurt 2007). In mammals, most of mRNPs are exported by a mRNA export receptor called NXF1-NXT1. This receptor consists of two subunits, a large subunit called nuclear export factor 1 (NXF1) and a small subunit named as nuclear export transporter 1 (NXT1) (Gruter, Tabernero et al. 1998; Herold, Suyama et al. 2000). The NXF1/NXT1 mRNP exporter can bind RNAs and export mRNPs through the nuclear pores. As the

mRNP is transported through the NPC, the mRNP composition changes and the proteins bound to the nuclear mRNPs are replaced by a different group of proteins. These proteins include the NXF1/NXT1 mRNP exporter, cap-binding complex (CBC) bound to the 5’ cap and PABPN1 bound to the poly (A) tail. Once the mRNP exits from the nuclear pore, the cytoplasmic RNA helicase (Dbp5) is recruited in order to remove NXF1/NXT1 complex and protects mRNPs to go back to nucleus and these proteins are then imported back at the nuclear side of the nuclear pore or in the nucleoplasm (Kohler and Hurt 2007; Kelly and Corbett 2009). In the cytoplasm, the CBC is replaced by the cytoplasmic cap-binding protein which is the translation initiation factor eIF4E. The PABPN1 is replaced by the PABPC1 at the polyA tail (Wahl, Will et al. 2009; Topisirovic, Svitkin et al. 2011).

Though many proteins are exchanged during or after the export to the cytoplasm, some proteins remain bound to the mRNPs in the cytoplasm. Among these proteins, there is a multiprotein complex called exon junction complex (EJC). EJC can be involved in mRNA export or subsequent mRNA cytoplasmic localization and plays an important role in the mRNA surveillance system called nonsense mediated mRNA decay (see below).

2. mRNA degradation pathways

Gene expression is the result of a balance between the synthesis of an mRNA including transcription and maturation, and the decay of this mRNA. mRNA degradation plays an essential role in the regulation of gene expression. mRNA synthesis is executed by RNA polymerase II only, but mRNAs are degraded by several exoribonucleases and endoribonucleases. In all species, 5'->3' and 3'->5' exoribonucleases and endoribonucleases act in the mRNA degradation, while decapping and deadenylation activities are specificities of eukaryotic cells because mRNAs in this type of cells possess the protective structures 5'-cap and 3'-poly (A) tail at the mRNA ends (Perez-Ortin, Alepuz et al. 2013). mRNA degradation can be divided by deadenylation -dependent mRNA decay and deadenylation-independent mRNA decay (Garneau, Wilusz et al. 2007).

2.1. Deadenylation-dependent mRNA decay

In eukaryotic cells, the majority of mRNA degradation is initiated by deadenylation which shortens poly (A) tails (Beelman and Parker 1995; Yamashita, Chang et al. 2005; Chen and Shyu 2011). Yamashita et al. have discovered that in mammalian cells deadenylation is biphasic. In the first phase, the 3' poly(A) tails of mRNAs are synchronously shortened to approximately 110 nucleotides without detecting the degradation of the rest of the mRNA; in the second phase the poly(A) tail of mRNAs is heterogeneously shortened from ~110nt to ~20nt, which triggers the degradation of the rest of the mRNA (Yamashita, Chang et al. 2005).

Several eukaryotic deadenylases have been identified such as PAN2-PAN3 complex, CCR4-NOT complex or PARN (Yamashita, Chang et al. 2005; Garneau, Wilusz et al. 2007). PAN2-PAN3 complex is a poly (A) binding protein (PABP)-dependent 3' to 5' poly (A) exoribonuclease which takes a role in trimming the 3' poly (A) tails in yeast (Mangus, Evans et al. 2004) and is activated as soon as the first phase of poly(A) tail deadenylation starts in mammalian cells (Yamashita, Chang et al. 2005). CCR4-NOT complex is comprised of nine subunits in yeast (Ccr4, Caf1, Caf40, Caf130, Not 1-5)

and most homologs of these subunits have also been identified in mammalian cells(Lau, Kolkman et al. 2009). CCR4-NOT complex whose activity can be inhibited by the PABP is the main deadenylase in yeast and functions in the second phase of deadenylation in mammalian cells (Yamashita, Chang et al. 2005; Collart and Panasenko 2012). PARN is a poly (A) 3'-5' ribonuclease and is only found in higher eukaryotes. PARN functions by interacting with cap-structure and its activity can be inhibited by the PABP and the nuclear cap-binding proteins (Utter, Garcia et al. 2011).

After poly(A) deadenylation (Figure 7), Sm-like (Lsm)1-7 complex binds to the 3' end of the mRNA and triggers decapping by the DCP1-DCP2 complex at the 5' termini (Sharif and Conti 2013). DCP2 is the most well-studied and conserved eukaryotic decapping enzyme, it has intrinsic decapping activity and its decapping activity needs the interaction with DCP1 (Lykke-Andersen 2002; She, Decker et al. 2008). The activity of DCP1-DCP2 complex can be stimulated by the enhancers of decapping such as enhancer of decapping (Edc) (Arribas-Layton, Wu et al. 2013).

The removing of the cap structure allows the 5'-3' exoribonuclease XRN1 to degrade the mRNA from the 5'-end to the 3'-end. The XRN family of 5'-3' exoribonucleases is comprised of the nuclear enzymes (XRN2/RAT1 and XRN3) and the cytoplasmic enzymes XRN1/PACMAN or XRN4 (Nagarajan, Jones et al. 2013). XRN1 can hydrolyze the decapped mRNAs in the 5'-3' direction and XRN2 is involved in the nuclear mRNA quality control (Nagarajan, Jones et al. 2013). It has been shown that XRN2 also can be involved cytoplasmic mRNA control called NMD because NMD factors (UPF1, UPF2 and UPF3X) can coimmunoprecipitate with XRN2(Lejeune, Li et al. 2003). When the 5' to 3' decay pathway is compromised, the mRNA is also degraded from the 3'-end to the 5'-end by a large complex called the exosome.

2.2. Deadenylation-independent mRNA decay

Although the bulk of mRNAs are degraded by deadenylation-dependent pathway, there are some special mRNAs such as the mRNAs encoding the ribosomal protein RPS28B or the enhancer of decapping EDC1 whose degradation is deadenylation–independent(Badis, Saveanu et al. 2004). In yeast, RPS28B mRNA is

subject to an autoregulatory mechanism. Indeed, RPS28B protein can directly bind to the hairpin at the 3’ untranslated region (UTR) of its corresponding mRNA and sequentially recruits an enhancer of decapping called Edc3 which can recruit other decapping factors and can induce deadenylation -independent decapping. Denise et al shown that in yeast, EDC1 mRNA encodes a protein that enhances decapping rate, which can let EDC1 mRNA bypassing deadenylation (Muhlrad and Parker 2005). Denise et al also discovered that the 3’ UTR of EDC1 mRNA protects mRNA from deadenylation and is sufficient for deadenylation-independent decapping because EDC1 mRNA becomes uncapped when a poly(G) tract is inserted in the 3’ UTR to block the deadenylation (Muhlrad and Parker 2005) .

There are also other patterns of deadenylation-independent mRNA decay involving the exosome or endonuclease cleavages. The exosome is a multi-subunit complex composed of ten to eleven proteins and has both endonuclease and exoribonuclease activities. The exosome has been shown to be involved in both the deadenylation-dependent and the deadenylation-independent mRNA decay (Chlebowski, Lubas et al. 2013). Some special mRNAs, including the mRNAs encoding avian apo-very low density lipoprotein, insulin-like growth factor II (IGF-II), Transferrin receptor (TfR), or α-globin mRNA possess sequences or structures sensitive that can trigger a cleavage by endonucleases leading to the production of two fragments (Schoenberg 2011).

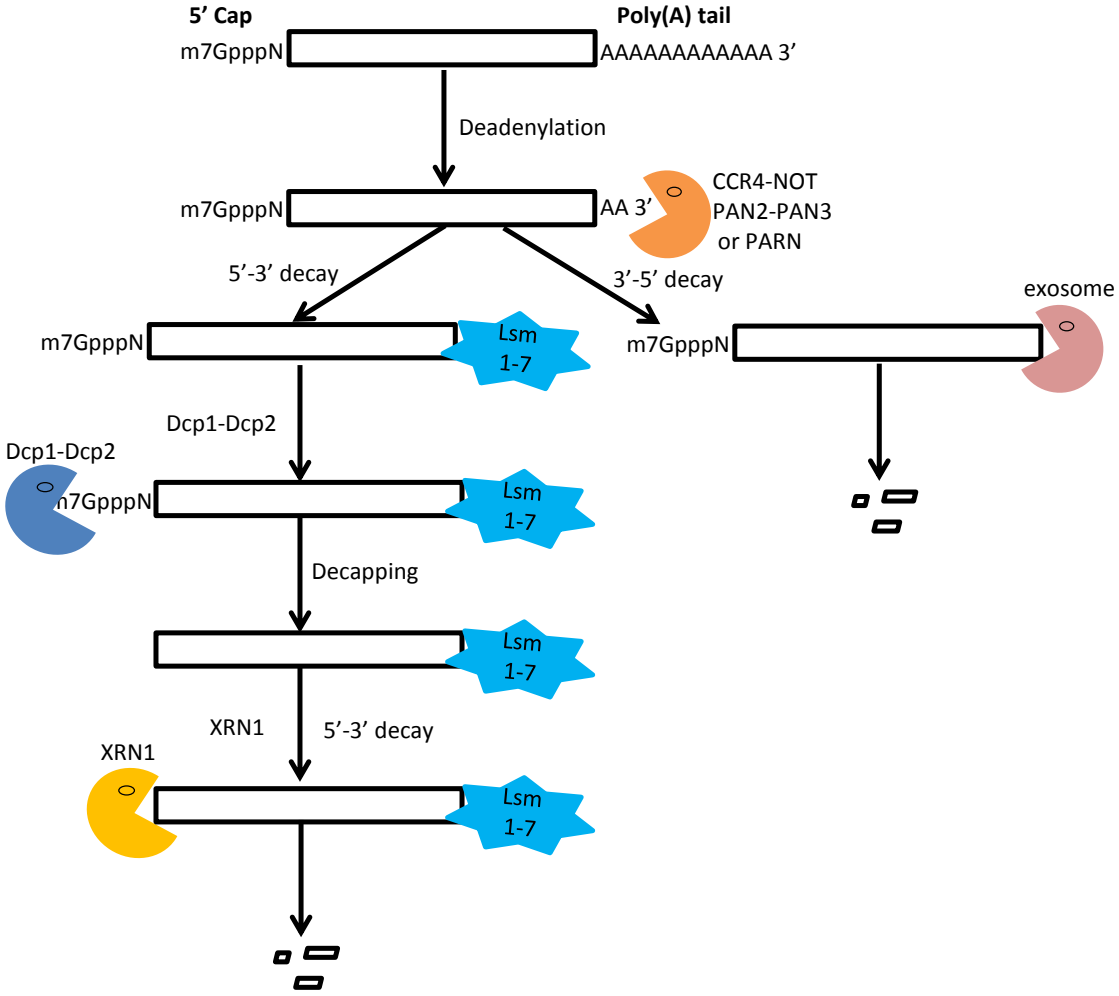

Figure 7: Deadenylation-dependent decay

During deadenylation-dependent decay, first deadenylases (CCR4-NOT, PAN2-PAN3, PARN) shorten the poly (A) tail of the mRNA, then Lsm1-7 complex binds to the 3'end of the mRNA which recruits decapping enzymes (DCP1-DCP2) and induces decapping at the 5'end. Finally mRNA is completely degraded by the exoribonuclease XRN1 in the 5'-3' direction or by the exosome from the 3' to the 5'end.

3. mRNA surveillance system

To synthesize a mature mRNA in eukaryotic cells, genes go through several processings: transcription, 5'capping, splicing and 3' polyadenylation. At each step, an aberrant mRNA can be produced which could be toxic or simply not functional. To maintain the fidelity of gene expression cells evolved several mRNA surveillance systems (also called as quality control systems) in both the nucleus and the

cytoplasm.

3.1. Nuclear mRNA surveillance

Nuclear mRNA surveillance has been studied mainly in Saccharomyces cerevisiae (Garneau, Wilusz et al. 2007). Before mRNAs are exported from nucleus to cytoplasm, the aberrant synthesis of mRNAs (incorrect or defective splicing, cap structure, cleavage or polyadenylation at 3' end) or the retention of mRNAs in the nucleus lead to activate different surveillance mechanisms. The nuclear retention of an mRNA that should be exported to the cytoplasm leads to a decay by nuclear surveillance systems (Vasudevan and Peltz 2003). One of the main components of nuclear surveillances is the nuclear exosome. The exosome is distributed in both nucleus and cytoplasm and the core exosome is composed by six proteins which form a ring-like structure. In yeast, these six proteins are Rrp41-43p, Rrp45p, Rrp46p, and Mtr3p. The ring structure is capped on the top by three proteins named Rrp4p, Rrp40p and Cs14p. In human, the homologs of most of these proteins have been found except for Rrp43p and Mtr3p. The human homolog of Rrp45p is named PM-Scl75 because it has been identified in the autoimmune sera of patients with polymyositis-scleroderma overlap syndrome (Alderuccio, Chan et al. 1991). Studies have found that the ring proteins in human and yeast have lost the activity required to carry out RNA cleavage. Nevertheless, to promote the RNA degradation, two 3'-5' exonucleases interact with the core exosome. The two exonucleases are Dis3p/Rrp44p and Rrp6p whose homolog in human is called PM-Scl100. Both proteins have been found to be present in the nucleus and in the cytoplasm(Lejeune, Li et al. 2003) (Allmang, Petfalski et al. 1999; Burkard and Butler 2000; Raijmakers, Egberts et al. 2002; Zenklusen, Vinciguerra et al. 2002). The nuclear exosome can lead the aberrant transcripts to accumulate at the site of transcription for degradation (Torchet, Bousquet-Antonelli et al. 2002). Recently, some studies have found that exosome activity could also require additional cofactors such as TRAMP, Rrp47 and MPP6.

Indeed, a new enzyme complex called TRAMP (for **Tr**f4/**A**ir2/**M**tr4p **P**olyadenylation complex) can enhance the RNA degradation supported by Dis3/Rrp44p and Rrp6 (Ghosh and Jacobson 2010; Schmidt and Butler 2013). Rrp47 whose mammalian homologue is called C1D can directly bind Rrp6, promote the stability and normal expression of Rrp6 and facilitate the Rrp6-mediated degradation (Butler and Mitchell 2010; Feigenbutz, Garland et al. 2013). Studies found Mpp6 coimmunoprecipates with the exosome complex but its role on the exosome function remains unclear (Chen, Gherzi et al. 2001; Lehner and Sanderson 2004).

3.2. Cytoplasmic mRNA surveillance

Cytoplasmic mRNA surveillance contains nonsense-mediated mRNA decay (NMD), no-go mRNA decay (NGD), non-stop mRNA decay (NSD). These surveillance systems can eliminate aberrant mRNAs which harbor premature termination codon (PTC), stalled ribosome or mRNAs lacking a stop codon, respectively. Interestingly, they are all related with the translation mechanism.

3.2.1. Nonsense-mediated mRNA decay (NMD)

NMD is the quality control system that recognizes and degrades mRNAs harboring a premature termination codon (PTC) to prevent the synthesis of truncated proteins which can be toxic to the cell or no functional. NMD involves many factors and genetic screens method initially identified three up-frameshift (UPF) proteins (UPF1-3) in yeast Saccharomyces cerevisiae, and seven suppressor with morphological effect on genitalia (SMG) proteins (SMG1-7) in Caenorhabditis elegans (Hodgkin, Papp et al. 1989; Cui, Hagan et al. 1995). In 2009 two novel NMD factors repectively called SMG8 and SMG9 were identified (Yamashita, Izumi et al. 2009). The homologous proteins between species are described in the table 1 (Conti and Izaurralde 2005; Behm-Ansmant, Kashima et al. 2007). The three UPF proteins (UPF1, UPF2, UPF3) are conserved in all eukaryotic organisms including yeast (S. cerevisiae),

worm (Caenorhabditis elegans), fruitfly (Drosophila melanogaster) and mammals. Interestingly, in mammals, UPF3 has two paralogous proteins named as UPF3 and UPF3X (also known as UPF3a and UPF3b, respectively). SMG1, SMG 5-7 are preserved in all multicellular organisms but not in yeast and with the exception of SMG7 that is not been identified in fruitfly (Behm-Ansmant, Kashima et al. 2007) and SMG8 and SMG9 were conserved among metazoans except in yeast and A. thaliana (Yamashita, Izumi et al. 2009).

Table 1 NMD factor homologous in different organisms

Organism	Yeast	Worm	Fruitfly	Mammals
NMD factors	**UPF1**	**SMG2 (UPF1)**	**UPF1**	**UPF1**
	UPF2	**SMG3 (UPF2)**	**UPF2**	**UPF2**
	UPF3	**SMG4(UPF3)**	**UPF3**	**UPF3/3X**
		SMG1	**SMG1**	**SMG1**
		SMG5	**SMG5**	**SMG5**
		SMG6	**SMG6**	**SMG6**
		SMG7		**SMG7**
		SMG8	**SMG8**	**SMG8**
		SMG9	**SMG9**	**SMG9**

3.2.1.1. NMD factors

a) UPF1

UPF1 was originally identified in yeast, and its orthologous protein were named as regulator of nonsense transcript 1 (Rent1) in mammals and SMG2 in fruitfly (Behm-Ansmant, Kashima et al. 2007). UPF1 is an RNA/DNA-dependent ATPase and 5’-3’ helicase. Both activities are required for NMD (Cheng, Muhlrad et al. 2007). In the eukaryotes, UPF1 sequence identities are 40-62% between the different

eukaryotic species from S. cerevisiae to human (Applequist, Selg et al. 1997; Culbertson and Leeds 2003). That means that the sequence of UPF1 is highly conserved in the eukaryotic cells, which hints that UPF1 is important in biological systems. Sequence analysis shows that UPF1 contains two conserved functional regions which are an N-proximal cysteine- and histidine-rich domain (CH domain) and a C-proximal helicase domain. UPF1 can bind to UPF2 and eRF3 by N-proximal CH domain. CH domain can force UPF1 to bind RNA to inhibit the ATPase activity and this inhibition can be relieved when UPF2 binds to this CH domain (Chakrabarti, Jayachandran et al. 2011). Kashima et al have shown that removing the N terminal can inhibit NMD (Kashima, Yamashita et al. 2006). The C-proximal helicase domain belongs to the superfamily 1 of DNA/RNA helicases and possesses the ATPase activity. UPF1 can use the energy of ATP hydrolysis to unwind double-stranded RNA (dsRNA) or alter RNA-protein interactions (Imamachi, Tani et al. ; Cheng, Muhlrad et al. 2007). During the decay process, the recycling of the associated proteins on mRNPs is very important, it is found that the ATPase activity of UPF1 is necessary to the departure of the NMD factors from mRNA during the late steps of the decay processing since the absence of the ATPase activity can induce NMD factors to accumulate in the cytoplasmic foci called P-bodies (Franks, Singh et al. 2010). In yeast and human, UPF1 orthologous have been well characterized. In comparison with the yeast UPF1, human UPF1 contains an additional serine/glutamine motif (SQ motif) at the C-terminus which possesses some phosphorylation sites **(Figure 8)** (Imamachi, Tani et al.). Now the phosphorylation and dephosphorylation cycle of UPF1 is thought to be the signal to elicit NMD on the mRNA. SMG1 can phosphorylate UPF1 at SQ motifs in the N-regions (site threonine (T)28) and C-terminal regions (site (serin) S1078, S1096 and S1116) and T28 and S1096 are separately required for association with SMG 6 and SMG5/7 complex (Okada-Katsuhata, Yamashita et al. 2012). Fiorini et al demonstrated that SQ domain also can directly interact with the helicase domain to prevent ATP hydrolysis and RNA unwinding until the binding of partners to UPF1 (Fiorini, Boudvillain et al. 2013).

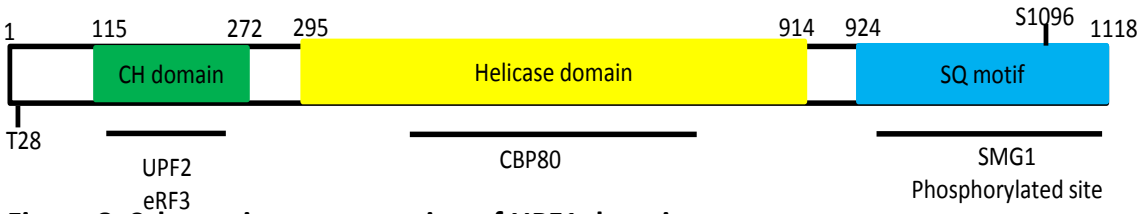

Figure 8: Schematic representation of UPF1 domains.

Functional and interacting domains of UPF1 are indicated. The amino acid positions are indicated by a number at the top of the structure. Cysteine/histidine-rich domain (CH domain) is located at the N-proximal region where UPF2 and eRF3 interact. serine/glutamine motif (SQ motif) is present at the C-terminus where phosphorylation sites are. The phosphorylation of AA site T28 and S1096 is important separately for SMG6 and SMG5/7 binding to UPF1.

UPF1 protein is concentrated in the cytoplasm and can shuttle between the nucleus and the cytoplasm (Mendell, ap Rhys et al. 2002). In all eukaryotic species UPF1 takes a key role in NMD (Hwang, Sato et al. 2010; Yamashita 2013). Beside of its role in NMD, UPF1 is also involved in other key processings such as the staufen 1 (STAU1)-mediated mRNA decay (SMD) (Imamachi, Tani et al. 2012). SMD is a post-transcriptional regulatory pathway that occurs when STAU1 together with UPF1 bind to the STAU1-binding site at the 3'-untranslated region of various mRNAs to promote the decay of these mRNAs. The binding site is located more than ～25nt downstream of translation termination codon. STAU1 is a dsRNA-binding protein which can recognize dsRNA structures and binds the STAU1-binding site in the 3' untranslated region of mRNAs to degrade it. STAU1 can directly interact with the CH domain of UPF1 and promote its helicase activity to induce SMD (Park and Maquat 2013). SMD is involved in some metabolic pathway such as myogenesis or adipogenesis. Studies show that down-regulation of STAU1 which inhibits SMD can increase the efficiency of NMD whereas down-regulation of UPF2 which inhibits NMD can increase the efficiency of SMD. These results suggest that SMD and NMD are in a competition for the recruitment of UPF1 (Park and Maquat ; Maquat and Gong 2009).

Recently some studies have uncovered that depletion of UPF1 but not UPF2 results in an S phase arrest in a NMD-independent manner and that UPF1 can interact with polymerase δ and plays a role in DNA synthesis during replication or

repair (Azzalin and Lingner 2006; Azzalin and Lingner 2006). All these studies contribute to demonstrate that UPF1 is involved in various key regulatory pathways and illustrates how one protein can have multi functions in the cell.

b) UPF2

UPF2 is a cytoplasmic protein concentrated at the perinuclear region. In the processing of NMD, UPF2 bridges UPF1 and UPF3/3X (Kunz, Neu-Yilik et al. 2006). UPF proteins are evolutionary conserved proteins. Indeed, UPF2 proteins from S. cerevisiae and from human are 22% identical and 39% similar (Culbertson and Leeds 2003). Human UPF2 contains three conserved MIF4G (Middle portion of eIF4G) domains **(Figure 9)** called like this due to their similarity with the middle domain of the eukaryotic translation initiation factor 4G (eIF4G). Interestingly, MIF4G domain is also found in CBP80 protein. UPF2 interacts with UPF3/3X and SMG1 via its third MIF4G domain and binds to the CH domain of UPF1 by its C-terminal region. The function of the first and the second MIF4G domains is not clear. Marcello *et al* have shown that deletion of the first MIF4G or/and the second MIF4G can partially impair NMD and these two domains are key bridging factors between the EJC and UPF1. UPF2 proteins containing only the third MIF4G domain and the UPF1-binding region can still partially activate NMD (Clerici, Deniaud et al.). That means the three MIF4G domain of UPF2 are all required for NMD.

Although UPF2 is essential for NMD, Gehring et al discovered an UPF2-independent NMD pathway by showing that UPF2 down-regulation does not inhibit all NMD reactions. They demonstrated that distinguishing UPF2-dependent and UPF2- independent NMD was dependent on EJC components. EJC components such as RNPS1 activated UPF2-dependent NMD and others such as Y14, MAGOH and eIF4A3 joined in the UPF2-independent NMD (Gehring, Kunz et al. 2005).

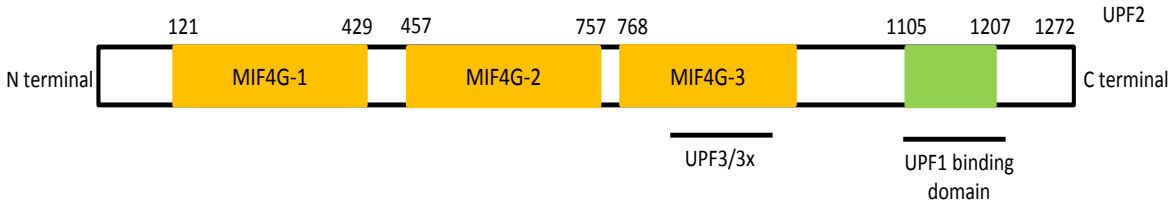

Figure 9: Schematic representation of UPF2 domains.
The amino acid positions are indicated by a number at the top of each structure.UPF2 contains three MIF4G domains and the C-terminal UPF1-binding region. The third MIF4G domain can be bound by UPF3/3X.

c) UPF3/3X

UPF3 is the least conserved protein among the UPF proteins with about 13-26% sequence identities between S. cerevisiae and human (Culbertson and Leeds 2003). A particularity in mammals is the presence of two genes corresponding to yeast UPF3 and encoding UPF3 located on the chromosome 13 and UPF3X located on the X-chromosome. UPF3 and UPF3X are also called UPF3a and UPF3b, respectively. UPF3 and UPF3X transcripts are subject to alternative splicing respectively on the exon 4 and on the exon 8 to synthesize two mRNA isoforms. RT-PCR experiments showed that all the UPF3/3X mRNAs and their splice variants are expressed in all human tissue types examined (Serin, Gersappe et al. 2001). UPF3 transcript harboring exon 4 has 99 nucleotides difference with UPF3 transcript lacking exon 4 that is translated into a protein called UPF3Δ (Serin, Gersappe et al. 2001). Serin et al also found that the difference of 99 nucleotides between UPF3 and UPF3Δ does not affect the interaction with UPF2 (Serin, Gersappe et al. 2001). However it is possible that there are different functions since the sequence of UPF3 transcript and UPF3Δ transcript is different. Schell et al did immunoprecipitation in HeLa cells and demonstrated that UPF3Δ associates stronger than UPF3 with UPF1; they also used molecular-mass- exclusion chromatography and found that UPF3Δ and UPF1 form a complex which excludes UPF3 and UPF2 and was different from the complex formed by UPF3 and UPF1 (Schell, Kocher et al. 2003). In S. cerevisiae, UPF3 mostly localizes in the cytoplasm but it shuttles between the nucleus and the cytoplasm. In contrast in mammals, UPF3 and UPF3X are mainly located in the nucleus and have the

capacity to shuttle between the nucleus and the cytoplasm. In human, UPF3/3X proteins contain a putative nuclear export signal (NES) and a nuclear localization signal (NLS) motifs. They also have an RNA recognition motif (RRM) suggesting that they can bind RNA even though this has not been demonstrated in mammals. Finally, a region at the N-terminal end of UPF3/3X proteins is dedicated to the interaction with UPF2 (Serin, Gersappe et al. 2001).

UPF3 or UPF3X are the first proteins to be recruited by the EJC in the nucleus and then UPF3/3X can recruit UPF2 (Ishigaki, Li et al. 2001). In normal mRNAs, the pioneer ribosome can remove UPF3/3X-UPF2-EJC complex and then the mRNAs mature to produce full-length proteins. When mRNAs contain a PTC at more than 50-55 nucleotides upstream of an exon-exon junction, UPF3/3X protein, UPF2 and EJC remain on the mRNP, then UPF2 recruits UPF1 and finally NMD is triggered. Kunz et al built the tethering system on the globin 5 boxB reporter mRNA and measured the function of UPF3 and UPF3X on NMD. They demonstrated that UPF3 was intrinsically much weaker than UPF3X in its ability to trigger NMD because of their different C-terminal sequences (Kunz, Neu-Yilik et al. 2006). Wai-kin Chan et al have shown a competitive relationship between UPF3 and UPF3X for the binding to UPF2: when the level of UPF3X is decreased by siRNA, more UPF3 binds to UPF2; in contrast, an overexpression of UPF3X decreases the binding of UPF3 to UPF2 (Chan, Bhalla et al. 2009). They also studied some endogenous NMD substrates and showed that all UPF3-dependent NMD substrates are also targeted by UPF3X but not all UPF3X-dependent NMD substrates are affected by the depletion of UPF3. These results indicate that UPF3X can replace UPF3 but UPF3 can only partially replace UPF3X.

Some UPF3-independent NMD pathways were also found (Avery, Vicente-Crespo et al. ; Chan, Huang et al. 2007). T-cell receptor (TCR) undergoes programmed genomic rearrangement which frequently results in the production of mRNAs with premature termination codons that activate NMD. Chan et al observed that deletion of UPF3 or/and UPF3X did not or lightly impair the efficiency of NMD on TCR mRNA containing PTC, which means that TCR NMD pathway is

UPF3/3X-independent (Chan, Huang et al. 2007). Paul et al also have shown that in Drosophila loss of UPF3 have no or very mild effect on some PTC-containing RNAs such as oda and tra and some NMD endogenous substrates such as cyp12c1 (Avery, Vicente-Crespo et al.).

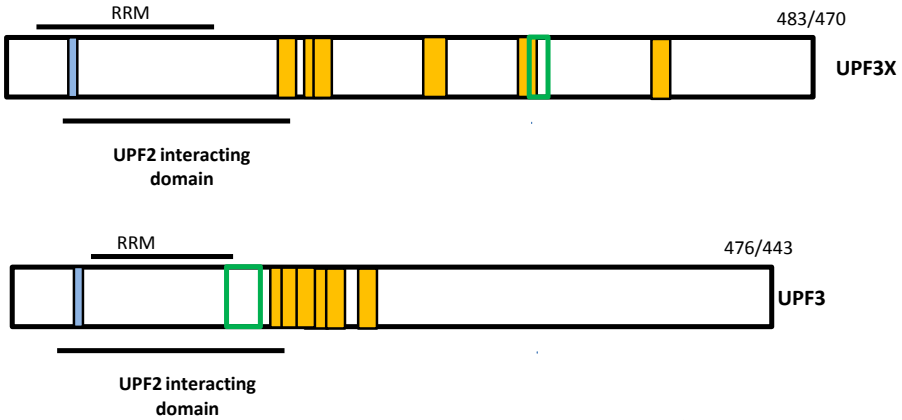

Figure 10: Schematic representations of human Upf3/3X proteins.

A blue box indicates a nuclear export signal (NES) and a yellow box represents a nuclear localization signal (NLS). Green box presents the alternatively spliced exon: UPF3 splices exon 4 (amino acids 141-173) and UPF3X splices exon 8 (amino acids 294-306). The regions of interaction with UPF2 are indicated by connecting lines. The numbers on the top of each protein correspond to the amino acid positions. RRM stands for RNA recognition motif.

d) SMG1, SMG5, SMG6, SMG7

Beside of UPF proteins, NMD also contains other central effectors named Suppressor with Morphogenetic effects on Genitalia (SMG) identified after a genetic screening in Cenorhabditis elegans. A group of 7 SMGs were identified and named SMG1, SMG2 (UPF1), SMG3 (UPF2), SMG4 (UPF3), SMG5, SMG6 and SMG7 proteins. In addition, Yamashita et al identified recently SMG8 and SMG9, 2 co-activators of SMG1 by biochemical studies in mammalian cells (Yamashita, Izumi et al. 2009). These SMG proteins are conserved in most of multicellular organisms, but in D. melanogaster SMG7 orthologue was not found. In S. cerevisiae there are homologues to SMG proteins and these proteins are the telomerase associated protein Est 1p and the related protein Ebs1p. Until now their putative role in NMD remains not clear (Behm-Ansmant, Kashima et al. 2007).

SMG1

SMG1 belongs to the phosphoinositide (PI) 3 –kinase-related kinase (PIKK) family. PIKK has serine/threonine kinase activity and can phosphorylate Ser and Thr amino-acids especially Ser/Thr-Gln (S/T-Q)-rich domains as the one presents in UPF1. PIKK also functions in cell growth, gene expression, genome surveillance and mitogenic and stress-induced signaling pathway in eukaryotic cells (Abraham 2001; Abraham 2004).

SMG1 plays a dual role in genotoxic stress response and mRNA surveillance processing such as NMD. Indeed, SMG1 is a stress-responsive protein and can be activated by ionizing radiation or UV light. SMG1 is required in the activation of p53 when cells are exposed to genotoxic stress such as UV or ionizing radiation (Brumbaugh, Otterness et al. 2004). The depletion of SMG1 results in spontaneous DNA damages and in increased sensitivity to ionizing radiations (Brumbaugh, Otterness et al. 2004). In NMD pathway, first SMG1, SMG8 and SMG9 form the SMG1 kinase complex then this complex binds UPF1 to form SMG1-UPF1 complex and interacts with eRF1 and eRF3 to build SMG1 kinase complex-UPF1 -eRF1-eRF3 complex (SURF) which associates with the ribosome **(Figure 11).** Finally, ribosome-SURF complex binds to the EJC to form the decay inducing complex (DECID) (the ribosome-SURF-EJC complex). The DECID complex can distinguish a PTC from a normal termination codon and induces SMG1-mediated UPF1 phosphorylation at the (S/T-Q) rich domains of UPF1. In SMG1 kinase complex, SMG8 mediates the recruitment of SMG1 to the ribosome-SURF complex and also suppresses SMG1 kinase activity until the DECID complex is formed. SMG9 is required to bridge SMG1 and SMG8 (Yamashita ; Kashima, Yamashita et al. 2006; Yamashita, Izumi et al. 2009).

SMG1 also plays a role in some NMD-independent biological processings. For example, SMG1 can inhibit the apoptosis induced by tumor necrosis factor α and can decrease the lifespan of C. elegans; SMG1 inactivation resists to oxidative stress in C. elegans; in human lung adenocarcinoma cell line A549, SMG1 has been shown to phosphorylate P53 in response to DNA double strand breaks and that function of

SMG1 is NMD-independent (Masse, Molin et al. 2008; Oliveira, Romanow et al. 2008).

SMG5, SMG6, SMG7

SMG5, SMG6 and SMG7 are evolutionally conserved from Drosophila to mammals and are required for NMD to dephosphorylate UPF1 by recruiting the protein phosphatase 2A (PP2A) (Anders, Grimson et al. 2003; Chiu, Serin et al. 2003; Gatfield, Unterholzner et al. 2003). Human SMG5, SMG6 and SMG7 share similar domains: two tetratricopeptide (TPR) repeats at the N-terminus of SMG5 and SMG7 or in the middle of SMG6, a PilT N-terminus (PIN) domain at the C-terminus of SMG5 and SMG6 (Fukuhara, Ebert et al. 2005) **(Figure 12)**. TPR domains contain the 14-3-3 like domain and helical hairpins domain and they regulate protein-protein interactions (Chakrabarti, Bonneau et al. 2014). SMG5, SMG6 and SMG7 all contain the conserved 14-3-3-like domain and these three proteins bind phosphorylated UPF1 (Figure 8) through this 14-3-3-like domain. 14-3-3 domains are the phosphoserine binding sites and are bound by phosphoserine-containing proteins (Rittinger, Budman et al. 1999). Interestingly, PIN domains have a nuclease activity (Schneider, Leung et al. 2009) .

It has been demonstrated by yeast two-hybrid assays and coimmmuno-precipitation that in C. elegans and human cells SMG5 and SMG7 interact with each other and share the similar structures to form SMG5/SMG7 heterodimer complex (Anders, Grimson et al. 2003; Ohnishi, Yamashita et al. 2003). Stafanie et al have studied the structure of SMG5 and SMG7 and found that SMG5 and SMG7 form the heterodimer by the 14-3-3-like domain in the back-to-back manner in which the peptide-binding sites face opposite directions. And they also found that this heterodimer is crucial for efficient NMD in human cells and this heterodimer can increase the affinity of the SMG5/SMG7 to UPF1 (Jonas, Weichenrieder et al. 2013). In contrast, the 14-3-3-like domain of SMG6 is a monomer. SMG5/SMG7 or SMG6 bind to the phosphorylation sites of UPF1 via the 14-3-3-like domain and then recruit PP2A which dephosphorylates UPF1. SMG1 can phosphorylate several serine

(S)/threonine (T)/glutamine (Q) sites of UPF1 and among them, the phosphorylation site S1096 is responsible for the recruitment of the SMG5/SMG7 heterodimer complex to the C-terminal SQ-rich region of UPF1 and the phosphorylation T28 is in charge of the recruitment of SMG6 to the N-terminal conserved region of UPF1 (Okada-Katsuhata, Yamashita et al. 2012). Interestingly, it has been shown that SMG6 has an endonucleolitic activity that would cut the PTC-containing mRNA close to the PTC (Huntzinger, Kashima et al. 2008; Eberle, Lykke-Andersen et al. 2009).

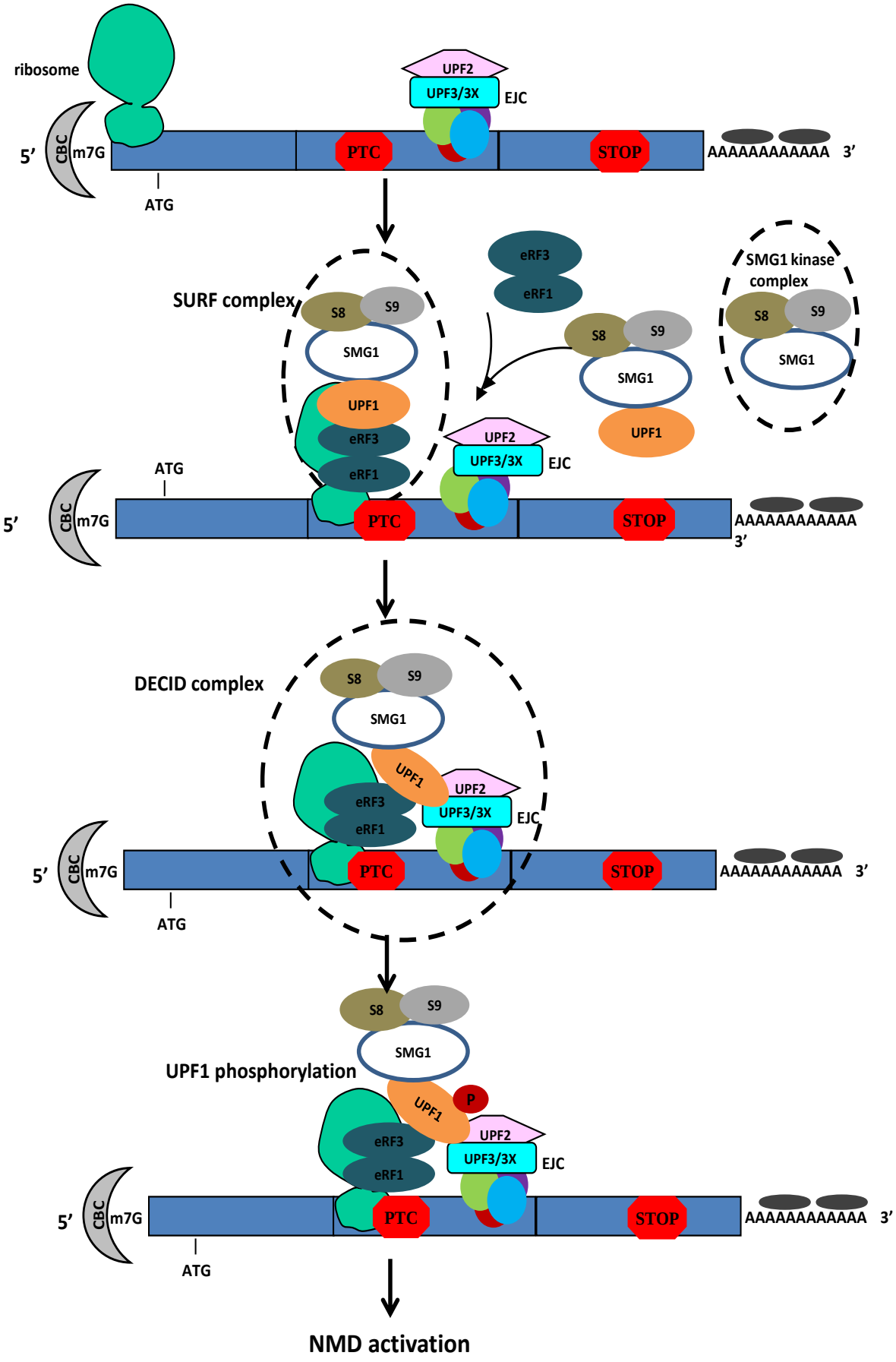
ribosome
UPF2
UPF3/3X
EJC
5'
CBC
m7G
PTC
STOP
AAAAAAAAAAA
3'
ATG
eRF3
eRF1
SMG1 kinase
complex
SURF complex
S8
S9
SMG1
UPF1
DECID complex
UPF1 phosphorylation
P
NMD activation

Figure 11: SURF complex and DECID complex

SMG1, SMG8 and SMG9 form a complex called SMG1 complex. This complex can bind UPF1 to form SMG1-UPF1 complex. When mRNA contains PTC, ribosome is stalled at PTC and recruits SMG1-UPF1 complex and eRF1 and eRF3 on mRNA to form SMG1-UPF1-eRF3-eRF1 complex called SURF complex. This complex associates with the ribosome. Then this complex binds to EJC by the interaction between UPF1 and UPF2 and form the ribosome-SURF-EJC complex called the decay inducing complex (DECID). DECID complex can induce UPF1 phosphorylation via SMG1. Finally NMD is activated and the RNA is degraded. Stop represents normal stop codon, S8 or S9 represents SMG8 or SMG9, P is for the phosphorylation.

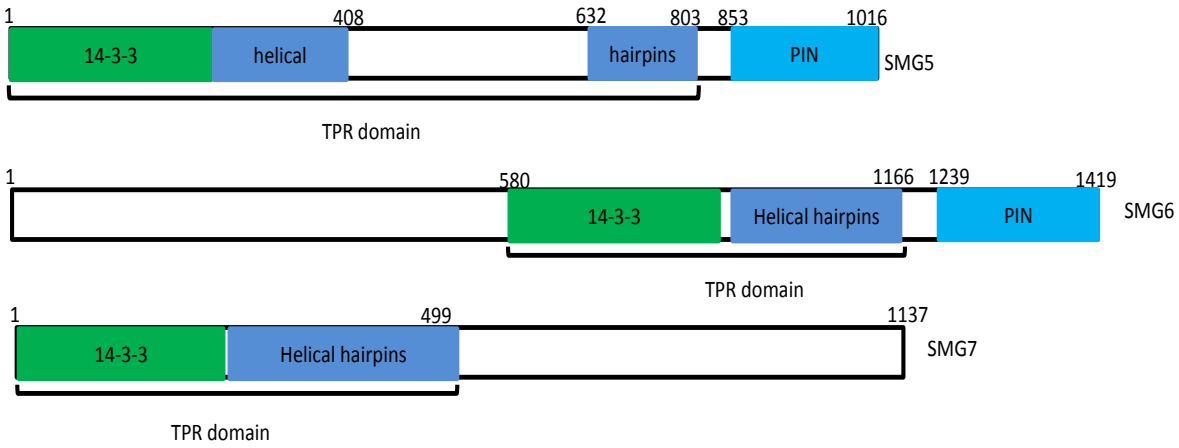

Figure 12: Schematic representation of SMG5, SMG6, SMG7 domains

The amino acid positions are indicated by a number on the top of each structure. The green boxes, deep blue boxes and light blue boxes separately indicate 14-3-3-like domain, helical hairpins and PIN domain, respectively.

3.2.1.2. The targets of NMD

a) mRNA containing premature termination codon

NMD targets and degrades mRNAs containing premature termination codons (PTCs) in order to prevent the synthesis of C-terminal truncated proteins with no activity or with potentially deleterious function to cells. PTCs arise in many ways: For example, PTCs can result either from mutations (nonsense mutations, frame-shifting, deletions or insertions) at the DNA level or from errors in RNA splicing. Indeed, more than 70% of pre-mRNAs undergo alternative splicing and one-third of the alternatively spliced transcripts contain PTCs which can be targeted for NMD (Lewis, Green et al. 2003; Chang, Imam et al. 2007). Another source of PTCs is the

programmed DNA rearrangements. In mammals, during lymphoid ontogeny, T-cell receptor (TCR) and immunoglobulin (Ig) genes undergo programmed rearrangements to generate large numbers of immune-system receptors which are important to recognize a diversity of antigens. However, two out of three times, these rearrangements result in the generation of PTCs which can elicit NMD (Li and Wilkinson 1998; Wang, Vock et al. 2002).

Importantly, in order that a PTC triggers NMD, it has to follow some specific rules in mammalian cells. Some studies have shown that the position of a PTC relative to the position of a downstream intron determines whether or not this PTC elicits NMD (Cheng, Belgrader et al. 1994; Thermann, Neu-Yilik et al. 1998; Zhang, Sun et al. 1998). Indeed, after pre-mRNA splicing, a protein complex called EJC (for exon junction complex) is deposited 20-24 nucleotides upstream of all exon-exon junctions as a consequence of splicing (Le Hir, Izaurralde et al. 2000). EJCs are working as residual marks of the splicing activity on mRNAs. It is actually the presence of EJC downstream of a stop codon that will elicit NMD on an mRNA. During the pioneer round of translation, ribosomes read the open reading frame and remove EJCs that they meet until to reach the first stop codon (Ishigaki, Li et al. 2001). In the case of a wild-type mRNA, no EJCs will be present on the mRNA after the pioneer round of translation due to the position of the normal termination codon in the last exon or at less than 50-55 nucleotides upstream of the last exon-exon junction. In the case of an mRNA harboring a PTC, the ribosome during the pioneer round of translation will stop on the PTC. Because of the position of the PTC (more than 50-55 nucleotides upstream of the last exon-exon junction), at least one EJC will be still present on the mRNA after the pioneer round of translation. It is the presence of this EJC after the pioneer round of translation that elicits NMD. According to this model, any PTC located at less than 50-55 nucleotides from the last exon-exon junction or in the last exon will not activate NMD. In addition, mRNAs deriving from naturally intronless genes or transfected cDNAs are immune to NMD **(Figure 13)**.

The activation of NMD seems to be species dependent since the rules are different between mammalian cells and S. cerevisiae, C. elegans cells or D.

melanogaster cells (Conti and Izaurralde 2005). For example, in S. cerevisiae PTCs are recognized by either an abnormally long 3' untranslated region (UTR) (also called faux 3' UTR) or a downstream sequence element (DSE) that recruits factors to distinguish between normal stop codons and PTCs (Zhang, Ruiz-Echevarria et al. 1995; Gonzalez, Ruiz-Echevarria et al. 2000; Das and Das 2013). It is worth noting that the model involving a DSE is now not favor since it has been only found in PGK1 mRNA (Zhang, Ruiz-Echevarria et al. 1995).

In mammalian cells, exceptions have also been described. One type of exception concerns the TCR-ß transcript and the immunoglobulin-µ (Ig-µ) transcript that they are still subject to NMD even when the distance between a PTC and the downstream exon-exon junction is less than 50-55 nucleotides (Carter, Li et al. 1996). PTCs on TCR-ß transcripts and Ig-µ transcripts result from the programmed DNA rearrangement which produces VDJ exon. Some studies have found that in VDJ exon there is a NMD- promoting sequence which is necessary for NMD because deletion of this sequence induces the mRNA escaping from NMD. But the composition of this sequence and the factors interacting with this sequence have not yet been identified (Gudikote and Wilkinson 2002; Buhler, Paillusson et al. 2004). Other possibility that explain why PTCs on TCR-ß transcript can break the position rule is that some sequences also can function under certain conditions to activate NMD: a fail-safe sequence in triosephosphate isomerase (TPI) or ß-globin mRNAs without downstream EJC seems to be able to elicit NMD (Cheng, Belgrader et al. 1994; Zhang, Sun et al. 1998).

Another exception is the ß-globin mRNA with PTCs on the first exon that is close to the initiation codon fail to elicit NMD although PTCs reside more than 50-55nt upstream of the last exon-exon junction (Romao, Inacio et al. 2000). Neu-YILIK et al showed that the first exon of ß-globin is divided by a sharp border which separates NMD-activating from NMD-resistant nonsense mutations because they found the expression level of ß-globin mRNA with nonsense mutations at codon from 2 to 23 is only slightly decreased but the abundance of mRNAs with nonsense mutations at codon 26 or further downstream are significantly decreased. They also found that

the ability of nonsense mutation to escape NMD is relative to a reinitiation of the translation downstream of a PTC (Zhang and Maquat 1997; Neu-Yilik, Amthor et al. 2011). This explanation is not so simple since Danckwardt et al have demonstrated that the translation reinitiation downstream of the PTC is not the reason why NMD fails to be activated on PTC located in the first exon of the β-globin gene (Danckwardt, Neu-Yilik et al. 2002). The failure of early PTCs on ß-globin mRNA to active NMD is still not clearly understood and it is possible that there are some specific sequences downstream of the PTC which can make early PTCs immune to NMD. Globin gene is not an isolate case since the same type of NMD activation failure occurs on the general control non- repressible (GCN4) mRNA and on the yeast AP-1 (YAP1) mRNA in S.cerevisiae (Ruiz-Echevarria and Peltz 2000).

Another example of this exception to the rule is the apolipoprotein (apo) B mRNA. Apo B mRNA undergoes Cytidine to Uridine (C to U) site specific RNA editing, which converts a CAA glutamine codon into a UAA PTC on exon 26 that will be used to incorporate a seleno-cysteine. On apo B mRNA all PTCs tested at different positions except the PTC resulting from the editing complex on exon 26 can trigger NMD. The failure of PTC to activate NMD is due to the formation of the editing complex which can prevent translation termination complex from interacting with PTC and EJC downstream of PTC (Kim, Ambroziak et al. 1998; Chester, Somasekaram et al. 2003).

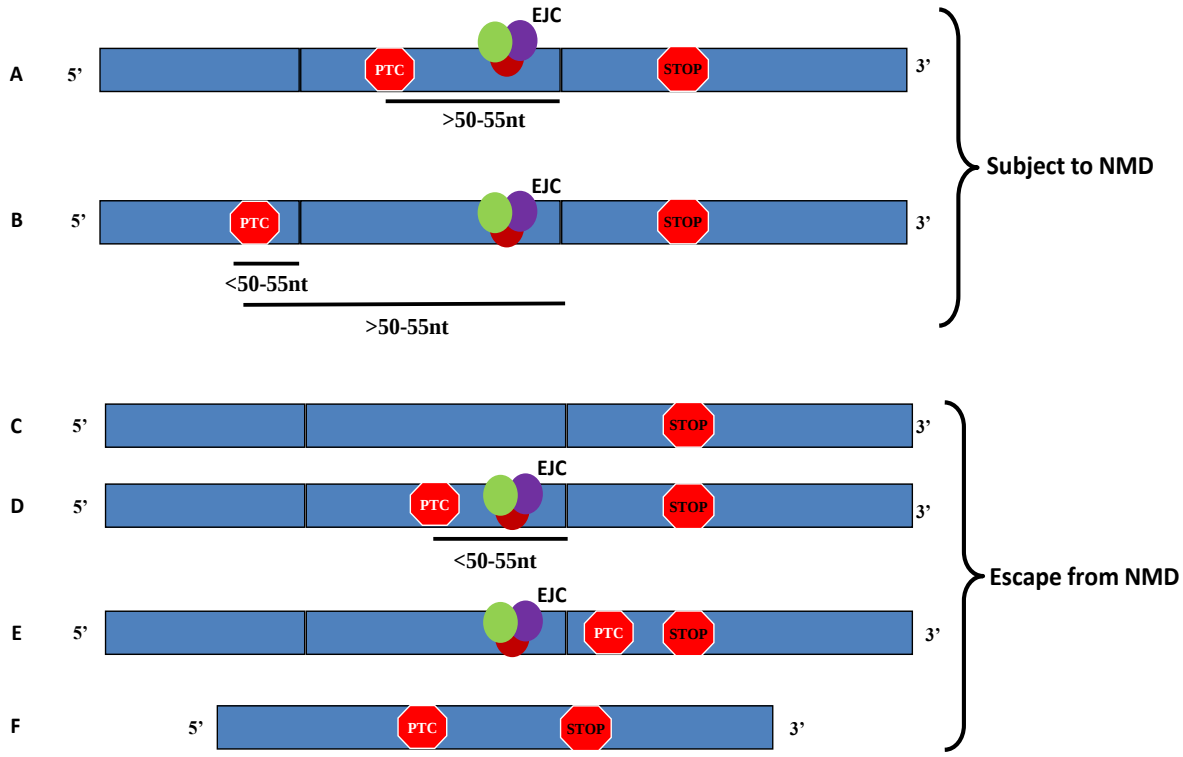

Figure 13: The targets of NMD

When PTC is located more than 50-55nt upstream of the last exon-exon junction, it will be subject to NMD (A and B). However under some situation, mRNAs can be immune to NMD. For example, if there is no PTC on mRNA (C), the distance between PTC on mRNA and the last exon-exon junction is less than 50-55nt (D), the PTC on mRNA is located in the last exon (E), or the mRNA has no intron(F). The blue rectangles represent exon, "Stop" represents normal stop codon.

b) Natural substrates of NMD

In the last 15 years, NMD has been shown to contribute to the post-transcriptional regulation of numerous physiological mRNAs which are natural substrates of NMD meaning that they are not carrying any nonsense mutations. Some studies have shown that 4-20% of the genome from various organisms is down-regulated by NMD (He, Li et al. 2003; Rehwinkel, Letunic et al. 2005; Ramani, Nelson et al. 2009; Yepiskoposyan, Aeschimann et al. 2011). To show that, authors inactivated one or more essential NMD factors in order to block NMD. But recently Chapin *et al* used rapid reactivation approach. They first measured the expression of genes in a D. melanogaster NMD factor UPF2 mutant and identified the genes down-regulated by NMD. Then they used a UAS/GAL4 expression system to reactivate the expression of UPF2 and measure the expression of the genes regulated

by NMD. It is expected that genes regulated directly by NMD should be rapidly degraded and expressions of the indirect substrates should be decreased after the direct substrates. Authors found that 81% of genes regulated by NMD are not direct NMD substrates and only recognized 168 candidate direct NMD targets in the total of 5682 studied genes (Chapin, Hu et al. 2014). Mendell *et al* detected the decay rates and the increased steady-state abundance of transcripts in the mammalian cells depleted in UPF1 using siRNA and found that only 4.9% of all the transcripts in HeLa cells were upregulated and the same proportion was down-regulated (Mendell, Sharifi et al. 2004). It is difficult to distinguish the direct and indirect substrates of NMD by only inactivating essential NMD factors because some NMD factors can function in NMD-independent manner like UPF1 that has been shown to be involved in the Staufen-mediated mRNA decay (SMD) system. It is essential to use several different methods to verify *bona fide* whether a putative NMD substrate is really a natural substrates for NMD.

Viegas et al did first microarray analysis by different probes representing about 14500 human genes in the UPF1-depleted HeLa cells and found that expression level of 2.8% genes was increased, in contrast 2.6% genes expression is decreased. To rule out the genes that are regulated by UPF1 depletion in an NMD-independent manner, they chose 16 genes whose expressions were increased after the depletion of UPF1; they compared the level of mRNA and pre-mRNA of these 16 genes in order to determine the impact of the UPF1 down-regulation on the transcription of these genes. Among the 16 genes, only two (NAT9 and TBL2 genes) showed an increased at the RNA level and not at the pre-mRNA level, which mean most of genes up-regulated after UPF1 depletion are not direct NMD substrates; they also checked the half-life of genes and down-regulated UPF2 by siRNA to further confirm that NAT9, TBL2 and some other genes (SC35 and GADD45B) which were taken as endogenous NMD substrates are *bona fide* NMD targets (Viegas, Gehring et al. 2007).

The principal source of NMD substrates appears to be the products from alternative pre-mRNA splicing since more than 70% of pre-mRNAs are alternatively spliced and among them about 30% of alternatively spliced forms harbor PTCs which

can activate NMD (Lewis, Green et al. 2003; Chang, Imam et al. 2007). One of examples that have been described is on the expression of the splicing factor SC35 (SRSF2). SC35 gene autoregulates its expression according to the level of protein SC35 present in the cell. In the physiological conditions, SC35 pre-mRNA is subject to only one splicing event in its coding sequence. When the level of SC35 protein become “abnormally high”, SC35 as a splicing factor, activates some cryptic splicing events in the 3’UTR of its pre-mRNA. The consequence is the deposit of several EJCs downstream of the normal stop codon that become located at more than 50-55 nucleotides upstream of an exon-exon junction, situation that triggers NMD (Sureau, Gattoni et al. 2001). The amount of SC35 protein will be therefore reduced until to reach the physiological level.

Another example for gene autoregulation using NMD comes from the regulation of the expression of the polypyrimidine tract binding protein (PTB), another splicing factor. The increased abundance of PTB protein can inhibit the use of the 3’ splice site of the exon 11 of its pre-mRNA which leads to exon 11 skipping and results in a frameshift and produces a nonsense codon on exon 12. Lareau et al have used expressed sequence tag (EST) libraries and have found that all human SR genes are alternatively spliced by exon skipping, intron-retention or alternative splicing in 3’ untranslated regions (Lareau, Inada et al. 2007). Alternative splicing in 3’ untranslated regions can introduce an exon-exon junction more than 50 nucleotides downstream of the normal stop codons which elicit NMD. Exon skipping and intron-retention can produce PTCs in mRNAs and if PTCs are located more than 50-55 nt upstream of the last exon-exon junction, the PTC-containing mRNAs are expected to be degraded by NMD. To confirm this expectation, they down regulated UPF1 expression to inhibit NMD and found that expression of the alternative splice forms were increased up to a 4 to 40 folds. To confirm these results and to measure a degradation time course to further support the expectation that SR genes alternatively spliced are direct NMD targets, they measured at different time points the level of these mRNAs in the presence of cycloheximide. Finally they concluded that the alternative splice forms are degraded by NMD. (Lareau, Inada et al. 2007).

Mendell et al have shown other resources of NMD substrates (Mendell, Sharifi et al. 2004): (1) mRNAs with upstream open reading frame (uORF) in the 5' untranslated region (e.g. mitogen-activated protein kinase kinase kinase 14 (MAP3K14), dual specificity phosphatase 10 (DUSP10)), (2) mRNA with intron in the 3' untranslated region (e.g. growth arrest and DNA-damage-inducible, beta (GADD45B), mitochondrial ribosomal protein L49 (MRPL49), (3) mRNA with selenocysteine codons (e.g. thioredoxin reductase 2 (TXNRD2), selenoprotein W, 1 (SEPW1)). They also found one special group of transcripts which are relative to amino acid starvation, and they observed that 12 of 80 tested genes were upregulated by inhibiting NMD with UPF1 siRNA, and that these genes contained uORF or were alternatively spliced to result in PTC.

Why are mRNAs with uORF subject to NMD? In the light of the current models, when the ribosome is paused at the normal translation termination codon, ribosome can interact with the eukaryotic release factor 1 (eRF1), eRF3 which binds to the poly (A) binding protein cytoplasmic 1 (PABPC1), to finally stimulate a correct and efficient translation termination event (Schweingruber, Rufener et al. 2013). Eberle *et al* demonstrated that the physical distance between the termination codon and the PABPC1 can regulate NMD pathway (Eberle, Stalder et al. 2008). They have shown that if the distance of termination codon to PABPC1 is extended, PABPC1 is not allowed to interact with the eRF3 and induces the ribosome to stall at the normal termination codon and normal termination codon is recognized as PTC, which will trigger NMD. The termination codon of uORF is located at a greater distance from PABPC1 and the long distance makes PABPC1 fail to interact with the termination complex of uORF and the termination codon of uORF is taken as PTC to elicit NMD (Barbosa, Peixeiro et al. 2013).

Why are mRNAs with intron in the 3' untranslated region degraded by NMD? Bicknell *et al* have shown that between ~6% (NCBI'S Reference Sequence) and ~16% (Vertebrate Genome Association) of human 3' untranslated region harbor introns. After removing the intron in the 3' untranslated region, an EJC is left

downstream of the normal termination codon and the normal termination codon is taken as PTC which can activate NMD(Bicknell, Cenik et al. 2012).

Some mRNAs with selenocysteine codons are also the substrates of NMD. Because UGA codons also can be recoded to specify selenocysteine rather than termination codon, mRNAs translated into selenoproteins contain one or more UGA codons. The synthesis of amino acid selenocysteine is regulated by the cis- or trans-acting factors. By these regulators translation into selenoproteins should compete with translation termination at a UGA codon. Therefore it is the regulation of the incorporation of the selenocysteine into the protein that will influence either the synthesis of a selenoprotein or the degradation of its RNA by NMD (Maquat 1995; Sun, Li et al. 2001).

3.2.1.3. The activation of NMD

a) NMD and the exon-junction complex

In mammalian cells, two models have been described to explain the recognition of PTCs and the activation of NMD. Historically, the first model associates the recognition of PTCs to the presence of a splicing event downstream of the PTC. Indeed, according to the first model, a stop codon has to be located more than 50-55 nucleotides upstream of an exon-exon junction to be detected as a PTC. The 50-55 nucleotide distance requirement is related with the presence of a protein complex deposited 20-24 nucleotides upstream of all exon-exon junctions as a consequence of splicing. This protein complex is called EJC for exon junction complex.

During the pioneer round of translation, ribosomes read the open reading frame from the initiation codon until the first stop codon removing EJCs that they meet. When the mRNA does not carry a PTC, all EJCs will be removed after the first round of translation since the normal stop codon is located either in the last exon or at less than 50-55 nucleotides upstream of the last exon-exon junction. In the case of an mRNA harboring a PTC located 50-55 nucleotides upstream of an exon-exon junction,

at least one EJC will still be present on this mRNA after the pioneer round of translation because ribosomes will not meet EJCs located after the PTC (Lejeune, Ishigaki et al. 2002; Gehring, Lamprinaki et al. 2009). The pause of the ribosome on the PTC and the presence of EJC, UPF3/3X and UPF2 downstream of the PTC will activate NMD by recruiting additional NMD factors such as UPF1, SMG1, SMG8, SMG9, SMG5, SMG6 and SMG7 for instance.

RNase protection assay and gel filtration analysis contributed to demonstrate that EJC is a multi-protein complex with an apparent molecular weight of 335 kDa composed by about 10 proteins at least (Le Hir, Izaurralde et al. 2000). EJC is comprised by core EJC proteins and those that are transient part of EJC. The EJC core proteins might act as a platform on which transient EJC components bind (Tange, Shibuya et al. 2005; Stroupe, Tange et al. 2006).

The EJC core proteins include four proteins: Y14, MAGOH, eIF4AIII and MLN51 (also named as Barentz (BTZ) or CASC3). RNase H footprinting studies, coimmunoprecipitation, cross-linking and negative-stain random-conical tilt electron microscopy showed that these four proteins form a stable heterotetramer bound to the spliced mRNA in vitro (Le Hir, Izaurralde et al. 2000; Tange, Shibuya et al. 2005; Stroupe, Tange et al. 2006). Y14 a mRNA localization factor, mainly present in the nucleus but shuttles between nucleus and cytoplasm. It can be bound to spliced mRNA and it is detected on nuclear and newly exported cytoplasmic mRNAs (Kim, Yong et al. 2001); Y14 is associated with MAGOH to form a stable heterodimer Y14/MAGOH deposited near exon-exon junctions of a mRNA during splicing (Fribourg, Gatfield et al. 2003). Y14 has also been shown to interact directly with eIF4AIII (Ballut, Marchadier et al. 2005). MAGOH shuttles from the nucleus to the cytoplasm and binds to Y14 and TAP (Kataoka, Diem et al. 2001). eIF4AIII is localized mainly in the nucleus but also shuttles to the cytoplasm and it belongs to the DEAD-box RNA helicase family serving as an anchor to bind the EJC to the RNA substrate. In vitro eIF4AIII binds some ATP molecules to stabilize the EJC core complex. X-ray crystallographic study showed that eIF4AIII is associated directly with the Y14/MAGOH heterodimer (Tange, Shibuya et al. 2005). MLN51 is the mammalian

ortholog of D. melanogaster Barentz (BTZ) and cross-linking analysis showed that MLN51 can bind spliced mRNA and interact with MAGOH and eIF4AIII (Stroupe, Tange et al. 2006).

EJC is a dynamic structure with a flexible composition according to the environment and the mRNA maturation step (Dreyfuss, Kim et al. 2002). Indeed, some proteins are transient EJC components including RNPS1, PYM, UAP56, REF/ALY, TAP, SRm160, PININ, ACINUS and SAP18. Among the transient EJC components, (1) Some EJC factors function in pre-mRNA splicing, RNPS1 is mostly nuclear but shuttles and functions in splicing and mRNA export in addition to be involved in NMD (Lykke-Andersen, Shu et al. 2001; Lejeune, Ishigaki et al. 2002). SRm160 is a member of the SR protein family, can co-activate splicing and also promotes cleavage of transcript at the 3' end (Le Hir, Izaurralde et al. 2000; McCracken, Lambermon et al. 2002). (2) Some EJC factors are involved in mRNA export, UAP56 is a nuclear factor that joins the EJC during the RNA splicing and mRNA export steps. Another characteristic of UAP56 is the presence of a DEAD-box RNA helicase domain. UAP56 is thought to recruit REF/ALY (Luo, Zhou et al. 2001). TAP is a nuclear protein, component of the nuclear pore complex with a function in the mRNA export (Stutz and Izaurralde 2003). REF/ALY also can shuttle from nucleus to cytoplasm and takes part in the mRNA export. REF/Aly mainly interacts with UAP56, Y14 and TAP (Stutz, Bachi et al. 2000). PININ is nuclear and functions in mRNA export. Its main partner is RNPS1 (Li, Lin et al. 2003). (3) For the rest transient EJC factors, their functions are not very clear, PYM is a cytoplasmic protein and associates with Y14/MAGOH heterodimer to form a trimeric complex. PYM has also been shown to be necessary for NMD (Bono, Ebert et al. 2004). ACINUS is a nuclear protein that can form a heterodimer with RNPS1 (Li, Lin et al. 2003). ACINUS has been shown to be involved in apoptosis pathway. SAP18 also is an EJC factor and can bind RNPS1 (Schwerk, Prasad et al. 2003). EJC also can contain additional transient proteins including UPF3 or UPF3X, UPF2 which can recruit UPF1 to elicit NMD. Not all the EJC components function in NMD and some join in the pre-mRNA splicing and/or mRNA export from nucleus to cytoplasm. And all the EJC core proteins, RNPS1 and PYM function in NMD

and serve as a platform where NMD UPF factors load.

In addition to the EJC-dependent NMD, some mammalian genes containing PTCs can activate NMD without the presence of a down-stream EJC. For example, Zhang *et al* have shown that nonsense codons on exon 2 of mRNA β-globin can elicit NMD when intron 2 is deleted from globin genes, which means this NMD is EJC-independent since β-globin gene has only 2 introns (Zhang, Sun et al. 1998). It has been shown that Ig-μ genes containing PTCs in the penultimate exon at 10 to 15 nucleotides upstream of the last exon exon junction were still degraded by UPF1-dependent NMD. They showed that as in yeast the distance between the termination codon and PABPC1 is very important to trigger NMD especially in this PTC-containing Ig-μ mRNA (Buhler, Steiner et al. 2006). Additional examples of EJC-independent NMD have been provided on human triosephosphate isomerase (TPI) mRNA and T-cell receptor-β (TCR-β) (Cheng, Belgrader et al. 1994; Wang, Gudikote et al. 2002). The mechanism of EJC-independent is not clearly understood. Studies on comparison of EJC-dependent and EJC-independent NMD in human cells found that (1) EJC- independent NMD is less efficient than NMD involving EJC, (2) EJC-independent NMD also is restricted to CBC-bound mRNA not eIF4E-bound mRNA, (3) UPF1 and SMG1 are the crucial factors for EJC-dependent and EJC–independent NMD, (4) it is dependent on different transcript whether UPF2, UPF3X, SMG5/7, SMG6 affect EJC-independent NMD (Matsuda, Hosoda et al. 2007; Metze, Herzog et al. 2013).

b) NMD and PABP protein

In mammals, the PTC position relative to the last exon-exon junction must be more than 50-55 nt toward the 5’ end to activate NMD. Some PTCs that follow this position rule and are located close to translation initiation codon can evade NMD (Silva, Ribeiro et al. 2008). This suggests that other determinant of NMD should exist. For example, in yeast PTCs are recognized by the long 3’ untranslated region not by EJCs and the distance between PABPC and the stop codon is key to elicit NMD (Das

and Das 2013). In D. melanogaster, Behm-Ansmant et al have shown that the position of PTC relative to the PABPC1 is also an important determinant to activate NMD (Behm-Ansmant, Gatfield et al. 2007). In 2008, Silva et al demonstrated that NMD can be activated according to the distance between the PTC and PABPC1 protein in HeLa cells. They found that tethering PABPC1 at 15 codons downstream from the PTC can suppress NMD. In contrast, tethering PABPC1 at 44 codons downstream from the PTC cannot inhibit NMD. Increase the distance between PTC and PABPC1 by inserting a pseudoknot can remove NMD suppression, which means that the distance between PABPC1 and PTCs is crucial to trigger NMD and that PABPC1 in the proximity to the PTC can inhibit NMD (Silva, Ribeiro et al. 2008).

The distance between PTC and the PABPC1 can also explain another type of exception to the 50-55nt rule. PTCs close to the translation initiation codon AUG often escape from NMD. It was thought at the beginning that translation reinitiate on the next following AUG making the PTC undetectable (Amrani, Ganesan et al. 2004). Another explaination would be that during translation initiation PABPC1 can interact with eIF4G and this interaction can bring PABPC1 close to AUG initiation codon and ribosome via the link between eIF4G and the 40S recruitment factor eIF3 (Martineau, Derry et al. 2008). When mRNAs contain an AUG-proximal PTC, PABPC1 is close to PTC and this proximity makes PABPC1 easily bind to eRF3 which can prevent UPF1 from interacting with eRF3 (Peixeiro, Inacio et al. 2011). It has been demonstrated that PABPC1 can compete with UPF1 for the interaction with translation termination factors. UPF1 interacts with translation termination factors to elicit NMD when PABPC1 binds to translation termination factors to promote a normal translation termination event (Ivanov, Gehring et al. 2008; Silva, Ribeiro et al. 2008; Singh, Rebbapragada et al. 2008; Silva and Romao 2009; Peixeiro, Inacio et al. 2011).

c) NMD and translation

It is well known that NMD is a translation-dependent process. For instance,

NMD can be inhibited by translation inhibitors such as cycloheximide, anisomysin, puromycin or emetine (Belgrader, Cheng et al. 1993; Qian, Theodor et al. 1993; Carter, Doskow et al. 1995). It is beneficial for the cells to remove mRNAs containing PTCs as early as possible because they will be translated into deleterious or no-functional truncated proteins to cells. It means that mRNAs containing PTCs must be recognized and degraded during the first few rounds of translation which are also called the pioneer rounds of translation. Many studies have provided the evidences that NMD occurs in the pioneer rounds of translation (Ishigaki, Li et al. 2001; Lejeune, Ishigaki et al. 2002; Kashima, Yamashita et al. 2006). These studies show a central role for the cap-binding complex (CBC). CBC is comprised by two proteins—CBP80 and CBP20. CBC directs the pioneer rounds of translation and CBC can be replaced by the eukaryotic translation initiation factor 4E (eIF4E) which directs the steady-state rounds of translation where mRNAs are translated into bulk of proteins. Ishigaki et al have shown that CBC-bound mRNA is the precursor of the eIF4E-bound mRNA (Ishigaki, Li et al. 2001).

The pioneer round of translation can be distinguished from the steady state rounds of translation not only by its role but also by the nature of the proteins bound to the 5’ Cap and the presence of EJC during the pioneer rounds of translation (Lejeune, Ishigaki et al. 2002); Another difference is that CBC-bound RNAs are associated with the poly (A)-binding protein N1 (PABPN1) and the poly (A)-binding protein C1 (PABPC1), in contrast eIF4E-bound mRNAs are bound by only PABPC1. Importantly, PTC-containing mRNAs bound by CBC are subject to NMD, but the PTC-containing mRNAs bound by eIF4E are not (Ishigaki, Li et al. 2001; Lejeune, Ishigaki et al. 2002); Chiu et al analyzed the distribution of CBP80 versus eIF4E-bound mRNA in a polysome profile. They concluded that eIF4E-bound mRNAs were concentrated in the late fractions of the polysome indicating that these RNAs carryed a high number of ribosomes when CBP80-bound mRNAs were present in the early fractions of the polysome reflecting the low number of ribosomes present on these mRNAs (Chiu, Lejeune et al. 2004). CBC-bound mRNA also shares some components with the eIF4E-bound mRNAs and the components are restructured from CBC-bound

mRNAs to eIF4E-bound mRNAs. Chiu et al did immunoprecipitation of CBP80 or eIF4E and found that some proteins such as eIF4GI, eIF3, eIF4AI, eIF2α and PABPC1 coimmunopurified with both CBP80 and eIF4E which indicates that (Chiu, Lejeune et al. 2004). eIF4G plays a central role in the structure of the translated mRNP by linking the 5' and the 3' end of the mRNA since it has been shown to interact with eIF4E and PABPC1. eIF4G has also been shown to function in the pioneer round and play a role in NMD because cleaving eIF4G by HIV-2 or poliovirus 2A protease impairs NMD. In addition, eIF4G can be coimmunoprecipitated with CBP80, CBP20, PABPC1, PABPN1 or NMD factors (UPF2 and UPF3X) suggesting that eIF4G supports the interaction between the 5' and the 3' end of the mRNA leading to a circularization of the mRNP during the pioneer round of translation (Lejeune, Ranganathan et al. 2004).

There are several lines of evidences that support the theory that NMD occurs on CBC-bound mRNAs. First, PTCs decrease the level of CBC-bound mRNAs, in contrast do not affect the level of eIF4E-bound mRNAs, indicating that NMD only acts on CBC-bound mRNAs (Ishigaki, Li et al. 2001). Second, EJCs and several NMD factors including SMG1 and eIF4AIII are only detected on CBC-bound mRNAs but not eIF4E-bound mRNAs (Ishigaki, Li et al. 2001; Lejeune, Ishigaki et al. 2002; Kashima, Yamashita et al. 2006). Third, the level of CBC-bound mRNAs containing PTCs is increased when translation is blocked (Ishigaki, Li et al. 2001; Lejeune, Ishigaki et al. 2002). Finally 4E-BP1 which is a translation inhibitor and can compete with eIF4G for the binding of eIF4E, inhibits the translation of eIF4E-bound mRNAs but not the translation of CBC-bound mRNAs and does not inhibit NMD (Chiu, Lejeune et al. 2004).

Recently Durand et al and Rufener et al have shown that eIF4E-bound mRNPs are also subject to NMD in mammalian cells. They used HeLa Tet-off cells to measure the degradation time of ß-globin mRNA containing a PTC or TCR-ß mRNA harboring a PTC under translation inhibition conditions or using UPF1 siRNA to knockdown UPF1 and to inhibit NMD. They found that eIF4E-bound mRNAs containing a PTC also prolong their degradation time when NMD is inhibited (Durand and Lykke-Andersen 2013; Rufener and Muhlemann 2013). Both groups concluded that eIF4E-bound

mRNAs are also subject to NMD. However, these results have to be confirmed by other studies since their demonstrations raised some questions. Indeed, in the study of the group of Muhlemann, they immunoprecipitated eIF4E and found UPF1 coimmunoprecipitated. However, their eIF4E immunoprecipitation also contained CBP80 indicating that their immunoprecipitation was not restricted to eIF4E-bound mRNPs suggesting that they were contaminated by CBC-bound mRNAs. In the paper of Durand et al, they used puromycine as NMD inhibitor. Puromycine induces the release of the ribosomes during the translation elongation. The consequences of using puromycine are to promote a continuum of translation initiation rounds that would favor the exchange of the cap binding protein from CBP80/20 to eIF4E. Another approach seems to be necessary to validate their results.

Since NMD likely degrades only the CBC-bound mRNAs containing PTCs, the function of CBC has been investigated further in NMD pathway. In 2005, Hosoda et al found that depletion of CBP80 in HeLa cells can increase the expression of PTC-containing genes and decrease the amount of UPF2 immunoprecipited by UPF1. Authors have also shown that using CBP80 antibody can immunopurified UPF1 suggesting an interaction between CBP80 and UPF1 (Hosoda, Kim et al. 2005). From these results, authors concluded that CBP80 plays an important part in NMD pathway and it can bind to UPF1 and promote the interaction between UPF1 and UPF2 to trigger NMD. For the role of CBP80 in NMD pathway, Hwang et al did further investigations by immunoprecipitation and they demonstrated that first CBP80 interacts temporarily or weakly with UPF1 at 5’ end of mRNA to assist the complex UPF1/SMG1 to interact with the translation termination factors eRF1-eRF3 heterodimer to form the SURF complex. Then CBP80 promoted UPF1 present in the SURF complex to bind to UPF2 poised on EJC (Hwang, Sato et al. 2010).

3.2.1.4 The model of NMD activation

Different models for NMD activation have been proposed according to the

studied species. In S.cerevisiae, as the mammalian cells, NMD is dependent translation but in contrast to the mammalian cells, NMD targets not only the CBC-bound newly synthesized mRNAs (CBC is comprised of Cbc1p and Cbc2p, orthologous to mammalian CBP80 and CBP20) but also the eIF4E-bound mRNAs (Das and Das ; Gao, Das et al. 2005). There are two main models which explain how PTCs are distinguished from nomal terminition codons in S.cerevisiae. The first model indicates that some mRNAs contain downstream sequence elements (DSEs) which function as an analogue of the mammalian EJCs to recruit NMD factors. But this model now is not prefered because DSE is only found in PGK1 mRNA (Zhang, Ruiz-Echevarria et al. 1995). The other model is the 'faux 3'-UTR model' which proposes that the distance between PTCs or normal termination codons and the poly (A) tail is the determinant to active NMD. The long distance from PTCs to the poly (A) binding protein (PABPC1) on the poly (A) tail can inhibit terminating ribosome to associate with PABPC1 and promotes terminating ribosome to bind to NMD factors to elicit NMD (Muhlrad and Parker 1999; Amrani, Sachs et al. 2006). In the faux 3'-UTR model **(Figure 14)**, first, when a ribosome stops at a termination codon and analyzes the context of termination codon. If the context is in line with the faux 3'-UTR model, termination factors eRF1-eRF3 complex is recruited to the A site of the ribosome. UPF1 is then recruited to associate with the mRNA and the eRF1-eRF3 complex and subseqently inhibits the translation. Second, eRF1 is dissociated from the ribosome after hydrolysis of the peptidyl-tRNA bound to ribosome, and the departure of eRF1 provides the place where UPF2 and UPF3 binds to eRF3 and UPF1. Third, the association of UPF2 and UPF3 releases eRF3 and forms UPF1-UPF2-UPF3-ribosome complex. Finally mRNAs are degraded in 5'-3' direction and/or in 3'-5' direction (Wang, Czaplinski et al. 2001; Das and Das 2013).

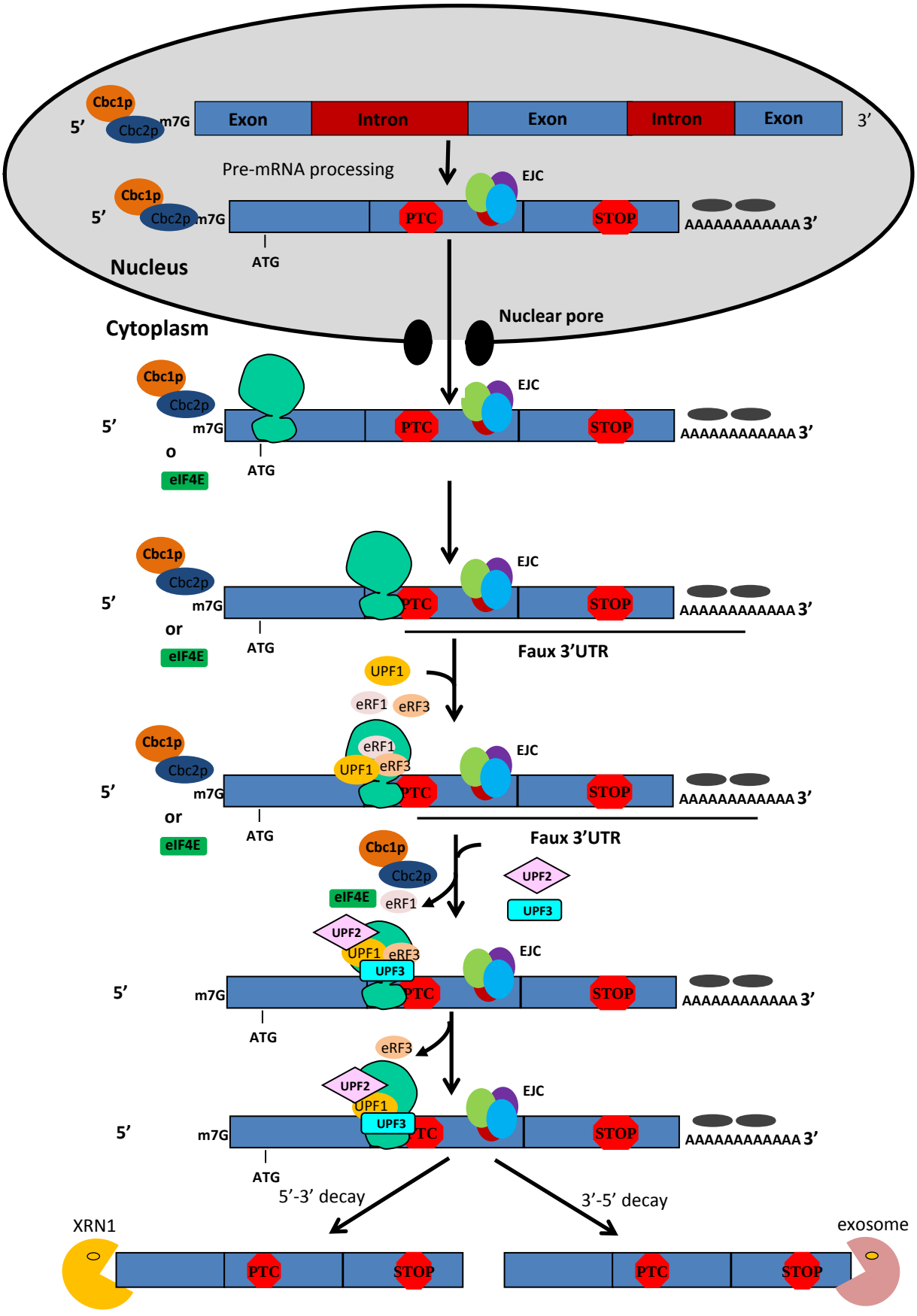
Cbc1p
Cbc2p
5'
m7G
Exon
Intron
Exon
Intron
Exon
3'
Pre-mRNA processing
EJC
PTC
STOP
AAAAAAAAAAAA 3'
ATG
Nucleus
Cytoplasm
Nuclear pore
o
eIF4E
or
Faux 3'UTR
UPF1
eRF1
eRF3
UPF2
UPF3
5'-3' decay
3'-5' decay
XRN1
exosome

Figure 14: Model of Faux 3'UTR in S. cerevisiae.

After pre-mRNAs undergo the processing of splicing, capping and poly (A) tail to become mature mRNAs, mRNAs are transported from nucleus to cytoplasm and go into translation processing. When mRNAs contain PTCs and have a faux 3' UTR, mRNAs are degraded by NMD. Whatever Cbc1p/Cbc2p-bound mRNAs (indicating pioneer round of translation) or eIF4E-bound mRNAs (indicating steady state round of translation) both containing PTCs are subject to NMD. In the model of faux 3' UTR, first ribosome is stalled at the position of PTC and recruits eRF1-eRF3 complex and UPF1 and sequentially represses translation; second because translation is repressed, cap-binding protein and eRF1 is removed from the ribosome and the dissociation of eRF1 provide the place where UPF2 and UPF3 associate the eRF3-UPF1 complex; third UPF2 and UPF3 bind to UPF1 and release eRF3; finally PTC-containing mRNAs are degraded in 5'-3' direction by Xrn1 or in 3'-5' direction by exosome. STOP represents normal stop codon, grey ovals represent poly (A) binding protein.

Here I will mainly describe the model in mammals. In mammalian cells, NMD pathway is mainly dependent on EJCs which are deposited 20-24 nt upstream of every exon-exon junctions after pre-mRNA splicing, although as described before, there are some PTC-containing genes which are degraded by EJC-independent NMD pathway (Zhang, Sun et al. 1998; Wang, Gudikote et al. 2002; Buhler, Steiner et al. 2006). In mRNAs with the normal termination codon, as ribosomes proceed translation on mRNAs these EJCs are removed by ribosomes. However, when mRNA carries a PTC, ribosomes are stalling at the PTC position and at least one EJC remains on the mRNA. mRNAs containing PTCs which can be degraded by NMD must respect the position rule that PTCs are localized more than 50-55 nt upstream of the last exon-exon junction in spite of several exceptions (Cheng, Belgrader et al. 1994; Wang, Vock et al. 2002; Neu-Yilik, Amthor et al. 2011). Besides the 50-55 nts position rule, it has been shown that the distance between PTCs and PABPC1 also affects NMD. When this distance is recognized as "short", the mRNA is not subject to NMD unlike when the distance is considerated as "abnormally long" (Ivanov, Gehring et al. 2008; Silva, Ribeiro et al. 2008; Singh, Rebbapragada et al. 2008; Silva and Romao 2009; Peixeiro, Inacio et al. 2011). In mammalian cells NMD occurs during the pioneer round of translation and degrades only CBC-bound mRNAs not eIF4E-bound mRNAs. CBC is comprised by CBP20 which can directly bind the cap structure and CBP80. During NMD processing, NMD factors play the key roles in activation of NMD and CBP80 also function in NMD pathway. In nucleus pre-mRNAs pass the processing

of 5'capping, splicing, 3' poly (A) tail before they become mature mRNAs. And in the nucleus, UPF3/3X is recruited to the EJC . When mature mRNAs are exported from the nucleus to the cytoplasm for translation by ribosomes, UPF3/3X recruit UPF2. When ribosomes reach a PTC **(Figure 15)**, (1) first CBP80 binds temporarily or weakly but directly to UPF1 which is already associated with SMG1 inside of the complex SMG1-SMG8-SMG9. CBP80 promotes the interaction between SMG1-SMG8-SMG9-UPF1 complex and eRF3. Since eRF3 forms an heterodimer with eRF1 which is responsible for the interaction with the ribosome, SURF complex is then assembled at the PTC position; (2) CBP80 facilitates the interaction between UPF1 and UPF2 present in EJC to form DECID complex (Hosoda, Kim et al. 2005; Hwang, Sato et al. 2010); (3) subsequently DECID complex induces UPF1 phosphorylation by SMG1 whose activity is suppressed by SMG8 during the formation of the SURF complex; (4) phosphorylated UPF1 can recruit SMG5/SMG7 complex and SMG6 seperately by its phosphorylation site serine 1096 and threonine 28 (Okada-Katsuhata, Yamashita et al. 2012). Phosphorylated UPF1 can also bind to eukaryotic initiation factor eIF3, a component of the translation preinitiation complex at the AUG translation initiation codon to inhibit further translation initiation (Isken, Kim et al. 2008); (5) the interaction between UPF1 and SMG5/SMG7 complex induces the release of the ribosome and the release factors as demonstrated by the depletion of SMG5 that results in the aggregation of phosphorylated UPF1 complex with the ribosome, the release factors and the EJC (Okada-Katsuhata, Yamashita et al. 2012); (6) finally PTC-containing mRNAs are degraded by SMG5/7 complex-mediated exonucleolytic decay via deadenylation and/or decapping followed by exonucleolytic decay from both ends or by SMG6-mediated endonucleolytic decay followed by the exonucleolytic from internal sites which is near the PTC position. There are several lines of evidence demonstrating PTC-containing mRNAs decay routes. In 2003, the group of Lynne Maquat found that the downregulation of the decapping protein DCP2 or one of the exosome component called PM/Scl100 or one of deadenylation factor called poly(A) ribonuclease (PARN) by siRNAs lead to the increase of the amount of nonsense-containing mRNAs and they showed that NMD factors (UPF1,

UPF2 and UPF3X) coimmunopurified with 5’-3’ exonuclease Xrn1 and PM/Scl100 and PARN, which demonstrated that NMD pathway involved decapping, deadenylation, exosome and exonucleolytic activities (Lejeune, Li et al. 2003). Unterholzner et al have shown that under confocal microscopy SMG5/7 complex colocalized with decapping activator LSm4 and the abundance of SMG7-tethered transcript which can elicit NMD is increased by downregulating XRN1 or DCP2 (Unterholzner and Izaurralde 2004). Loh et al have demonstrated that SMG5/7 interacts with deadenylase complex CCR4-NOT to induce deadenylation (Loh, Jonas et al. 2013). Some studies used RNAi or catalytic residues mutation to deplete the endogenous activity of SMG6 and found that PTC-containg mRNAs expression level are increased and endonucleolytic cleavage site is near PTC (Huntzinger, Kashima et al. 2008; Eberle, Lykke-Andersen et al. 2009). The circle of phosphorylation and deposphorylation of UPF1 is very important to elicit NMD, but it is still not very clear how UPF1 is dissociated from mRNAs.Recently Okada-Katsuhata et al have shown that the dissociation of UPF1 from mRNA needs the simultaneous binding of SMG5/7 complex and SMG6 to phosphorylated UPF1 (Okada-Katsuhata, Yamashita et al. 2012). To demonstrate that authors down-regulated SMG6 that leaded to the accumulation of phosphorylated UPF1 complexed with SMG5/SMG7 complex and the EJC but without the ribosome and the release factors.

NMD pathway involves some nuclear and cytoplasmic events. Indeed, the EJC is deposited on the mRNA after pre-mRNAs splicing in the nucleus. NMD targets CBP80/CBP20-bound mRNAs which are the nuclear cap-binding protein complex (Le Hir, Izaurralde et al. 2000; Le Hir, Moore et al. 2000). The recognition of the PTC involves the translation machinery indicating that this step occurs in the cytoplasm (Lykke-Andersen, Shu et al. 2000; Serin, Gersappe et al. 2001). According to cell fractionation assaies, NMD can takes place either in the nuclear fraction, we then talk about nucleus-associated NMD, or in the cytoplasmic fraction which is called cytoplasmic NMD. Since NMD has been demonstrated to be cytoplasmic, nucleus-associated NMD which is thought to occur during or after mRNA transport across the nuclear pore complex when cytoplasmic NMD which takes place in

cytoplasm (Maquat 2002; Dahlberg, Lund et al. 2003). The studies showed that the majority of mammalin mRNAs are subject to nucleus-associated NMD, whereas a small number of mRNAs are subject to cytoplasmic NMD (Cheng and Maquat 1993; Cheng, Belgrader et al. 1994; Thermann, Neu-Yilik et al. 1998; Zhang, Sun et al. 1998). ß-globin containing PTC at position 39 is proved to be only subject to nucleus-assocaited NMD because the amount of this PTC-containing mRNA was much less than wild-type mRNA in the nuclear fraction (Maquat, Kinniburgh et al. 1981). The mRNA expression level of glutathione peroxiase 1 (GPx1) is selenium-dependent because this mRNA habors a UGA codon that can be translated into selenocysteine or be recognized as a stop codon activating NMD. Inefficient selenium causes this mRNA to be degraded by NMD. Analyses of nuclear and cytoplasmic fractions showed that selenium deprivation did not affect the level of nuclear GPx1 mRNA but decreased the amount of cytoplasmic GPx1 mRNA, which means GPx1 mRNA is subject cytoplasmic NMD (Moriarty, Reddy et al. 1998; Sun, Moriarty et al. 2000). It is still not clear what dictates mRNAs to undergo nucleus-associated NMD or cytoplasmic NMD. For instance, TPI mRNA is subject to nucleus-associated NMD but only keeping the last intron would promote TPI to be subject to cytoplasmic NMD (Sun, Moriarty et al. 2000).

And where are mRNAs containing PTCs degraded after NMD is activated? Sheth et al and Durand et al answered this question separately in yeast and in mammalian cells (Sheth and Parker 2006; Durand, Cougot et al. 2007). Sheth et al have found that in yeast NMD factors (UPF1, UPF2,UPF3) and mRNAs containing nonsense mutation colocalized with P-bodies marker Dcp2 or Dcp1. Durand et al demonstrated in HeLa cells that when NMD is inhibited by the molecule NMDI 1 NMD factors (UPF1, UPF3/3X) and NMD substrates mRNAs containing nonsense mutation accumulated in P-bodies. P-bodies have the decapping enzyme and 5’-3’ exonuclease and in P-bodies mRNAs with PTCs can be degraded (Eulalio, Behm-Ansmant et al. 2007). Since these two studies showed that NMD factors and substrates were recruited to P-bodies, these tranports to P-bodies may be via cytoskeleton because cytoskeleton regulate the intracellular movement (Rogers and

Gelfand 2000) and it is also demonstrated that the P-bodies are interacted with cytoskeleton (Kulkarni, Ozgur et al. 2010). So my third project is to find the link between NMD and cytoskeleton.

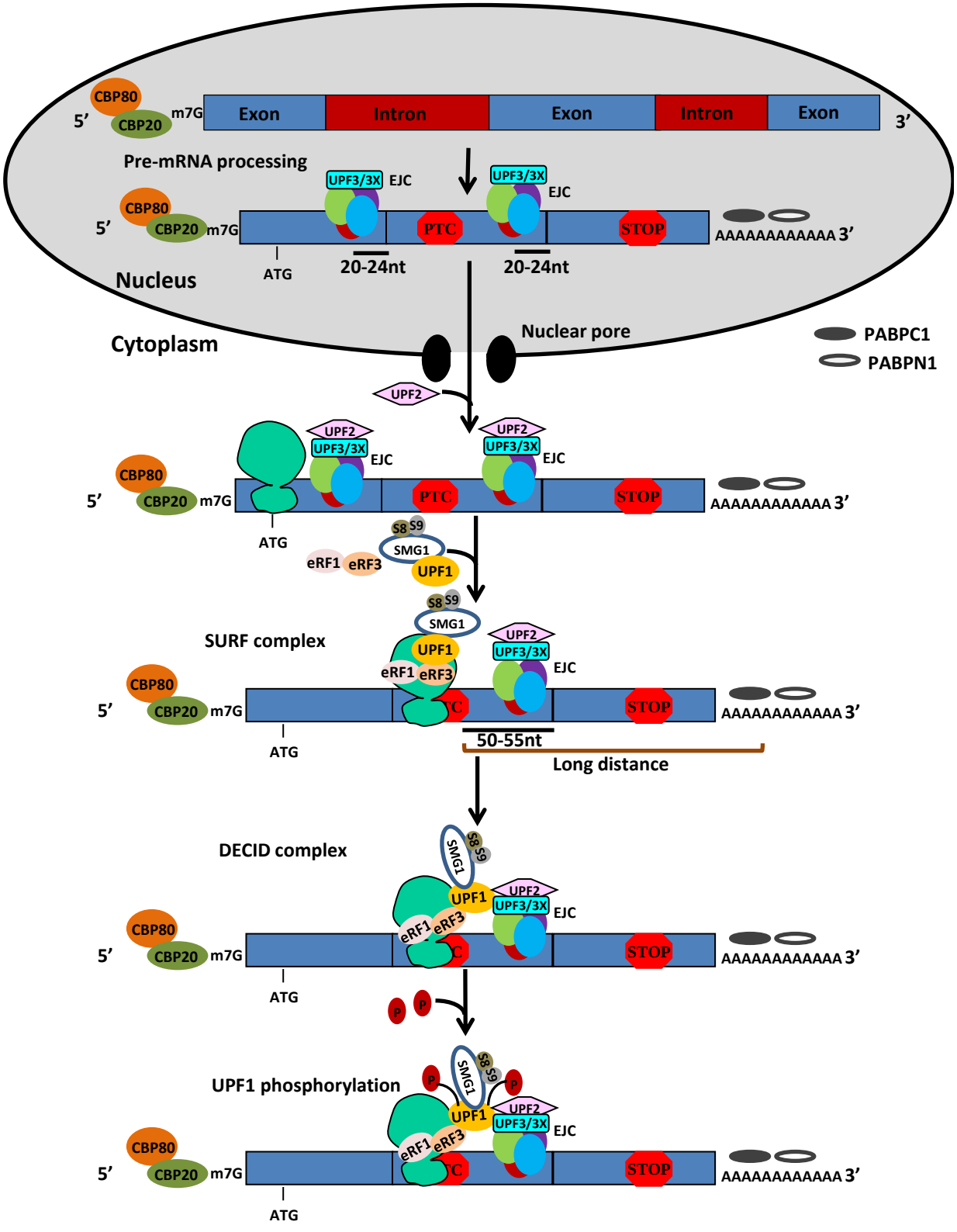

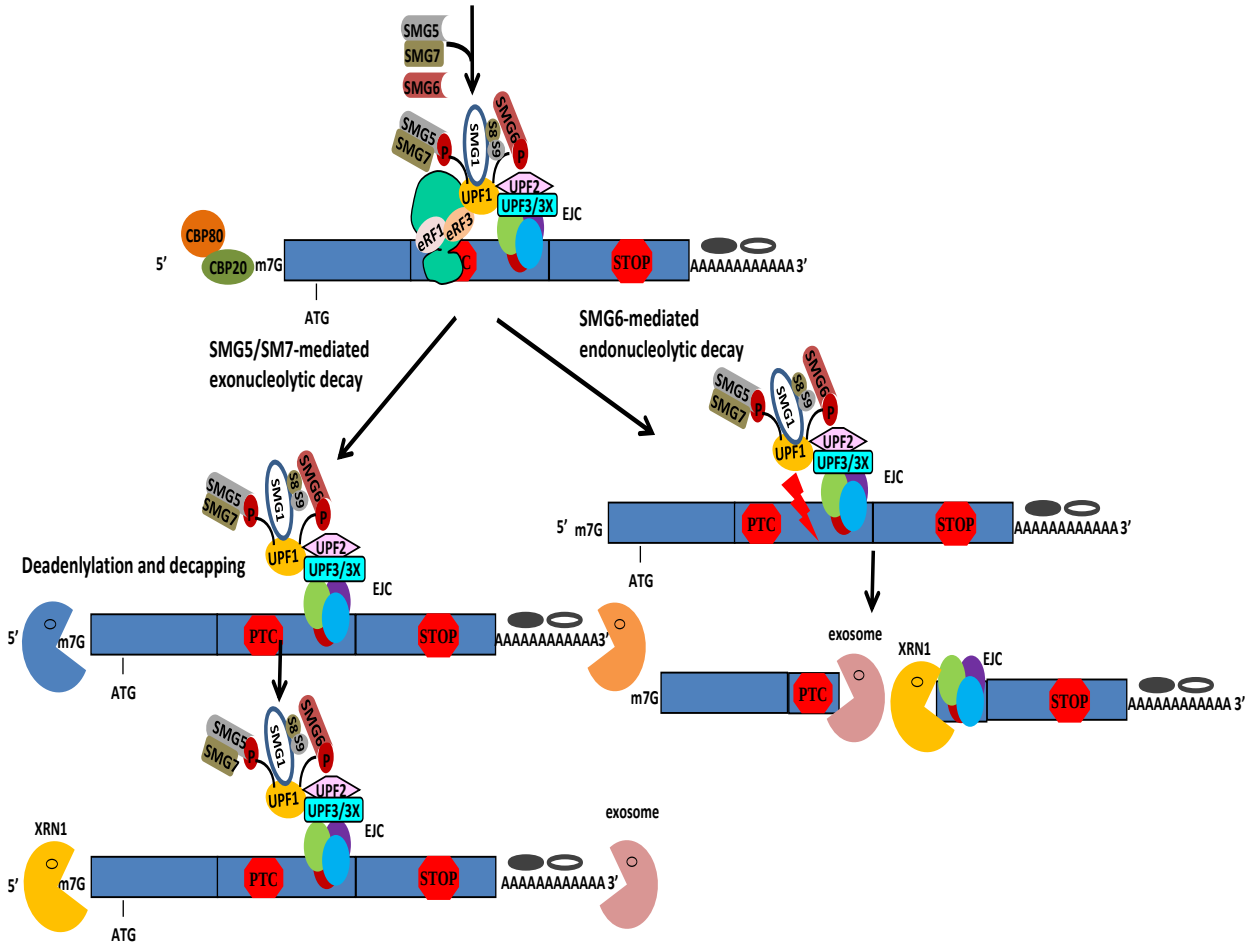

Figure 15: Model of NMD in mammals.

In nucleus pre-mRNAs go through the processing of 5'capping, splicing, and 3' poly (A) tail before to be mature mRNAs. After splicing a complex called EJCs are left 20-24nt upstream of exon-exon junction and EJCs can recruit UPF3/3X as the temporary composition in nucleus. When mRNAs are transported from nucleus to cytoplasm, UPF3/3X recruits UPF2 in the cytoplasm. During translation processing EJCs are removed but when mRNAs contain a PTC, ribosome pauses at the position of PTC and leaves at least one EJC downstream of PTC, and if PTC is poised 50-55nt upstream of exon-exon junction and there is a long distance between PTC and PABPC1, this PTC-containing mRNA is subject to NMD. In mammals only CBC (which consists of CBP80 and CBP20)-bound mRNAs harboring PTCs are subject to NMD. In the model of NMD in mammals, first ribosome stops at PTC and recruits eRF1-eRF3 complex and SMG8-SMG9- SMG1-UPF1 complex to form SURF complex; second UPF1 in the SURF complex binds to UPF2 in EJC to form DECID complex which promotes SMG1 to phosphorylate UPF1(SMG8 binds to SMG1 via SMG9 and inhibits SMG1 kinase activity before the DECID complex is formed), and CBP80 can directly associate with UPF1 to promote the formation of SURF complex and DECID complex; third phosphorylated UPF1 recruits SMG5/SMG7 complex and SMG6, the association of SMG5/SMG7 releases ribosome and release factors; finally PTC-containing mRNA is degraded in 5'-3' or 3'-5' direction via decapping and deadenylation mediated by SMG5/SMG7 complex or degraded near the position of PTC via SMG6 which contains endonucleolytic activity.

3.2.2. Non-stop mRNA decay (NSD)

Non-stop mRNA decay recognizes and degrades mRNAs with no stop codon. mRNAs without a stop codon can arise when transcription is broken, when polyadenylation takes place prematurely or when mutations disrupt the stop codon (Klauer and van Hoof 2012). In silico analysis found that premature polyadenylation arises in approximately 1% of yeast and human cDNA clones (Graber, Cantor et al. 1999; Frischmeyer, van Hoof et al. 2002). Because mRNAs are short of a stop codon, it leads to ribosomes to cross the poly (A) tail and remove the poly (A)-binding protein (PABP) and stall at the 3’ end of the mRNA. mRNAs without stop codon are degraded in the cytoplasm and NGD is translation-dependent because the degradation of the nonstop mRNAs is inhibited by cycloheximide (Chatr-Aryamontri, Angelini et al. 2004). Now there are two distinct pathways of NSD. The first one, which is conserved in yeast and mamalian cells, requires the cytoplasmic exosome, the Ski complex and the adaptor protein Ski7. The Ski complex consists of the DEVH-box RNA helicase Ski2, the tetratricopeptide repeat protein Ski3 and two copies of the WD repeat protein Ski8. Ski7 is a exosome-associated protein and because its structure is similar to the GTPase domain of elongation factor-1A which can bind to the A site of the ribosome when a sense codon is present at A site and eRF3 which can recognize the A sites of ribosome when A site is occupied by a nonsense codon, Ski7 can interact with the A site of the ribosome stalling at the 3’ end of mRNA by its C-teminal domain. It is not very clear what is the function of Ski complex and Ski7 in NSD but all these proteins are necessary for NSD (Klauer and van Hoof 2012). Now some studies have shown that the interaction between ribosome and Ski7 can release the ribosome and then recruit the exosome and the Ski complex to degrade the poly (A) tail and the mRNA in the 3’-5’ direction. The Ski complex and Ski7 can interact with the exosome and facilitate the degradation of normal or aberrant mRNAs in the cytoplasm (Frischmeyer, van Hoof et al. 2002; van Hoof, Frischmeyer et al. 2002; Inada and Aiba 2005). Kong et al found that dominant negative form of the deadenylase enzyme did not affect the expression of α-globin

without stop codon, which means the nonstop decay is deadenylation- independent (Kong and Liebhaber 2007). When Ski7 is absent, the second pathway will be activated and this pathway is found in S. cerevisiae. It seems that in S. cerevisiae the removing of PABP by the translating ribosome makes the mRNA subject to decapping and 5'-3' decay mediated by the 5'-3' exoribonuclease Xrn1 (Inada and Aiba 2005). The mechanism of nonstop decay is not very clear and should be further studied.

Nonstop decay is also relative to some disease. For example, about 100 out of millions people have nonstop mutation on the DEFB126 gene which encodes ß-defensin protein. ß-defensin protein is important for human sperm function and approximately 20% of males are homozygous for nonstop mutation on DEFB126 gene, which results in a lower fertility (Tollner, Venners et al. 2011).

3.2.3. No-go mRNA decay (NGD)

NGD is the least understood pathway and is studied only in S.cerevisiae. NGD can recognize ribosomes stalled on mRNAs and degrade such mRNAs by endonucleolytic cleavage. The full mechanism of NGD is not very clear. It has been demonstrated that when mRNAs containing stalled ribosomes, Dom34/Hbs1 complex can interact with the A site of the stalled ribosome and induce peptidyl-tRNA and the nascent peptide released from the ribosome. After this step, three events may occur. First the mRNA is cleaved near the stalled ribosome, but the nuclease is not yet identified; second ribosomes are released for recycling or degradation by an unknown mechanism; third, peptidyl-tRNA is hydrolyzed to release tRNA for recycling and the nascent peptide are subject to ubiquitin-proteasome mediated degradation. In any case the cleaved mRNA fragment is degraded by the exosome and Xrn1 (Doma and Parker 2006; Passos, Doma et al. 2009).

NGD may be involved in some biological processing. In yeast depletion of dom34 gene cause the slower growth rates, cell-cycle delay in the G1 phase (Passos, Doma et al. 2009). Saito et al have shown that the Dom34/Hbs1 complex can bind to the Ski complex and be also involved in nonstop decay (Saito, Hosoda et al. 2013). The

full mechanism and biological function of non-go decay should be further studied in order to understand better the involvement of NGD as a cytoplasmic quality control of the gene expression.

4. Introduction on the work in our lab

Nonsense mutations account for many diseases (inherited genetic disease, cancers, etc). Our lab mainly studies two strategies to correct nonsense mutations which are the inhibition of NMD and the activation of the PTC-readthrough. The NMD machinery comprises four core *trans*-acting factors, called up-frameshift proteins (UPF1, UPF2, UPF3 and UPF3X) (Chang, Imam et al. 2007). It has been shown that the presence of at least one of UPF proteins downstream of a nonsense codon is sufficient to elicit NMD even though this nonsense codon is the normal termination codon (Lykke-Andersen, Shu et al. 2000). Based on that, our lab decided to identify molecules capable of inhibiting NMD by screening compounds for their aptitude in interfering with the function of UPF factors. For that, we use a screening system that measures a luciferase activity in HeLa cells expressing a Firefly luciferase mRNA harboring 8 highly specific binding sites for the viral protein MS2 and a fusion protein made of the association of the viral protein MS2 and one of the UPF proteins. Indeed, when molecules do not interfere with the UPF protein function, the firefly luciferase mRNA is degraded by NMD and no luciferase activity is measured. In contrast, when a molecule blocks the function of one of the UPF proteins, the firefly luciferase is stabilized and a luciferase activity can be measured above background (Figure 16). In our lab, about 30 000 compounds belonging to about seven small compound libraries have been tested during the past 6 years and several molecules have been identified (Gonzalez-Hilarion, Beghyn et al. 2012)(Jia et al, in press). Using the results of these several rounds of screening, we decided to test molecules that have been identified by screening on rare disease models harboring a nonsense mutation and check the inhibition of NMD and the activation of PTC-readthrough. Our lab has several cell lines containing a nonsense mutation in P53, CFTR or dystrophin gene and a mouse model containing a nonsense mutation in dystrophin gene.

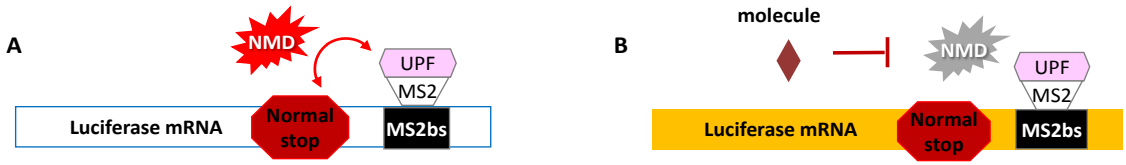

Figure 16: Our NMD inhibitor screening principle

A. One of UPF factors is bound downstream of the normal stop codon of the luciferase mRNA, which can active NMD and degrade luciferase mRNA. The consequence is the absence of luciferase activity so the absence of luminescence. B. if molecules can inhibit NMD, luciferase mRNA escapes from NMD, luciferase protein is expressed and can act on its substrate, a luminescence is then detected.

To illustrate the efficiency of our screening system, we selected amlexanox as a putative NMD inhibitor. After characterization of this molecule, we have shown that amlexanox not only inhibits NMD but also activates PTC readthrough in several cell lines containing a nonsense mutation (Gonzalez-Hilarion, Beghyn et al. 2012). We found amlexanox is more effective than already known readthrough molecules such as G418 or PTC124. But its efficacy remains very low. We decided to continue to look for molecules having a higher efficiency of correcting nonsense mutations.

RESULTS

1. Project 1: Rescue of nonsense mutations by amlexanox in human cells

1. 1. A summary for the project

About 10% of inherited genetic diseases result from nonsense mutations. In our lab we study two strategies to correct nonsense mutations which are the NMD inhibition and/or the activation of the PTC readthrough. Such molecules represent a new therapeutic approach for the treatment of genetic diseases caused by a nonsense mutation. In 2008, our lab screened a chemical library made of compounds already used as a medicine. One molecule was selected and it called amlexanox which is a drug for the treatment of asthma and mouth ulcers. We validated the screening results by demonstrating a stabilization of several PTC-containing mRNAs. We then looked for the presence of the truncated protein that should be synthesized from the stabilized PTC-containing mRNA. Surprisingly, we were able to find the truncated protein but also the full length protein indicating that amlexanox can activate readthrough. We then demonstrated that the full length proteins are functional demonstrating the potential of such molecules as a therapeutic approach.

This result has been published in Orphanet Journal of Rare Diseases

1.2 Results

Title: Rescue of nonsense mutations by amlexanox in human cells

Authors: Sara Gonzalez-Hilarion[1,2,3,13], Terence Beghyn[3,4,5,6], Jieshuang Jia[1,2,3], Nadège Debreuck[3], Gonzague Berte[3,4,5,6], Kamel Mamchaoui[7,8,9,10], Vincent Mouly[7,8,9,10], Dieter C. Gruenert[11,12], Benoit Déprez[3,4,5,6] and Fabrice Lejeune[1,2,3*].

Address

[1] Université Lille Nord de France, IFR142, Lille, France

[2] Inserm, Equipe AVENIR, Lille, France

[3] Institut Pasteur de Lille, Lille, France

[4] INSERM U761 Biostructures and Drug Discovery, Lille F-59000, France, www.deprezlab.fr

[5] Faculté de Pharmacie, Université Lille Nord de France, F-59000 Lille, France

[6] PRIM (www.drugdiscoverylille.org)

[7] Institut de Myologie, UM76, Paris, France

[8] Université Pierre et Marie Curie, Faculté de Médecine Pierre et Marie Curie, Paris, France

[9] Inserm, UMRS 974, Paris, France

[10] CNRS, UMR 7215, Paris, France

[11]Departments of Otolaryngology-Head and Neck Surgery and of Laboratory Medicine, Eli and Edythe Broad Center for Regenerative Medicine and Stem Cell Research, Helen Diller Family Comprehensive Cancer Center, Institute for Human Genetics, University of California, San Francisco, San Francisco, CA, USA

[12] Department of Pediatrics, University of Vermont College of Medicine, Burlington,

VT, USA

[13] Present address: Unité des Aspergillus, Institut Pasteur, 25 rue du Dr Roux, 75015 Paris

*Corresponding author: Fabrice Lejeune (fabrice.lejeune@inserm.fr) Institut Pasteur de Lille – 1 Rue du Professeur Calmette – 59019 Lille, France; Tel : 33-3-20-87-71-21

Abstract

Background: Nonsense mutations are at the origin of many cancers and inherited genetic diseases. The consequence of nonsense mutations is often the absence of mutant gene expression due to the activation of an mRNA surveillance mechanism called nonsense -mediated mRNA decay (NMD). Strategies to rescue the expression of nonsense-containing mRNAs have been developed such as NMD inhibition or nonsense mutation readthrough.

Methods: Using a dedicated screening system, we sought molecules capable to block NMD. Additionally, 3 cell lines derived from patient cells and harboring a nonsense mutation were used to study the effect of the selected molecule on the level of nonsense-containing mRNAs and the synthesis of proteins from these mutant mRNAs.

Results: We demonstrate here that amlexanox, a drug used for decades, not only induces an increase in nonsense-containing mRNAs amount in treated cells, but also leads to the synthesis of the full length protein in an efficient manner. We also

demonstrated that these full length proteins are functional.

Conclusions: As a result of this dual activity, amlexanox may be useful as a therapeutic approach for diseases caused by nonsense mutations.

Keywords: NMD/nonsense mutation/readthrough/RNA/small molecules

Background

One third of genetic inherited diseases involve a premature termination codon (PTC) (Frischmeyer and Dietz 1999). In most cases, the primary mechanism whereby a nonsense mutation has an effect is through the degradation of that mRNA by a surveillance mechanism called nonsense-mediated mRNA decay (NMD) and not through translation of the mutant mRNA into a truncated protein (for reviews see (Rehwinkel, Raes et al. 2006; Chang, Imam et al. 2007; Isken and Maquat 2007; Muhlemann, Eberle et al. 2008; Rebbapragada and Lykke-Andersen 2009)). Several therapeutic strategies have been developed to overcome the presence of nonsense mutations. One approach consists in promoting PTC-containing exon skipping during the RNA splicing process. For example, this approach has been successfully used to eliminate exon 51 mutations of dystrophin gene of patients with Duchenne muscular dystrophy (DMD) (Chaouch, Mouly et al. 2009; Goyenvalle, Babbs et al. 2009). The limitations of this approach are: 1) to ensure that the truncated protein is functionally viable, 2) to control the number of exons skipped such that the resultant mRNA is in-frame with an intact open reading frame (ORF), and 3) to reach a sufficiently high level of the skipped exon mRNA to have functional significance.

A second strategy involves the incorporation of a random amino-acid at the PTC position through PTC read-through mechanism. PTC read-through results in the synthesis of a full-length protein that is functional when the PTC is not at a crucial position (i.e. the original amino-acid can be replaced without loss of function). A few molecules have been shown to activate PTC read-through. These include aminoglycoside family members such as G418, or PTC124 (ataluren) (Keeling, Du et al. 2006; Welch, Barton et al. 2007). However, even in presence of these molecules, the efficiency of PTC read-through is low (Bidou, Hatin et al. 2004; Welch, Barton et al. 2007). One reason for this low read-through efficiency is that mutated mRNAs are often substrates for NMD, depleting substrates available for read-through. Therefore, inhibition of NMD may augment PTC read-through (Linde, Boelz et al. 2007). Because NMD occurs upstream of the bulk of translation, regardless of the functional status of the truncated protein, its inhibition may represent an attractive way to treat nonsense-mutation mediated genetic diseases, associated or not to read-through activation (Kuzmiak and Maquat 2006; Bhuvanagiri, Schlitter et al. 2010).

Although NMD has been found in eukaryotes from Yeast to Human, the mechanism underlying degradation of PTC-containing mRNAs appears to be species-specific. In mammalian cells, NMD involves 4 main factors: UPF1, UPF2, UPF3 (also called UPF3a) and UPF3X (also called UPF3b). The actual role of UPF proteins remains unclear and certain UPFs are not required for all NMD reactions (Gehring, Kunz et al. 2005; Kunz, Neu-Yilik et al. 2006; Chan, Bhalla et al. 2009). UPF proteins are recruited to the mRNP in a sequential manner: UPF3 or UPF3X arriving first, then UPF2 and

finally UPF1. It is the presence of UPF proteins downstream of a PTC that promotes the activation of NMD on a specific mRNA during the first/pioneer round of translation (Ishigaki, Li et al. 2001). As was first demonstrated by tethering any UPF protein to the 3'UTR of β-globin mRNA (Lykke-Andersen, Shu et al. 2000), the presence of UPF proteins downstream of a normal mRNA stop codon activates NMD.

In our attempt to identify NMD inhibitors that could potentially enhance PTC-read-through as new therapies for nonsense mutation-mediated diseases, we previously identified the first NMD-specific inhibitor, NMDI 1 (Durand, Cougot et al. 2007). However, this compound is a new chemical entity based on an indole structure that will require a long and risky optimization and development process before any clinical use. In order to accelerate access to the clinic, we have screened a library of 1200 marketed drugs. We present here evidences that amlexanox stabilizes nonsense mutation containing mRNAs and induces the synthesis of full-length proteins from these mRNAs. Amlexanox might therefore represent a potential new therapeutic molecule to abolish the consequences of a nonsense mutation.

Methods

Chemistry

NMR spectra were recorded on a Bruker Avance 300. Chemical shifts are in parts per million (ppm). Mass spectra were recorded with a LCMS (Waters ZQ Micromass). HPLC analyses were performed using a C18 XBridge 3.5 µm particle size column (50 x 4.6 mm). HPLC gradient started from 98 % H2O/0.1 % formic acid, reaching 98 %

CH3CN/0.1 % formic acid within 5 or 10 min at a flow rate of 2 mL/min. All commercial reagents and solvents were used without further purification. Purification yields were not optimized.

3-(N-Hydroxycarbamimidoyl)-benzoic acid methyl ester

3.398 mmol of 3-Cyano-benzoic acid (Sigma Aldrich Fluka, 15,716-3, CAS 1877-72-1) were suspended in dichloromethane (10 mL) containing 5 % of methanol. A 0.1 equivalent of 4dimethylaminopyridine and 1.1 equivalent of dicyclohexyl carbodiimide was added at 0 °C and stirred for 5 hours. Dicyclohexylurea was then filtered, and the solvent was removed by evaporation. After a second precipitation of dicyclohexylurea in diethylether, filtration and evaporation to dryness, 3-Cyano-benzoic acid methyl ester was obtained as a white powder. The crude residue was then dissolved in absolute ethanol (10 mL) containing a 1.4 equivalent of diisopropylethylamine. Hydroxylamine chlorhydrate (1.3 eq) was added to the mixture, which was refluxed for 4 hours and then ethanol was evaporated to dryness. The residue was dissolved in ethyl acetate and washed with water and brine. The organic layer was dried over magnesium sulfate and evaporated to dryness to yeld 510 mg of a white powder (yield = 77 %, Purity LC = 88 %)

LC: tR = 1.07 min (5 min), MS (ESI+): m/z = 195.1 $[M + H]^+$

The 3-(N-Hydroxycarbamimidoyl)-benzoic acid methyl ester (2.626 mmol) was suspended in toluene (10 mL) in presence of pyridine (1.1 eq), followed by the addition of 2-Fluorobenzoyl chloride (Sigma Aldrich Fluka, 120847-25 G, CAS

393-52-2) and 3 hours of reflux. Toluene and pyridine were removed by evaporation. The crude residue was then dissolved in ethyl acetate and washed with aqueous acidic and basic solutions. The organic layer was dried over magnesium sulfate and evaporated to dryness to give 700 mg of a white powder (yield = 89 %, Purity LC = 92 %).

LC: tR = 3.35 min (on 5 min), MS (ESI+): m/z = 298.91 [M + H]+

The 3-[5-(2-Fluoro-phenyl)-[1,2,4] oxadiazol-3-yl]-benzoic acid methyl ester (2.35 mmol) was suspended in a 1 M NaOH solution in methanol 1 M (10 mL). After 2 hours, the suspension was heated to 50 °C and stirred overnight. After 16 hours, the reaction mixture was acidified to pH 4 with 1 M chlorhydric acid. The methanol was evaporated and the product was extracted from aqueous solution with ethyl acetate. The organic layer was then dried over MgSO4. The product was crystallized in a mixture 60/40 ethanol/DCM and yielded 245 mg of a white crystal (yield = 36 %, purity LC = 97 %).

LC: tR = 6.64 min (on 10 min), MS (ESI+): m/z = 284.95 [M + H]+

1 H NMR (CD2Cl2): δ 8.61 (t, J=1.4 Hz, 1 H), 8.30 (dt, J= 7.8 Hzand J =1.2 Hz 1 H), 8.24 (td, J =7.6 Hz and J=1.7 Hz, 1 H), 8.15 (dt, J= 7.8 Hz and J=1.4 Hz, 1 H), 7.9 (m, 1 H), 7.72 (t, J= 7.7 Hz, 1 H), 7.55 (d, J=8.5 Hz, 1 H), 7.49 (q, J=7.6 Hz, 1 H).

The library of drugs contains more than 1200 pure active pharmaceutical compounds from international pharmacopeias as pure powders. Screening of the compounds was carried out from 96-well plates at 10 µM in DMSO.

Cell culture and chemical exposure

HeLa cells, expressing firefly luciferase mRNA and one of the fusion protein MS2-UPF, were grown in DMEM supplemented with 10 % FBS, 2.5 mg/ml blasticidin and a mixture of 1 U/ml penicillin and 1 mg/ml of streptomycin at 37 °C and 5 % CO2. Calu-3 and Calu-6 cells were grown in RPMI medium supplemented with 10 % FBS and a mixture of 1U/ml penicillin and 1 mg/ml of streptomycin at 37 °C and 5 % CO2. DMD cells were grown in DMEM/199 medium (4:1) supplemented with 20 % FBS, 10-7 M dexamethasone, 2.5 ng/ml HGF and a mixture of 1 U/ml penicillin and 1 mg/ml streptomycin at 37 °C and 5 % CO2. Cell differentiation was initiated in DMEM supplemented with 10 µg/ml insulin and 100µg/ml transferrin. 6CFSMEo-cells [21, 22] were grown in α-MEM supplemented with 10 % FBS, 1 mM L-glutamine and a mixture of 1 U/ml of penicillin and 1 mg/ml of streptomycin at 37 °C and 5 % CO2. Compounds were added 20 hours before harvesting the cells with the exception of the DMD cells which were exposed to the compounds for 48 hours starting with the addition of the differentiation medium.

Immortalization of DMD cells

hTERT and Cdk4 cDNA were cloned into distinct lentiviral vectors containing respectively the puromycin and neomycin selection markers. Transduction with lentiviral vectors were performed overnight in the presence of Polybrene (4 mg/ml; Sigma-Aldrich). Transduced cell cultures were submitted to selection in the presence of puromycin (0.2 µg/ml) and/or neomycin (0.3 mg/ml) for 8 days. The infected cells were then seeded at clonal density. Clones selected were isolated using glass

cylinders and their proliferation and differentiation capacities were characterized in the culture conditions described above. The clone used in this study presented growth and differentiation capacity similar to that observed on the original primary culture.

Expression constructs

HeLa cells stably expressing firefly luciferase mRNA with MS2 binding sites (bs) in the 3'UTR were obtained by transferring Fluc cDNA with MS2 bs from pCFluc (gift from Dr. Jens Lykke-Andersen) to the pLenti6/V5 using the PCR-based TOPO directional cloning system (Life Technologies) (sense primer: 5'CACCATGGAAGACGCCAAAAAC AT3' and antisense primer: 5'TGACACTATAGAATAGGGCC3'). The lentiviral particles produced with ViraPower Lentiviral Expression System (Life Technologies) were used to transduce the HeLa cells. Stable Fluc expressing clones were selected and isolated using a selective medium containing 2.5 mg/ml Blasticidin. The MS2-UPF expression vectors were constructed by transferring MS2-UPF cDNA from the pMS2-UPF proteins vector (gift from Dr. Jens Lykke-Andersen) into pLenti4/V5-DEST vector using Gateway Cloning according the manufacturer's instructions. Each MS2-UPF cDNA was cloned using the following primers: sense: 5'GGGGACAAGTTTGTAC AAAAAAGCAGGCTCACCATGGCTTCTAACTTTACTCAG3'; and antisense: 5'GGGGACCA CTTTGTACAAGAAAGCTGGGTTAATTTAGGTGACACTATAGAA 3'

Screening

HeLa cells stably expressing firefly luciferase were transduced with the recombinant

lentiviral constructs containing one of the four pLenti4/V5-MS2-UPF plasmids. Cells were seed into 96 well plates two days after infection and then exposed to the chemical compounds for 20 hours. Plates were loaded into a Tristar LB 941 microplate reader (Berthold) after the addition of Steadylite luciferase substrate (PerkinElmer) in order to measure Luciferase activity in each well for 1 second. Each plate was read 3 times.

RNA analysis

RNA was purified using RNazol (MRC) according to the manufacturer's instructions. A portion (1/5) of the RNA preparation was evaluated by reverse-transcription (RT) PCR (RTPCR) using Superscript II (Life Technologies) for 2 hours at 42 °C in presence of random hexamer for RT. The resultant cDNAs were PCR amplified in presence of dCTP (α33P) (Perkin Elmer) with primers indicated in Table 1. PCR products were quantified using Personal Molecular Imager and QuantityOne quantification software (Bio-Rad).

Table 1 listing of primer sequences used in this study for PCR amplification

Primers		**Sequences**
GAPDH	Sense	5'-CATTGACCTCAACTACATGG-3'
	Antisense	5'-GCCATGCCAGTGAGCTTCC-3'
p53	Sense	5'-ATGTGCTCAAGACTGGCGC-3'
	Antisense	5'-GACAGCATCAAATCATCC-3'
Dystrophin	Sense	5'-TCCTGGCATCAGTTACTGTG-3'
	Antisense	5'-CCAGTGGAGGATTATATTCC-3'
CFTR	Sense	5'-GGCCAGAGGGTGGGCCTCTT-3'
	Antisense	5'-CACCCTGTCGGAGGGGCTGA-3'
p21	Sense	5'-CGAGGCACTCAGAGGAG-3'
	Antisense	5'-TCCAGGACTGCAGGCTTCC-3'

Glycosylation analysis of CFTR and CFTR immunoprecipitation

Cells were lysed in RIPA buffer (1 % deoxycholic acid, 1 % Triton x100, 0.1 % SDS, 50 mM Tris pH7.4 and 150 mM NaCl) containing HALT protease inhibitor cocktail (Pierce). Then lysats were incubated with 10,000 units of PNGase (New England Biolabs) or 10,000 units of EndoH (New England Biolabs) for 4 hours at 37°c. Cells extracts were then used for the immunoprecipitation of CFTR. Briefly, non specific interactions with protein G agarose were removed by incubating protein extracts with 50 µl of protein G agarose beads (Pierce) for 30 minutes at 4°c. Then protein extracts were incubated with mAb 24–1 antibody for 2 hours at 4°c before to add 50 µl of protein G agarose beads and incubate for an additional 2 hours at 4°c. Beads were finally washed three times with RIPA buffer. Elution of CFTR was obtained by adding 50 µl of 2x sample buffer and vortexing before centrifuging samples and collecting the supernatant.

Western blot hybridization

Proteins were isolated in the following lysis buffer: 50 mM Tris pH7, 20 mM EDTA and 5 % SDS. All protein extracts, with the exception of dystrophin, were analyzed by 10 % SDSPAGE. Dystrophin analysis was carried out using 7.5 % SDS-PAGE. After migration, proteins were transferred onto a nitrocellulose membrane and then exposed to the primary antibody. The primary antibodies used were: anti-p53 (D01; Santa-Cruz), anti-dystrophin against an N-terminal epitope (4C7; Santa-Cruz), anti-dystrophin against a C-terminal epitope (exons 77–78) (Abcam), anti-CFTR against an N-terminal epitope (MM13-4; Millipore), anti-tubulin (Epitomics) and

anti-phosphorylated eIF2α (Epitomics). The primary antibody incubation is followed by a secondary antibody incubation using anti-mouse or rabbit antibody (Jackson Immuno Research). Proteins finally detected using SuperSignal West Femto Maximum Sensitivity Substrate (Pierce).

SPQ Halide-efflux Assay

Cells were seeded in 96-well plates and loaded overnight with 10 mM SPQ fluorophore (6methoxy-N-(3-sulfopropyl)-quinolinium) (Life technologies). Cells were washed twice with buffer (135 mM NaI, 2.4 mM K2HPO4, 0.6 mM KH2PO4, 1 mM MgSO4, 1 mM CaSO4, 10 mM dextrose and 10 mM Hepes, pH 7.3) and then incubated in iodide buffer for 30 min. After establishing the basal fluorescence (2 min), the iodide buffer was replaced with NO3buffer (135 mM NaNO3 instead of NaI) containing 20 µM forskolin and 200 µM IBMX. Fluorescence was the evaluated for a further 10 min. Fluorescence intensities were measured every 15 seconds using the Tristar LB 941 microplate reader (Berthold) equipped with a 340 nm excitation filter and a 450 nm emission filter.

Translation efficiency

Calu-6 cells were incubated with DMSO or 25 µM amlexanox for 20 hours before harvesting cells, or with cycloheximide (200µg/ml) 4 hours before harvesting cells. Newly synthesized proteins were measured using Click-iT AHA for Nascent Protein Synthesis kit (Life Technologies). Briefly, 30 min. before harvesting cells, L-AHA (L-azidohomoalanine) is added to the cell culture medium in order to be

incorporated into newly synthesized proteins. Then Cells were washed three times with PBS and lysis buffer was added to the cells. After 30 min. on ice, lysat was centrifuged and supernatant was collected. TAMRA molecule was then bound to the L-AHA modified amino acid using Clik-iT reaction buffer (Life technologies) by following the recommendations of the manufacturer. Finally, TAMRA was detected and quantified by western-blot using a DNR MF-ChemiBIS 3,2 (DNR) and Multi Gauge software (FUJIFILM).

Cell viability

Cells were harvested after trypsin treatment, centrifuged 3 min at 200 g and resuspended in PBS. Tali dead cell red (propidium iodide) reagent was then added to the cells. After a 5 min incubation in the dark, the cells were loaded into Tali image-based cytometer (Life Technologies).

Immunofluorescence

DMD cells were grown on ibiTreat surface µ-dishes (Ibidi) and differentiated as described above. Cells were fixed 10 min in 95 % ethanol at room temperature 48 hours after initiating differentiation. The fixed cells were washed twice in PBS and incubated with the C-terminal anti-dystrophin antibody for 1 hr at room temperature, washed twice with PBS and incubated with the secondary anti-rabbit antibody conjugated with Alexa 488 fluorophore (Life Technologies) for 1 hr at room temperature. The cells were then incubated with Hoechst stain for 1 min at room temperature before adding Vectashield (ABCYS) mounting medium and sealing a

coverslip.

Results and discussion

Identification of amlexanox as an NMD inhibitor

A tethering-based screening system (Lykke-Andersen, Shu et al. 2000) has been developed to identify NMD inhibitors from chemical libraries. Briefly, firefly luciferase (Fluc) mRNA was stabilized when the function of hUPF1, hUPF2, hUPF3 or hUPF3X was blocked by a chemical molecule. The assay relies on the transfection of a cell line that stably expresses a Fluc mRNA with 6 MS2-binding sites in the 3'UTR, with vectors that express MS2 fusion protein with one of the four hUPF proteins. Cells were incubated in 96 well-plates with the test compounds. Luciferase activity after adding a luciferase substrate mixed with a lysis buffer was measured three times. All drugs have been tested once. The hit selection threshold is the mean plus 3 standard deviation. Hit rates were 0.44%; 0.18%; 0.18% and 0.36% in UPF1; 2; 3 and 3X respectively. Amlexanox (Sequoia Research Products, UK) is the only one drug confirmed on the primary assay after screening. It significantly increases the luciferase activity in the four cell lines expressing one of the MS2-UPF proteins, suggesting that this compound might block NMD after recruitment of hUPF1, which is the most downstream factor among the four tested (Fig. 1 and Tables S1-4 for tables of luciferase measures).

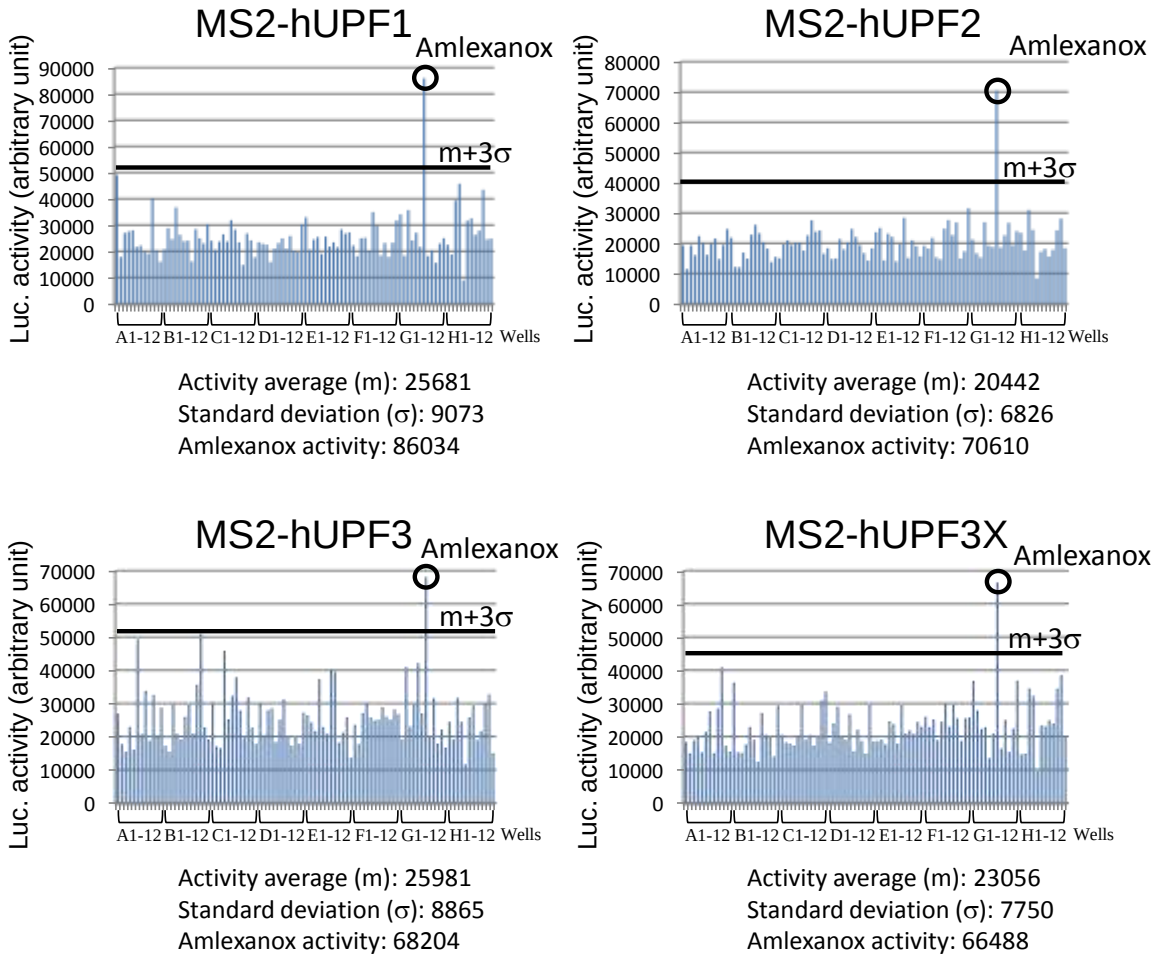

Figure 1 Identification of amlexanox as putative NMD inhibitor.

Luciferase activity was measured from cells expressing the Firefly luciferase with MS2 binding sites in its 3'UTR and MS2-UPF1 (up and left), MS2-UPF2 (up and right), MS2-UPF3 (down and left) or MS2-UPF3X (down and right). Tested drugs were added in columns 2 to 11 of each 96-well plate, the vehicle (DMSO) was added in positions A1, B1 and C1. No compounds were added in the rest of column 1 and column 12 of each plate, as negative controls. The luciferase activity is provided in arbitrary units. The mean luminescence values were calculated from all test compounds and for each plate. The threshold of hit selection was calculated for each plate and is represented by the black thick line: m + 3σ (mean plus 3 standard deviations)

To further characterize amlexanox, we determined whether it is able to increase the amount of endogenous nonsense mutation-containing mRNAs in cell lines issued from patients suffering from nonsense-mutation-mediated lung cancer, Duchenne muscular dystrophy (DMD) or cystic fibrosis (CF). In these cells the mutated mRNAs code for truncated p53, dystrophin and the CF transmembrane conductance regulator (CFTR),

respectively. Interestingly, with these cell lines, it was possible to measure the effect of our compound on the three possible nonsense codons located in three different nucleotide environments.

The lung cancer cell line, Calu-6 (ATCC, USA) has a homozygous TGG→TGA mutation at codon 196 of p53. These cells were incubated with increasing concentrations of amlexanox ranging from 0.2 to 25 μM for 20 hours or with DMSO as a control (Fig. 2A). Reverse transcribed RNAs from Calu-3 cells (ATCC, USA) were used as a reference. Calu-3 cells are derived from a lung adenocarcinoma and they express both p53 and CFTR at relatively high level (RNA and protein). A greater than 2-fold increase in the p53 mRNA amount was observed at 25 μM of amlexanox in Calu-6 cells suggesting an inhibition of NMD. At higher concentrations, a change in the cell morphology was observed, suggesting that amlexanox concentrations higher than 25 μM might interfere with cellular metabolism. However, the cell viability even at 125 μM was comparable to that observed with the DMSO alone (Fig. 3A). Therefore, to avoid any confounding results, 25 μM was the highest concentration used. A faint band corresponding to p53 mRNA was detected in the DMSO sample. This residual expression of p53 in Calu-6 cells has already been observed previously (Caamano, Ruggeri et al. 1991) and could represent a subpopulation of NMD-protected p53 mRNAs (such as nuclear p53 mRNAs) or cytoplasmic untranslated p53 mRNAs.

We then tested an immortalized myocyte cell line from a DMD patient with nonsense mutation (TCT→TAA) in exon 71 at codon 3420 of the dystrophin gene (see Methods). These cells were treated with amlexanox for 48 hours while they were exposed to

conditions that promote differentiation and dystrophin expression. As with the Calu-6 cells, increasing concentrations of amlexanox resulted in increased levels (up to 5-fold) of the mutant mRNA (Fig. 2B).

The third cell line used (6CFSMEo- cells) is an immortalized cystic fibrosis (CF) airway epithelial cell line derived from a population enriched for submucosal gland epithelial cells (Cozens, Yezzi et al. 1992; da Paula, Ramalho et al. 2005). These cells are from a patient who is compound heterozygous: one allele is a CTT deletion spanning codons 507 and 508 of CFTR that results in the in frame deletion of a phenyalanine (ΔF508), the other allele is a CAG→TAG nonsense mutation at the codon 2 (Q2X) of the CFTR gene (Cozens, Yezzi et al. 1992). A previous study indicated that there was little or no expression of the ΔF508 nor of the Q2X alleles in the 6CFSMEo- cells (da Paula, Ramalho et al. 2005). When the cells were treated with increasing concentrations of amlexanox a 3- to 4-fold increase in the CFTR mRNA amount was detected at 25 μM of amlexanox (Fig. 2C). Even though we favor the hypothesis that amlexanox stabilized PTC-containing mRNAs, we cannot exclude the possibility that amlexanox activated the expression of the ΔF508 CFTR allele. As with Calu-6 cells (p53 PTC-containing mRNA), 25 μM was the most effective for facilitating CFTR mRNA increase in 6CFSMEo- cells (Figs. 2A,C). Altogether results from figures 1 and 2 confirm that molecule amlexanox blocks NMD in various PTCs and PTC environments.

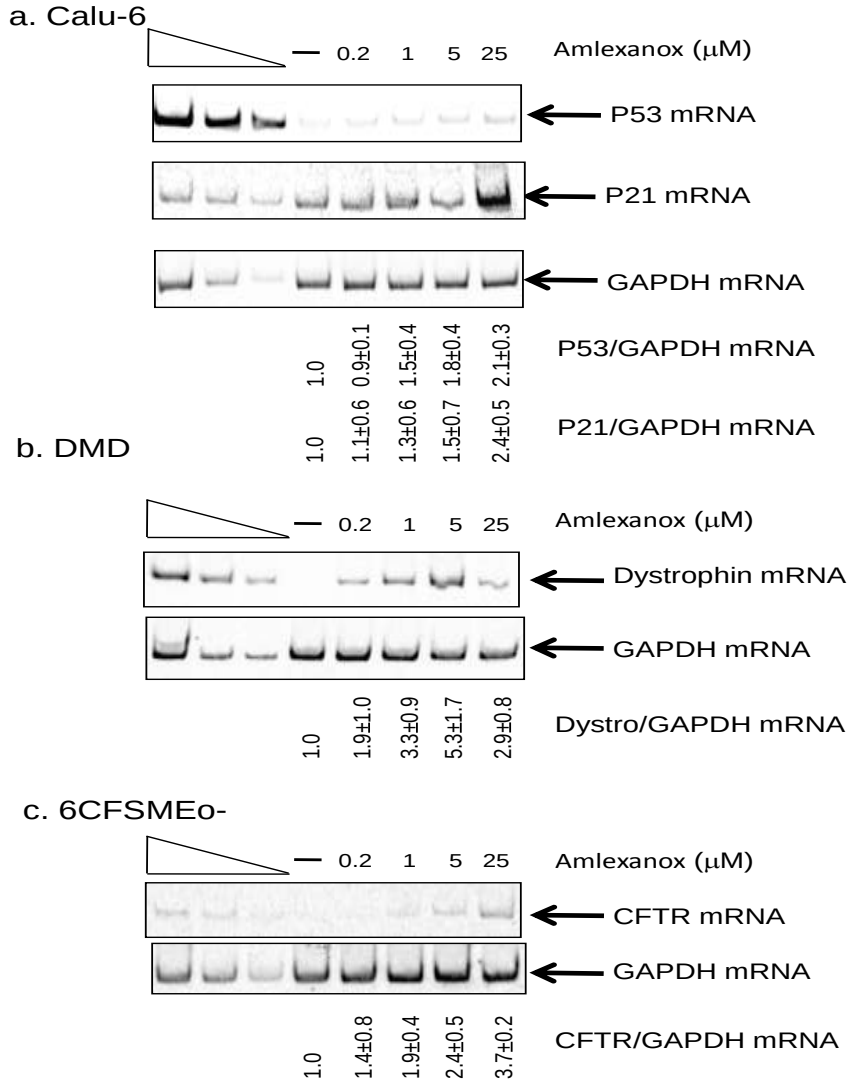

Figure 2 Amlexanox increases the amount of nonsense mutation-containing mRNAs. Increasing amounts of amlexanox are added to the cell culture medium of Calu-6 cells (A), DMD cells (B) or 6CFSMEo-cells (C). RNAs are purified, reverse transcribed and PCR is performed to measure the level of p53, dystrophin or CFTR mRNA, respectively. GAPDH level is used to normalize the amount of the nonsense mutation-containing mRNAs level. The three left lanes represent a two-fold serial dilution of RNA from untreated cells (Calu-3 cells for (A) and (C) or WT myoblasts for (B)). Quantifications are given as a ratio of P53 or P21 mRNA on GAPDH mRNA level and normalized to DMSO treatment which is given as 1. Quantifications are based on at least 3 independent experiments and the average quantification is indicated under each gel with standard deviation.

Cytotoxicity, translation efficiency and stabilization of natural NMD targets

The specificity and cytotoxicity of the amlexanox were evaluated on Calu-6 cells. The effect of amlexanox on cell survival was evaluated after a 20 hours treatment at the working concentrations (0.2 to 25 μM) or at 125 μM of amlexanox. The viability after

amlexanox or DMSO incubation was between 95 and 98% (Fig. 3A), indicating that amlexanox is not toxic for cells even at 125 μM in the conditions described above.

Inhibition of translation by amlexanox was assayed by incorporating an L-AHA (L-azidohomoalanine) modified amino-acid in newly synthesized proteins. L-AHA is then detected and measured using Click-iT AHA new protein synthesis kit (Life Technologies) (See methods). Results of Fig. 3B show that amlexanox has no significant effect on the level of fluorescence, in contrast to cycloheximide which strongly reduces it, suggesting that the efficiency of translation is not altered by amlexanox.

In addition, the phosphorylation status of eIF2α after amlexanox treatment was assessed since the induction of eIF2α phosphorylation as a function of inhibiting NMD has been demonstrated (Chiu, Lejeune et al. 2004; Wang, Zavadil et al. 2011) and that would impair translation process. The expression of eIF2α was analyzed in both the DMD and 6CFSMEo- cells with an antibody specific for the phosphorylated isoform of eIF2α (Fig. 3C). No increase in the eIF2α phosphorylation was observed, suggesting that NMD inhibition does not always require an induction of eIF2α phosphorylation.

The effect of amlexanox-mediated-NMD inhibition was also assessed on genes that normally use the NMD pathway to regulate their expression. The mRNA levels of three genes that are natural NMD targets (Nat9, Tbl2 and SC35) (Viegas, Gehring et al. 2007) were assayed in Calu-6 cells (Fig. 3D). For each of these targets, we measured an average of 1.2 -fold increase in mRNA level and no dose-related effect. This suggests that amlexanox does not affect the regulation of these (and possibly all) natural targets

of NMD and also suggests that the increase observed in nonsense-containing mRNAs is not simply due to a general transcriptional up-regulation by amlexanox.

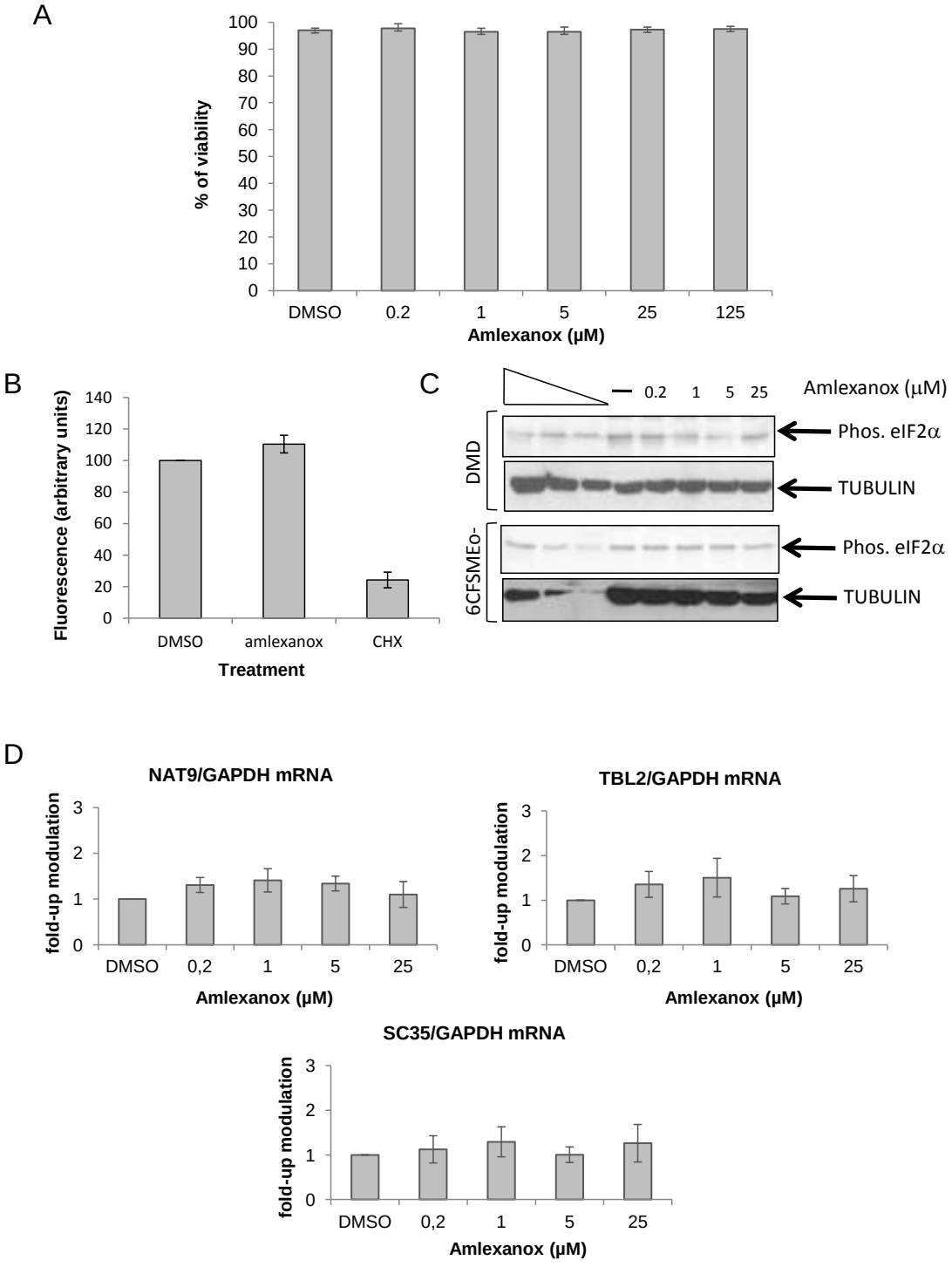

Figure 3 Amlexanox is not toxic, does not inhibit general translation and does not affect natural NMD substrates expression.

(A) Calu-6 Cell viability was measured after 20 hours of cell incubation with increasing amounts of amlexanox or with DMSO. These results combine three independent experiments. (B) Measure of

translation efficiency after amlexanox treatment. Calu-6 Cells were incubated with DMSO, amlexanox or cycloheximide (CHX) before to measure translation efficiency using Click-iT AHA for nascent protein synthesis kit (Life technologies). This result is representative of 2 independent experiments. (C) Western-blot showing that the level of phosphorylated (Phos.) eIF2α does not increase in the presence of amlexanox in DMD cells (upper panels) or 6CFSMEo-cells (lower panels). The three left lanes represent a two-fold serial dilution of cell extract from untreated WT myoblasts (upper panels) or Calu-3 cells (lower panels). (D) The level of three NMD natural target mRNAs was measured from Calu-6 cells as described in Materials and Methods from three independent experiments

Amlexanox induces protein synthesis from nonsense mutation-containing mRNA

Protein synthesis from nonsense mutation mRNAs was analyzed after amlexanox inhibition of NMD. All three cell lines with the PTCs described above were assayed by Western-blot for the presence of truncated p53, dystrophin or CFTR protein. An N-terminal antibody was initially used to detect truncated as well as full-length proteins (Fig. 4). After amlexanox treatment, a truncated p53 protein was well detected in Calu-6 cells. This truncated protein was not present in DMSO treated Calu-6 cells or in whole-cell extracts from Calu-3 cells. In addition, a very low level of full-length p53 was also detected when cells were treated with 1 to 25 μM amlexanox. In Calu-6 cells, it appears that the PTC-containing P53 mRNA stabilized by amlexanox can be translated into proteins. These results also suggest that amlexanox can directly or indirectly elicit PTC-readthrough on this particular PTC.

Previous studies clearly demonstrated that PTC-readthrough depends on the identity of the PTC and its nucleotide context (Bonetti, Fu et al. 1995; Namy, Hatin et al. 2001; Bidou, Hatin et al. 2004; Tork, Hatin et al. 2004). To determine whether the dystrophin and CFTR PTCs resulted in full-length and/or truncated protein, the two other cell lines were also treated with amlexanox. Increasing concentrations of amlexanox in the

culture medium of DMD cells during differentiation induced the synthesis of dystrophin protein with maximum synthesis at a concentration of 5μM amlexanox, as detected with an anti-N-term antibody (Fig. 4B, upper gel). This result was consistent with the observation that maximal dystrophin mRNA stabilization also occurs at 5μM (Fig. 2B). However, it was difficult to distinguish the full length from the truncated form of dystrophin with this antibody because of their high and similar molecular weights (427 vs 400 kDa). Therefore, a C-terminal anti-dystrophin antibody (with an epitope in exons 77-78 of dystrophin so downstream of the PTC position) was used. This antibody also detected dystrophin produced upon amlexanox treatment indicating that at least a portion of the dystrophin synthesized in the presence of amlexanox is the full-length protein (Fig. 4B middle gel).

Analysis of CFTR protein expression in 6CFSMEo- cells after treatment with increasing concentrations of amlexanox was a bit more challenging, since the truncated CFTR protein with a stop at the second codon would be purely theoretical (da Paula, Ramalho et al. 2005). As with the other two cell lines, bands were detected that were consistent with the full-length wild-type CFTR protein produced in Calu-3 cells (Fig. 4C).

Interestingly, CFTR is subject to 2 steps of glycosylation occurring first in the endoplasmic reticulum to give the core glycosylated band B CFTR, and then in the Golgi to give the fully mature band C CFTR. To assess the glycosylation level of the CFTR protein isoform obtained after amlexanox treatment, we incubated protein extracts from Calu-3 or 6CFSMEo- cells treated or not with amlexanox with PNGaseF

or endoH glycosydases before to immunoprecipate CFTR (Fig. S1). The resulting CFTR protein after amlexanox treatment in 6CFSMEo- cells is processed like the wild-type CFTR from Calu-3 cells with a band C showing some sensitivity to PNGaseF and resistance to endoH. Band B is sensitive to both glycosidases but this isoform was not observed in 6CFSMEo- cells after amlexanox treatment likely due to the low amount of CFTR synthesized.

Fig. 4 shows that full-length proteins are synthesized after amlexanox treatment from mRNAs containing nonsense mutations. This strongly suggests that amlexanox promotes PTC-readthrough. However, it was not possible to determine whether amlexanox was equally efficient on any PTC, because the appropriate cell models were not available. For example Calu-3 cells over-express CFTR and synthesize relatively high levels of p53 protein. In the case of DMD cells, both cell lines come from different patients and cannot be effectively compared, because inter-individual variation in the expression of the same gene (Storey, Madeoy et al. 2007). However, it does appear that amlexanox induces, at low micromolar concentrations, the synthesis of full-length proteins from any PTC at a level detectable by Western blot.

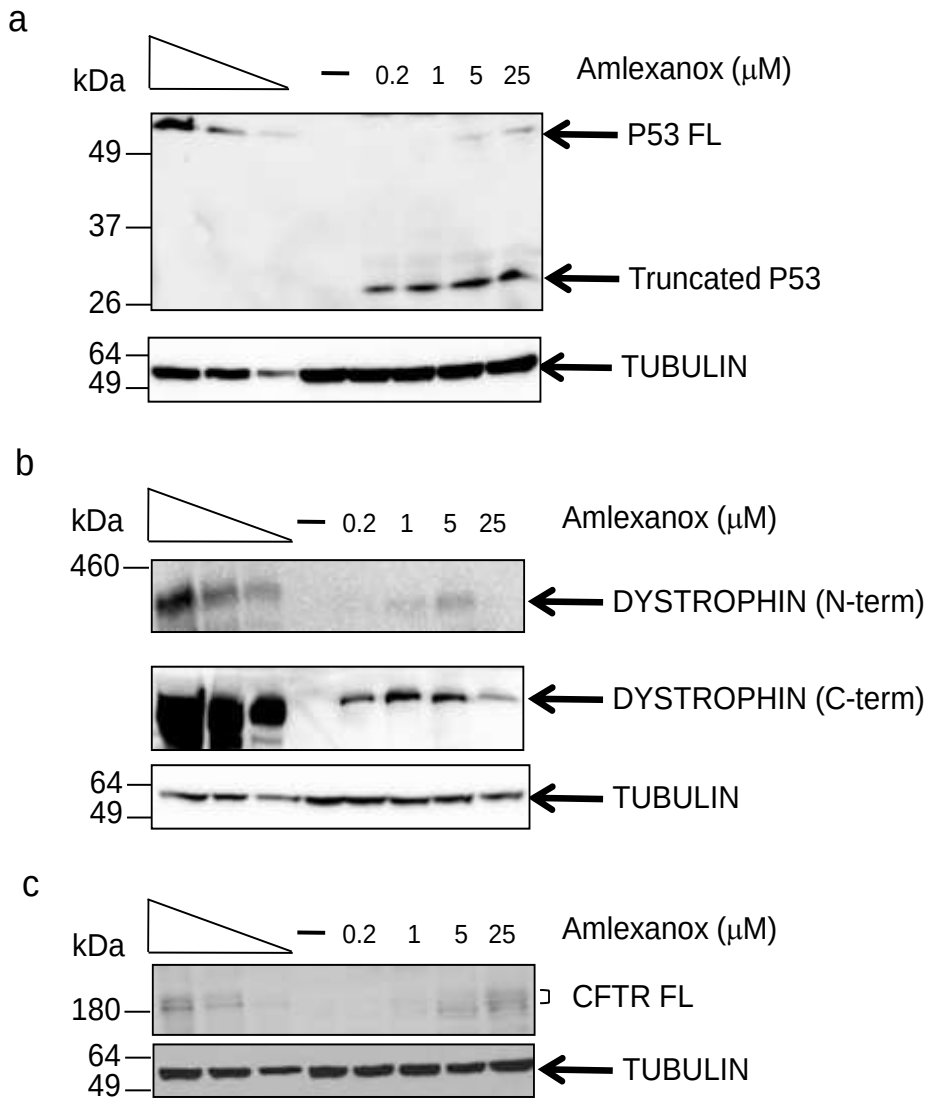

Figure 4 Amlexanox treatment leads to the synthesis of truncated and/or full length proteins from nonsense mutation-containing mRNAs.

Calu-6 (A), DMD (B) or 6CFSMEo-(C) cells were incubated with amlexanox molecule or with DMSO (−) as a control before purifying proteins and performing Western blot to detect p53, dystrophin or CFTR protein, respectively, using antibodies raised against N-terminal part of the proteins (and C-terminal part of the dystrophin protein as mentioned). The three left lanes represent a two-fold serial dilution of cell extract from untreated cells (Calu-3 cells for (A) and (C) or WT myoblasts for (B)). Each gel is representative of at least 2 independent experiments. On the left of each gel is indicated the molecular weight ladder (BenchMark pre-stained for A and C, or HiMark pre-stained for B (Life Technologies)).

Functional analysis of proteins generated after amlexanox treatment

Truncated dystrophin from our DMD cell line would be as functional as the wild-type dystrophin (Crawford, Faulkner et al. 2000). Therefore, we analyzed the cellular

localization of dystrophin in this cellular model. Dystrophin immunolocalization using the antibody that recognizes an epitope in exons 77-78 was distinctly different when comparing WT cells to DMD cells (Fig. 5). An intense fluorescent signal (green) was observed under the cytoplasmic membrane of WT cells, but not in the DMD cells treated with DMSO where there appears to be some weak non specific staining. Additionally, DMD cells keep a small size under differentiation conditions unlike WT cells or DMD cells after amlexanox treatment. Indeed, about 20% of cells (n=329) show a large size representing cells that are in the process of differentiate into myotubes. In presence of amlexanox, dystrophin staining becomes more apparent and can be easily detected at the plasma membrane of 75% of large cells (n=76), in a pattern similar to what is observed with the wild-type DMD cells (Fig. 5, right panel). Thus, these images are consistent with the Western blot analysis, and confirm that full-length dystrophin is synthesized after amlexanox treatment.

Since the Calu-6 and 6CFSMEo- cell lines encode a nonfunctional truncated p53 or CFTR proteins, respectively, it was interesting to determine whether a treatment with amlexanox actually rescues the lost functions in these cells. The function of the full-length p53 protein in the Calu-6 cells was determined by measuring the level of p21 mRNA (a transcriptional target of p53 (el-Deiry, Tokino et al. 1993)). The rationale for this analysis was that amlexanox-induced increases in functional p53 should result in an increase in the amount of p21 mRNA. The level of p21 mRNA was correlated with the increase in p53 mRNA (at 5 and 25 μM in particular) (Fig. 2A). The function of CFTR in 6CFSMEo- cells was evaluated by measuring cAMP-dependent halide

efflux as a function of SPQ fluorescence (Mansoura, Biwersi et al. 1999). Cells were loaded with SPQ and incubated with increasing amounts of amlexanox or with DMSO alone. The medium was sequentially switched to 1) an iodide solution to quench the SPQ fluorescence, and 2) to a nitrate solution containing forskolin and IBMX to increase intracellular cAMP levels and activate the CFTR. If CFTR is functional, iodide will be secreted from cells after cAMP stimulation and replaced by nitrate on the anion binding site of SPQ. Unlike iodide, nitrate does not quench the fluorescence of SPQ. Therefore the presence of functional CFTR will be assessed by a rapid increase in the SPQ fluorescence. A dose-dependent in iodide efflux with a maximum effect at 25 μM amlexanox was clearly observed in 6CFSMEo- (Fig. 6). Although, a direct comparison cannot be made between 6CFSMEo- cells and Calu-3 cells due to the fact that the latter overexpress CFTR, a set of measures of CFTR functionality in Calu-3 cells using the same SPQ assay is presented in supplemental figure S2 and shows that the CFTR activity that we measured in 6CFSMEo- cells after amlexanox treatment is about 20% of the CFTR activity that is measured in Calu-3 cells. Overall, these results demonstrate that amlexanox induces the synthesis of functional CFTR protein in 6CFSMEo- cells.

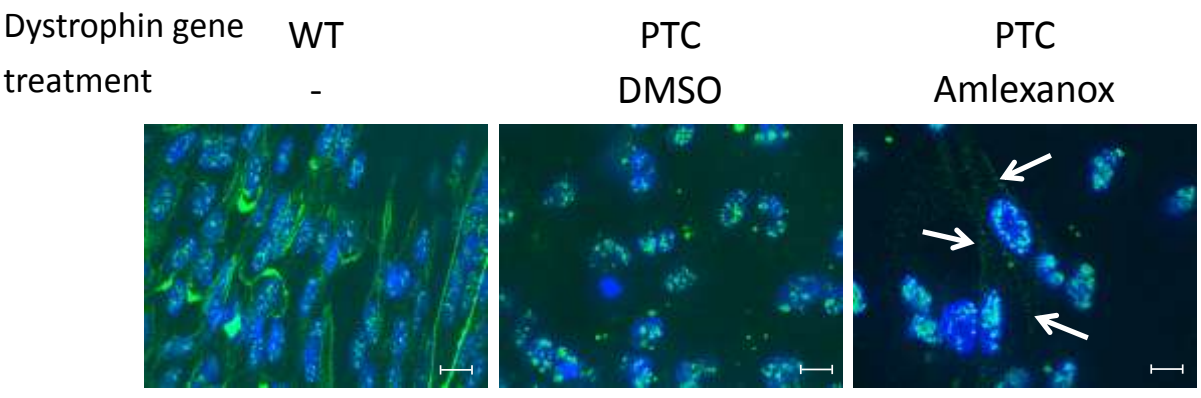

Figure 5 Dystrophin is found at the cell membrane of DMD cells after amlexanox treatment. WT (left panel) or DMD cells (two right panels) were incubated in differentiation medium in presence of DMSO or 5 **µ**M of amlexanox for 48 hours. Then cells were fixed and nuclei (blue) were stained using Hoechst reagent and dystrophin (green) was localized using anti-dystrophin raised against the C-terminal part of the protein. White arrows indicate dystrophin localization at the cellular membrane. Scale bar represents 10 **µ**m.

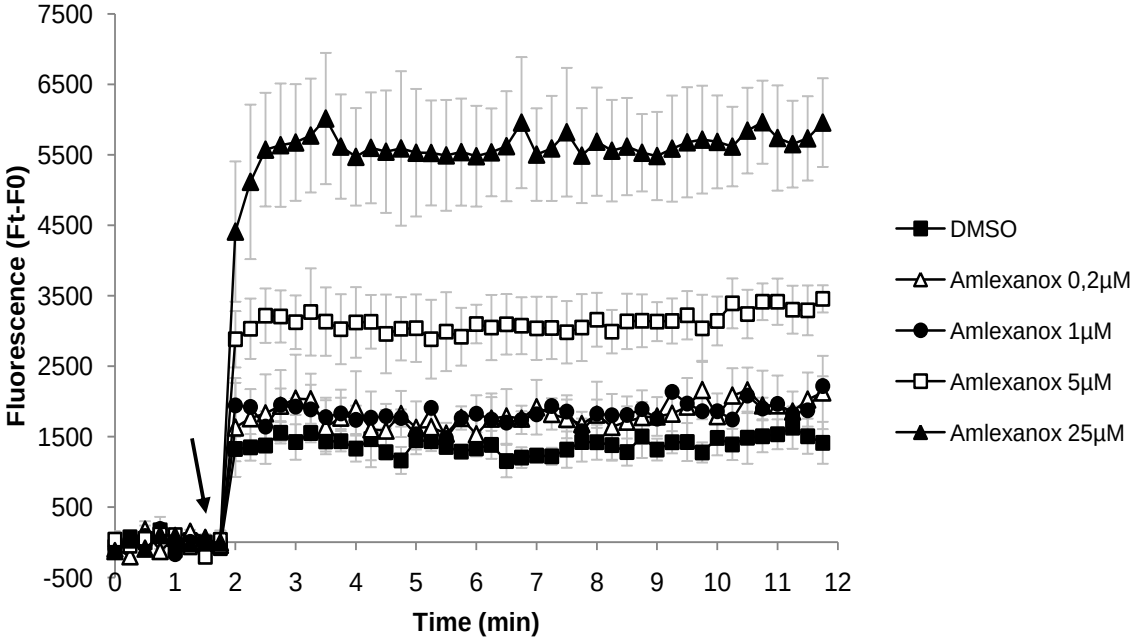

Figure 6 Amlexanox treatment of 6CFSMEo-cells leads to the synthesis of functional CFTR. 6CFSMEo-cells were loaded with the halide-sensitive fluorophore SPQ and treated with DMSO (■), 0.2 **µ**M amlexanox (Δ), 1 µM amlexanox (●), 5 **µ**M amlexanox (□) or 25 µM amlexanox (▲) for 20 hours. At time (t) = 2 min cAMP-stimulating cocktail was added (arrow). The increase in iodide efflux is shown as mean ± SEM from at least four independent experiments. Ft represents the measure of the fluorescence at the reading time; F0 is an average fluorescence before addition of cAMP agonists

Comparison of amlexanox with PTC-readthrough molecules

Since amlexanox was able to induce the synthesis of full-length proteins from nonsense mutation-containing mRNAs, it was interesting to compare its efficacy to that of G418 or PTC124, which have already been shown to facilitate PTC-readthrough (Correa-Cerro, Wassif et al. 2005; Welch, Barton et al. 2007; Kerem, Hirawat et al. 2008). The effect of each molecule and their combinations was evaluated quantitatively by measuring iodide efflux across the plasma membrane. Amlexanox,

G418 or PTC124 (for synthesis of PTC124 see Methods) were added to 6CFSMEo- cells for 20 hours either alone or in combinations (Fig. 7). Amlexanox was used at 5 μM (suboptimal) and 25 μM (optimal) and G418 was used at 100 and 400 μM, concentrations used previously to show G418 readthrough (Bedwell, Kaenjak et al. 1997; Bidou, Hatin et al. 2004; Murphy, Mostoslavsky et al. 2006). PTC124 was used at 5 and 25 μM, which were previously shown to be optimal for readthrough (Welch, Barton et al. 2007). First of all, a significant increase in the export of iodide was observed for the 3 components, compared to treatment with DMSO and amlexanox at 5μM is as potent as G418 at 400μM or PTC124 at 5μM (Fig.7A). Although combinations behave with similar efficacy, the combination of amlexanox (5 μM) and PTC124 (25 μM) seems to be slightly more efficient than each molecule alone (Fig. 7A lower panel). Interestingly, amlexanox at 25 μM was at least 3 times more effective than any of the single other molecules or combinations (Fig. 7B), an important result which could be due to the combined function of amlexanox in both NMD and readthrough processes.

A

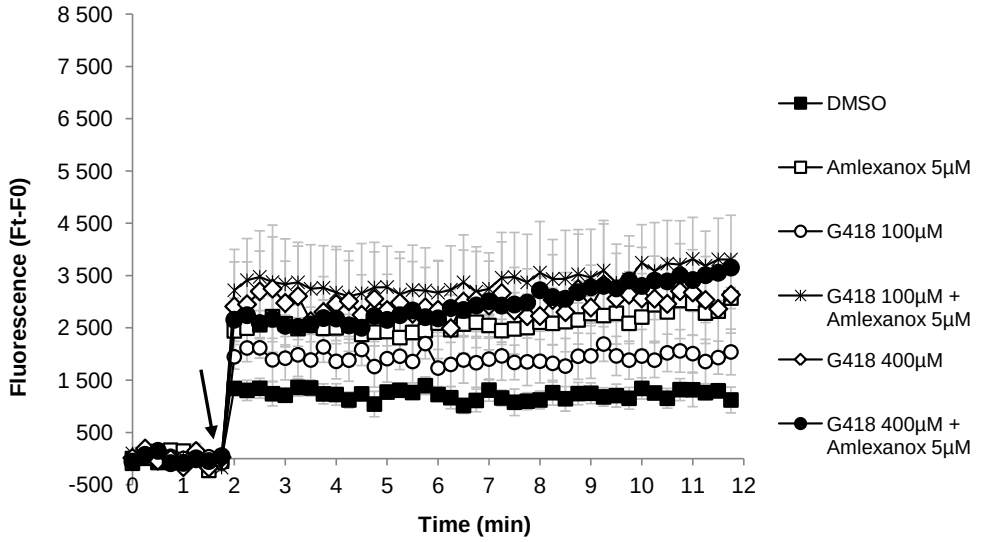
8 500
7 500
6 500
5 500
4 500
3 500
2 500
1 500
500
-500
0 1 2 3 4 5 6 7 8 9 10 11 12
Fluorescence (Ft-F0)
Time (min)
DMSO
Amlexanox 5µM
G418 100µM
G418 100µM + Amlexanox 5µM
G418 400µM
G418 400µM + Amlexanox 5µM

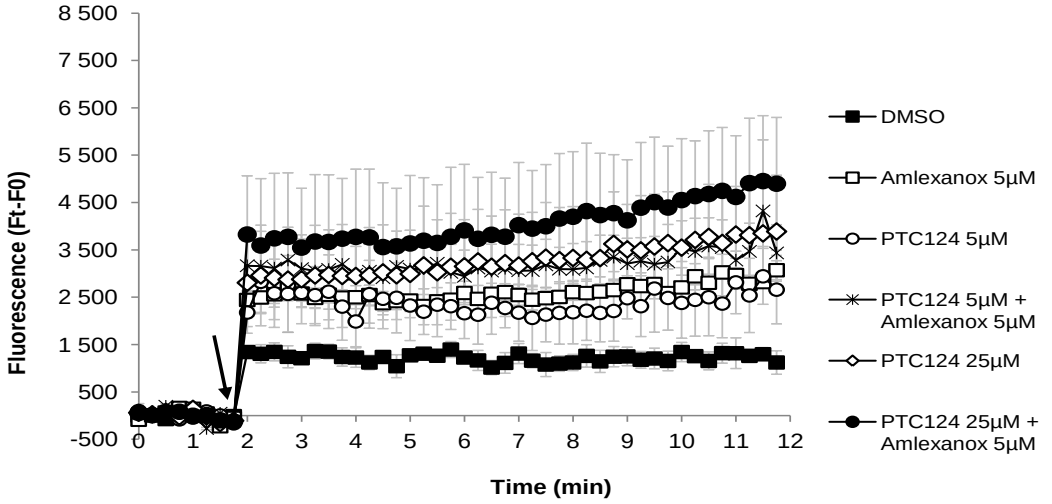
8 500
7 500
6 500
5 500
4 500
3 500
2 500
1 500
500
-500
0 1 2 3 4 5 6 7 8 9 10 11 12
Fluorescence (Ft-F0)
Time (min)
DMSO
Amlexanox 5µM
PTC124 5µM
PTC124 5µM + Amlexanox 5µM
PTC124 25µM
PTC124 25µM + Amlexanox 5µM

B

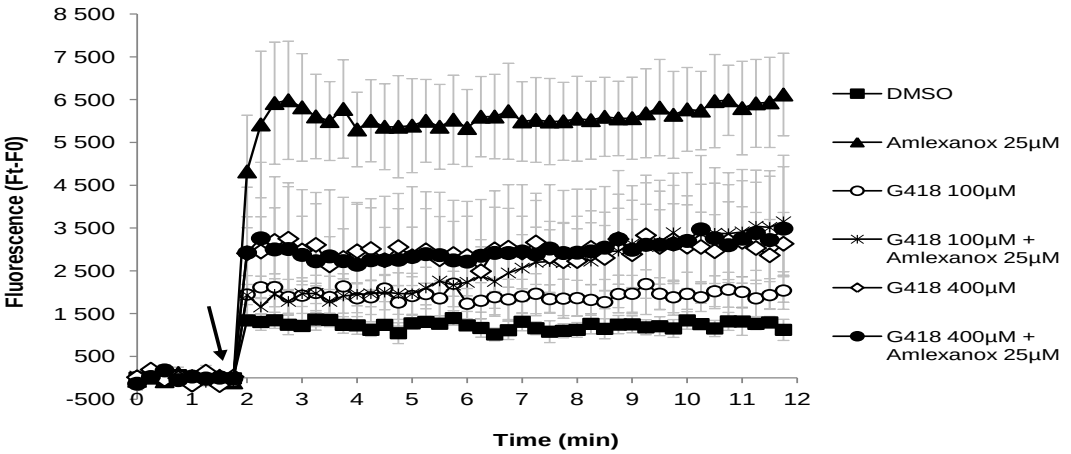
8 500
7 500
6 500
5 500
4 500
3 500
2 500
1 500
500
-500
0 1 2 3 4 5 6 7 8 9 10 11 12
Fluorescence (Ft-F0)
Time (min)
DMSO
Amlexanox 25µM
G418 100µM
G418 100µM + Amlexanox 25µM
G418 400µM
G418 400µM + Amlexanox 25µM

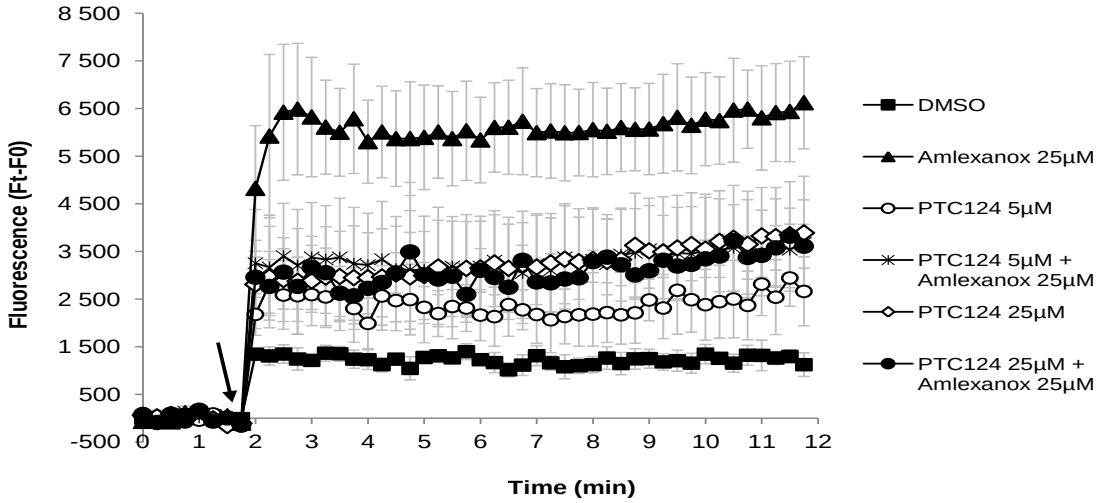

Figure 7 Comparison of the efficiency of amlexanox alone or in combination with PTC-readthrough molecules.

6CFSMEo-cells were incubated with 5 µM (A) or 25 µM (B) of amlexanox alone or with G418 (upper panel) or PTC124 (lower panel). At time (t) = 2 min cAMP-stimulating cocktail was added (arrow). The increase in iodide efflux is shown as mean ± SEM from at least four independent experiments. Ft represents the measure of the fluorescence at the reading time; F0 is an average fluorescence before addition of cAMP agonists.

Conclusions

The studies presented here outlined the features of a new NMD inhibitor, amlexanox (Fig. 1). It is probable that amlexanox inhibits NMD at a late stage, since its effect is not abolished by tethering the MS2-UPF1 protein in the 3'UTR of the Fluc mRNA (Fig. 1). Amlexanox is shown to stabilize the three different nonsense mutation-containing mRNAs from three cellular human disease models (Fig. 2). The work presented here also demonstrates that it is possible to inhibit the degradation of nonsense mutation containing mRNAs without dramatically altering cellular metabolism. Both cell viability (Fig. 3A) and translation are not affected by amlexanox treatment (Fig. 3B). The observed lack of toxicity of amlexanox could be explained by the redundancy of

mRNA level regulation. In our study, the levels of natural NMD substrates are not up-regulated after treatment with amlexanox (Fig. 3D), a point that can be explained by the fact that genes using NMD to regulate their expression often use several regulatory mechanisms. For example, SR protein genes use NMD to regulate their expression (Lareau, Inada et al. 2007). The regulation of SR protein gene expression also involves transcription, splicing, translation and/or post-translational events to maintain a functional level of SR proteins (Bourgeois, Lejeune et al. 2004; Ni, Grate et al. 2007). These are likely backup regulatory mechanisms to compensate for a lack of response in a specific regulatory pathway. Furthermore, an unusual event must occur to involve NMD regulation as with the SR proteins that employs an NMD mechanism that reduces the amount of translated mRNA and is activated only when the level of a specific SR protein becomes abnormally high (Sureau, Gattoni et al. 2001; Lareau, Inada et al. 2007). These previous studies and the present studies suggest that robustness of gene regulation allows some inhibition of NMD without significantly affecting the profile of gene expression (Fig. 3D).

Interestingly, amlexanox not only increases the amount of nonsense mutation-containing mRNAs, but also induces the synthesis of truncated and/or full-length proteins from PTC-containing mRNAs, suggesting activation of PTC-readthrough (Fig. 4). This ability to both stabilize nonsense mutation-containing mRNA and promote PTC readthrough has been previously described for G418 (Correa-Cerro, Wassif et al. 2005). G418 is an aminoglycoside analog, which unfavorable therapeutic index makes it unsuitable for medical applications. Amlexanox

is effective at concentrations (5 or 25 μM) that are generally lower than those required for aminoglycosides. We have observed with amlexanox some variations in the sensitivity of cells to treatment which would be due to the nature of the nonsense mutation, the nucleotide environment, and the nature of mRNA or the cell type. Therefore, each cell model with a nonsense mutation needs to be independently assayed to determine the most effective amlexanox working concentration. In our study, The DMD cell model was the most sensitive to amlexanox (Figs 2 and 4). However, DMD cells are distinct from the other cell systems studied, since they require cellular differentiation to activate expression of nonsense-mutation containing dystrophin mRNA. Furthermore, the decrease of the efficacy of amlexanox at 25 μM when compared to effect at 5 μM may be due to a cellular defense that inhibits the entrance of amlexanox into the cells when a specific concentration is reached. We cannot exclude some cellular toxicity at the highest concentration that we didn't detect in Fig. 3A due to the difference of cellular model. Alternatively, amlexanox could affect muscle differentiation process or dystrophin expression.

The ability of amlexanox to inhibit NMD and facilitate PTC-readthrough of all the PTCs tested suggests that its mode of action is different from molecules that only activate PTC-readthrough and for which the efficacy is strongly influenced by the identity of the PTC and its nucleotide environment (Bidou, Hatin et al. 2004).

Recent studies have shown that protein synthesis occurs during the pioneer round of translation (Apcher, Daskalogianni et al. 2011). Amlexanox could cause nonsense-mutation read-through during this round of translation, if NMD inhibition

and readthrough are concomitant. If readthrough occurs after the pioneer round, it would suggest that NMD inhibition and read-through promotion are two distinct molecular intervention of amlexanox. Clearly, further analysis of the mode of action of amlexanox will be important for its development as a novel therapy for nonsense mutation mediated diseases. These studies may also provide a better understanding of NMD mechanism. While amlexanox appears to be the most potent molecule of the three tested (Figs 6 and 7), further studies using other quantifiable PTC-readthrough systems will be required to determine whether this is a specific or a general property of amlexanox. Indeed, PTC124 has been shown to be efficacious for some nonsense-mutations (Welch, Barton et al. 2007; Du, Liu et al. 2008) and totally ineffective with others (Brumm, Muhlhaus et al. ; Dranchak, Di Pietro et al. 2011).

Amlexanox has anti-allergic (Saijo, Kuriki et al. 1985; Saijo, Makino et al. 1986) and anti-inflammatory properties (Saijo, Kuriki et al. 1985; Sakakibara 1988). It has been used for more than 30 years *per os* or topically to treat asthma and aphthous ulcers (Saijo, Kuriki et al. 1985; Meng, Dong et al. 2009). Together with its activity on nonsense mutation containing genes, the relative safety of amlexanox and its current use as an oral treatment of asthma, encourage us to investigate in details its therapeutic potential in other pulmonary diseases such as nonsense mutation mediated cystic fibrosis but not only. To our opinion, amlexanox appears to be a reasonable candidate for a novel therapy to treat disease states that are the result of nonsense mutations. Along with PTC124, amlexanox provides another opportunity for the development of a disease modifying, personalized therapy against several genetic diseases.

Abbreviations

BS, binding site; CF, cystic fibrosis; CFTR, cystic fibrosis transmembrane conductance regulator; DMD, Duchenne muscular dystrophy; Fluc, firefly luciferase; Min, minute; NMD, nonsense-mediated mRNA decay; ORF, open reading frame; PCR, polymerase chain reaction; Phos., phosphorylated; PPM, parts per million; PTC, premature termination codon; RT, reverse transcription; UTR, untranslated region

Competing interest

Authors declare that they have no competing interests.

Authors' contribution

SGH, JJ, ND, KM and FL performed experiments. SGH, TB, GB, VM, DCG, BD and FL interpreted results. SGH, TB, VM, DCG, BD and FL wrote the paper. All authors read and approved the final manuscript.

Acknowledgements

Authors thank Jens-Lykke Andersen, Lynne Maquat and Lee Sweeney for reagents. We also would like to thank France Leturcq and Valérie Allamand for technical advices, and James Stévenin and Florence Petit for critical reading of the manuscript. We thank the BICeL facility for the access to instruments and technical advices. This work was supported by Inserm Avenir program, the Association Française contre les Myopathies, Vaincre la Mucoviscidose, la Fondation pour la Recherche Médicale, la Ligue Régionale du Nord-Pasde-Calais contre le Cancer and l'Institut Pasteur de Lille. SGH is supported by a grant Inserm/Région Nord-Pas-de-Calais. JJ is supported by a

grant from Vaincre la mucoviscidose. KM and VM received funding from TREAT-NMD (contract LSHM-CT2006-036825) from the European Commission 6th FP, the ANR Genopath-INAFIB, the Duchenne Parent Project Netherlands, CNRS, INSERM, University Pierre and Marie Curie, Parents Project of Monaco, and European Parent Project. DCG is supported by funds from CF Research, Inc and Pennsylvania CF, Inc.

Additional files

					average							
well	reading	reading	reading	well	readings 1-3		E01	30785	33080	35331	E01	33065.3333
A01	49170	48839	49528	A01	49179		E02	20244	20654	21387	E02	20761.6667
A02	17199	17888	18708	A02	17931.6667		E03	23359	24127	26309	E03	24598.3333
A03	27042	26815	27417	A03	27091.3333		E04	24049	25209	27295	E04	25517.6667
A04	27146	27574	28211	A04	27643.6667		E05	18412	19118	19764	E05	19098
A05	27958	27871	28438	A05	28089		E06	24467	25436	27190	E06	25697.6667
A06	21186	21544	22530	A06	21753.3333		E07	20707	21771	23132	E07	21870
A07	22173	21902	22714	A07	22263		E08	22975	23368	24223	E08	23522
A08	19563	19825	20549	A08	19979		E09	21361	21413	22042	E09	21605.3333
A09	18778	19101	19738	A09	19205.6667		E10	27321	28281	29694	E10	28432
A10	38874	40130	41945	A10	40316.3333		E11	25227	26946	28385	E11	26852.6667
A11	19947	20471	21335	A11	20584.3333		E12	25942	26736	29258	E12	27312
A12	16012	15672	16701	A12	16128.3333		F01	21998	22146	22836	F01	22326.6667
B01	20061	20558	22033	B01	20884		F02	17530	18246	18848	F02	18208
B02	28569	28167	30026	B02	28920.6667		F03	24380	24878	25986	F03	25081.3333
B03	24267	24310	25602	B03	24726.3333		F04	24720	24878	26186	F04	25261.3333
B04	35113	36588	38726	B04	36809		F05	19485	20131	21448	F05	20354.6667
B05	25654	26282	27181	B05	26372.3333		F06	32731	34607	37774	F06	35037.3333
B06	22714	23935	25183	B06	23944		F07	26893	29720	32687	F07	29766.6667
B07	23342	23787	25331	B07	24153.3333		F08	17993	18185	19293	F08	18490.3333
B08	15995	16248	16501	B08	16248		F09	22504	23220	24083	F09	23269
B09	27321	28028	30183	B09	28510.6667		F10	17618	17618	18647	F10	17961
B10	24101	24991	26056	B10	25049.3333		F11	22068	23097	24965	F11	23376.6667
B11	22513	23019	23752	B11	23094.6667		F12	31082	31422	33054	F12	31852.6667
B12	29590	30244	31727	B12	30520.3333		G01	33141	33996	35392	G01	34176.3333
C01	24511	23604	24258	C01	24124.3333		G02	17522	18333	19406	G02	18420.3333
C02	20209	20776	21108	C02	20697.6667		G03	34022	35445	37940	G03	35802.3333
C03	24302	23298	23822	C03	23807.3333		G04	23455	23987	25253	G04	24231.6667
C04	26492	26178	27085	C04	26585		G05	25087	27338	29101	G05	27175.3333
C05	22574	23656	25235	C05	23821.6667		G06	20942	21344	22932	G06	21739.3333
C06	31431	31762	32783	C06	31992		G07	91910	84179	82015	G07	86034.6667
C07	27399	27696	30008	C07	28367.6667		G08	17356	18150	19310	G08	18272
C08	22871	23176	24520	C08	23522.3333		G09	18874	20515	22268	G09	20552.3333
C09	14310	14686	15628	C09	14874.6667		G10	14939	15515	16693	G10	15715.6667
C10	24816	26693	29101	C10	26870		G11	21902	22426	24747	G11	23025
C11	23298	24083	25410	C11	24263.6667		G12	24284	24363	26631	G12	25092.6667
C12	17452	17382	18490	C12	17774.6667		H01	21474	22408	23857	H01	22579.6667
D01	22103	23185	25375	D01	23554.3333		H02	17618	18848	20122	H02	18862.6667
D02	22164	22801	23918	D02	22961		H03	39022	38952	40401	H03	39458.3333
D03	22495	22443	23010	D03	22649.3333		H04	41753	46143	49685	H04	45860.3333
D04	15392	16047	16623	D04	16020.6667		H05	8586	8892	9598	H05	9025.33333
D05	20829	20995	21632	D05	21152		H06	30462	31413	33368	H06	31747.6667
D06	22426	22949	24302	D06	23225.6667		H07	30523	32652	34729	H07	32634.6667
D07	24223	24729	26152	D07	25034.6667		H08	25113	26082	27914	H08	26369.6667
D08	20279	20977	22033	D08	21096.3333		H09	26736	27748	29424	H09	27969.3333
D09	25628	25445	26710	D09	25927.6667		H10	40994	43272	46396	H10	43554
D10	18944	20480	21605	D10	20343		H11	23874	24450	25715	H11	24679.6667
D11	18804	19598	20637	D11	19679.6667		H12	23682	24878	26248	H12	24936
D12	29555	30157	31771	D12	30494.3333					average:		25681.9826

Table S1: Measures of the luciferase activity of plate figure 1 with MS2-UPF1 strain.
Reading 2 was performed 2 minutes after reading 1 and reading 3 was performed 2 minutes after reading 2.
Amlexanox position (G07) is highlight

					average						
well	reading	reading	reading	well	readings 1-3		E01	22661	23708	24860	E01	23743
A01	18883	19188	20078	A01	19383		E02	24651	24886	25802	E02	25113
A02	11195	11509	11954	A02	11552.6667		E03	13769	14197	15270	E03	14412
A03	18682	19293	20087	A03	19354		E04	22129	23001	24555	E04	23228.3333
A04	15366	16108	16902	A04	16125.3333		E05	21501	21719	23429	E05	22216.3333
A05	22225	22277	22932	A05	22478		E06	13647	13953	14651	E06	14083.6667
A06	19485	20131	20689	A06	20101.6667		E07	18813	19607	20759	E07	19726.3333
A07	15654	16125	16972	A07	16250.3333		E08	28045	28167	29310	E08	28507.3333
A08	19537	19921	20061	A08	19839.6667		E09	14136	15340	16178	E09	15218
A09	21876	21248	21771	A09	21631.6667		E10	20480	20881	21858	E10	21073
A10	14302	14808	15488	A10	14866		E11	18988	19223	19153	E11	19121.3333
A11	18665	19363	20436	A11	19488		E12	15244	15715	16335	E12	15764.6667
A12	23761	24502	26047	A12	24770		F01	18586	19049	20096	F01	19243.6667
B01	21727	21623	22364	B01	21904.6667		F02	17748	18167	19057	F02	18324
B02	11623	12312	12766	B02	12233.6667		F03	20872	21902	22871	F03	21881.6667
B03	11701	12112	12557	B03	12123.3333		F04	14642	15201	16379	F04	15407.3333
B04	16274	17260	17513	B04	17015.6667		F05	14101	14555	15637	F05	14764.3333
B05	14878	14790	15392	B05	15020		F06	24459	24511	25724	F06	24898
B06	22382	22740	23621	B06	22914.3333		F07	27460	27155	28586	F07	27733.6667
B07	25227	25960	27338	B07	26175		F08	22042	22696	23551	F08	22763
B08	22635	23185	24345	B08	23388.3333		F09	25898	26579	28377	F09	26951.3333
B09	19913	20218	21300	B09	20477		F10	14651	14782	15698	F10	15043.6667
B10	17731	18124	19075	B10	18310		F11	17207	17321	17775	F11	17434.3333
B11	13298	13822	14529	B11	13883		F12	30148	31396	33411	F12	31651.6667
B12	15192	15384	16099	B12	15558.3333		G01	20200	21300	22399	G01	21299.6667
C01	15000	14886	15506	C01	15130.6667		G02	15672	16570	17949	G02	16730.3333
C02	19398	19310	20296	C02	19668		G03	14782	15139	16248	G03	15389.6667
C03	20366	21082	21666	C03	21038		G04	25523	26588	28996	G04	27035.6667
C04	18621	19380	20305	C04	19435.3333		G05	18778	19049	19982	G05	19269.6667
C05	20008	20131	20820	C05	20319.6667		G06	17993	18481	20035	G06	18836.3333
C06	19939	20017	20925	C06	20293.6667		G07	75043	70226	66561	G07	70610
C07	16998	17618	18359	C07	17658.3333		G08	17687	18595	19659	G08	18647
C08	21605	22295	24162	C08	22687.3333		G09	21972	22591	23534	G09	22699
C09	26919	27260	28795	C09	27658		G10	25305	26474	28734	G10	26837.6667
C10	23106	23857	24729	C10	23897.3333		G11	18377	18953	20803	G11	19377.6667
C11	23726	24363	24755	C11	24281.3333		G12	23150	23857	25209	G12	24072
C12	16195	16361	17303	C12	16619.6667		H01	22216	23446	24921	H01	23527.6667
D01	17871	18063	19424	D01	18452.6667		H02	16605	17504	19049	H02	17719.3333
D02	14354	14860	15419	D02	14877.6667		H03	30261	30654	32373	H03	31096
D03	14293	15009	15881	D03	15061		H04	22783	24371	26370	H04	24508
D04	21108	21213	22077	D04	21466		H05	8063	8377	8970	H05	8470
D05	17705	17879	18577	D05	18053.6667		H06	16387	17094	18298	H06	17259.6667
D06	19555	20349	21492	D06	20465.3333		H07	17338	17958	19302	H07	18199.3333
D07	24415	24869	25183	D07	24822.3333		H08	15314	15427	16370	H08	15703.6667
D08	20986	21902	23551	D08	22146.3333		H09	17251	17644	18804	H09	17899.6667
D09	19162	19328	19773	D09	19421		H10	22932	24110	25994	H10	24345.3333
D10	16248	16640	17565	D10	16817.6667		H11	27356	27923	29380	H11	28219.6667
D11	14005	14241	14834	D11	14360		H12	17120	18272	20008	H12	18466.6667
D12	17583	18202	19537	D12	18440.6667					average:		20442.0694

Table S2: Measures of the luciferase activity of plate figure 1 with MS2-UPF2 strain.
Reading 2 was performed 2 minutes after reading 1 and reading 3 was performed 2 minutes after reading 2.
Amlexanox position (G07) is highlight

					average						
well	reading	reading	reading	well	readings 1-3		E01	26012	26771	26762	E01	26515
A01	27478	26710	26911	A01	27033		E02	24459	24206	24502	E02	24389
A02	17382	17932	18228	A02	17847.3333		E03	21911	21597	21867	E03	21791.6667
A03	15611	15410	15541	A03	15520.6667		E04	37111	37050	38010	E04	37390.3333
A04	22591	23080	23429	A04	23033.3333		E05	23272	22740	22949	E05	22987
A05	16091	16082	16283	A05	16152		E06	20925	20820	21090	E06	20945
A06	48420	49711	50209	A06	49446.6667		E07	40209	40401	40837	E07	40482.3333
A07	20235	21021	21213	A07	20823		E08	40383	38813	39607	E08	39601
A08	34144	33708	33734	A08	33862		E09	18333	18202	18604	E09	18379.6667
A09	18612	18979	19005	A09	18865.3333		E10	21492	21536	21073	E10	21367
A10	32408	32530	33054	A10	32664		E11	26439	25532	25898	E11	25956.3333
A11	19921	20619	20951	A11	20497		E12	13246	13604	14372	E12	13740.6667
A12	29031	28691	28787	A12	28836.3333		F01	23621	23534	23813	F01	23656
B01	17286	17382	17321	B01	17329.6667		F02	17844	17652	17906	F02	17800.6667
B02	15471	15392	15689	B02	15517.3333		F03	27373	26789	27460	F03	27207.3333
B03	29965	29607	29598	B03	29723.3333		F04	30488	30261	30288	F04	30345.6667
B04	20619	21160	21169	B04	20982.6667		F05	26117	25584	25846	F05	25849
B05	19337	19197	19206	B05	19246.6667		F06	24878	25052	24904	F06	24944.6667
B06	25986	25951	26274	B06	26070.3333		F07	24991	25131	25471	F07	25197.6667
B07	30384	29747	28822	B07	29651		F08	28542	28769	29677	F08	28996
B08	21300	20942	20707	B08	20983		F09	25864	26117	26518	F09	26166.3333
B09	35244	35427	36605	B09	35758.6667		F10	25357	25096	25070	F10	25174.3333
B10	50060	51221	51797	B10	51026		F11	27993	28254	28577	F11	28274.6667
B11	23124	22705	22975	B11	22934.6667		F12	26387	26570	27574	F12	26843.6667
B12	19389	19223	19171	B12	19261		G01	18647	19049	19834	G01	19176.6667
C01	30069	30898	30628	C01	30531.6667		G02	40034	40671	42111	G02	40938.6667
C02	16509	17007	17836	C02	17117.3333		G03	22530	22879	24145	G03	23184.6667
C03	16474	16562	16745	C03	16593.6667		G04	28813	29965	30436	G04	29738
C04	45209	45863	46849	C04	45973.6667		G05	40872	41893	43979	G05	42248
C05	24537	25340	26186	C05	25354.3333		G06	26963	26937	27478	G06	27126
C06	32286	32007	32740	C06	32344.3333		G07	73882	66073	64659	G07	68204.6667
C07	37582	37626	38909	C07	38039		G08	20017	19738	20043	G08	19932.6667
C08	27626	27984	28473	C08	28027.6667		G09	30706	31352	33028	G09	31695.3333
C09	19389	19598	19817	C09	19601.3333		G10	17461	17879	18516	G10	17952
C10	31378	31998	32600	C10	31992		G11	22164	22042	22408	G11	22204.6667
C11	22426	22600	23473	C11	22833		G12	16579	16509	17242	G12	16776.6667
C12	17661	17844	18132	C12	17879		H01	24267	24494	24904	H01	24555
D01	30165	30035	30881	D01	30360.3333		H02	19040	19197	19494	H02	19243.6667
D02	20209	20654	20916	D02	20593		H03	31806	31797	31937	H03	31846.6667
D03	27373	28097	28839	D03	28103		H04	24188	24354	25131	H04	24557.6667
D04	27958	28420	29345	D04	28574.3333		H05	11256	11684	12330	H05	11756.6667
D05	18630	18420	18560	D05	18536.6667		H06	25567	25942	26230	H06	25913
D06	24720	25131	25689	D06	25180		H07	28630	29162	30558	H07	29450
D07	30925	31003	32050	D07	31326		H08	18298	18892	19974	H08	19054.6667
D08	19982	20227	20358	D08	20189		H09	21588	21605	22059	H09	21750.6667
D09	17146	17356	17548	D09	17350		H10	29668	30131	31012	H10	30270.3333
D10	19642	19790	20139	D10	19857		H11	32050	32958	33464	H11	32824
D11	17757	17836	18202	D11	17931.6667		H12	14677	15105	15611	H12	15131
D12	26893	27382	27783	D12	27352.6667					average:		25981.6458

Table S3: Measures of the luciferase activity of plate figure 1 with MS2-UPF3 strain.
Reading 2 was performed 2 minutes after reading 1 and reading 3 was performed 2 minutes after reading 2.
Amlexanox position (G07) is highlight

					average							
well	reading	reading	reading	well	readings 1-3		E01	18822	18586	18918	E01	18775.3333
A01	18377	18324	18647	A01	18449.3333		E02	18385	19014	19947	E02	19115.3333
A02	14590	15288	15436	A02	15104.6667		E03	17016	17748	18473	E03	17745.6667
A03	18813	18918	19145	A03	18958.6667		E04	23944	24511	25785	E04	24746.6667
A04	19921	20488	20890	A04	20433		E05	23202	23577	24598	E05	23792.3333
A05	15384	15235	15480	A05	15366.3333		E06	17679	17783	18289	E06	17917
A06	20654	21893	22138	A06	21561.6667		E07	29110	29424	30165	E07	29566.3333
A07	26954	27670	28499	A07	27707.6667		E08	20296	20907	21815	E08	21006
A08	14703	15279	15375	A08	15119		E09	21501	21946	22661	E09	22036
A09	27504	29031	29040	A09	28525		E10	20427	20864	21457	E10	20916
A10	39886	40863	41867	A10	40872		E11	23324	24782	25515	E11	24540.3333
A11	16693	17469	17801	A11	17321		E12	22827	22844	23455	E12	23042
A12	14939	15750	15995	A12	15561.3333		F01	26483	25829	26230	F01	26180.6667
B01	35471	36221	37478	B01	36390		F02	22652	22757	23464	F02	22957.6667
B02	15043	15349	15715	B02	15369		F03	25078	25017	25750	F03	25281.6667
B03	14913	15035	15689	B03	15212.3333		F04	18743	18979	19153	F04	18958.3333
B04	17495	17714	18019	B04	17742.6667		F05	24293	24328	25192	F05	24604.3333
B05	22460	23246	23351	B05	23019		F06	29319	29764	31553	F06	30212
B06	18673	18848	19703	B06	19074.6667		F07	22469	22836	24319	F07	23208
B07	12321	12426	12766	B07	12504.3333		F08	28734	29284	30916	F08	29644.6667
B08	27338	27286	27260	B08	27294.6667		F09	25925	24738	26099	F09	25587.3333
B09	20323	20576	20864	B09	20587.6667		F10	18342	18499	19502	F10	18781
B10	20113	20314	20349	B10	20258.6667		F11	24816	25357	26719	F11	25630.6667
B11	13691	14119	14502	B11	14104		F12	24747	25619	27103	F12	25823
B12	27975	29214	30959	B12	29382.6667		G01	36282	36544	37897	G01	36907.6667
C01	19939	20628	21344	C01	20637		G02	26597	27705	29607	G02	27969.6667
C02	18045	18246	18839	C02	18376.6667		G03	21605	22251	23368	G03	22408
C03	17661	18036	18272	C03	17989.6667		G04	21789	22862	24249	G04	22966.6667
C04	17085	17260	17975	C04	17440		G05	13290	13525	14153	G05	13656
C05	20157	20227	21003	C05	20462.3333		G06	20218	20942	21981	G06	21047
C06	29083	29642	30261	C06	29662		G07	72504	65619	61343	G07	66488.6667
C07	18830	19136	19590	C07	19185.3333		G08	16012	16474	17007	G08	16497.6667
C08	20000	20541	21169	C08	20570		G09	24241	24729	26300	G09	25090
C09	16710	17251	18028	C09	17329.6667		G10	15017	15366	16003	G10	15462
C10	19180	19817	20698	C10	19898.3333		G11	21981	22321	23385	G11	22562.3333
C11	30462	30872	31658	C11	30997.3333		G12	34877	37085	39109	G12	37023.6667
C12	32085	34127	34895	C12	33702.3333		H01	13778	14703	15742	H01	14741
D01	17766	18124	19005	D01	18298.3333		H02	14180	14921	15698	H02	14933
D02	23516	24005	24790	D02	24103.6667		H03	34520	34179	35130	H03	34609.6667
D03	27652	28874	30994	D03	29173.3333		H04	30349	32687	34127	H04	32387.6667
D04	19913	20157	20698	D04	20256		H05	9127	9729	10026	H05	9627.33333
D05	18857	19014	19555	D05	19142		H06	22155	23621	24712	H06	23496
D06	26021	26597	27844	D06	26820.6667		H07	22173	23054	24328	H07	23185
D07	15384	15689	16099	D07	15724		H08	23743	24991	26213	H08	24982.3333
D08	21710	22312	22670	D08	22230.6667		H09	23394	23769	24982	H09	24048.3333
D09	18150	18612	19450	D09	18737.3333		H10	32818	34415	36500	H10	34577.6667
D10	14869	14721	15201	D10	14930.3333		H11	37137	38193	40497	H11	38609
D11	28246	29267	31448	D11	29653.6667		H12	19066	20078	21413	H12	20185.6667
D12	18289	18464	19267	D12	18673.3333					average:		23056.7049

Table S4: Measures of the luciferase activity of plate figure 1 with MS2-UPF3X strain.
Reading 2 was performed 2 minutes after reading 1 and reading 3 was performed 2 minutes after reading 2.
Amlexanox position (G07) is highlight

Additional file 1 Tables S1 to S4: measures of the luciferase activity obtained with the plate presented Figure 1 for the 4 MS2-UPF strains. For each strain, the plate was read 3 times by the luminometer (reading 1 to 3) in order to control the luminometer variability. It is an average of these 3 readings that is presented Figure 1.

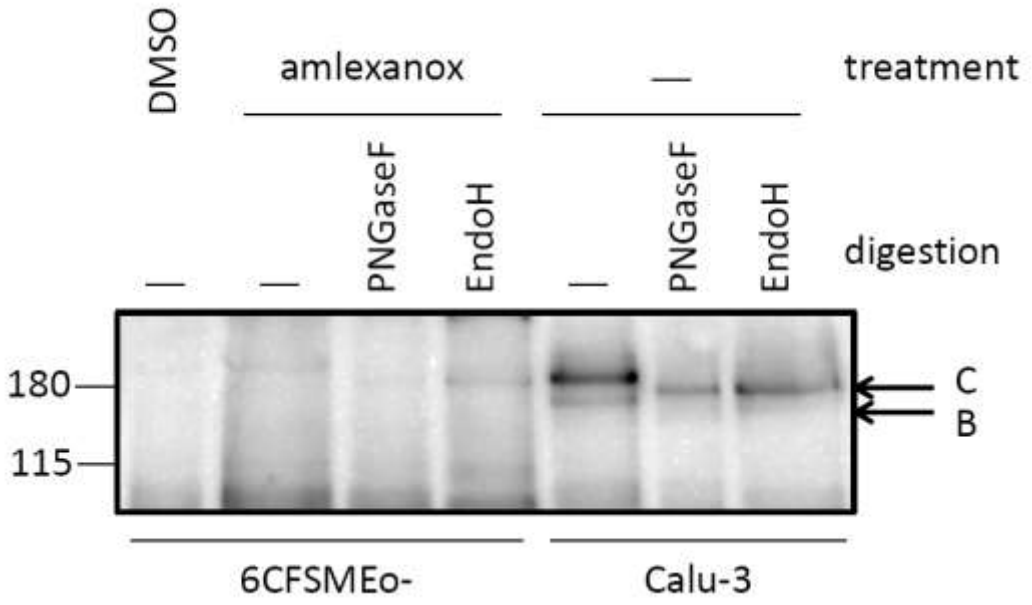

Additional file 2 Figure S1: Analysis of the glycosylation status of CFTR in 6CFSMEo- treated with DMSO or 25 µM of amlexanox for 24 hours and Calu-3 cells. 1/10 of CFTR immunoprecipitation from Calu-3 cells and 1/2 of CFTR immunoprecipitation from 6CFSMEo-cells were analyzed by western-blot. Molecular weight marker is indicated on the left side of the gel. Band B (B) and band C (C) are indicated on the right side of the gel. This analysis is representative of three independent experiments.

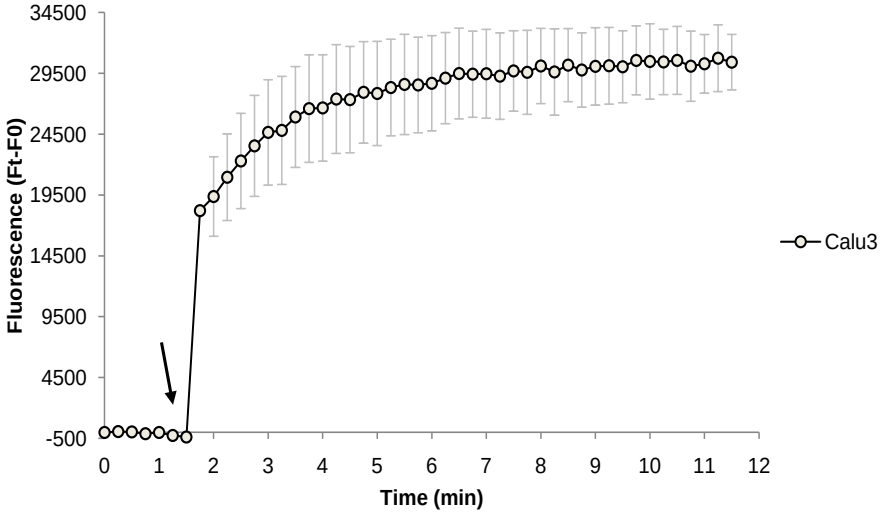

Additional file 3 Figure S2: Measure of iodide transport through Calu-3 cell membrane using halide-sensitive fluorophore SPQ assay. At time (t) = 2 min cAMP-stimulating cocktail was added (arrow). The increase in iodide efflux is shown as mean ± SEM from at least four independent experiments. Ft represents the measure of the fluorescence at the reading time; F0 is an average fluorescence before addition of cAMP agonists.

2. Project 2: Caspases shut down nonsense-mediated mRNA decay during apoptosis

2. 1 A summary for the project

Nonsense mutation-containing mRNAs can be degraded by a quality control called NMD to prevent the synthesis of deleterious or non functional truncated proteins. In our lab we used screening system to identify molecules that can inhibit NMD. Among the selected molecules, we found the doxorubicin which is a very well known as a putative NMD inhibitor. Based on that, we investigated on the possibility that NMD is inhibited during apoptosis. I compared several apoptosis inducers such as doxorubicin, staurosporine, cis-platin, etoposide or apoptosis activator 2 and validate the result of the screen and our hypothesis since with all these molecules I observed an inhibition of NMD. For product availability reason, I mainly used staurosporine but most of the results were also confirmed with another apoptosis inducer. I found staurosporine can increase the mRNA level of nonsense mutation-containing mRNAs and cleave NMD factors (UPF1 protein at position 37 and UPF2 protein at position 741) and these effects can be reversed by a pan-caspase inhibitor, which demonstrated that during apoptosis some NMD factors are cleaved by caspases and NMD is inhibited. I also identified caspase 3 and caspase 7 as the caspases responsible for the UPF protein cleavages. I demonstrated that the NMD inhibition observed on cell culture also occurs in vivo after injection of anti-Fas antibody in mice to induce a massive liver apoptosis. My study also provide new insight in the property of N and C terminal domain of UPF1 and UPF2 since I showed that N-terminal domain of UPF1 and UPF2 can induce apoptosis and C-terminal domain of UPF1 and N-terminal domain of UPF2 are NMD inhibitors.

This result has been accepted for publication in Cell Death and Differentiation

2.2 Results

Title: Caspases shut down nonsense-mediated mRNA decay during apoptosis

Running Title: apoptosis inhibits NMD

Authors: Jieshuang Jia[1,2,3], Alessandro Furlan[1,2,3], Sara Gonzalez-Hilarion[4], Catherine Leroy[1,2,3], Dieter C Gruenert[5,6], David Tulasne[1,2,3] and Fabrice Lejeune[1,2,3]*

[1] Université de Lille, FRE 3642, Lille, France

[2]CNRS UMR 8161, Institut de Biologie de Lille, Lille, France

[3] Institut Pasteur de Lille, Lille, France

[4]Unité Biologie et Pathogénicité Fongiques, Institut Pasteur, 25 rue du Dr Roux, 75015 Paris

[5]Department of Otolaryngology-Head and Neck Surgery, Eli and Edythe Broad Center for Regenerative Medicine and Stem Cell Research, Helen Diller Family Comprehensive Cancer Center, Institute for Human Genetics, Cardiovascular Research Institute, University of California, San Francisco, San Francisco, CA, USA

[6]Department of Pediatrics, University of Vermont College of Medicine, Burlington, VT, USA

*Corresponding author – E-mail: fabrice.lejeune@inserm.fr

Keywords: NMD, apoptosis, caspase, mRNA quality control, UPF protein, cell death

Abstract

Nonsense-mediated mRNA decay (NMD) is an mRNA surveillance mechanism that plays integral roles in eliminating mRNAs with premature termination codons to prevent the synthesis of truncated proteins that could be pathogenic. One response to the accumulation of detrimental proteins is apoptosis, which involves the activation of enzymatic pathways leading to protein and nucleic acid cleavage and culminating in cell death. It is not clear whether NMD is required to ensure the accurate expression of apoptosis genes or is no longer necessary since cytotoxic proteins are not an issue during cell death. The present study shows that caspases cleave the two NMD factors UPF1 and UPF2 during apoptosis impairing NMD. Our results demonstrate a new regulatory pathway for NMD that occurs during apoptosis and provide evidence for role of the UPF cleaved fragments in apoptosis and NMD inhibition.

Introduction

Cell death is a natural process that occurs throughout development and the life of a multicellular organism removing cells that are no longer needed or have become pathogenic, thereby organizing tissues and participating in their homeostasis. There are many pathways leading to cell death that are activated by numerous external and/or internal stimuli (Elmore 2007). Cell death can occur via programmed processes such as apoptosis, autophagy, necrosis (a more passive process) or necroptosis (a type of programmed necrosis) (Galluzzi, Vitale et al. 2012).Apoptosis can be activated either through extrinsic or intrinsic pathways that involve programmed cell-death receptors or mitochondria, respectively.

During apoptosis, specific gene networks and protein-cleavage programs are activated sending the cells on a death spiral (Zhang, Yang et al. 2002; Reimertz, Kogel et al. 2003; Johnson, Sengupta et al. 2004) through a family of cysteine-aspartate proteases (caspases) (Alnemri, Livingston et al. 1996). Caspases are classified by their role in the apoptotic pathway, into (i) initiator caspases (such as caspases 2, 8, 9 and 10) or (ii) effector caspases (such as caspases 3, 6 or 7) (Frejlich, Rudno-Rudzinska et al. 2013). Initiator caspases cleave the inactive precursor of the effector caspases (pro-caspases) into their active forms. Effector caspases are then responsible for cleaving protein targets to interfere with cellular processes, and in particular, with the activation of some endonucleases that degrade genomic DNA.

Throughout the process of mRNA maturation, numerous quality control mechanisms verify the integrity of the information carried by mRNAs. One of these, nonsense-mediated mRNA decay (NMD), leads to the rapid decay of mRNAs harboring a premature termination codon (PTC) to prevent the synthesis of non-functional and/or potentially detrimental truncated

proteins (Muhlemann, Eberle et al. 2008; Karam, Wengrod et al. 2013; Popp and Maquat 2014). In addition to its role in quality control, NMD also regulates gene expression of so-called natural substrates of NMD (Sureau, Gattoni et al. 2001; Mendell, Sharifi et al. 2004; Wollerton, Gooding et al. 2004; Lareau, Inada et al. 2007; Viegas, Gehring et al. 2007). NMD has been observed in all eukaryotic organisms studied and appears to operate according to species-specific mechanisms (Conti and Izaurralde 2005). Proteins that play a central role in NMD, such as UPF1, UPF2, UPF3 (UPF3a), and UPF3X (UPF3b) are highly conserved from yeast to human. The requirement for these UPF proteins in NMD is illustrated by the fact that the down-regulation of any one of them results in an inhibition of NMD (Mendell, ap Rhys et al. 2002; Chan, Bhalla et al. 2009). UPF proteins are sequentially loaded onto the mRNP with the initial recruitment of UPF3 or UPF3X by a protein complex located 20-24 nucleotides upstream of all exon-exon junctions (EJC or exon junction complex) (Le Hir, Izaurralde et al. 2000; Le Hir, Moore et al. 2000). UPF3 or UPF3X then recruits UPF2 and finally UPF1 into the complex. UPF1 is then subjected to a cycle of phosphorylation and dephosphorylation if the mRNA harbors a PTC, initiating exoribonucleolytic as well as endoribonucleolytic cleavage of the PTC-containing mRNA (Cao and Parker 2003; Lejeune, Li et al. 2003; Mitchell and Tollervey 2003; Huntzinger, Kashima et al. 2008; Eberle, Lykke-Andersen et al. 2009). NMD is a necessary component in the development and maintenance of healthy cells and organisms. For example, UPF1 is an essential gene since inactivation of UPF1 protein leads to early embryonic death in mouse (Medghalchi, Frischmeyer et al. 2001), thus implicating NMD as a critical proof-reading and/or regulatory component in early organismal development. However, the question of whether NMD is

required after cells have committed to proceed along a pathway that culminates in cell death has not been investigated. To address this question, NMD efficiency was studied during apoptosis. The studies presented here show that NMD factors UPF1 and UPF2 are cleaved by caspases 3 and 7 during apoptosis. The functional consequences of these cleavages are a general shutdown of NMD activity leading to stabilization of both PTC-containing mRNAs and natural substrates of NMD, and also the production of caspase-cleaved UPF fragments that induce apoptosis and inhibit NMD. Furthermore, our studies show that NMD inhibition during apoptosis occurs both in tissue culture models and in mice.

Results

UPF proteins are cleaved during apoptosis

Since apoptosis effectors such as caspases target various proteins (Shi 2004), studies were carried out to investigate the possibility that components of the NMD system could themselves be targets. Putative caspase cleavage sites in UPF proteins were identified using the Support Vector Machine technology for predicting caspase substrate cleavage sites (Wee, Tan et al. 2006). As shown in supplementary Figure S1, several putative caspase cleavage sites are present in human UPF1, UPF2 or UPF3X. This suggests that these proteins could be targeted by caspases during apoptosis.

To determine if UPF proteins are targeted for degradation during apoptosis, the detection of the full-length proteins and putative UPF cleavage fragments was assessed in apoptotic cells. As an initial step, HeLa cells, incubated with increasing amounts of staurosporine (Zwelling, Altschuler et al. 1991; Koh, Wie et al. 1995), were assayed for the rate of apoptosis after 24

hrs by quantifying the incorporation of annexin V and propidium iodide into the cells (Figure 1A). This shows that treatment with 2 or 4 µM staurosporine results in about 50% apoptotic cells. At higher staurosporine concentrations, killing was much quicker and more extensive and therefore unsuitable for further NMD efficiency analysis (data not shown). Subsequent studies used 2 µM staurosporine as a working concentration combined with a 24 hrs exposure.

Next, HeLa cells were incubated with staurosporine as described above using caspase cleavage of PARP or caspase 3 proteins to monitor caspase activation (Figure 1B) and any variations in the levels of UPF proteins (Figure 1C). UPF1 and UPF2 protein levels were lower in cells treated with staurosporine compared to those exposed to DMSO alone. An about 110 kDa UPF1 cleavage fragment was detected in staurosporine-treated extracts using an anti-UPF1 antibody, raised against the C-terminus of UPF1, that corresponds to the molecular weight expected for a UPF1 C-terminal fragment that would be generated upon cleavage at the putative caspase cleavage sites $EFTD_{37}$ or $DEED_{111}$ (supplemental Figure S1).

Western-blot analysis of UPF2 protein with an antibody recognizing the amino terminal residues identified a new UPF2 isoform of about 75kDa in staurosporine-treated cells (Figure 1C). This UPF2 isoform appears to correspond to the expected N-terminal fragment generated by a cleavage either after $DLID_{585}$ or $MHLD_{741}$ (supplemental Figure S1).

UPF3X level was not affected and additional fragments were not detected by staurosporine treatment even though there are at least two putative canonical caspase cleavage sites present in this protein (Figure 1C and supplemental Figure S1). Overall, the results show that staurosporine-induced apoptosis reduced the level of UPF1 and UPF2 proteins suggesting a

possible inhibition of NMD during apoptosis. Specifically, the putative UPF1 caspase cleavage site would separate the N-terminal conserved region of UPF1, shown to be essential for the function of UPF1 in NMD (Kashima, Yamashita et al. 2006), from the rest of the protein (Figure 2). Little is known about the role of UPF2 in NMD; however, a recent study has shown that the first and/or the second MIF4G domains of UPF2 are essential for NMD (Clerici, Deniaud et al. 2013). Given that the UPF2 caspase cleavage site is predicted to be located in the second middle domain of eIF4G (MIF4G) (Figure 2), UPF2 would become nonfunctional during apoptosis following it cleavage by caspases.

To identify of the UPF protein species detected by Western-blot in the presence of staurosporine, UPF1 or UPF2 were targeted with siRNAs and almost abolished UPF1 or UPF2 related bands, respectively, but not the non-specific bands (supplemental Figure S2A).

To evaluate if UPF1 and UPF2 protein cleavage was restricted to staurosporine, the other apoptosis activators were assessed for their effect on the integrity of both UPF proteins (supplemental Figure S2B). These studies showed that anisomycin, etoposid, apoptosis activator 2 and cisplatin also promote cleavage of UPF1 and UPF2, indicating that the effect of staurosporine is not specific to staurosproine, but may be a generalized feature of apoptosis inducers (supplemental Figures S2B and S5).

A caspase inhibitor prevents UPF factors cleavage during apoptosis

To investigate the possible role of caspases in the cleavage of NMD factors UPF1 and UPF2 during apoptosis, HeLa cells were incubated with staurosporine in the presence or in the absence of benzyloxycarbonyl-Val-Ala-DL-Asp-fluoromethylketone (zVAD-fmk), a pan-caspase

inhibitor. As expected, staurosporine-induced apoptosis, as measured using the annexin V staining assay (Figure 3A) and caspase activation, was reversed in the presence of the zVAD-fmk since there was no detectable cleavage of either PARP or caspase 3 (Figure 3B).

To demonstrate that caspases are responsible for the cleavage of NMD factors UPF1 and UPF2 after staurosporine treatment, the levels of UPF1 and UPF2 proteins in cells incubated with or without zVAD-fmk were analyzed by western blotting (Figure 3C). As expected (Figure 1), staurosporine treatment decreased the levels of full-length UPF1 and UPF2 and showed the appearance of UPF1 and UPF2 cleavage products (Figure 3C). In contrast, in the presence of staurosporine and zVAD-fmk, the levels of full-length UPF1 and UPF2 were almost identical to those in the presence of the DMSO vehicle control, and no UPF1 and UPF2 cleavage products were detected (Figure 3C). Overall, these results indicate that caspases are responsible for the cleavage of UPF1 and UPF2 during apoptosis.

Caspase 3 and caspase 7 can cleave UPF1 and UPF2 NMD factors

To identify the caspases responsible for UPF1 and UPF2 cleavage, HeLa-cell extracts were incubated with purified caspases 3, 6, 7, 8 or 9. The results indicate that UPF1 and UPF2 levels were reduced in the presence of caspase 3 (Figure 4). Consistent with fragments generated during apoptosis (Figures 1 and 3), a shorter isoform of UPF1 of about 110kDa, corresponding to a C-terminal UPF1 fragment, and the cleavage product of UPF2 of about 75kDa, corresponding to the N-terminal UPF2 fragment, were also detected after treatment of the HeLa cell extract with caspase 3.

Although the amount of full-length UPF1 and UPF2 proteins decreased in the presence of

caspase 7, no cleavage fragments were detected. This suggests that caspase 7 generated cleavage fragments that are unstable or that the presence of another protease activity in the purified caspase 7 solution making the UPF1 and UPF2 cleavage fragments undetectable. Nevertheless, the results presented in Figure 4 indicate that UPF1 and UPF2 are targeted by caspase 3 and/or caspase 7 suggesting that NMD can be inhibited during apoptosis.

NMD is inhibited during staurosporine- or apoptosis activator 2-induced apoptosis

To characterize the functional consequences of UPF1 and UPF2 cleavage during apoptosis, the efficiency of NMD was first measured in HeLa cells. Cells were transfected with □-*globin* gene expression vectors encoding mRNA that was either wild-type (Norm) or harbored a nonsense mutation at codon 39 (Ter) which is an NMD target (Thermann, Neu-Yilik et al. 1998; Zhang, Sun et al. 1998). After a 24 hrs exposure to 2 µM staurosporine or DMSO (negative control), the level of globin Ter mRNA in the cells was about 3 times higher in the presence of staurosporine than in the presence of DMSO alone, as determined using quantitative RT-PCR (Figure 5A). These results indicate that NMD is inhibited during apoptosis induced by staurosporine.

The efficiency of NMD during apoptosis was also evaluated in other cell lines that produce an endogenous mutated mRNA targeted for NMD. Immortalized cystic fibrosis (CF) airway epithelial cells, IB3, that contain one *CF transmembrane conductance regulator* (*CFTR*) allele harboring the W1282X nonsense mutation and the other allele harboring a F508del mutation or, alternatively, 6CFSMEo-, that contains one *CFTR* allele harboring the Q2X nonsense mutation and the other allele harboring the F508del mutation (Supplemental

Figure S3) (Cozens, Yezzi et al. 1992; da Paula, Ramalho et al. 2005) were also assayed. Previous studies demonstrated that no or extremely low CFTR protein is detected in these cell lines (Hamosh, Rosenstein et al. 1992; da Paula, Ramalho et al. 2005). We first determined that 2 □M staurosporine was the lowest concentration that provided efficient apoptosis in each cell line (Supplemental Figure S3A) even though this level of apoptosis is about 2 fold less than that obtained in HeLa cells. Under these conditions, CFTR mRNA levels were about 2.5 to 4 fold higher in the presence of staurosporine than in the presence of DMSO alone (Supplemental Figure S3B). Inhibition of NMD in the presence of staurosporine was even greater than that observed in the presence of amlexanox, a molecule we recently identified as an inhibitor of NMD (Gonzalez-Hilarion, Beghyn et al. 2012). This observation suggests that staurosporine could be a more efficient NMD inhibitor than amlexanox (Supplemental Figure S3B). To evaluate whether the staurosporine effect observed on PTC-containing mRNAs was not the result of a general increase in transcription, the level of CFTR pre-mRNA was assayed and shown not to significantly change in the presence of staurosporine (Supplemental Figure S4). Overall, these results demonstrate that NMD can be inhibited in several cell-types during staurosporine-induced apoptosis and are consistent with the notion that caspase-cleaved UPF1 and UPF2 impair NMD during the process of apoptotic programmed cell death. Due to the higher level of apoptosis measured in HeLa cells when compared to that in IB3 and 6CFSMEo- cells, further experiments were performed in HeLa cells.

Since NMD is inhibited during apoptosis, studies were undertaken to determine whether natural substrates of NMD were also stabilized during apoptosis. The mRNA levels of three

different natural NMD substrates, i.e., SC35, NAT9 and TBL2 (Sureau, Gattoni et al. 2001; Mendell, Sharifi et al. 2004; Viegas, Gehring et al. 2007), were measured in cells incubated with staurosporine or DMSO. The mRNA levels of these three substrates were compared to the level of three reference mRNAs that are not subject to NMD (i.e. GAPDH, Actin or RPL32 mRNA). The level of the three natural substrates of NMD showed a two to four fold of increase compared to the level of the three reference mRNAs (Figure 5B). This result shows that the NMD regulation occurring on natural substrates of NMD is also inhibited during apoptosis.

To demonstrate the involvement of caspases in the inhibition of NMD during apoptosis, NMD efficiency was assessed in the presence of zVAD-fmk. The Figure 6 shows that NMD inhibition caused by staurosporine treatment was also reversed in the presence of zVAD-fmk, consistent with the previous findings (Figure 3) showing that NMD inhibition occurring during apoptosis involves caspase activity. It is noteworthy that the presence of the zVAD-fmk alone had no effect on NMD efficiency when apoptosis is not activated, likely because caspases are not in play (Figure 6).

To exclude the possibility that UPF1 and UPF2 cleavage, and NMD inhibition observed during apoptosis is an indirect effect related to staurosporine exposure, NMD was evaluated after exposure to another inducer of apoptosis, apoptosis activator 2 (AA2) (Nguyen and Wells 2003). AA2 activates caspases in a cytochrome c dependent manner to potentiate apoptosis. After a 16 hrs exposure to 50 □M AA2 more than 20% of the HeLa cells went through apoptotic cell death (supplemental Figure S5A). Under these conditions, the level of exogenous Globin Ter mRNA was about 4 fold higher than in vehicle-treated cells

(supplemental Figure S5B). AA2 exposure also caused a decrease of the full-length UPF1 and UPF2 proteins, and the appearance of caspase cleavage products, thereby demonstrating that different inducers of apoptosis can also inhibit NMD (supplemental Figure S5C).

Caspase cleavage fragments from UPF1 or UPF2 are inducers of apoptosis and/or NMD inhibitors

The presence of cleaved UPF1 or UPF2 fragments during apoptosis in cells treated with staurosporine or AA2 raises the question of their role in NMD inhibition and/or in apoptosis. The specific identity of the caspase cleavage sites in the UPF1 and UPF2 proteins was deteremined by mutating aspartic acid to asparagine at positions 37 or 111 in UPF1 and 585 or 741 in UPF2 to block caspase cleavage. CFP-tagged constructs were used in order to discriminate full-length proteins and their cleavage products from their endogenous counterparts. Overexpression of the full-length wild-type or D111N UPF1 transgene, showed a baseline presence of the UPF1 cleavage fragment that increased in the presence of staurosporine. No cleavage fragment was detected with the full-length D37N UPF1 construct (Figure 7A). With regard to UPF2, the caspase cleavage product was not detected under any conditions using the CFP-UPF2 constructs for reasons that remain unclear. A decrease in full-length CFP-UPF2 protein was observed with the wild-type or the D585N UPF2 construct, while no decrease was observed with the D741N UPF2 construct (Figure 7B). These results indicate that the caspase cleavage site in UPF1 is located at position 37 in UPF1 and at position 741 in UPF2 (Figure 7).

To evaluate the impact of N- or C-terminal UPF1 or UPF2 fragments generated by caspase

cleavage on apoptosis, HeLa cells were transfected with an expression vector encoding a CFP-fusion peptide with the N-terminal part of UPF1 (amino-acids 1 to 37: CFP UPF1-Nter), C-terminal part of UPF1 (amino-acids 38 to 1118: CFP UPF1-Cter), N-terminal part of UPF2 (amino-acids 1 to 741: CFP UPF2-Nter) or the C-terminal part of UPF2 (amino-acids 742 to 1272: CFP UPF2-Cter) corresponding to each UPF1 or UPF2 caspase-cleaved fragments. Protein expression and apoptosis were analyzed 48 hours after transfection. The expression level of each exogenous caspase cleaved UPF protein fragments was assessed by western-blotting analysis (Supplemental Figure S6). At the expression levels of exogenous UFP1 or UFP2 fragments indicated there was an ~ 10-fold increase in apoptosis in cells expressing the N-terminal caspase-cleavage fragment from UPF1 or UPF2, while cells expressing the C-terminal fragments or the full length UPF1 or UPF2 proteins showed no such increase (figure 8A). These results suggest that the N-terminal caspase-cleaved fragment from both UPF1 and UPF2 proteins promote apoptosis when they are generated in cells.

To determine the contribution of UPF caspase cleavage fragments to the rate of staurosporine-induced apoptosis, UPF1 or UPF2 were down-regulated with siRNAs (supplemental Figure S7). Although, UPF1 or UPF2 caspase cleavage fragments were not detectable in the presence of UPF1 or UPF2 siRNAs, respectively, the rate of staurosporine -induced apoptosis remains unchanged (supplemental Figure S7B), suggesting that the production of UPF1 and UPF2 apoptotic cleavage fragments play only a modest role in cell death and that this is likely due to the wide range of targets impaired during apoptosis even though the down-regulation by itself of UPF1 or UPF2 by siRNAs induces apoptosis.

To assess the effect of the caspase UPF1 and UPF2 cleaved fragments on NMD, HeLa cells were transfected with expression vectors encoding Globin Norm or Ter, MUP and one of the caspase-generated N- or C-terminal fragments, or the full length UPF1 or UPF2 (Figure 8B). Assessment of NMD at each condition showed about 2-3 fold NMD inhibition in cells expressing either the C-terminal fragment of UPF1 or the N-terminal fragment of UPF2. The dominant negative interference of the C-terminal fragment of UPF1 on NMD is consistent with what has been previously reported (Kashima, Yamashita et al. 2006). Interestingly, the N-terminal UPF2 fragment shows the capacity of both inducing apoptosis and inhibiting NMD.

Assessment of NMD inhibition during apoptosis in vivo

Our previous results indicate that NMD is inhibited as a consequence of activating the cell-intrinsic apoptotic pathway. To generalize these results we interrogated whether the activation of the cell-extrinsic (death receptor) apoptotic pathway is also able to inhibit NMD and whether the shutdown of NMD can occur *in vivo*. Accordingly, mice were injected with an agonistic anti-Fas antibody to ligate the Fas death receptor (CD95) and initiate cell-extrinsic apoptosis in hepatocytes as previously described (Lefebvre, Muharram et al. 2013). The impact of hepatic apoptosis on NMD was assessed through the analysis of liver mRNAs and proteins after anti-Fas antibody exposure. The apoptotic status of hepatocytes was monitored by the presence of cleaved caspase 3 (Figure 9A). As predicted for the human sequence, several putative caspase cleavage sites in mouse UPF3X were predicted *in silico* and caspase cleavage sites identified for UPF1 and UPF2 are conserved between mice and

human (supplemental Figure S1). In apoptotic livers, a decrease was observed in the level of UPF1 protein, without a corresponding decrease in UPF3X (Figure 9A). UPF1 cleavage products were not detected, suggesting that they may be more unstable *in vivo* than *in vitro* or that the apoptosis was too massive and the UPF cleavage fragments are already degraded at the time of the cell harvesting. Analysis of UPF2 levels was not possible, since none of the UPF2 antibodies used could detect mouse UPF2 protein (data not shown).

NMD efficiency in mice was measured by exploiting the conservation of the alternative splicing between human and mouse at intron 3 of the mouse *Srsf7* gene that encodes for the 9G8 splicing factor (Lejeune, Cavaloc et al. 2001; Lareau, Inada et al. 2007). The retention of intron 3 in Srsf7 mRNA introduces PTCs that leads to the degradation of this alternatively spliced mRNA by NMD (Lejeune, Cavaloc et al. 2001; Lareau, Inada et al. 2007). Quantification of the alternative Srsf7 transcripts in mice exposed to anti-Fas antibody showed a 5-fold increase in intron 3 containing mRNA transcript (i.e. NMD inhibition) compared to mice injected with saline (Figure 9B). General inhibition of splicing during apoptosis can be excluded since retention of intron 4 in Srsf7 mRNA was not detected in the PCR amplification product encompassing intron 3 to exon 5 used in this analysis (Figure 9B). Overall, the results in Figure 9 indicate that NMD is inhibited during apoptosis both *in vitro* and *in vivo*.

Discussion

During apoptosis, caspases target a wide panel of proteins to promote cell death. *In silico*

prediction programs reveal putative caspase cleavage sites in proteins encoding key NMD factors UPF1, UPF2 and UPF3X at least (Supplemental Figure S1), and we experimentally demonstrate that UPF1 and UPF2 but not UPF3X are cleaved during staurosporine-induced apoptosis (Figure 1) with initially putative cleavage sites at amino-acid 37 or 111 for UPF1 and at amino-acid 585 or 741 for UPF2 (Figure 2). These cleavages are prevented when the pan-caspase inhibitor zVAD-fmk is added in the presence of staurosporine, indicating that caspases are responsible for the cleavage of UPF proteins 1 and 2 during apoptosis (Figure 3). *In vitro* results implicate caspase 3 at least in mediating UPF1 and UPF2 cleavage (Figure 4). Due to the central role of UPF proteins in NMD, the functional consequence of the cleavage of NMD factors UPF1 and UPF2 is the inhibition of NMD, as demonstrated for transfected PTC-containing Globin mRNA as well as for endogenous nonsense mutation-containing genes and natural substrates of NMD in different cell lines (Figure 5 and Supplemental Figure S3). Moreover, staurosporine-induced NMD inhibition was reversed with the pan-caspase inhibitor, zVAD-fmk (Figure 6). These findings are further reinforced by the use of another apoptosis activator, apoptosis activator 2 (AA2), which confirmed the cleavage of UPF1 and UPF2 and the inhibition of NMD during apoptosis (Supplemental Figure S5). Together, these results indicate that both staurosporine and AA2 represent two new non-specific NMD inhibitors that may be useful as tools to study mechanisms that underlie NMD. Moreover, AA2 has also previously been shown to induce apoptosis via the activation of caspase 3 (Nguyen and Wells 2003). More importantly, this study demonstrates that the inhibition of NMD observed during apoptosis in cultured cells also extends to tissues undergoing apoptosis *in vivo* (Figure 9).

It was particularly noteworthy that apparently only UPF1 and UPF2 were targeted by caspases, while UPF3X was not, despite the presence of putative caspase cleavage sites in UPF3X (supplemental Figure S1). Targeting UPF1 to efficiently inactivate NMD is reasonable since all NMD pathways are unified by their requirement for UPF1, unlike UPF2 (Gehring, Kunz et al. 2005). The targeting of UPF2 by caspases suggests that either UPF2 plays a more central role in NMD than previously thought or other functions of UPF2 unrelated to its role in NMD must be inhibited for apoptotic cell death to progress. The absence of cleavages of UPF3X by caspases during apoptosis raises the hypothesis that UPF3X plays a role in apoptosis progression. Overall, these results suggest that NMD inhibition during apoptosis is a component of the apoptotic programmed response rather than a default response. It is possible that there are other proteins, such as SMG proteins or EJC components (also involved in the NMD) targeted by caspases to ensure the complete arrest of NMD. For example, proteins from the translation initiation complex have been shown to be targeted by caspases during apoptosis to block more than 60% of the protein synthesis (Clemens, Bushell et al. 2000). Among these proteins, eIF4G which plays a central role in the pioneer round of translation through its interaction with PABPC1 and CBP80, is targeted and inactivated by caspase 3 (Marissen and Lloyd 1998). Since down-regulation of eIF4G by siRNA or by viral proteases leads to the inhibition of NMD (Lejeune, Ranganathan et al. 2004), it is clear that NMD is also indirectly inhibited during apoptosis by cleavage of translation factors.

The work presented here shows that UPF1 and UPF2 cleavage occurs at positions D37 and D741, respectively (Figure 7) not only to inactivate both NMD factors *per se* but also to generate fragments that induce apoptosis (Figure 8A). However, this contribution to

apoptosis appears to be modest and is likely due to the wide spectrum of caspase targets that influence apoptosis (Zhang, Yang et al. 2002; Reimertz, Kogel et al. 2003; Johnson, Sengupta et al. 2004). Further investigations will be necessary to elucidate the mechanism underlying the induction of apoptosis by these UPF cleavage fragments, to identify the proteins that bind these fragments and in particular the highly conserved N-terminal UPF1 fragment for which there is, as yet, no clear function. With respect to UPF2, specific functions have not been correlated with the different regions of UPF2 other than the interaction domain in the C-terminal region with UPF1 and SMG1 (Clerici, Deniaud et al. 2013). This C-terminal region partially retains the UPF2 function in NMD and is consistent with findings showing a dominant negative effect of the N-terminal caspase-cleavage UPF2 fragment on NMD, which is not observed with the C-terminal caspase-cleavage fragment (Figure 8). Our study shows that the N-terminal part of UPF2 (amino-acids 1-741) has the dual property to induce apoptosis and to inhibit NMD making this region of interest to understand the function of the full length UPF2.

During apoptosis, various pathways that ultimately lead to cell death are either inhibited or activated. Until the present study, there was little known about the relationship between cellular quality control mechanisms such as NMD that maintain mRNA integrity and apoptosis. It has been assumed that quality control mechanisms remain in place during apoptosis to ensure the fidelity of proteins required for progression towards programmed death. However, NMD no longer appears to be required during apoptosis, given that the level of PTC-containing mRNAs increase in the presence of apoptosis activators (Figures 5, 6 and 9 and supplemental Figures S3 and S5). The levels of natural substrates of NMD are also

upregulated during apoptosis (Figure 5B and Figure 9B) which could promote apoptosis by allowing the expression of toxic proteins. The upregulation of natural substrates of NMD was not observed during the NMD inhibition by two other NMD inhibitors, NMDI 1 and amlexanox (Durand, Cougot et al. 2007; Gonzalez-Hilarion, Beghyn et al. 2012). The inhibition of NMD by the two last ones appears to be milder than the NMD inhibition observed during apoptosis. This difference in the level of NMD inhibition might be explained by the difference in the way to inhibit NMD since apoptosis promotes the cleavage of several central NMD factors and translation factors when NMDI 1 or amlexanox interfere with protein-protein interactions between NMD factors (Clemens, Bushell et al. 2000; Durand, Cougot et al. 2007) (Jia and Lejeune, unpublished data). This highlights the complexity of NMD and its putative regulation at different levels.

There are several reasons why NMD as a quality control mechanism or as a regulator of gene expression could become unnecessary during apoptosis. Since the goal of apoptosis is cell death, there is no further need to prevent the synthesis of harmful proteins including those synthesized by PTC-containing mRNAs. In contrast, one could imagine a scenario where NMD inhibition might facilitate cell death by allowing the synthesis of toxic truncated proteins that are normally repressed by NMD or alternatively the synthesis of proteins encoded by natural NMD substrates. It is also possible that most quality controls are, at the very least, inhibited if not shutdown completely during apoptosis to spare some energy required for the proper execution of apoptosis.

In this study, the results show a bidirectional link between NMD and apoptosis in the sense that apoptosis induces NMD inhibition and caspase-cleaved UPF fragments promote

apoptosis. The induction of apoptosis by NMD inhibition has previously been demonstrated during embryogenesis in particular. Apoptosis, as well as NMD, is essential during embryogenesis, and is involved in removing unnecessary cells to help shape and define tissues (Suzanne and Steller 2013) and organs. NMD is likely involved in degrading inaccurate mRNAs that could interfere with the normal developmental program. In the event of a molecular dysfunction, such as NMD arrest during embryogenesis, apoptosis and eventually embryonic lethality can occur. For instance, the absence of UPF1 in 3.5 days post coitum (dpc) results in blastocysts death by apoptosis (Medghalchi, Frischmeyer et al. 2001), while the lack of SMG1 leads to embryonic death at day 8.5 dpc by apoptosis (McIlwain, Pan et al. 2010). However, NMD inhibition *in vivo* does not always lead to activation of apoptosis. This is illustrated by the UPF2 knock-out mice that do not undergo apoptotic embryonic death (Thoren, Norgaard et al. 2010). Other examples include NMD inhibition by amlexanox where there is no effect on cell viability (Gonzalez-Hilarion, Beghyn et al. 2012), or more recently, by a new set of NMD inhibitors targeting the interaction between UPF1 and SMG7 proteins with a low cellular toxicity (Martin, Grigoryan et al. 2014). Whether NMD inhibition can activate apoptosis might be dependent on the degree of NMD inhibition.

Apoptosis impairs cell metabolism at different stages such as cell membrane shape, protein synthesis, post-translational processes or DNA integrity for instance. In addition, we show now that apoptosis can also act at the RNA level by interfering with the mRNA surveillance mechanism NMD. This supports the idea that apoptosis affects a large spectrum of cellular pathways by targeting their specific key components in order to reach very efficiently the cell death.

The data presented here demonstrate that apoptosis regulates NMD in addition to other already identified molecular pathways such as miRNAs, Staufen-mediated mRNA decay or the response to stress (for review see (Karam, Wengrod et al. 2013)). The data also raise the question of whether there are other cell death pathways that promote NMD inhibition. For example, apoptotic-like programmed cell death does not involve caspases activation, but rather an apoptosis-inducing factor (AIF) (Susin, Zamzami et al. 1996). Recent studies have also suggested that inhibition of NMD can lead to autophagy (Wengrod, Martin et al. 2013) ; however, whether NMD is inhibited during distinct autophagic inductions has yet to be determined. Cell death by necrosis is yet another mechanism that involves a family of proteases, the calpains rather than caspases. It would therefore be of interest to assess whether NMD is also active during these other cell death pathways.

Material and methods

Cell Culture

HeLa cells were incubated in DMEM supplemented with 10% foetal bovine serum (FBS) and ZellShield (Minerva Biolabs). IB3 cells were grown in LHC-8 supplemented with 10% FBS and ZellShield, and 6CFSMEo- (Cozens, Yezzi et al. 1992; Gruenert, Willems et al. 2004; da Paula, Ramalho et al. 2005) and 16HBE14o- (Cozens, Yezzi et al. 1994; Gruenert, Willems et al. 2004) were grown in □-MEM supplemented with 10% FBS, 1mM L-glutamine and ZellShield. Chemical treatment of the cells involved: Staurosporine (Sigma-Aldrich) - at 2 µM for 24 hrs; Z-VAD-FMK (Santa Cruz Biotechnology) - 20µM added 30 min before incubating the cells with

staurosporine; amlexanox (Sequoia Research) - 25µM for 24hrs; apoptosis activator 2 (Santa Cruz Biotechnology) - 50µM for 16 hrs; Anisomycin (Santa Cruz Biotechnology) at 50 µM, Etoposide (Sigma) at 50µM, or Cisplatin at 50µg/ml for 24hrs.

qRT-PCR analysis

qRT-PCR analysis was performed as previously described (Durand, Cougot et al. 2007; Gonzalez-Hilarion, Beghyn et al. 2012). The list of primer sequences used in this study is: Globin (sense: 5'GGACGAGCTGTACAAGTATC3', antisense:5'GGGTTTAGTG GTACTTGTGAGC3'), MUP (sense: 5'CTGATGGGGCTCTATG3', antisense: 5'TCCTGGTGAGAAG TCTCC3'), CFTR mRNA (sense: 5'GGCCAGAGGGTGGGCCTCTT3', antisense: 5'AGGAAACTGTTCTATCACAG3'), CFTR pre-mRNA (sense: 5'TTGATGCCTAGA GGGCAGAT3', antisense 5'TGTCAAAGGGATTGGGAGGG3'), SC35 (sense: 5'CCTCTTAAGAAAA TGCTGCGGTCTC3',antisense: 5'ATCAGCCAAATCAGTTAAAATCTGC3'), NAT9 (sense: 5'ATTGTG CTGGATGCCGAGA3', antisense: 5'ACCTAGCGTGGTCACTCCGTA3'), TBL2 (sense: 5'GCAGTCAT TTACCACATGC3', antisense: 5'TATTGTTTCTGCTTCTTGGAT3'), GAPDH (sense: 5'CATTGACCTC AACTACATGG3', antisense: 5'GCCATGCCAGTGAGCTTCC3'), Actin (sense: 5'ATGAGGTAGTCAGT CAGGTCCC3', antisense: 5'CAGAAGGATTCCTATGTGGGCG3'), RPL32(sense:5'TTGACAACA GGGTTCGTAG3',antisense:5'TTCTTGGAGGAAACATTGTG3'), mouse SRSF7 (sense (intron 3):5'CTTCGTTTGAGTCAGTCGCC3', antisense (exon 5): 5'AAGCTGATCTTGATCTACG3').

Western blot analysis

Proteins were extracted in lysis buffer (50mM Tris pH7, 20mM EDTA and 5% SDS) and then

loaded on a 10% SDS-PAGE (except UPF1 which was loaded on 6% SDS-PAGE). After migration, proteins were transferred to a nitrocellulose membrane. The membrane was incubated with a primary antibody overnight at 4°C and then with a secondary antibody coupled to HRP activity (Jackson Immuno Research) at 4°C for 2hrs. Finally, proteins were detected using SuperSignal West Femto Maximum Sensitivity Substrate (Pierce). Primary antibodies used were: rabbit anti-hUPF1 at 1/5000 (Abcam), rabbit anti-hUPF2 at 1/5000 (antibody raised against the following synthetic peptide: H2N - MPA ERK KPA SME EKD C - CONH2 (Eurogentec)), rabbit anti-UPF3X at 1/5000 (Aviva Systems Biology), rabbit anti-PARP at 1/1000 (Santa Cruz Biotechnology), rabbit cleaved Caspase-3 (Asp175) at 1/1000 (Cell Signaling Technology), rabbit anti-tubulin at 1/1000 (Epitomics), mouse anti-eIF4E at 1/200 (Santa Cruz Biotechnology) and rabbit anti-GFP at 1/5000 (Sigma).

Apoptosis assays

Apoptosis was measured according to the manufacturer's protocol (Life Technologies) using the Tali Apoptosis Kit – containing annexin V Alexa Fluor 488 and propridium iodide. Measurements were performed on a Tali cytometer (Life Technologies). Apoptotic cells were identified as the cells incorporating only annexin V.

In vivo apoptosis assay

Mouse experiments were performed according to institutional guidelines. Briefly, 6-week old male C57BL/6 mice, fasted overnight and were then intraperitoneally injected with the anti-Fas Jo2 antibody (BD Pharmingen) at 0.2µg/g body weight or saline buffer vehicle as a

control. After 4 hrs, mice were euthanized and livers were harvested.

Caspase cleavage reaction

Assessment of caspase cleavage was as previously described (Foveau, Leroy et al. 2007). Briefly, 3 x 10^5 HeLa cells/well were distributed in 6 well-plates. After 24hrs, cells were lysed in 80 □l of the lysis buffer (20mM Pipes pH7.2, 100 mM NaCl, 1% Chaps, 10% Sucrose + 5 mMDTT+50 □M EDTA). Cell extracts were then incubated with 1µl of purified caspase for 4hrs at 37°C before loading on a 10% SDS-PAGE for western-blot analysis. Purified, active caspases were generously provided by Dr GS Salvesen (The Burnham institute, La Jolla, CA, USA). The concentration of purified caspase 3 is 13.9 □M, 7.5 µM for caspase 6, 19.7 □M for caspase 7, 15 □M for caspase 8 and 41.5 □M for caspase 9.

Construction of the plasmids expressing UPF fragments

UPF1 derived plasmids: CFP-UPF1 cDNA was introduced into pUNO vector (Cayla) linearized by BamHI using the Infusion cloning kit (Clontech). CFP-UPF1 was amplified by PCR with primer for CFP: sense: 5'AGATCACCGGCGTGTCGACGATGGTGAGCAAGGGCGAGGA3'; antisense: 5'CGTACGCCTCCACGCTCATCTTGTACAGCTCGTCCATGCC3'; primers for UPF1: sense: 5'ATGAG CGTGGAGGCGTACG3'; antisense: 5'TGGCTGCAGAGCGCTGGATCTTAATACTGGGACAGCC3'). The same method was used to amplify CFP-UPF1Nter (amino-acid 1 to 37) using the same primer sense as for CFP-UPF1 and the antisense primer: 5'TGGCTGCAGAGCGCTGGATCTTAG TCGGTGAACTCGAACTCGG3'), and CFP-UPF1Cter (amino-acid 38 to 1118) was amplified using the sense primer: 5'TTTACTCTTCCTAGCCAGACG3' and the same antisense primer as for

CFP-UPF1.

UPF2 derived plasmids were constructed according to Gateway cloning technology (Life Technologies) using empty vector pSPO-CFP-rfc. The list of primers used to amplify UPF2 full length or fragments is: for the full length the full-length UPF2 (called as CFP UPF2 expressing amino acid from 1 to 1272) (sense: 5'GGGGACAAGTTTGTACAAAAAAGCAGGCT CCATGCCAGCTGAGCGTAAAAAGCCAG3', antisense: 5'GGGGACCACTTTGTACAAGAAAGCTGGG TTCAACGTCTCCTCCCACCAGTCTTA3'), the N-terminal fragment of UPF2 (called as CFP UPF2-Nter expressing amino acids from 1 to 741) (sense: 5'GGGGACA AGTTTGTACAAAAAA GCAGGCTCCATGCCAGCTGAGCGTAAAAAGCCAG', antisense: 5'GGGGACCACTTTGTACAAGAAA GCTGGGT ATCAAGATG CATTGCTTGCTTCTTT 3'), the C-terminal fragment of UPF2 (called as CFP UPF2-Cter expressing amino acids from 742 to 1272) (sense: 5' GGGGACAAGTTTGTAC AAAAAAGCAGGCTCCGCGAGATACGTCACAATGGTAGAGA 3', antisense: 5' GGGGACCACTTTGTA CAAGAAAGCTGGG TTCAACGTCTCCTCCCACCAGTCTTA 3').

Construction of mutant UPF plasmids

Aspartic acid was changed to asparagine using QuikChange Site-Directed Mutagenesis Kit (Stratagene) and the following primers: UPF1 D37N (sense: 5' CCGAGTTCGAGTTCACCAAC TTTACTCTTCCTAGC3'; antisense: 5' GCTAGGAAGAGTAAAGTTGGTGAACTCGAACTCGG3'); UPF1 D111N(sense: 5'CTTCGAGGAAGATGAAGAAAACACCTATTACACGAAGG3'; antisense: 5'CCTTC GTGTAATAGGTGTTTTCTTCATCTTCCTCGAAG3') UPF2 D585N (sense: 5'CAACCGAGATCTGAT AAACAAGGCAGCAATGGATTTTTGC3'; antisense 5'GCAAAAATCCATTGCTGCCTTGTTT ATCAGAT CTCGGTTG3'), UPF2 D741N (sense: 5' GCAAGCAATGCATCTTAATGCGAGATACGTCACAATGG3';

antisense: 5’ CCATTGTGACGTATCTCGCATTAAGATGCATTGCTTGC3’).

UPF Knockdown by short interfering RNA (siRNA):

HeLa cells were transfected with the ICAFectin™ 442 reagent (In Cell Art) complexed with either 100 nM of siControl (Eurogentec), or with siUPF1 (5’-AAGATGCAGTTCCGCTCCATTTT-3’) or siUPF2 (5’-GAAGTTGGTACGGGCACTC-3’). At 24h post-transfection, cells were incubated with DMSO or 2µM of Staurosporine for an additional 24h. The cells were then collected to measure apoptosis by AnnexinV or were extracted in lysis buffer for western blot analysis.

Author contribution

JJ, AF, SGH, CL and FL performed experiments. JJ, AF, CL, DT, DCG and FL wrote the manuscript. JJ, AF, SGH, CL, DCG, DT ad FL designed the experiments and analyzed data.

Acknowledgments

Authors would like to thank Dr. Jérome Vicogne for helpful discussions and Pr. Lynne Maquat, Dr Edouard Bertrand and Dr. GS Salvesen for reagents and comments on the paper. We also thank the mouse facility of Institut Pasteur de Lille. JJ is funded by Vaincre la mucoviscidose. FL received fundings for this project from Vaincre la mucoviscidose, l’Association Française contre les myopathies and la Fondation ARC. DCG was supported by funds from Pennsylvania Cystic Fibrosis, Inc and Cystic Fibrosis Research, Inc.

Authors declare that they have no conflict of interest.

Jia_Fig1

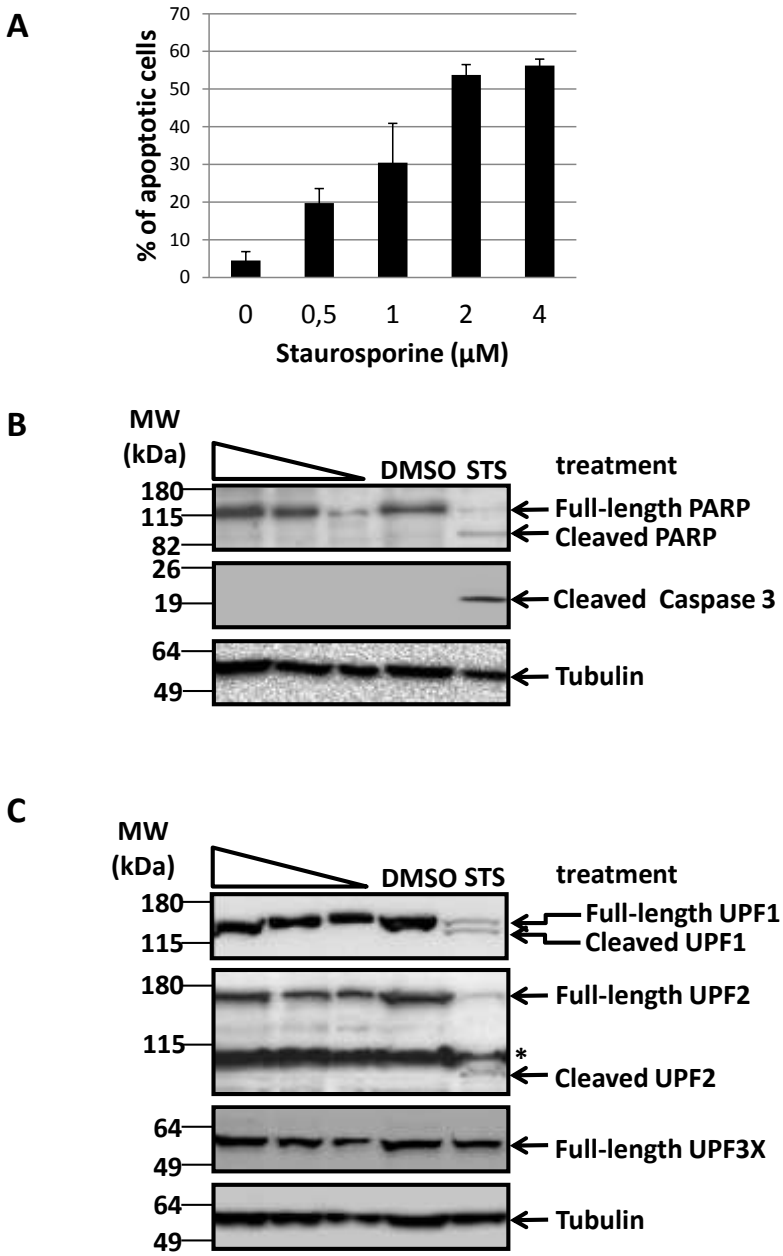
A
% of apoptotic cells
70
60
50
40
30
20
10
0
0
0,5
1
2
4
Staurosporine (µM)
B
MW
(kDa)
DMSO STS
treatment
180
115
82
Full-length PARP
Cleaved PARP
26
19
Cleaved Caspase 3
64
49
Tubulin
C
MW
(kDa)
DMSO STS
treatment
180
115
Full-length UPF1
Cleaved UPF1
180
115
Full-length UPF2
*
Cleaved UPF2
64
49
Full-length UPF3X
64
49
Tubulin

Jia_Fig 2

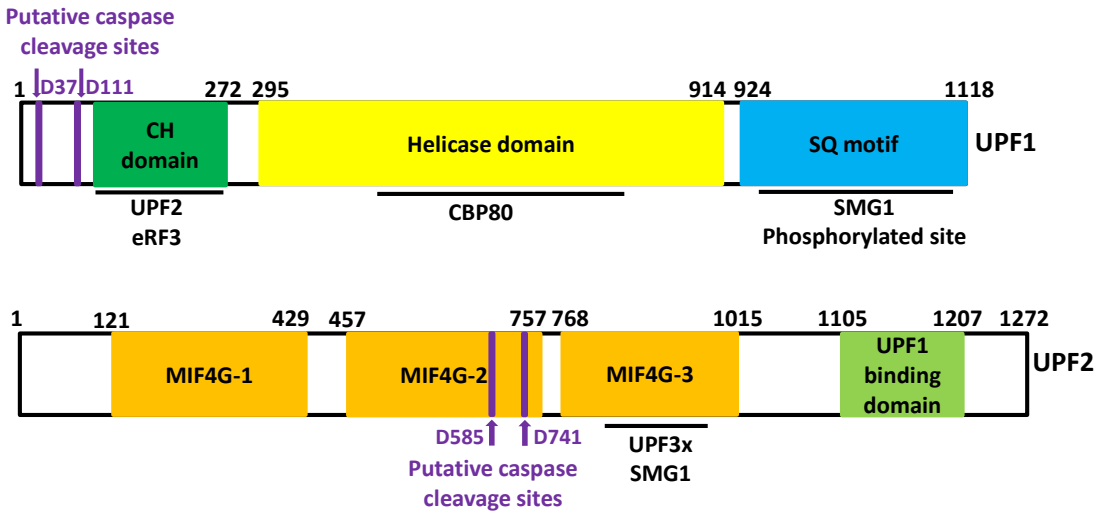
Putative caspase cleavage sites
1
D37
D111
272
295
914
924
1118
CH domain
Helicase domain
SQ motif
UPF1
UPF2 eRF3
CBP80
SMG1 Phosphorylated site
1
121
429
457
757
768
1015
1105
1207
1272
MIF4G-1
MIF4G-2
MIF4G-3
UPF1 binding domain
UPF2
D585
D741
Putative caspase cleavage sites
UPF3x SMG1

Jia_Fig 3

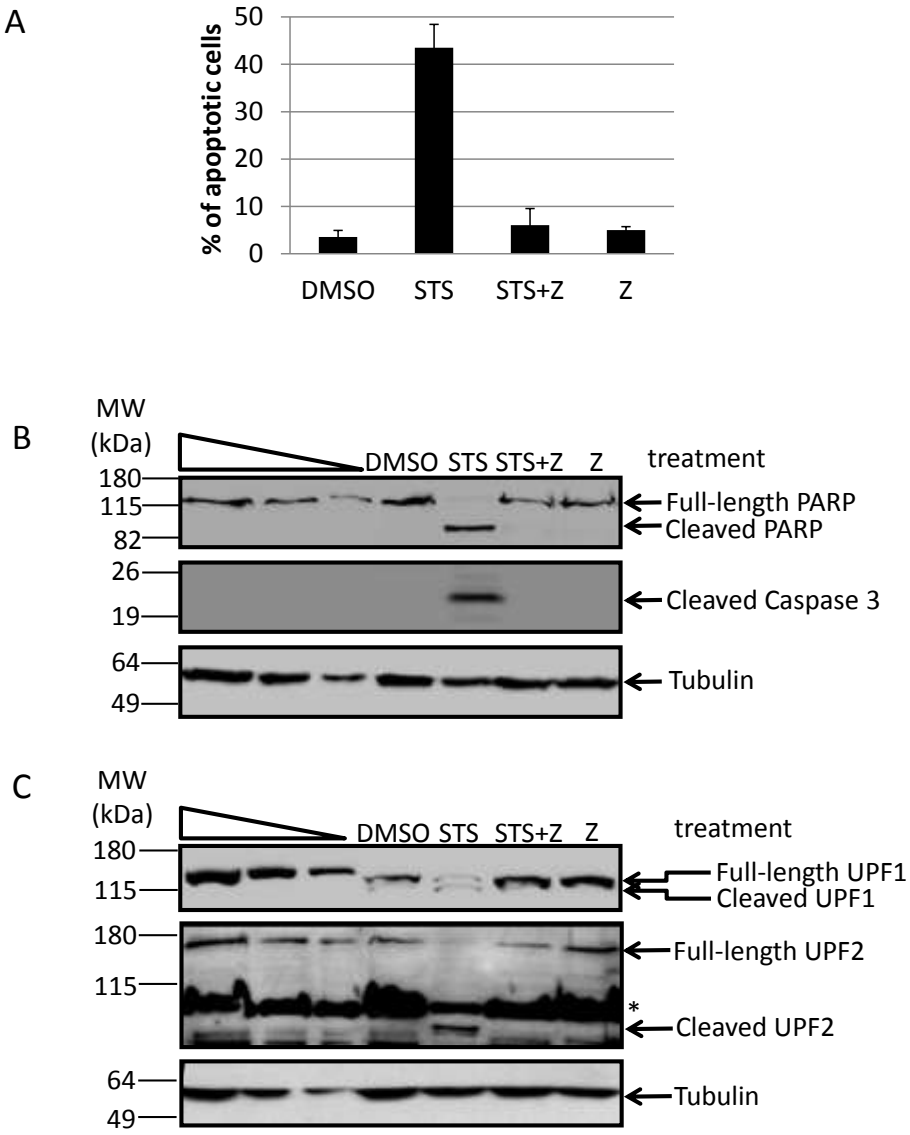
A
% of apoptotic cells
50
40
30
20
10
0
DMSO
STS
STS+Z
Z
B
MW
(kDa)
DMSO STS STS+Z Z
treatment
180
115
82
Full-length PARP
Cleaved PARP
26
19
Cleaved Caspase 3
64
49
Tubulin
C
MW
(kDa)
DMSO STS STS+Z Z
treatment
180
115
Full-length UPF1
Cleaved UPF1
180
115
Full-length UPF2
*
Cleaved UPF2
64
49
Tubulin

Jia_Fig 4

UPF1 analysis

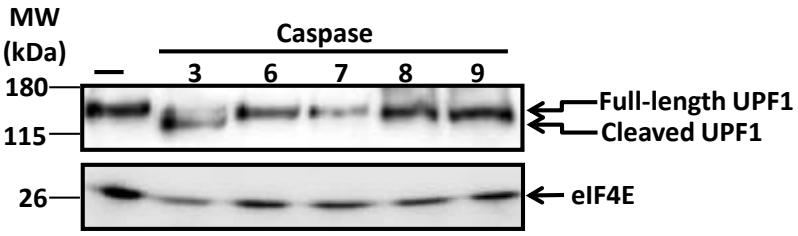

UPF2 analysis

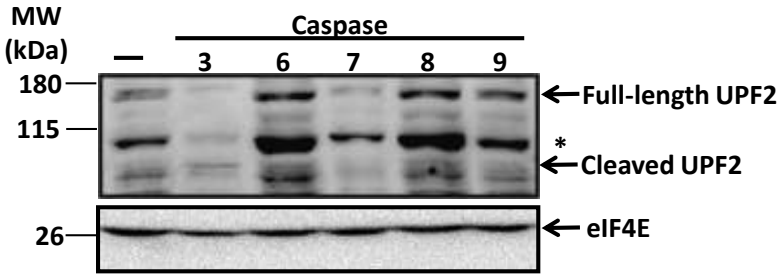

Jia_Fig 5

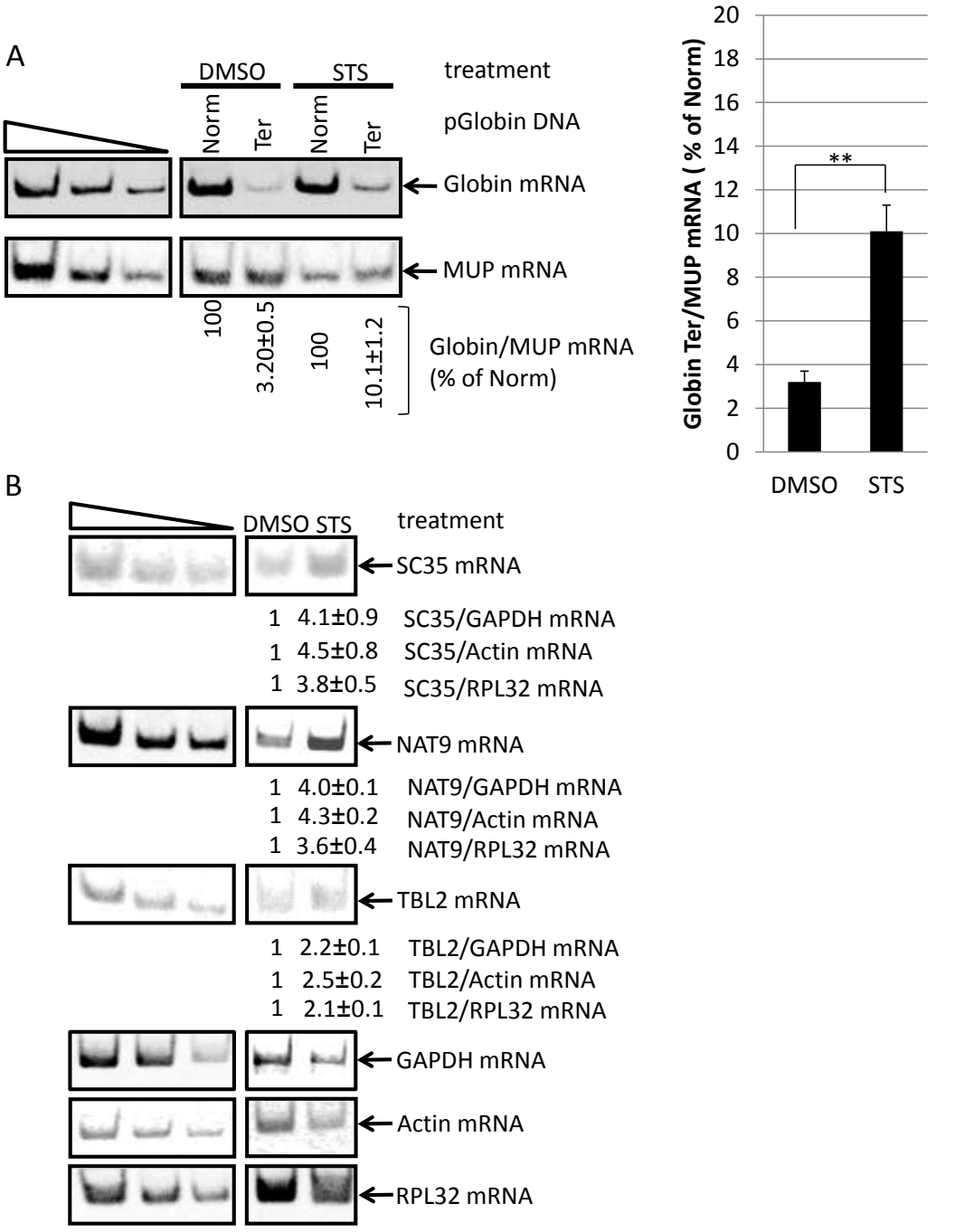
A
DMSO
STS
treatment
Norm
Ter
Norm
Ter
pGlobin DNA
Globin mRNA
MUP mRNA
100
3.20±0.5
100
10.1±1.2
Globin/MUP mRNA
(% of Norm)
Globin Ter/MUP mRNA (% of Norm)
20
18
16
14
12
10
8
6
4
2
0
**
DMSO
STS
B
DMSO STS
treatment
SC35 mRNA
1 4.1±0.9 SC35/GAPDH mRNA
1 4.5±0.8 SC35/Actin mRNA
1 3.8±0.5 SC35/RPL32 mRNA
NAT9 mRNA
1 4.0±0.1 NAT9/GAPDH mRNA
1 4.3±0.2 NAT9/Actin mRNA
1 3.6±0.4 NAT9/RPL32 mRNA
TBL2 mRNA
1 2.2±0.1 TBL2/GAPDH mRNA
1 2.5±0.2 TBL2/Actin mRNA
1 2.1±0.1 TBL2/RPL32 mRNA
GAPDH mRNA
Actin mRNA
RPL32 mRNA

Jia_Fig 6

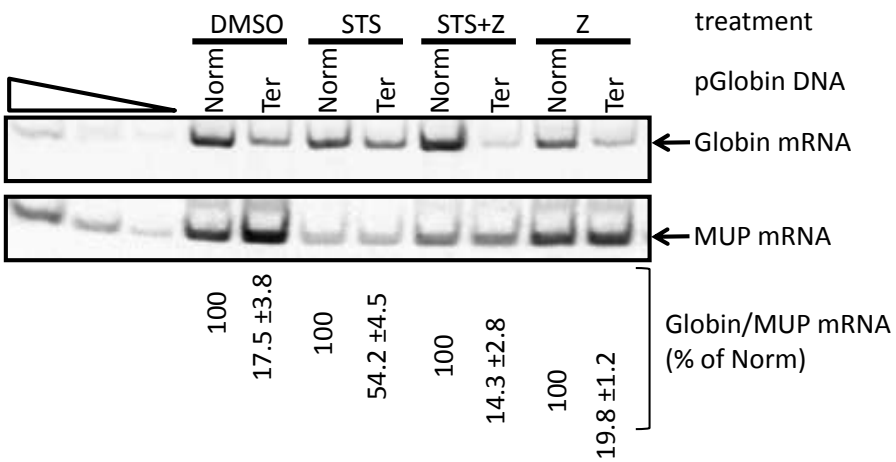
DMSO
STS
STS+Z
Z
treatment
Norm
Ter
pGlobin DNA
Globin mRNA
MUP mRNA
100
17.5 ±3.8
100
54.2 ±4.5
100
14.3 ±2.8
100
19.8 ±1.2
Globin/MUP mRNA
(% of Norm)

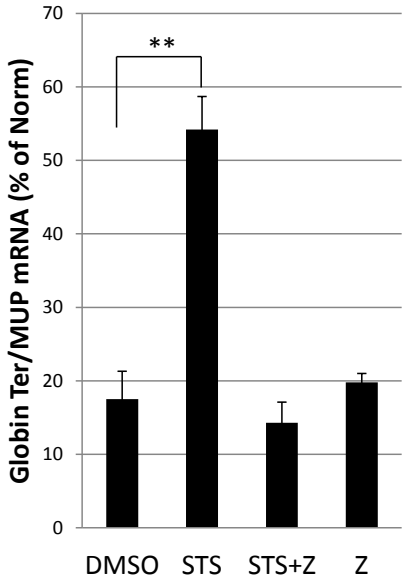
Globin Ter/MUP mRNA (% of Norm)
70
60
50
40
30
20
10
0
**
DMSO
STS
STS+Z
Z

Jia_Fig 7

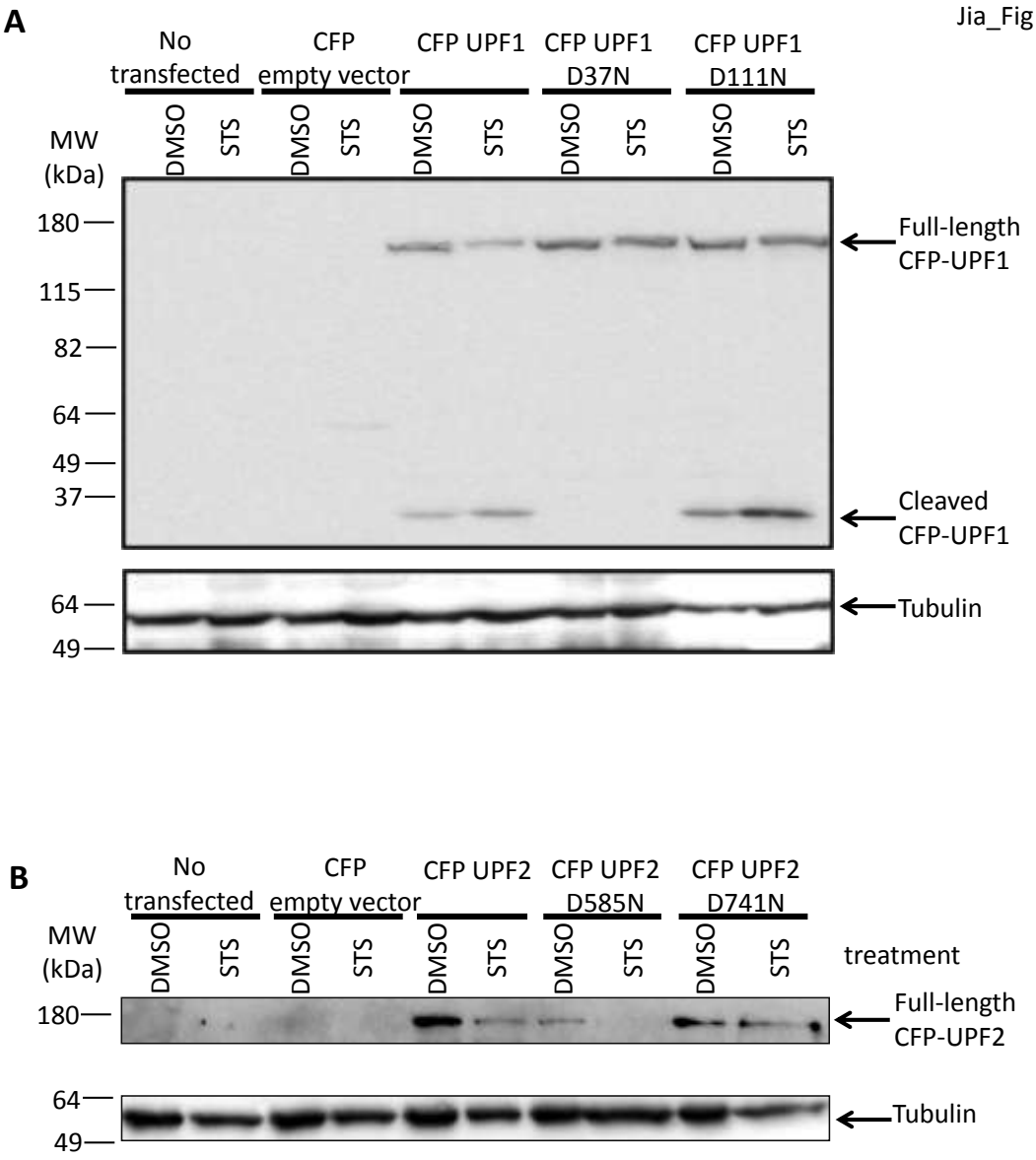
A
No transfected
CFP empty vector
CFP UPF1
CFP UPF1 D37N
CFP UPF1 D111N
DMSO
STS
MW (kDa)
180
115
82
64
49
37
Full-length CFP-UPF1
Cleaved CFP-UPF1
Tubulin
B
No transfected
CFP empty vector
CFP UPF2
CFP UPF2 D585N
CFP UPF2 D741N
treatment
Full-length CFP-UPF2
Tubulin

Jia_Fig 8

A

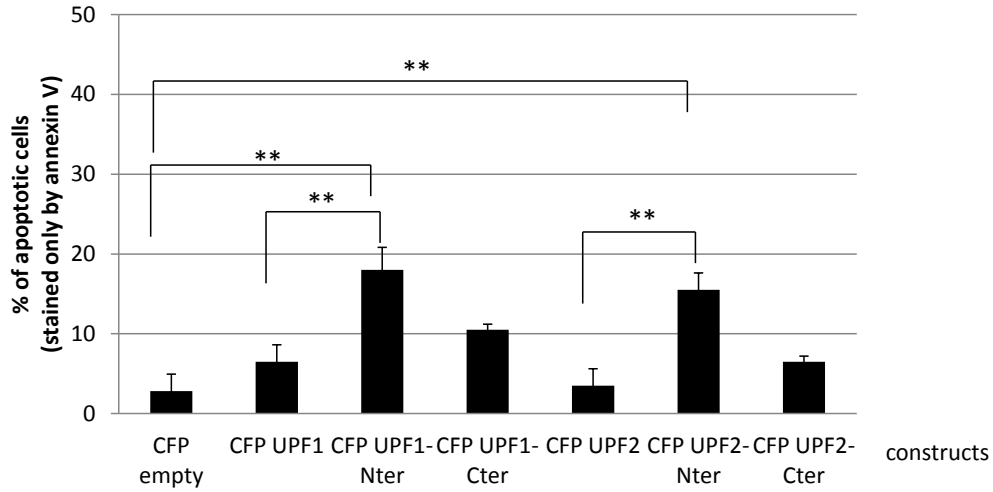
% of apoptotic cells (stained only by annexin V)
50
40
30
20
10
0
**
**
**
**
CFP empty
CFP UPF1
CFP UPF1-Nter
CFP UPF1-Cter
CFP UPF2
CFP UPF2-Nter
CFP UPF2-Cter
constructs

B

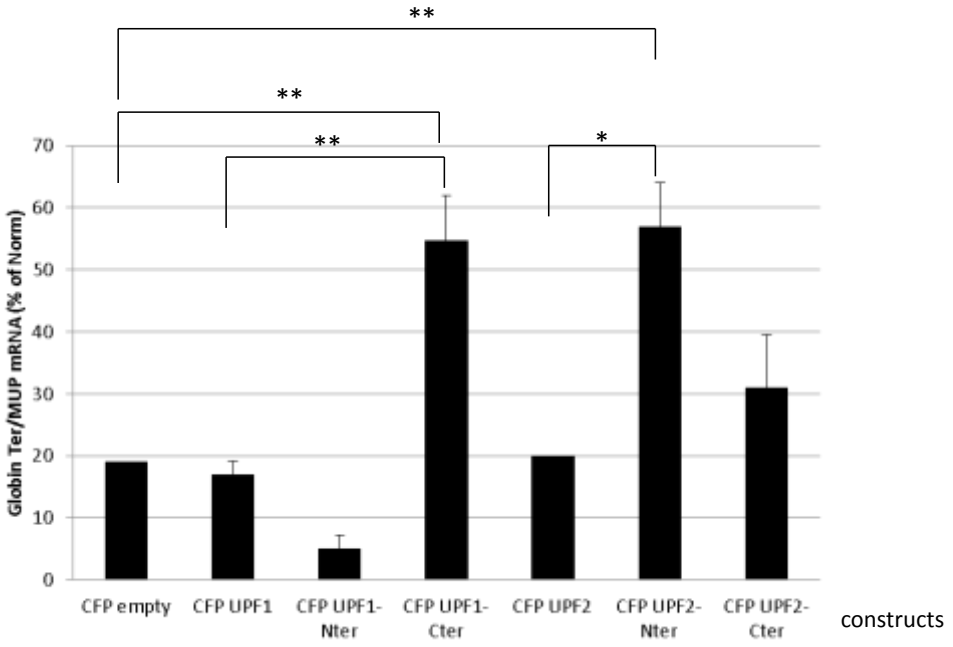
Globin Ter/MUP mRNA (% of Norm)
70
60
50
40
30
20
10
0
**
**
**
*
CFP empty
CFP UPF1
CFP UPF1-Nter
CFP UPF1-Cter
CFP UPF2
CFP UPF2-Nter
CFP UPF2-Cter
constructs

Jia_Fig 9

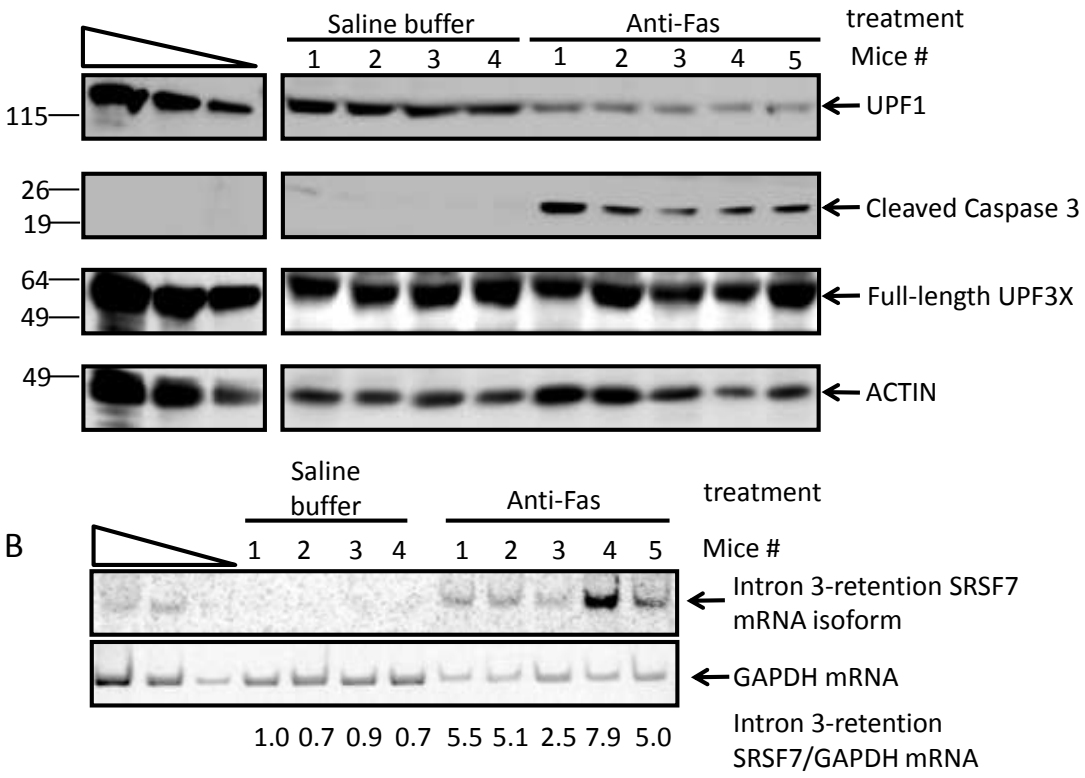
A
Saline buffer
Anti-Fas
treatment
1 2 3 4 1 2 3 4 5
Mice #
115
UPF1
26
19
Cleaved Caspase 3
64
49
Full-length UPF3X
49
ACTIN
B
Saline buffer
Anti-Fas
treatment
1 2 3 4 1 2 3 4 5
Mice #
Intron 3-retention SRSF7 mRNA isoform
GAPDH mRNA
1.0 0.7 0.9 0.7 5.5 5.1 2.5 7.9 5.0
Intron 3-retention SRSF7/GAPDH mRNA

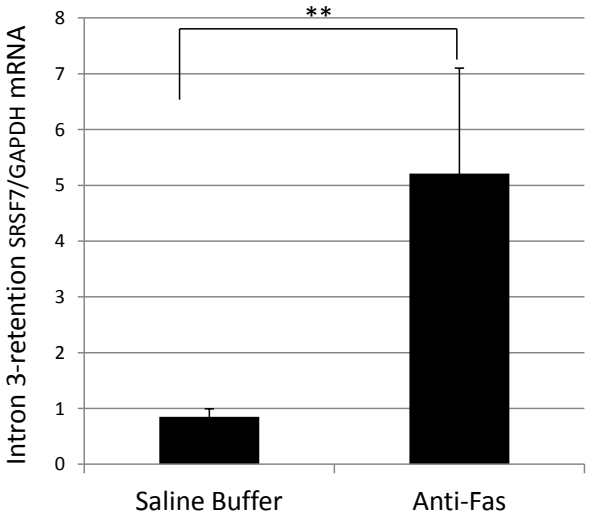
**
Intron 3-retention SRSF7/GAPDH mRNA
0
1
2
3
4
5
6
7
8
Saline Buffer
Anti-Fas

Jia_Suppl. Fig S1

UPF1 protein sequence

UPF2 protein sequence

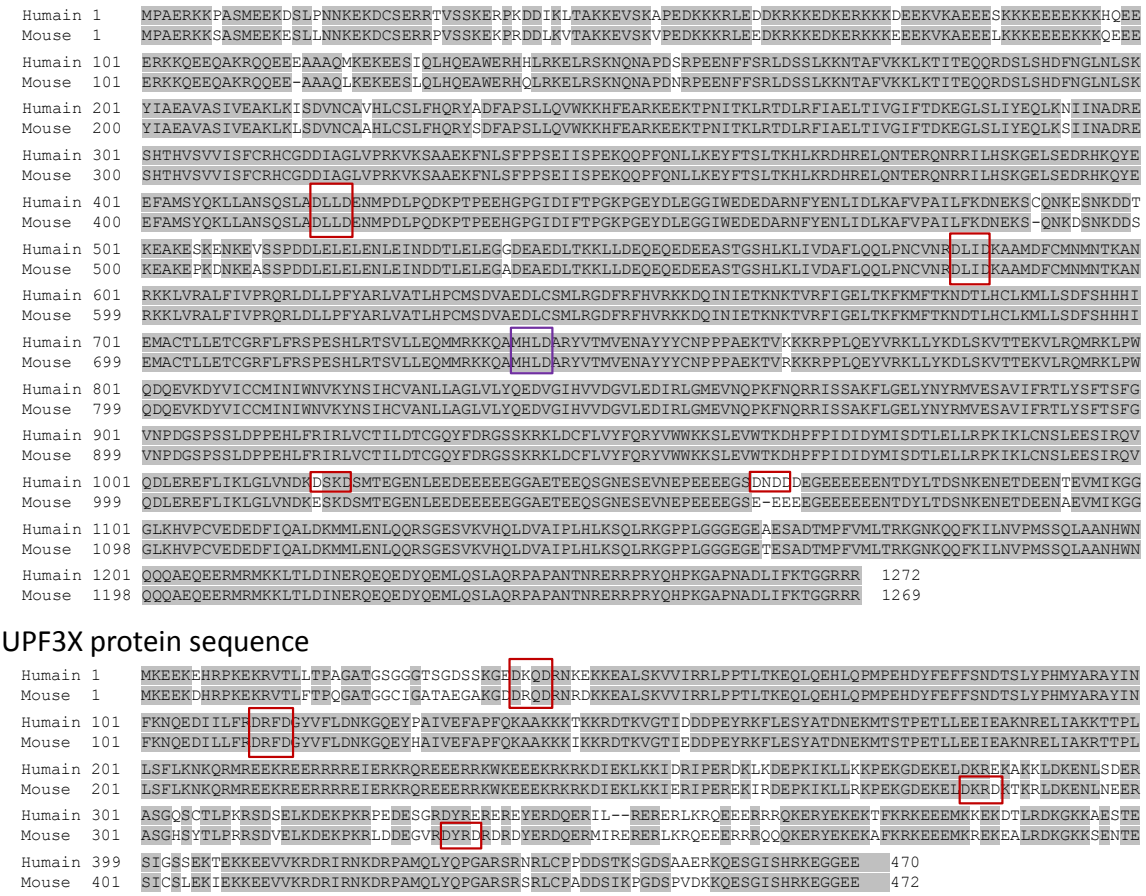

UPF3X protein sequence

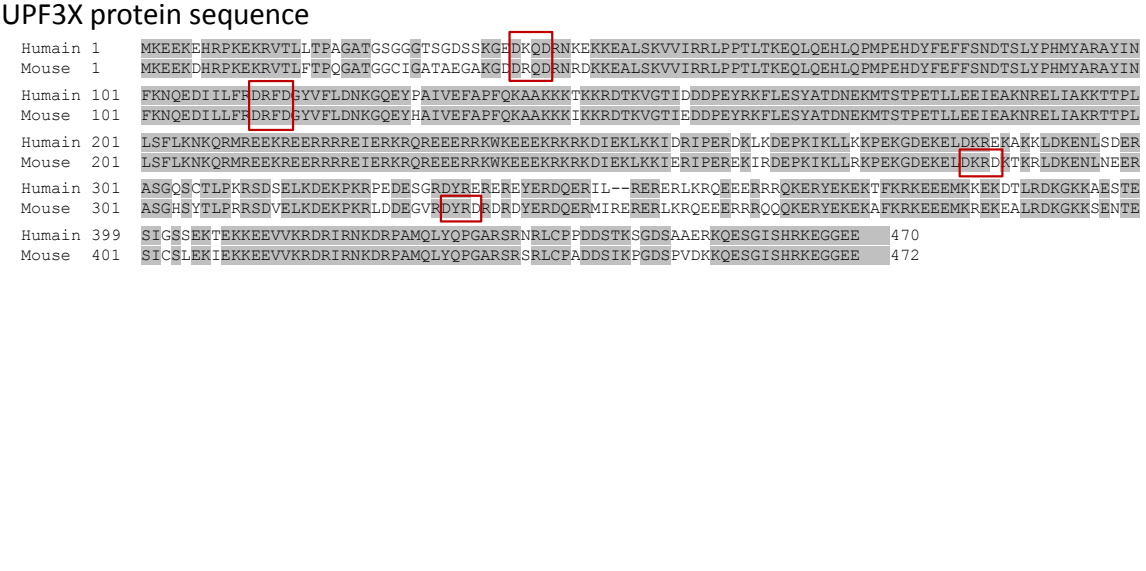

Jia_Suppl. Fig S2

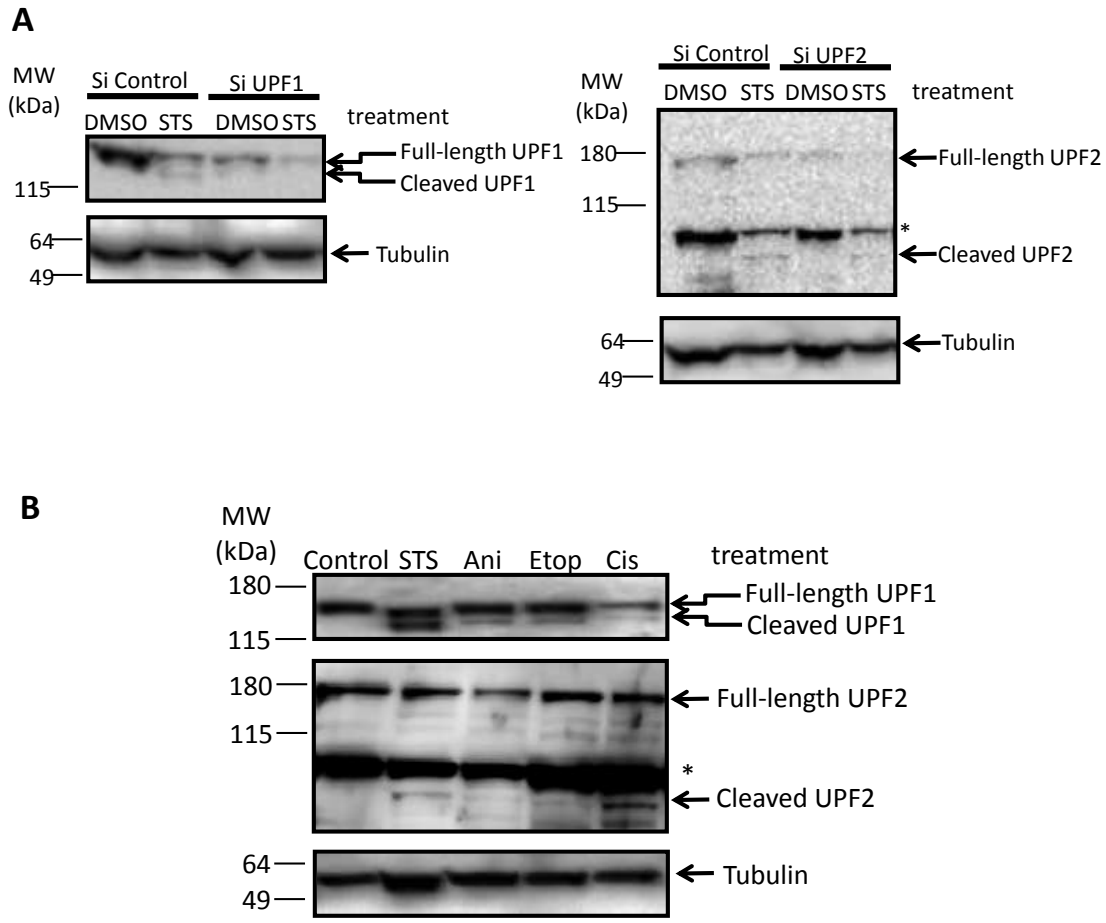

Jia_Suppl. Fig S3

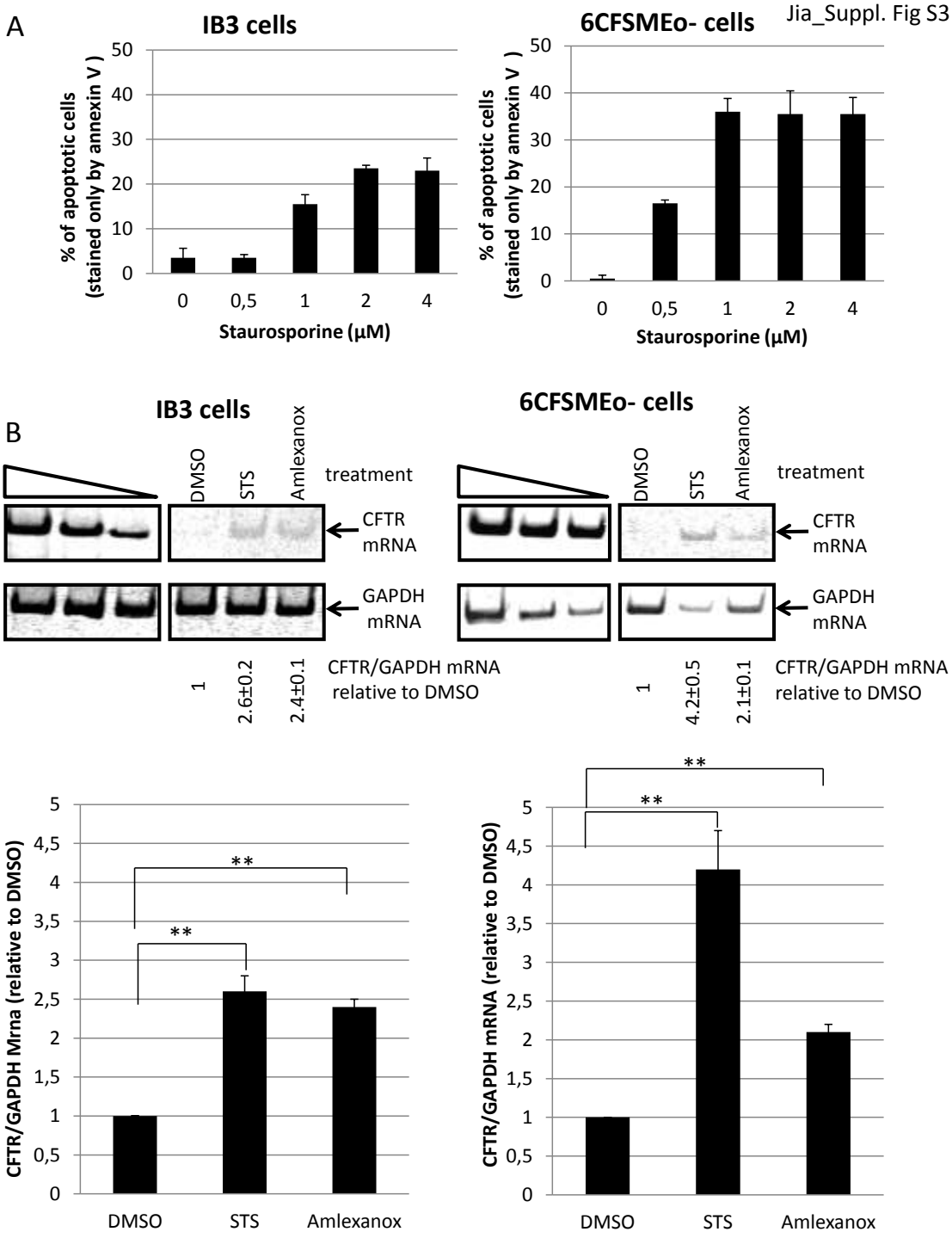

Jia_Suppl. Fig S4

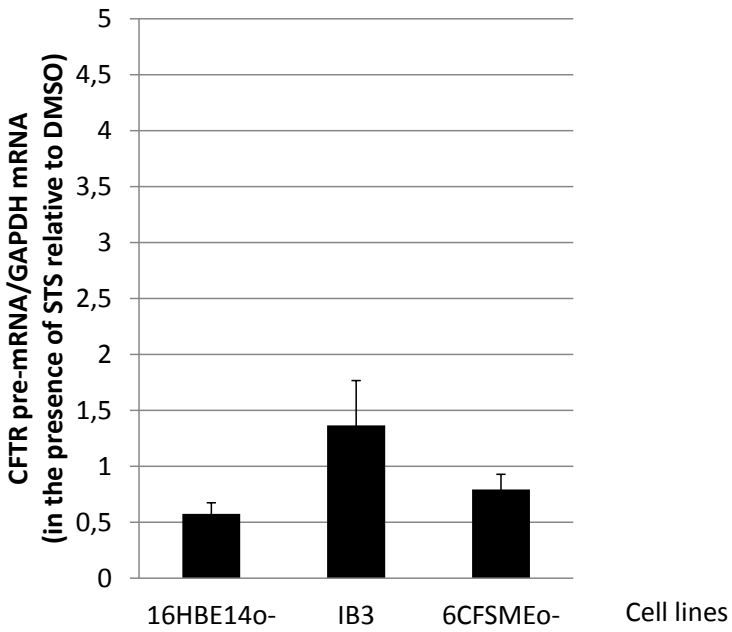

Jia_Suppl. Fig S5

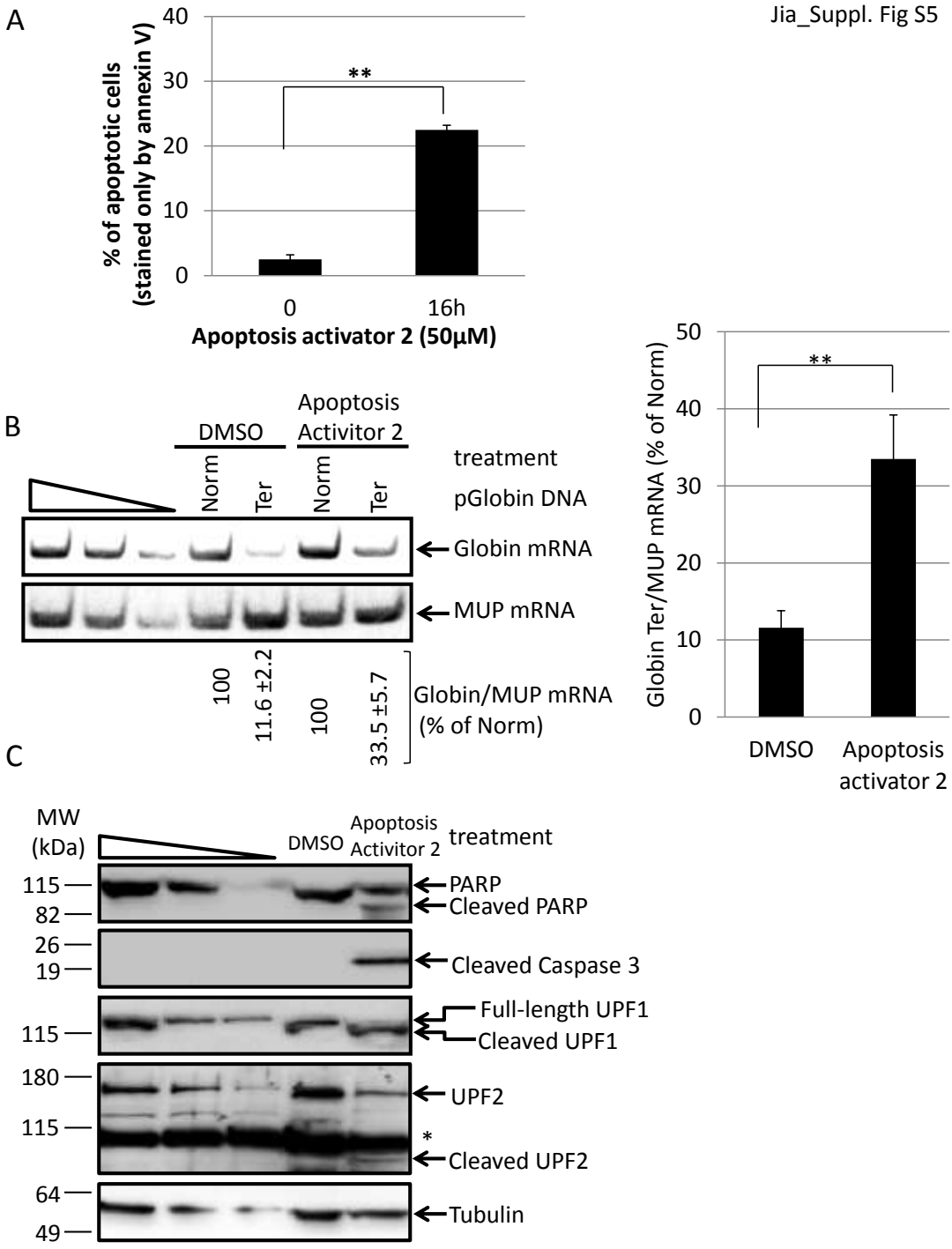

Jia_Suppl. Fig S6

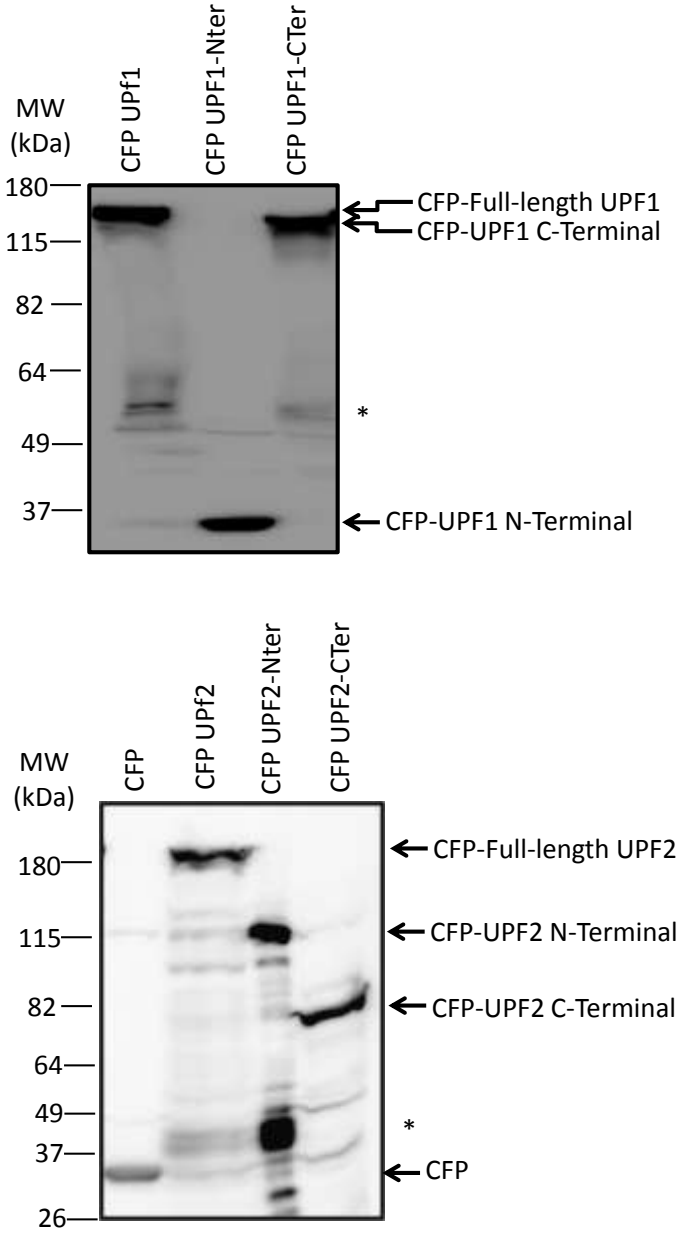

Jia_Suppl. Fig S7

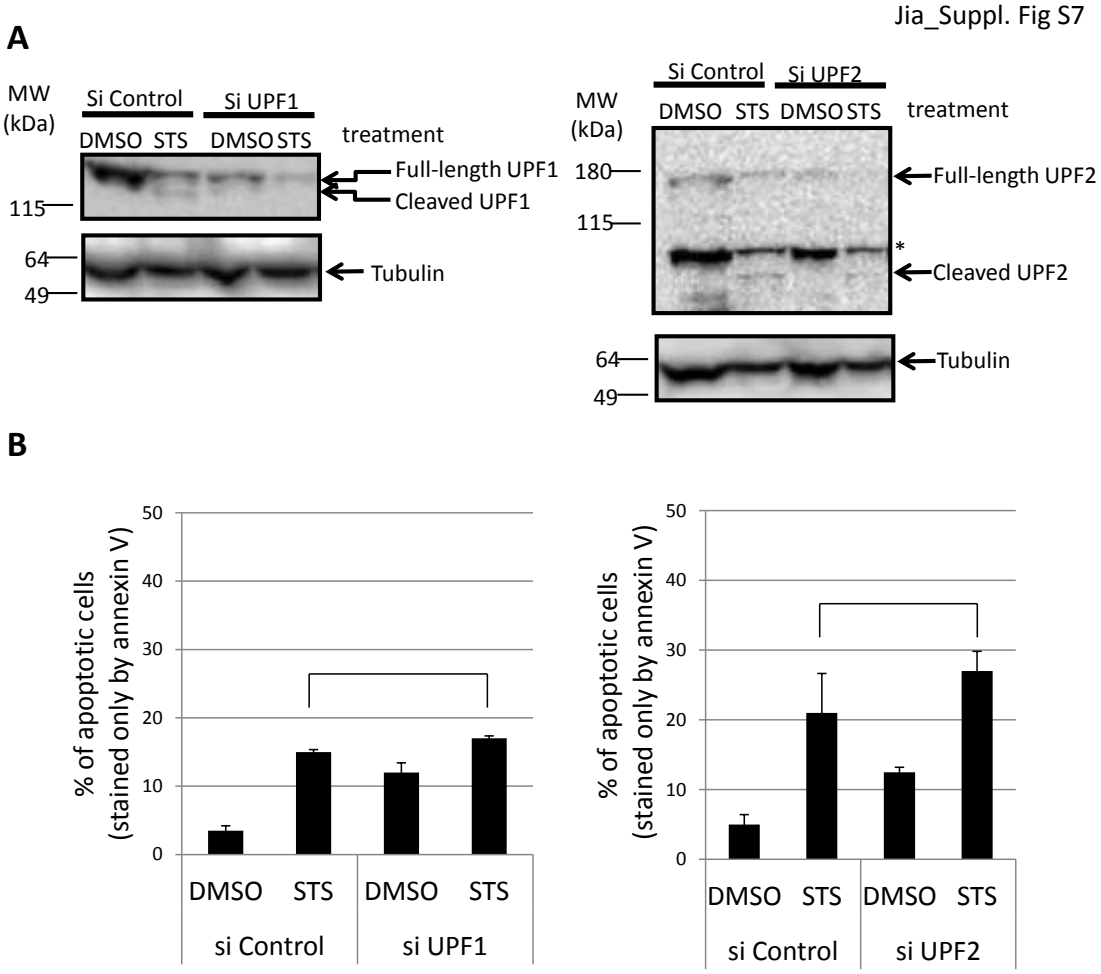

Figure legends

Figure 1: NMD factors UPF1 and UPF2 are cleaved during apoptosis. (A) Determination of the working concentration of staurosporine (STS) to induce apoptosis in HeLa cells. Cells were incubated for 24 hrs with increasing amounts of STS before measuring the apoptosis. (B) STS treatment of HeLa cells induces the activation of caspases. The western-blot analysis of PARP or caspase 3 shows the presence of the cleavage product of both proteins demonstrating the activation of caspases, but not of tubulin. (C) Western-blot analysis shows that the level of UPF1 and UPF2, but not UPF3X proteins decreases in cells treated by STS. Cleavage products of UPF1 and UPF2 are indicated on the right side of the figure. UPF1 and UPF2 are degraded during apoptosis; however,UPF3X was not. The three left-most lanes correspond to a two-fold dilution of a wild-type protein extract symbolized by a triangle. The molecular weight scale is presented on the left of all western-blot. The results presented here are representative of three independent experiments. * indicates non-specific protein species.

Figure 2: Schematic representation of UPF1 and UPF2 domains. Functional and interacting domains of UPF1 (upper) and UPF2 (lower) are as indicated. The positions of putative caspase cleavage sites are shown by purple arrows. The amino acid positions are indicated by a number at the top of each structure.

Figure 3: Caspases are responsible for the cleavage of NMD factors UPF1 and UPF2 during apoptosis. (A) Measure of the apoptosis level in cells treated with DMSO, staurosporine (STS), STS and the caspase inhibitor zVAD-fmk (Z) or Z alone. (B) Western-blot analysis of PARP and caspase 3 shows the presence of cleavage product in the presence of STS, but not in the presence of STS

with Z or Z alone. (C) Western-blot analysis of UPF1 or UPF2. Tubulin protein is used as control to ensure that the analysis of each lane can be comparable. * indicates non-specific protein species. The three most-left lanes of each analysis represent a serial dilution from an untreated cell extract symbolized by a triangle. The protein molecular weight is indicated on the left side of each western-blot analysis. The protein cleavage products are indicated on the right side of the western-blot analysis. Error bar=SD. Results showed in figure 3 are representative of at least three independent experiments.

Figure 4: Identification of caspases responsible for the UPF1 or UPF2 cleavage during apoptosis. HeLa cell extract was incubated with purified caspases 3, 6, 7, 8 or 9 before western-blot analysis for the presence of UPF1 (upper panel) or UPF2 (lower panel). The molecular weight scale is indicated on the left and UPF1 or UPF2 species are shown on the right side of gels. The three left-most lanes correspond to a serial dilution of untreated extract. * indicates non-specific protein species.The results shown in figure 4 are representative of three independent experiments.

Figure 5: NMD is inhibited during apoptosis. (A) Measure of NMD efficiency as determined by quantitative RT-PCR in HeLa cells transfected with expression vectors for Globin (Norm or Ter) and an expression vector for MUP in the presence of DMSO (as a negative control) or STS. The three left-most lanes represent a serial dilution of Norm RT in the PCR. A histogram representation of the results is presented under the gel. (B) Natural substrates of NMD are up-regulated during staurosporine (STS)-induced apoptosis. HeLa cells were incubated either

with DMSO or with STS for 24 hrs before purifying RNAs and measured by quantitative RT-PCR the level of natural NMD substrates SC35, Nat9 or Tbl2 mRNAs. GAPDH, Actin or RPL32 mRNA were used to normalize the level of SC35, Nat9 or Tbl2 mRNA level at each condition as indicated. The three left-most lanes represent a serial dilution of Norm RT in the PCR symbolized by a triangle. Error bar=SD, student t-test: **=p<0.05. Results are representative of three independent experiments.

Figure 6: Caspases are responsible for the NMD inhibition during apoptosis. HeLa cells were transfected with expression vectors encoding globin mRNA either WT (Norm) or harboring the 39-PTC (Ter) or MUP mRNA and then incubated with DMSO, staurosporine (STS), STS with zVAD-fmk (Z) or Z alone. The level of Globin and MUP mRNA was quantified by RT-PCR.The three left-most lanes represent a serial dilution of Norm RT in the PCR symbolized by a triangle. A histogram representation of the mRNA measures is presented on the right side of the gel. Results are representative of three independent experiments. Error bar=SD, student t-test: **=p<0.05.

Figure 7: Identification of the caspase cleavage sites in UPF1 and UPF2. (A) Identification of the caspase cleavage site in UPF1. Western-blot analysis using an anti-GFP antibody from protein purified from HeLa cells that were either not transfected or transfected with an expression vector encoding the CFP tag, a fusion protein CFP-UPF1 or a fusion protein CFP-UPF1 with a D37N or D111N missense mutation, with or without staurosporine (STS) treatment. (B) Identification of the caspase cleavage site in UPF2. Western-blot analysis using an anti-GFP antibody from protein purified from HeLa cells that were either not transfected or transfected with an expression vector

encoding the CFP tag, a fusion protein CFP-UPF2 or a fusion protein CFP-UPF2 with a D585N or D741N missense mutation, with or without staurosporine (STS) treatment. The molecular weight scale is shown on the left side of each gel and the identity of each species is shown on the right side of each gel. The results presented Figure 7 are representative of 3 independent experiments.

Figure 8: UPF caspase-cleavage fragments induce apoptosis and/or NMD inhibition. (A) Measure of apoptosis as described before in HeLa cells expressing one of the UPF caspase-cleavage fragment or as a control the empty expression vector (CFP) or the full length UPF protein UPF1 (CFP UPF1) or UPF2 (CFP UPF2). The N-terminal caspase cleavage fragment of UPF1, UPF2 or the C-terminal caspase cleavage fragment of UPF1 or UPF2 are noted CFP UPF1-Nter, CFP UPF2-Nter, CFP UPF1-Cter or CFP UPF2-Cter respectively. (B) Effect of the UPF caspase cleavage fragments on NMD efficiency. HeLa cells were transfected with expression vectors encoding globin mRNA Norm or Ter, MUP mRNA as a loading control, one of the UPF caspase cleavage fragments or as a control the empty expression vector or the expression vector encoding the full length UPF1 or UPF2. The level of NMD efficiency was measured by RT-PCR after quantifying the level of Globin and MUP mRNA. A histogram representation of the mRNA measures is presented. The results of figure 8 are representative of two independent experiments. Error bar=SD, student t-test: *=$p<0.1$; **=$p<0.05$.

Figure 9: NMD inhibition during apoptosis *in vivo*. Mice injected with saline buffer or with anti-Fas antibody 4hrs before harvesting the liver. Proteins were analyzed by western-blot (A) and mRNAs by quantitative RT-PCR (B). The three most-left lanes correspond to a serial dilution of

untreated extract symbolized by a triangle. A histogram representation of the mRNA measures of panel B is presented under the gel. Error bar=SD, student t-test: **=p<0.05.

Supplemental Figure S1: Human and mouse sequence alignments of UPF1, UPF2 and UPF3X proteins and identification of putative caspase cleavage sites in UPF proteins. The amino acid sequence of UPF1, UPF2 and UPF3X is given where putative caspase cleavage sites have been highlighted by a red box around the cleavage site. The cleavage sites used by caspase are indicated by a purple rectangle. The predicted cleavage sites were determined using the following URL: http://casbase.org/casvm/server/index.html. The conserved amino acids between human and mouse are on black background.

Supplemental Figure S2: UPF1 and UPF2 are cleaved in response in various apoptosis inducers. (A) Western-blot analysis of the level of UPF1 or UPF2 in the presence of siRNAs under DMSO or STS treatment in HeLa cells to validate the identity of UPF1 or UPF2 derived species. (B) HeLa cells were incubated with staurosporine (STS), anisomycin (ani), etoposide (etop) or cisplatin (cis) before to extract protein and analyze the presence of UPF1, UPF2 or tubulin as a loading control. The molecular weight scale is indicated on the left side of each gels and the identity of each species is shown on the right side of each gel. * indicates non-specific protein species. Results presented in this supplemental figure are representative of two independent experiments.

Supplemental Figure S3: Inhibition of endogenous NMD during apoptosis. (A) Determination of

the working concentration of STS in IB3 (left panel) or 6CFSMEo- (right panel) cells giving the highest degree of apoptosis. Cells were incubated with either DMSO (as a negative control) or STS at different concentrations before assessing apoptosis using annexin V and propridium iodide. (B) IB3 (left panel) or 6CFSMEo- (right panel) cells were incubated with 2 μM of STS, DMSO (as a negative control) or 25 μM of amlexanox as a positive control. The level of CFTR mRNA was determined by quantitative RT-PCR and compared to the level of CFTR in DMSO treated cells. The three left-most lanes represent a serial dilution of a WT bronchial epithelial cells (16HBE14o-) RT symbolized by a triangle. A histogram representation of the results is presented under each gel. All results are representative of three independent experiments. Error bar=SD, student t-test: **=$p<0.05$.

Supplemental Figure S4: Staurosporine does not affect the transcription level of CFTR gene. 16HBE14o-, IB3 or 6CFSMEo- cells were incubated with DMSO or staurosporine (STS) before to purify RNA and perform a quantitative RT-PCR to measure the level of CFTR pre-mRNA or GAPDH mRNA. All results are representative of three independent experiments. Error bar=SD.

Supplemental Figure S5: Another apoptosis activator reproduces the effect of staurosporine on NMD. HeLa cells were transfected with expression vectors encoding Globin mRNA either WT (Norm) or harboring the 39-PTC (Ter) or MUP mRNA before exposure to DMSO (negative control) or apoptosis activator 2 (AA2). Proteins and mRNAs were then analyzed to measure the degree of apoptosis (A), the efficiency of NMD as assessed by quantitative RT-PCR (B), and the cleavage of PARP, caspase 3, UPF1 or UPF2 by western-blot analysis (C). * indicates non-specific protein

species. The three left-most lanes in B and C represent a serial dilution of a Norm RT (B) or untreated extract (C) symbolized by a triangle. The molecular weight scale is indicated on the left side of the gel in C. A histogram representation of the mRNA measures of panel B is shown on the right side of the gel. The results are representative of two independent experiments. Error bar=SD, student t-test: **=p<0.05.

Supplemental Figure S6: Expression of UPF caspase-cleavage fragments in HeLa cells. Cells were transfected with 2 μg of expression vector for 48 hours before to harvest cells and extract proteins to perform western-blot analysis using anti-GFP antibody to detect UPF1 isoforms (A) or UPF2 isoforms (B). The N-terminal caspase cleavage fragment of UPF1, UPF2 or the C-terminal caspase cleavage fragment of UPF1 or UPF2 are noted CFP UPF1-Nter, CFP UPF2-Nter, CFP UPF1-Cter or CFP UPF2-Cter, respectively. Empty vector, UPF1 or UPF2 full length expression vectors are noted CFP, CFP UPF1 or CFP UPF2, respectively. * indicates non-specific protein species.

Supplemental Figure S7: Determination of the contribution of UPF1 or UPF2 caspase cleavage fragments to apoptosis. (A) Western-blot analysis of the level of UPF1 or UPF2 in the presence of siRNAs under DMSO or staurosporine (STS) treatment in HeLa cells. The molecular weight scale is indicated on the left side of each gels and the identity of each species is shown on the right side of each gel. * indicates non-specific protein species. These are the same samples as in supplemental Figure S2A. (B) Measure of apoptosis in the same samples as in (A) using incorporation of annexin V. Error bar=SD, the bracket indicate that the student t-test did not show any significant differences between these coditions. Results are representative of 2 independent experiments.

3. Project 3: Evidence for the involvement of the cytoskeleton in NMD mechanism

3. 1 A summary for the project

Like the second project, results from screening of chemical library brought us to consider Taxol as a putative NMD inhibitor. Taxol is known to interfere with cytoskeleton so we decided to investigate the putative involvement of cytoskeleton in NMD. To do that, I chose to use 2 molecules affecting acting filaments and 2 molecules interfering with microtubules and took amlexanox as a positive control. The two actin filaments inhibitors (cytochalasin D and jasplakinolide) and two microtubules inhibitors (colchicine and taxol) have been very well characterized for their property of impairing cytoskeleton structure. On the mRNA level, these four drugs can inhibit NMD with a similar or more efficient capacity than amlexanox and on the protein level cytochalasin D and jasplakinolide like amlexanox can induce the synthesis of full length proteins of CFTR from nonsense mutation-containing mRNA when colchicine or taxol can not. To investigate the mechanism by which cytoskeleton inhibitors can inhibit NMD, I used immunoprecipitation and microscopy approaches. I found that these four cytoskeleton inhibitors can decrease the interaction between cytoskeleton and NMD factors (UPF1, UPF2 and UPF3X) and can induce UPF1 and NMD substrates partially or totally to colocalize in P-bodies. I also identify new cytoplasmic foci that are still under investigation to determine their composition and their role. The involvement of cytoskeleton in NMD raises the question of the localization of the different steps of NMD and using cytoskeleton inhibitors might be a convenient approach to study that point.

3.2 Results

Introduction

Several lines of evidences let us think that molecules that interfere with the integrity of cytoskeleton could be inhibitors of NMD. First, taxol which inhibits microtubule depolymerization was identified in our screening system as a putative NMD inhibitor. Then, we and others showed that NMD factors and substrates transit through cytoplasmic foci called P-bodies (Sheth and Parker 2006; Durand, Cougot et al. 2007) meaning that PTC-containing mRNAs have to be targeted to P-bodies and this process could be performed by the cytoskeleton. Indeed, cytoskeleton regulates various cellular and molecular events, such as intracellular transport of organelles, cell signaling, cell movement, cellular transport, maintenance of cell shape and mRNAs trafficking (Pollard 2003). However, until now no relationship has been made between NMD and cytoskeleton. Therefore, we were interested to demonstrate a link between NMD and cytoskeleton, to test molecules interfering with cytoskeleton as NMD inhibitors and to compare their NMD inhibition efficiency with the one observed after amlexanox treatment (Gonzalez-Hilarion, Beghyn et al. 2012).

The cytoskeleton is made of three kinds of protein filaments: actin filaments, intermediate filaments and microtubules. I decided to focus on actin filaments and microtubules since intermediate filaments are less dynamic structures than the 2 other types of filaments and their role is more involved in the cell shape and anchor of cellular organelles (Fletcher and Mullins 2010). To interfere with actin filaments or microtubules, I chose two well-known actin-targeted agents (cytochalasin D and jasplakinolide (JPK)) and two microtubule-targeted agents (colchicine and taxol). Cytochalasin D inhibits actin polymerization when JPK induces actin polymerization and stabilizes actin filaments. Colchicine inhibits microtubules polymerization when taxol stabilizes the microtubule polymers and protects them from disassembly (Geipel, Just et al. 1990; King-Smith, Basciano et al. 2001; Bhattacharyya, Panda et al. 2008).

We choose the cystic fibrosis model since we have two nonsense mutation-containing cystic fibrosis cellular models in our lab and all the techniques and reagents to study the expression of CFTR (Gonzalez-Hilarion, Beghyn et al. 2012).

Results

Cytoskeleton inhibitors can inhibit NMD

First, to analyze the effect of cytoskeleton on NMD, I used HeLa cells stably transfected with a plasmid that encodes either the pYFP-Globin 39Ter containing nonsense mutation at the position 39 or pYFP-GPx1 46Ter harboring nonsense mutation at the position 46. Importantly, Globin (Gl) mRNA is subject to nucleus-associated NMD in non erythroid cells whereas GPx1 mRNA is subject to cytoplasmic NMD (Maquat, Kinniburgh et al. 1981; Sun, Moriarty et al. 2000). Cells were incubated with 1µM cytochalasin D, 1µM jasplakinolide, 10µM colchicine, 1µM taxol (the concentrations of drugs were chosen according to the literature (Thuret-Carnahan, Bossu et al. 1985; Geipel, Just et al. 1990; Boll, Partin et al. 1991; Cronstein, Molad et al. 1995; King-Smith, Basciano et al. 2001; Vanden Berghe, Hennig et al. 2004; Mseka and Cramer)), or DMSO as the negative control (Figure1). After 24h, total RNAs were purified and analyzed by RT-PCR. GAPDH mRNA was used as a reference. The level of Gl mRNA (Figure1A) or GPx1 mRNA (Figure1B) in the presence of jasplakinolide, colchicine, taxol relative to control was increased by 2-3 folds. Cytochalasin D at 24h did not affect the expression of Gl mRNA or GPx1 mRNA.

Since the three other drugs have an effect on NMD, I decided to verify that the no effect of cytochalasin D was not due to suboptimal experimental conditions. I tested the NMD efficiency in the presence of cytochalasin D on Gl mRNA (Figure1C) and GPx1 mRNA (Figure1D) at 48h since literature indicates that this drug can be used for 48h in order to cause cell retraction and to destroy actin filaments (Oh, Beckmann et al. 2011). A 2-3 folds of stabilization of Gl mRNA or GPx1 mRNA were detected with cytochalasin D treatment after 48h (Figure1C). Our results show that jasplakinolide, colchicine, taxol at 24h can inhibit nucleus-associated and cytoplasmic

NMD when cytochalasin D requires 48h to inhibit NMD. Overall, our results suggest that interfering with cytoskeleton integrity leads to inhibit NMD.

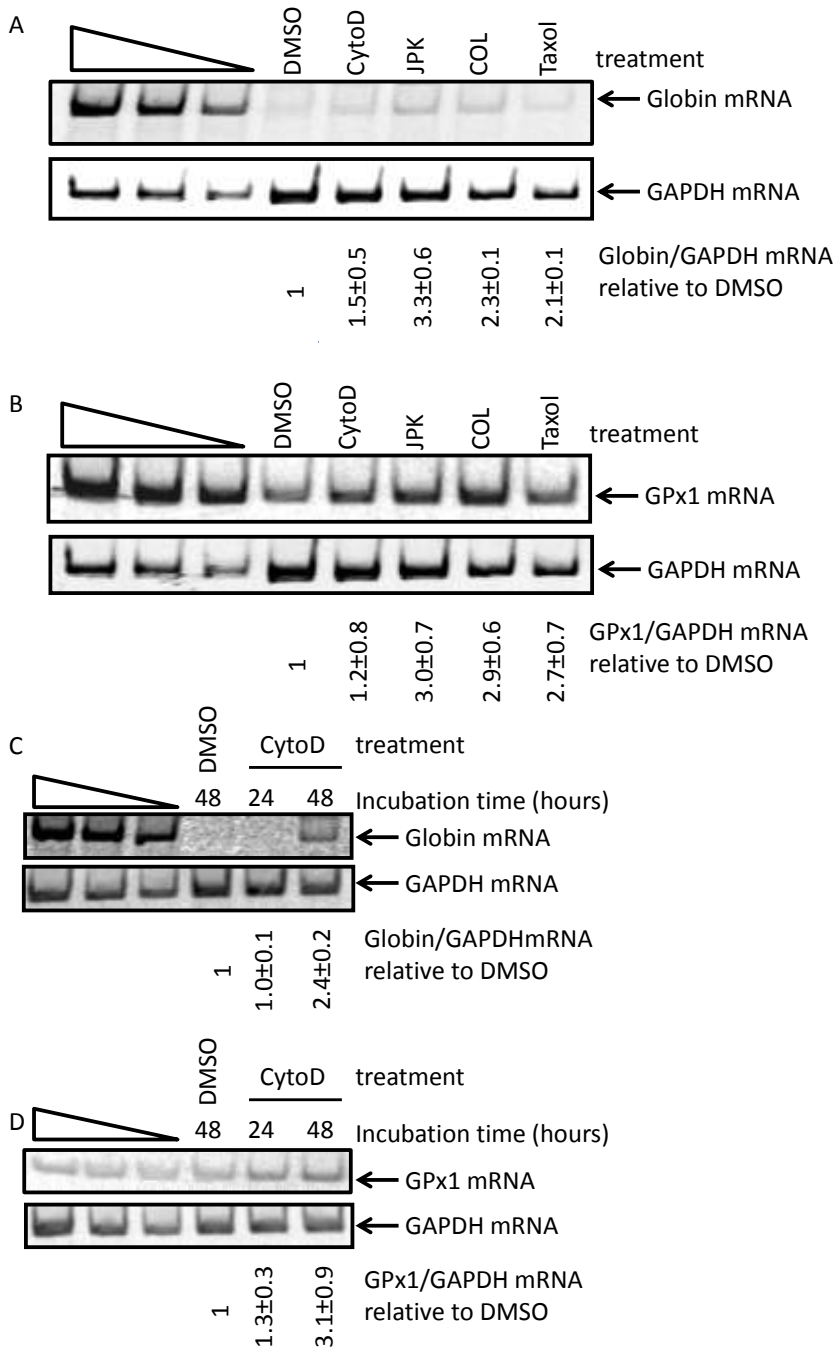

Figure 1: Stabilization of nonsense mutation-containing Globin or GPx1 mRNA by cytoskeleton inhibitors

HeLa cells were stably transfected with the plasmids that encode either the pYFP-Globin 39Ter (A, C) or pYFP-GPx1 46Ter (B, D). A,B, Cells were incubated respectively with DMSO, 1µM cytochalasin D (CytoD), 1µM jasplakinolide (JPK), 10µM colchicine (COL), 1µM Taxol for 24 hours. C,D Cells were treated with DMSO for 48h, 1µM CytoD for 24h and 48h. RNAs were purified, reverse transcribed and amplified by PCR to measure the level of Globin mRNA (A, C) or GPx1 mRNA (B, D). The level of Globin

mRNA or GPx1mRNA was normalized to the level of GAPDH mRNA. The three left lanes represent a two-fold serial dilution of RNA from the HeLa cells that were transfected with pYFP-globin (wild type) Norm (A, C) or pYFP-GPx1 Norm (B, D). These results are representative of three independent experiments.

In order to determine whether endogenous nonsense-containing mRNAs can also be stabilized when cytoskeleton integrity is affected, I decided to incubate IB3 cells (that harbor ΔF508/W1282X mutations on CFTR mRNA) (Figure2A) or 6CFSMEo- cells (that harbor ΔF508/Q2X mutations on CFTR mRNA) with one of the four cytoskeleton inhibitors or with amlexanox for 48h (Figure2B). Cells were incubated with 1µM cytochalasin D, 1µM jasplakinolide, 10µM colchicine, 1µM taxol, 25µM amlexanox or DMSO as the negative control. After 48h, total RNAs were purified and analyzed by RT-PCR. The level of CFTR mRNA was normalized to the level of GAPDH mRNA. Two to four folds of increase of CFTR mRNA expression were measured with the four cytoskeleton inhibitors treatment relative to control GAPDH mRNA. In IB3 cells, the efficiencies of the four cytoskeleton inhibitors were similar to amlexanox, but in 6CFSMEo- cells, it seemed that the four drugs were more efficient than amlexanox. The results show that the four drugs at 48h can inhibit NMD in IB3 and 6CFSMEo- cells in a similar or more efficient way than amlexanox.

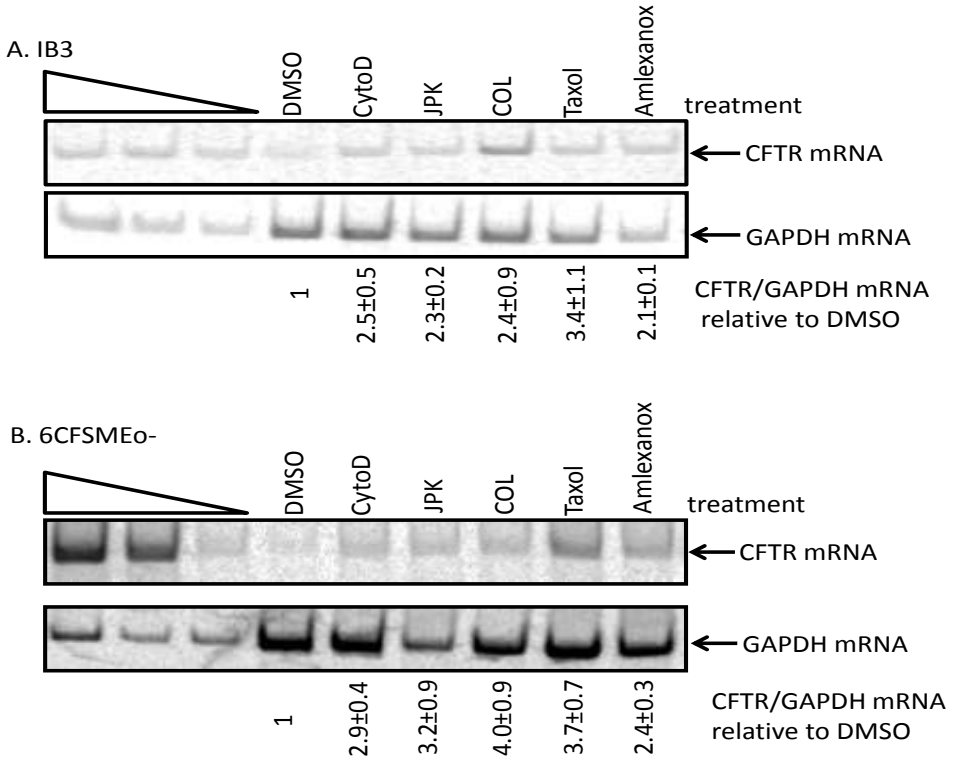

Figure 2: The cytoskeleton inhibitors increase the level of CFTR mRNA

IB3 cells (A) or 6CFSMEo- (B) were incubated respectively with DMSO, 1µM cytochalasin D (CytoD), 1µM jasplakinolide (JPK), 10µM colchicine (COL), 1µM Taxol or 25µM amlexanox for 48 hours. RNAs were purified, reverse transcribed and amplified by PCR to measure the level of CFTR mRNA. The level of CFTR mRNA was normalized to the level of GAPDH mRNA. The three left lanes represent a two-fold serial dilution of RNA from Calu3 cells that overexpress CFTR mRNA. These results are representative of three independent experiments.

Cytoskeleton inhibitors destroy cytoskeleton structure

Since I was able to show that these drugs can affect NMD, I wanted to verify that under my experimental conditions, cytoskeleton structure was affected. I decided to observe by fluorescence microscopy, the staining of actin or tubulin after cell treatment with 1µM cytochalasin D, 1µM jasplakinolide , 10µM colchicine, 1µM taxol for 48h in HeLa (Figure3A), in IB3 (Figure3B) or in 6CFSMEo- cells (Figure3C).

Actin is localized mainly in the cytoplasm, especially at the cell membrane in DMSO-treated cells. Cytochalasin D-treated cells showed some actin granules in the cytoplasm. In jasplakinolide -treated cells, actin staining was concentrated to the cell membrane and the cell size was reduced. Colchicine-treated cells or Taxol-treated cells had no significant changes in their morphology or in the actin staining compared to DMSO treatment. These results show that cytochalasin D and jasplakinolide can destroy actin filaments structure in the three cell lines unlike colchicine or taxol as expected.

In DMSO-treated cells, the tubulin staining showed numerous long and thin silk-like structures in the cytoplasm. The shape of cytochalasin D-treated cells remained intact and did not show any changes in the tubulin staining. Jasplakinolide -treated cells have a size reduction but did not show any tubulin staining changes. Colchicine-treated cells displayed numerous aggregated tubulin foci. Taxol-treated cells show some bulk silk-like structures concentrated at the cell membrane. Then I concluded that colchicine or taxol can interfere with microtubules structure in the three cell lines unlike cytochalasin D or jasplakinolide, as expected.

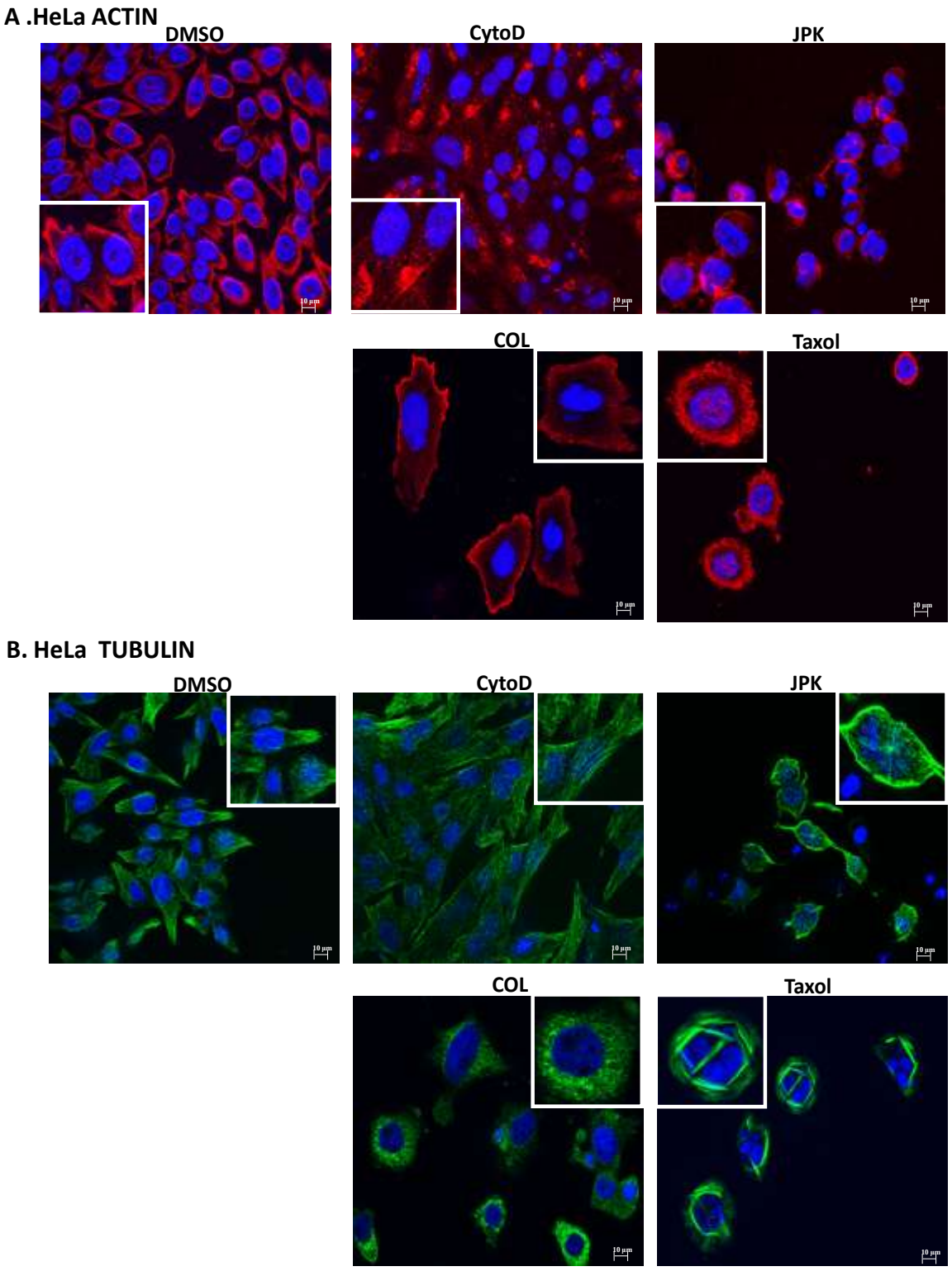

Figure 3A: Actin or tubulin staining in HeLa cells under DMSO, CytoD, JPK, COL or Taxol treatment.

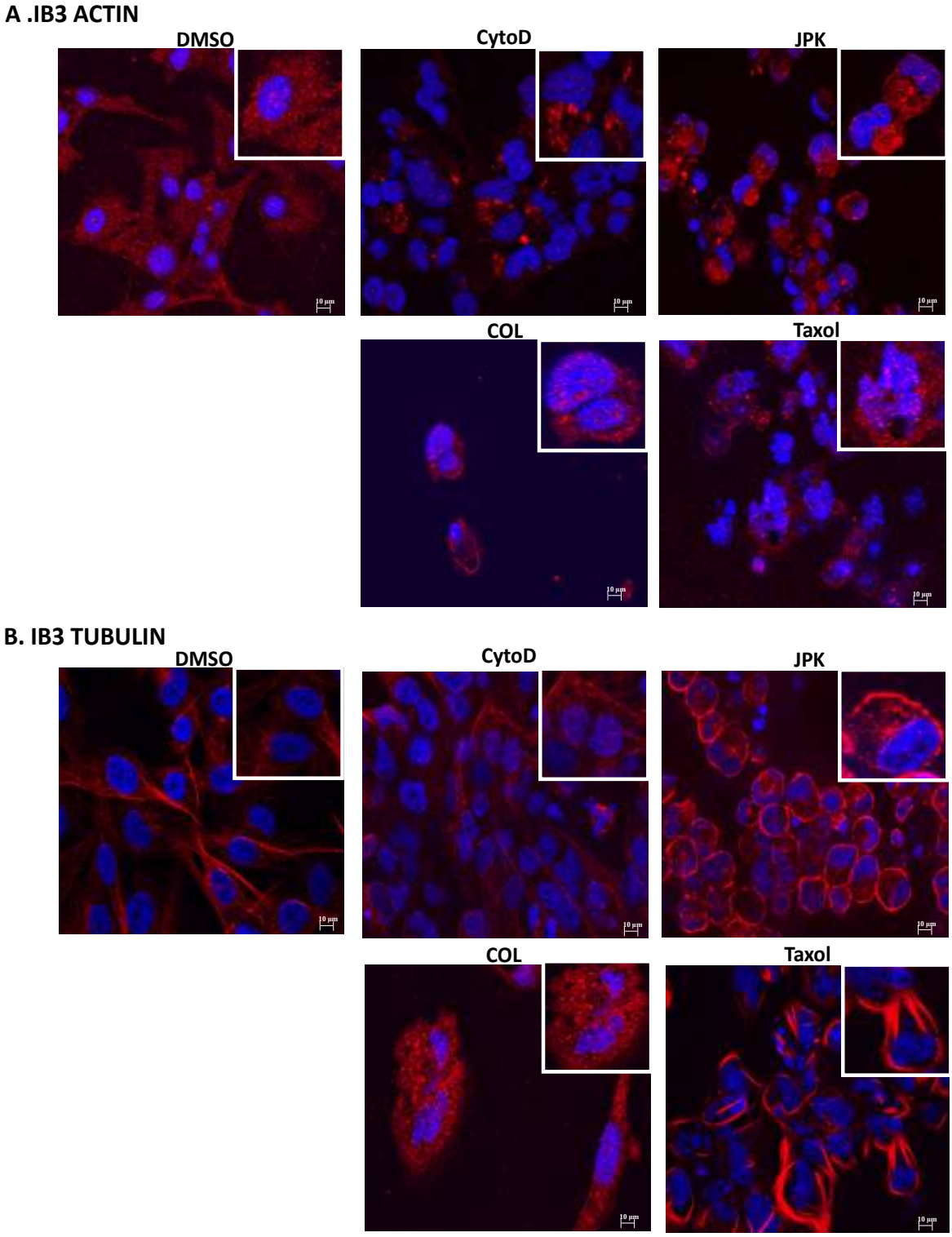

Figure 3B: Cellular distribution of actin or tubulin with DMSO, CytoD, JPK, COL, Taxol in IB3 cells

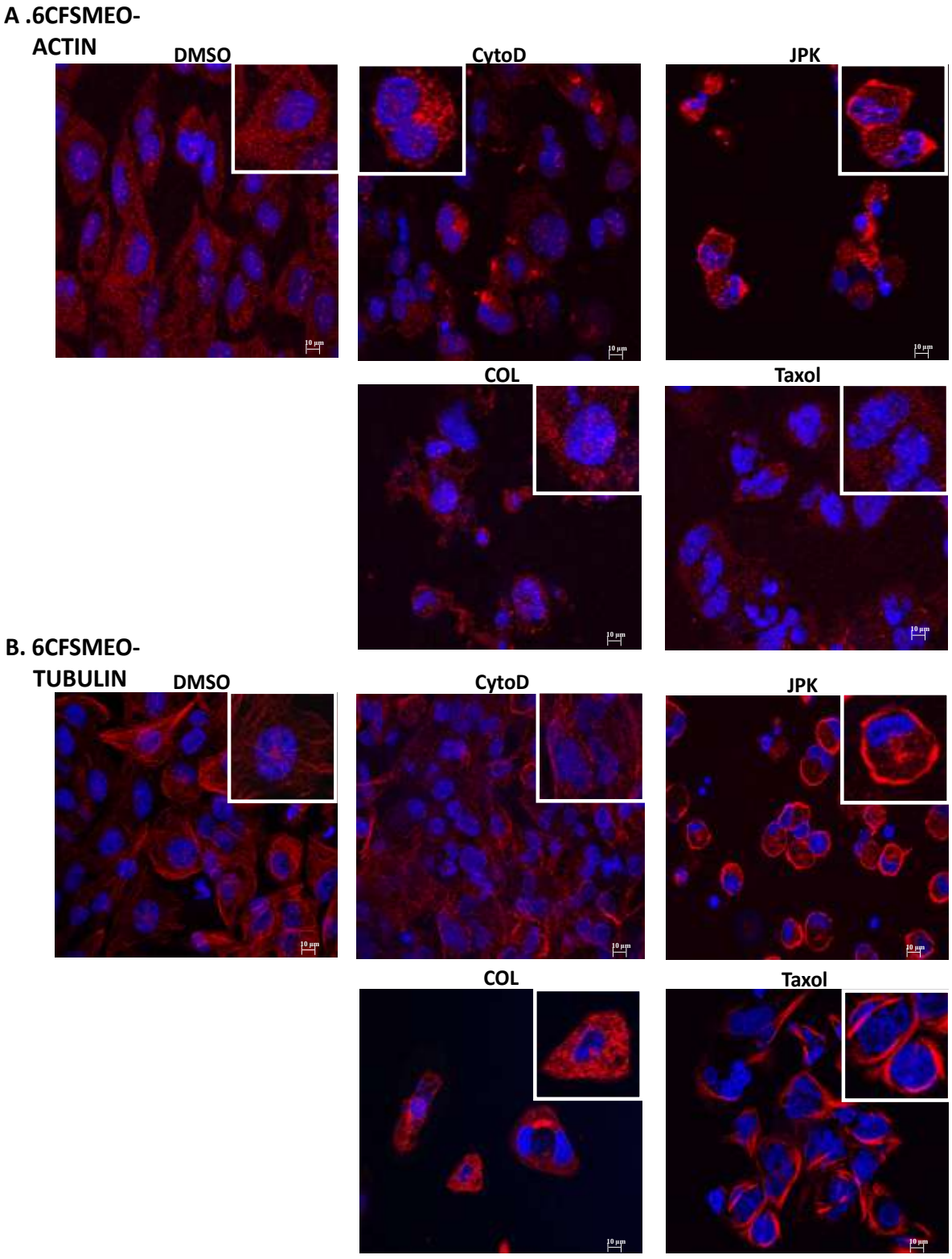

Figure 3C: Cellular distribution of actin or tubulin with DMSO, CytoD, JPK, COL, Taxol in 6CFSMEo-cells

Figure 3: Cellular distribution of actin or tubulin under DMSO, CytoD, JPK, COL or Taxol treatment.

HeLa (3A), IB3 (3B) or 6CFSMEo-(3C) cells were incubated respectively with DMSO, 1µM CytoD, 1µM JPK, 10µM COL or 1µM Taxol. 48 hours later, cells were fixed using formalin solution for 10 min at room temperature and permeabilized in 70% ethanol at 4°C for 1 hour. Cells were incubated with the primary antibodies (A actin, B tubulin) 1 hour at room temperature, washed three times with PBS and incubated with anti-rabbit goat antibody Alexa Fluor 594 (red) or anti-rabbit goat antibody Alexa Fluor 488 (green). Cells were washed three times with PBS and incubated with Hoechst stain blue) for 2 min at room temperature.

Cytoskeleton inhibitors do not affect natural NMD targets

It has been demonstrated that NMD modulates the expression of about 5% of the human genome (Viegas, Gehring et al. 2007). Since the cytoskeleton inhibitors can increase the level of nonsense-containing mRNAs, I investigated whether these drugs can affect the expression of natural NMD targets that use NMD to regulate their expression. In order to verify the impact of the four drugs on natural substrates of NMD, I measured the level of SC35, NAT9 and TBL2 mRNAs (Viegas, Gehring et al. 2007). For that, I incubated HeLa cells with the four cytoskeleton inhibitors for 48h and did RT-PCR to detect the mRNA levels of SC35, NAT9 or TBL2 (Figure 4). My results show that the mRNA level fluctuation was between 0.9 and 1.4 folds after the drug treatment compared to DMSO treatment for the three tested genes expression. We therefore concluded that the cytoskeleton inhibitors do not affect the natural NMD targets regulation and this also suggests that the detected increase of mRNA level for the nonsense mutation-containing mRNAs cannot be attributed to a general up-regulation of the transcription.

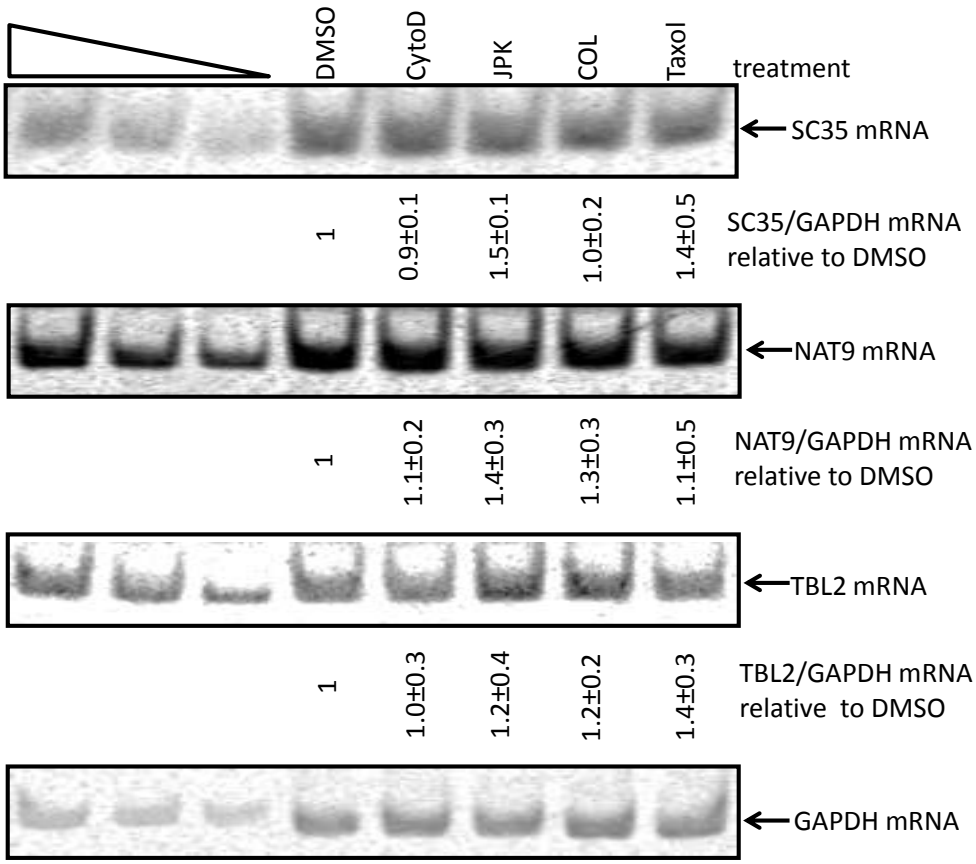

Figure 4: Cytoskeleton inhibitors do not affect natural NMD targets

HeLa cells were stably transfected with the plasmids that encode either the pYFP-Globin 39Ter or pYFP-GPx1 46Ter. Cells were incubated respectively with DMSO, 1µM cytochalasin D (CytoD), 1µM jasplakinolide (JPK), 10µM colchicine (COL) or 1µM Taxol for 48hours. RNAs were purified, reverse transcribed and amplified by PCR to measure the level of SC35 mRNA, NAT9 mRNA, and TBL2 mRNA. The level of mRNA was normalized to the level of GAPDH mRNA. The three left lanes represent a two-fold serial dilutions of RNA from the HeLa cells. These results are representative of three independent experiments.

Cytoskeleton inhibitors do not induce apoptosis

Because cytoskeleton regulates cell division, cell movement and shape, I was interested in determining whether these four drugs can affect cell growth in my experimental conditions. Another reason was that my other project showed that NMD is inhibited during apoptosis and drugs like taxol are used as an anti-cancer drug so I wanted to exclude the possibility that the effect on NMD observed with the cytoskeleton targeted drug was due to an activation of apoptosis. I measured apoptosis level using Annexin V and PI staining. HeLa, IB3 or 6CFSMEo- cells were treated by the four drugs for 48h before to measure the apoptosis rate. The results

showed that cytochalasin D, jasplakinolide , colchicine, taxol did not induce apoptosis in IB3 or 6CFSMEo- cells. Surprisingly, jasplakinolide, colchicine or taxol induced 30%-50% of apoptosis in HeLa cells (Figure 5). These results might suggest some differences in the treatment sensitivity between different cell-type. Altogether, my results indicate that cytoskeleton integrity is required for NMD process and that can not be related with an eventual apoptotic status of the cells due to the drug treatment, at least in IB3 or 6CFSMEo- cells. To exclude any influence of apoptosis in my further results, all experiments were performed in IB3 or 6CFSMEo- cells and not in HeLa cells.

A.

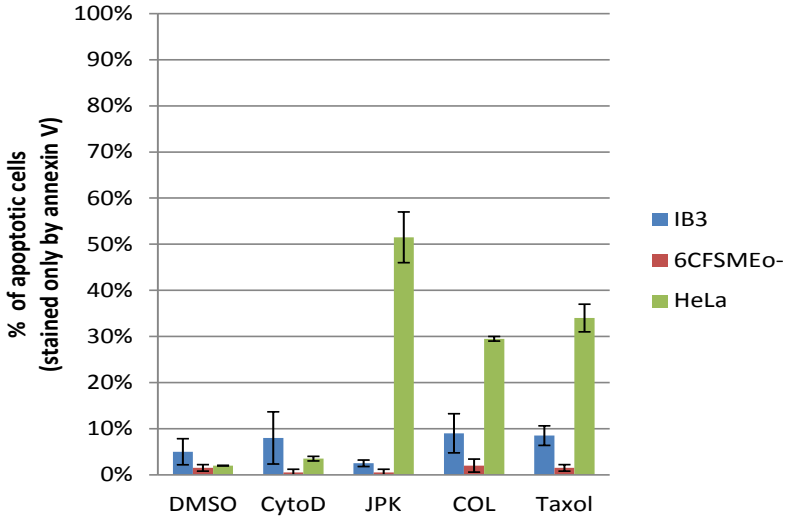

B.

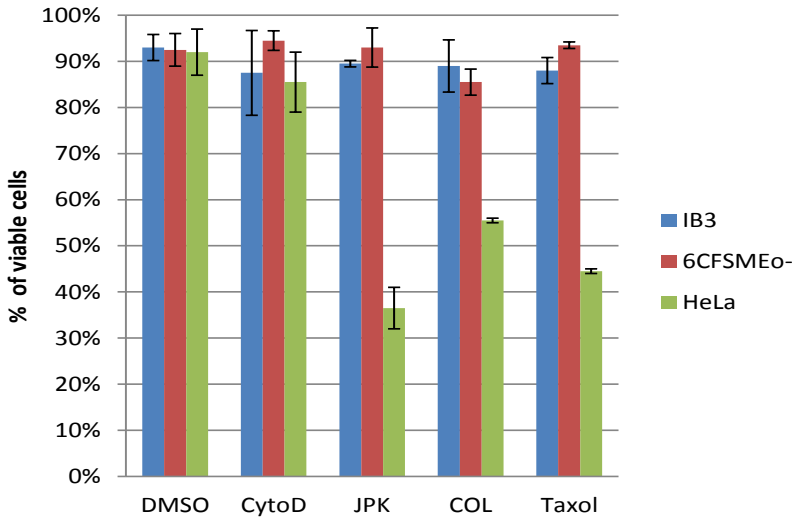

Figure 5: The percentage of apoptotic/viable cells induced by cytoskeleton inhibitors

HeLa, IB3, 6CFSMEo-Cells were incubated respectively with DMSO, 1µM cytochalasin D (CytoD), 1µM jasplakinolide (JPK), 10µM colchicine (COL), 1µM Taxol. 48 hours later, the attached cells were stained by Annexin V and PI. These results are representative of three independent experiments.

Cytoskeleton inhibitors do not affect total protein translation

NMD requires translation to identify PTCs on mRNA (Lejeune, Ishigaki et al. 2002). I wanted to know whether NMD inhibition by the cytoskeleton inhibitors was due to an indirect effect via an inhibition of translation. For that, I measured the translation efficiency in 6CFSMEo- cells by incubating these cells with an L-AHA (L-azidohomoalanine) modified amino-acid in order to detect and quantify newly synthesized proteins. To detect L-AHA proteins after protein extraction, I used the Click-iT Protein Analysis Detection Kit (Life technologies) (figure 6). The result showed that there was no significant effect on the level of translation with the treatment of cytochalasin D, jasplakinolide, colchicine or taxol relatively to the DMSO sample used as a control unlike with the protein extract from cells incubated with cycloheximide which is well known to inhibit translation. This result might be surprising since we could expect that by interfering with cytoskeleton, we will impact on translation but it has already been documented that cytochalasin D, colchicine or Taxol did not affect total protein synthesis (Le Marchand, Patzelt et al. 1974; Sauman and Berry 1993; Martin, Angeloni et al. 2004; Mileusnic, Lancashire et al. 2005; Sun, Chen et al. 2010). In the case of jasplakinolide, there were very few articles talking about the relation between jasplakinolide and total protein translation. Only Sebastian et al has showed that jasplakinolide increased the total protein synthesis in the mouse portal veins cells which is consistent with the slight increase of translation that I observe in my cells (Albinsson and Hellstrand 2007). So I concluded that the NMD inhibition that we observed after the drugs treatment is not related with a putative translation inhibition.

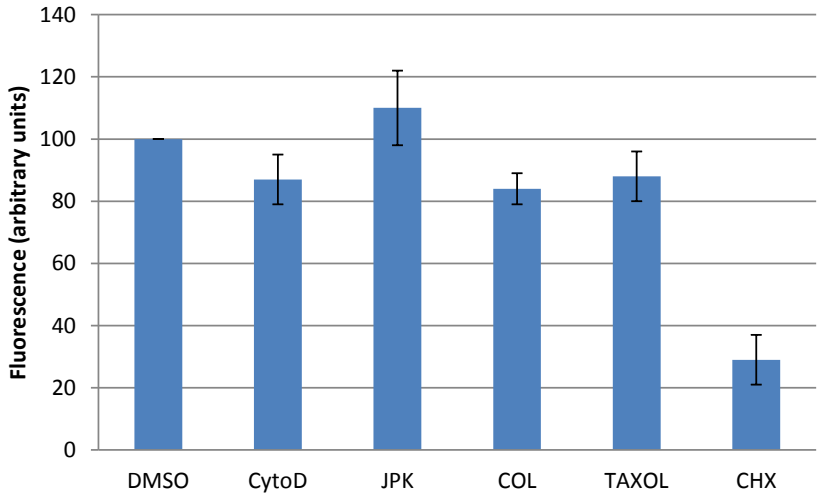

Figure 6: Cytoskeleton inhibitors do not affect translation in 6CFSMEo- cells

6CFSMEo-Cells were incubated respectively with DMSO, 1µM cytochalasin D (CytoD), 1µM jasplakinolide (JPK), 10µM colchicine (COL) or 1µM Taxol for 48 hours or incubated with 200µg/ml cycloheximide (CHX) (as positive control) for 4h. 1h before harvesting cells, 25µM L-azidohomoalaine (L-AHA) was added to the cell culture medium to be incorporated into newly synthesized proteins. Then cells were collected to measure translation efficiency using Click-iT Protein Analysis Detection Kit (Life technologies). These results are representative of three independent experiments.

Some cytoskeleton inhibitors induce readthrough

Since cytoskeleton inhibitors can stabilize nonsense mutation-containing mRNAs, I wanted to determine whether these stabilized nonsense mutation -containing mRNAs can be translated into proteins. First, I analyzed the protein expression from the well-studied NMD substrates encoding Globin Ter subject to nucleus-associated NMD or GPx1 Ter subject to cytoplasmic NMD (Maquat, Kinniburgh et al. 1981; Sun, Moriarty et al. 2000). I transfected HeLa cells with a plasmid encoding YFP-Globin Ter or YFP-GPx1 Ter and a plasmid called flag-SRSF7 that carries the SRSF7 cDNA which is not subject to NMD and codes for the SRSF7 protein (a splicing factor). 24h after transfection, I added cytoskeleton inhibitors or amlexanox as positive control to the cells. After 48h of treatment, I extracted proteins to analyze the level of Globin (Figure 7A) or GPx1 protein (Figure 7B). Under cytochalasin D, jasplakinolide or amlexanox treated cells, truncated Globin or GPx1 protein was found. Surprisingly, the full-length GPx1 protein was also synthesized meaning that cytochalasin D and jasplakinolide inhibit both nucleus- associated and cytoplasmic NMD and also activate PTC readthrough as amlexanox does. Interestingly,

these three drugs (cytochalasin D, Jasplakinolide and amlexanox) can not induce the synthesis of full length Globin protein suggesting either the PTC-readthrough of nucleus-associated and cytoplasmic NMD involves different mechanisms or it is more likely that the PTC on Globin is very difficult to readthrough. Colchicine and taxol did not induce the synthesis of truncated or full-length protein eventhough both molecules inhibit NMD (Figures 1-2). In addition, Figure 6 shows that colchicine or taxol does not affect the general translation in cells. Since under cytochalasin D and jasplakinolide treatment full-length or truncated proteins are present, that excludes the possibility that the proteins are not stable. The absence of proteins translated from Globin or GPx1 mRNA under colchicine or taxol treatment raises the possibility that nonsense mutation-containing mRNAs are protected from translation as it could be by sequestration in the cytoplasmic foci called P-bodies where translation does not happen (Durand, Cougot et al. 2007). To validate this hypothesis, I first measured the protein expression from endogenous nonsense mutation-containing mRNA to confirm that cytochalasin D or jasplakinolide can induce the synthesis of truncated and full length protein when colchicine or taxol cannot.

To do that, IB3 (Figure 8A) or 6CFSMEo- cells (Figure 8B) were incubated with 1µM cytochalasin D, 1µM jasplakinolide, 10µM colchicine, 1µM taxol, 25µM amlexanox or DMSO. 48h after, proteins were extracted before to perform a Western blot analysis for CFTR protein. As a loading control, I analyzed the KU80 protein which is a DNA double strand's molecular detector and has helicase activity, a protein that is not expected to be related with NMD or readthrough mechanism. Interestingly, full length CFTR protein was detected in the presence of cytochalasin D, jasplakinolide or amlexanox in IB3 or 6CFSMEo- cells but not after treatment with colchicine or taxol. No truncated proteins were found. However, the truncated CFTR protein cannot be detected in 6CFSMEo- cells since the PTC replaces the second codon of CFTR making undetectable the putative truncated protein. In the case of IB3 cells, the truncated CFTR protein was also not observed suggesting that it could be unstable. Results of the cytoskeleton inhibitors on endogenous nonsense mutation-containing mRNAs are consistent with the results obtained with

transfected PTC-containing Globin or GPx1 mRNAs. Overall, my results suggest that actin filaments are not necessary for PTC readthrough since readthrough can occur in the absence of actin filaments.

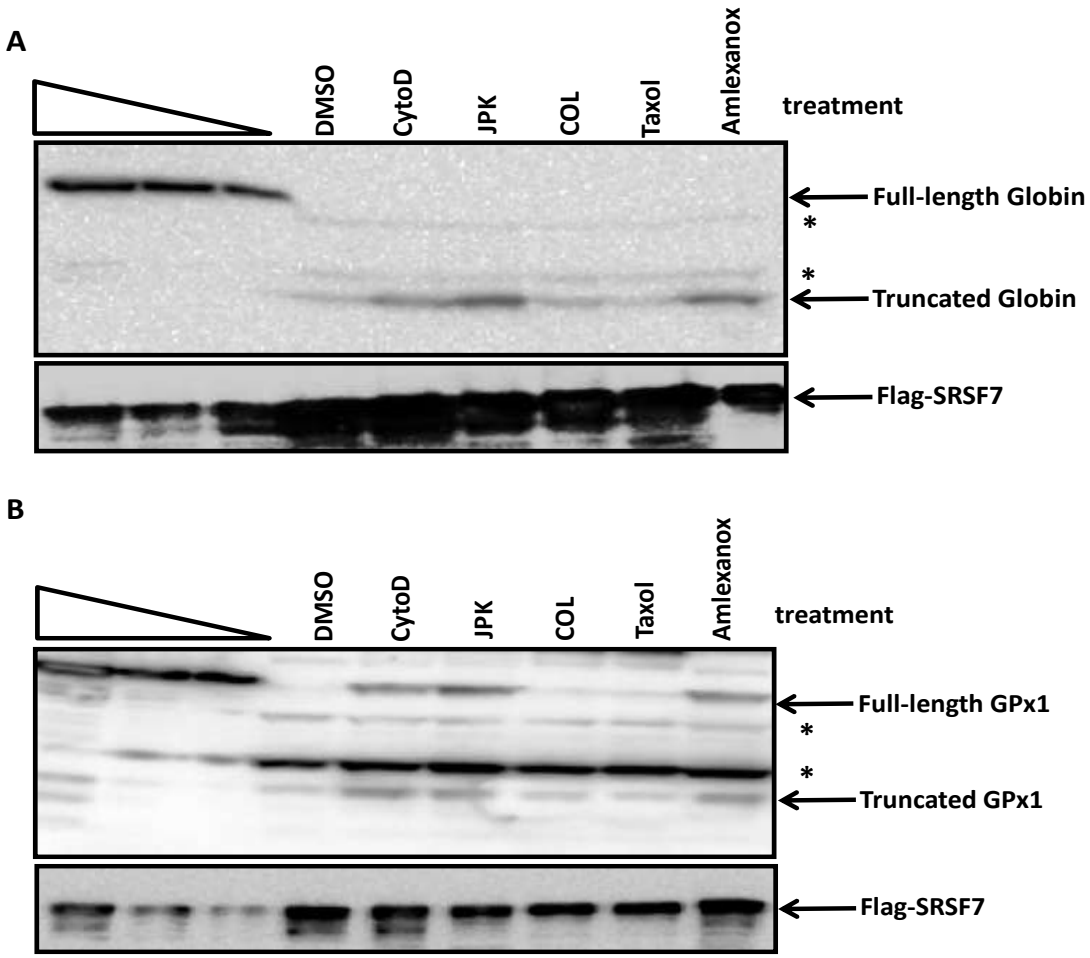

Figure 7: Effect of cytoskeleton inhibitors on the translation of nonsense mutation- containing mRNAs

HeLa cells were transfected with YFP-Globin 39Ter (A) or YFP-GPx1 46 Ter (B) and flag-SRSF7 as reference plasmid. Transfected cells were incubated respectively with DMSO, 1µM cytochalasin D (CytoD), 1µM jasplakinolide (JPK), 10µM colchicine (COL), 1µM Taxol or 25µM amlexanox for 48 hours. Proteins were purified to do western blot to detect Globin or GPx1 protein by GFP antibody. SRSF7 protein was detected by flag as a loading control. The three left lanes represent a two-fold serial dilutions of protein extract from HeLa cells transfected with Globin Norm (A) or GPx1 Norm (B). These results are representative of three independent experiments. *indicates non-specific protein species.

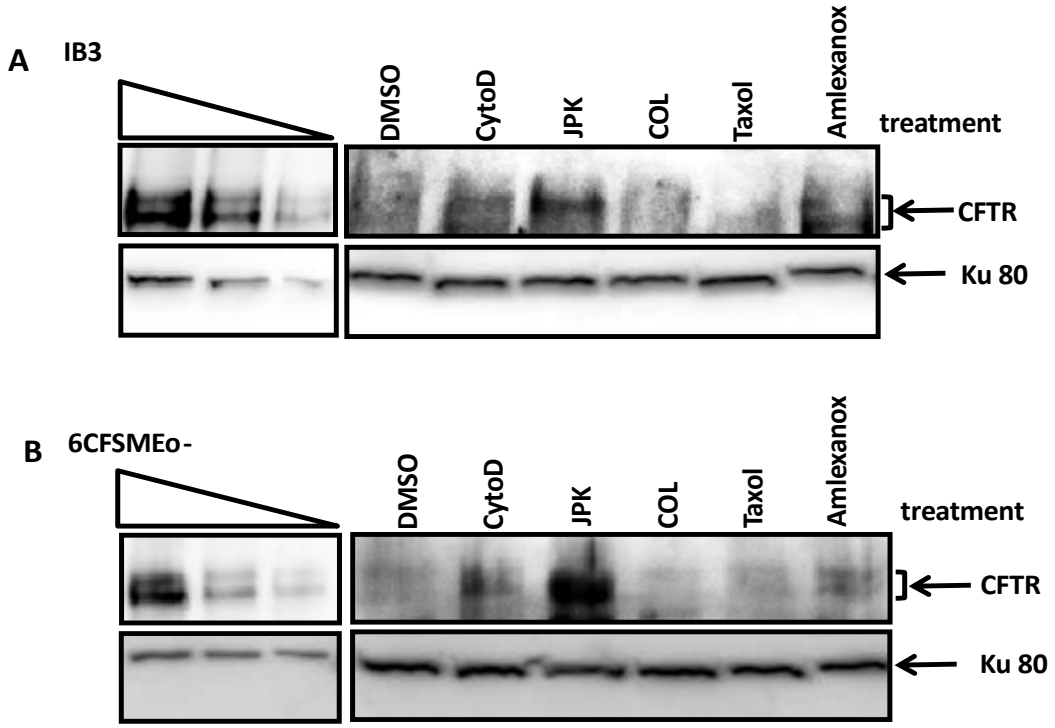

Figure 8: Effect of cytoskeleton inhibitors on the translation of nonsense mutation -containing CFTR mRNA

IB3 (A) or 6CFSMEo-Cells (B) were incubated respectively with DMSO, 1µM cytochalasin D (CytoD), 1µM jasplakinolide (JPK), 10µM colchicine (COL), 1µM Taxol or 25µM amlexanox for 48 hours. Proteins were purified to detect CFTR protein by western blot. KU80 protein was detected as a loading control. The three left lanes represent a two-fold serial dilutions of protein extract from Calu3 cells. These results are representative of three independent experiments.

The different stages of the CFTR maturation are well described in the literature. After translation, CFTR proteins go through post-translational processes. First, CFTR protein is transported through the rough endoplasmic reticulum (RER) to form a core-glycosylated immature CFTR protein and then through the Golgi apparatus with the formation of full glycosylated mature CFTR protein before to be localized at the apical plasma membrane where CFTR protein functions (Kopito 1999; Lubamba, Dhooghe et al. 2012). Since actin filaments inhibitors (cytochalasin D and japlakinolide) can induce the synthesis of full length CFTR protein, I continued to investigate whether the full length CFTR protein produced after cytochalasin D or japlakinolide treatment could be transported to the plasma membrane. For that, I incubated 6CFSMEo- cells or 16HBE14o- cells which express wild-type CFTR as positive control on the coated slides, with 1µM cytochalasin D, 1µM jasplakinolide, 10µM colchicine, 1µM taxol or DMSO.

After 48h of drugs treatment, cells were incubated sequentially with anti-CFTR primary antibody and then with a fluorescence secondary antibody. Finally I observed the cellular CFTR localization (red) under the microscope (Figure 9). I found that in 6CFSMEo- cells CFTR staining was detected on the cell membrane in the presence of cytochalasin D or jasplakinolide as it is in the wild-type 16HBE14o- cells. Consistent with the western blot results, no CFTR protein was detected at the membrane or anywhere else in the cell in the presence of colchicine or taxol. My results demonstrate that actin filaments inhibitors (cytochalasinD and jasplakinolide) allow the synthesis of the full length CFTR protein and this protein localizes to the membrane of 6CFSMEo- cells. This result suggests that the transport of CFTR to the cell membrane does not required actin filaments. My results are consistent with a previous study that reported that in the absence of actin filaments, CFTR can be transported to the cell membrane (Lee, Ferguson et al. 1989; Tousson, Fuller et al. 1996; Klopfenstein, Kappeler et al. 1998).

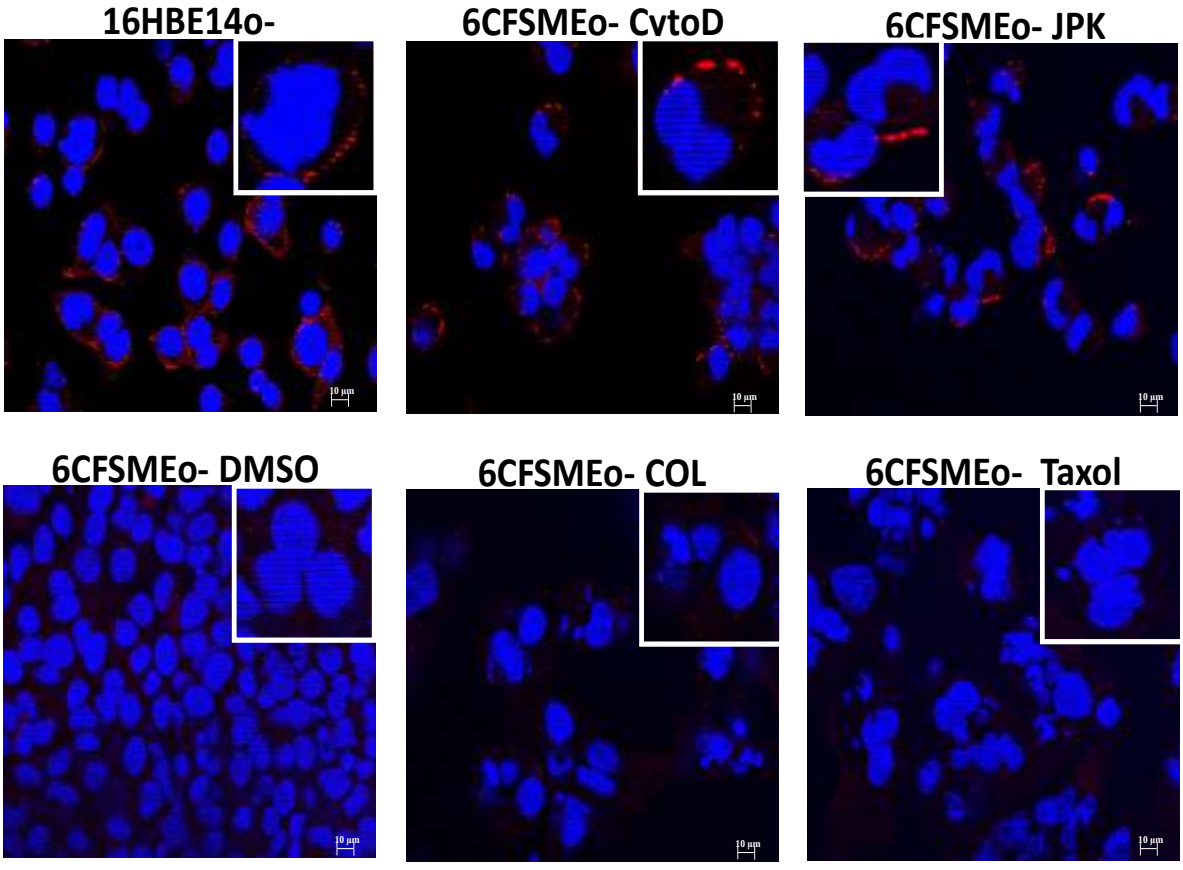

Figure 9: CFTR localization after cytoskeleton inhibitors treatment

6CFSMEo- cells were incubated on the coated coverslip with 1µM cytochalasin D, 1µM jasplakinolide, 10µM colchicine, 1µM taxol or DMSO for 48h. 16HBE14o- cells which express wild-type CFTR proteins were used as a positive control. Cells were fixed by methanol, permeated by 0.2% TritonX-100, blocked by BSA and incubated sequentially by the primary antibody anti-CFTR overnight at 4°C and the secondary antibody anti-CY3 for 1h at room temperature, before a final stained by DAPI and observed under microscopy. These results are representative of three independent experiments.

Cytoskeleton inhibitors affect the localization of NMD factors and substrates.

Under our experimental conditions, the four cytoskeleton inhibitors inhibit NMD and affect the integrity of cytoskeleton structure leading to the actin or tubulin concentration in the cytoplasm (Figure 3ABC). Based on this, I was interested in determining whether these four drugs can change the cellular localization of the NMD factors and substrates. For that, 6CFSMEo- cells were transfected with an expression vector encoding YFP-UPF1 or YFP-UPF3X and one of NMD substrates called pCMV-GPx1 46Ter containing nonsense mutation at the position 46 of the GPx1 gene before to be incubated with 1µM cytochalasin D, 1µM jasplakinolide, 10µM colchicine, 1µM taxol or DMSO. After 48h, cells were fixed and permeabilized before to be incubated with actin or tubulin primary antibody and then with a fluorescent secondary antibody. Finally under microscope, I observed the location of actin (or tubulin) (in red) and NMD factors (UPF1 (Figure 10A) or UPF3X (Figure 10B) in green). In DMSO-treated cells, UPF1 is distributed in the cytoplasm and UPF3X localized in the nucleus as expected (Durand, Cougot et al. 2007). Interestingly the four drugs induce UPF1 to aggregate in the cytoplasm without colocalization with actin or tubulin. Surprisingly, only jasplakinolide can also affect UPF3X location and makes it to concentrate in the cytoplasm without colocalization with actin.

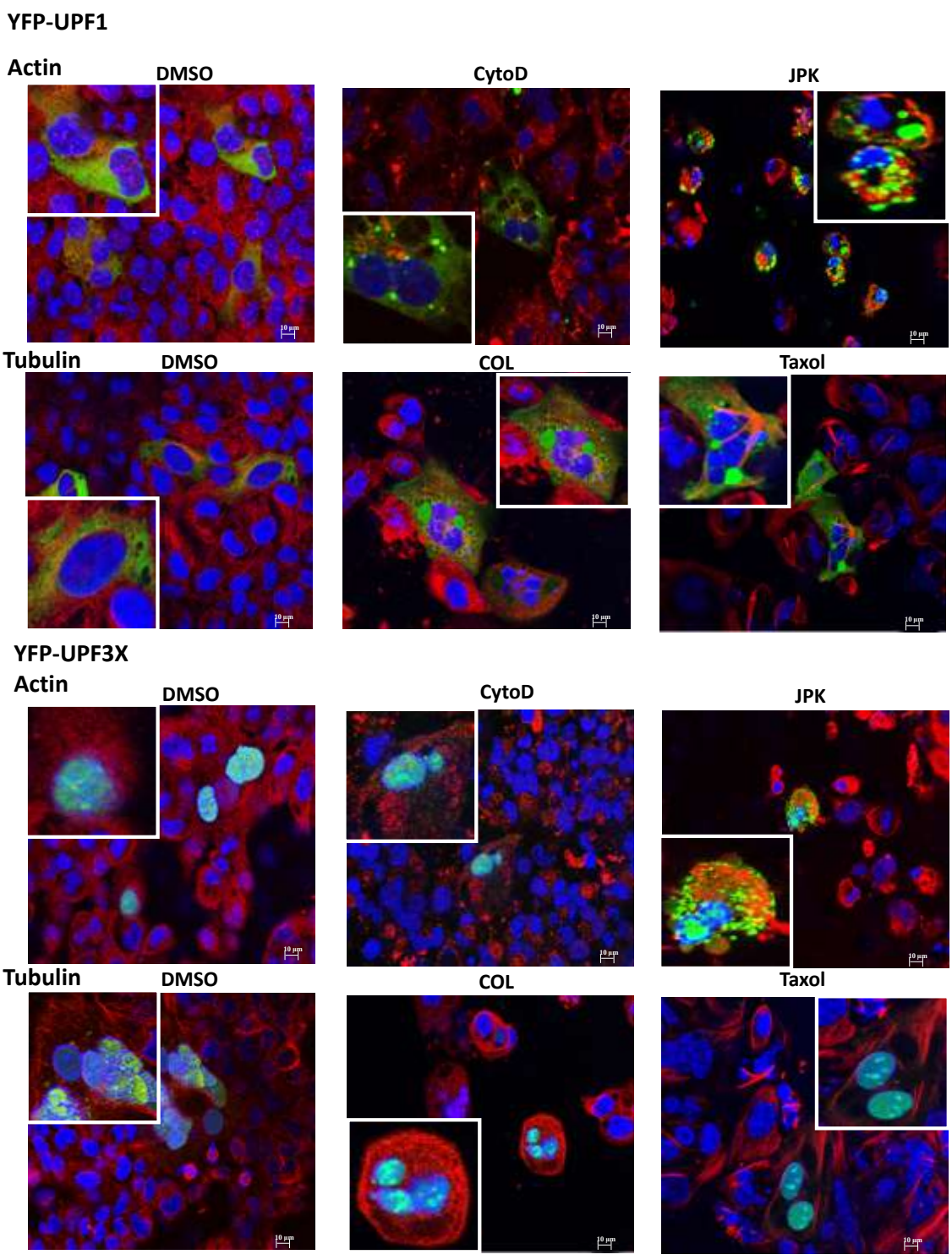

Figure 10: NMD factors do not colocolize with actin or tubulin under the treatment of cytoskeleton inhibitors in 6CFSMEo-cells

6CFSMEo-cells transfected with YFP-UPF1 or YFP-UPF3X and pCMV-GPx1 46Ter were incubated respectively with DMSO, 1µM CytoD, 1µM JPK, 10µM COL or 1 µM Taxol. 48 hours later cells were fixed using formalin solution for 10 min at room temperature and permeabilized in 70% ethanol at 4°C for 1 hour. Cells were incubated sequentially with the primary antibodies (actin or tubulin) 1 hour at room temperature, anti-rabbit goat second antibody Alexa Fluor 594 (red), finally with Hoechst stain (blue) for 2 min at room temperature.

Since the cellular location of NMD factors UPF1 and/or UPF3X are changed by the cytoskeleton inhibitors, I also wanted to determine whether NMD substrates are localized in the same place as NMD factors under cytoskeleton inhibitor treatment. I used two reference NMD substrate plasmids: one is pCMV-Globin 39Ter, the other is pCMV-GPx1 46Ter. For comparison, I also used pCMV-Globin Norm or pCMV-GPx1 Norm which have normal termination codon. 6CFSMEo- cells were respectively transfected with pCMV-Globin 39Ter or Norm or pCMV-GPx1 46Ter or Norm and an expression vector encoding either YFP-UPF1 protein or YFP-UPF3X protein before treatment. 48h after the four cytoskeleton inhibitors treatment, Globin or GPx1 mRNAs were detected by Fluorescence in situ hybridization (FISH) probe. The results showed that wild-type mRNAs (Globin in red (Figure 11A) or GPx1 in red (Figure11C)) location is not affected by any of the cytoskeleton inhibitors and mainly show a homogenous cytoplasmic distribution like in DMSO-treated cells. As expected and due to NMD, In contrast, no Globin Ter (Figure 11B) or GPx1Ter (Figure 11D) mRNA was detected in DMSO-treated cells. Globin Ter or GPx1 Ter (red) mRNAs were detected and concentrated in the cytoplasm when cells were incubated with the 4 drugs, which is consistent with the RT-PCR results demonstrating their capacity at inhibiting NMD. Interestingly, I observed a colocalization between the nonsense mutation-containing Globin or GPx1 mRNA and UPF1 (Figure 11 B, D) under the treatment of the four drugs. In addition, a colocalization was detected between UPF3X and NMD substrates (Figure 12) in the presence of JPK only.

A red color represents Globin Norm, green color represents UPF1

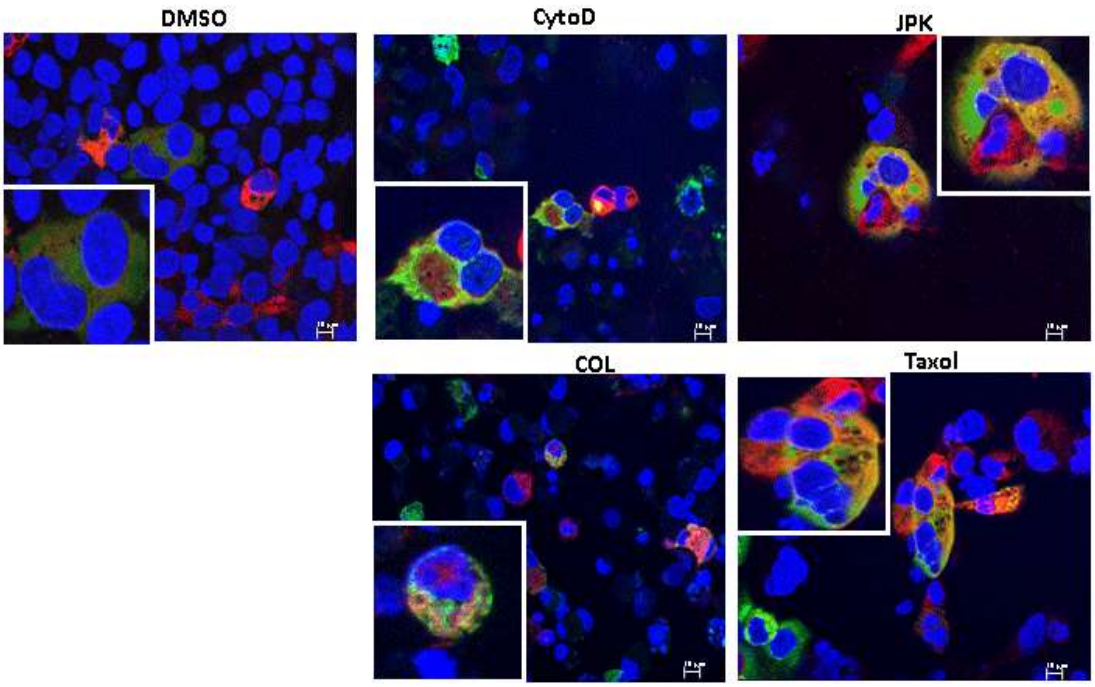

B red color represents Globin Ter, green color represents UPF1

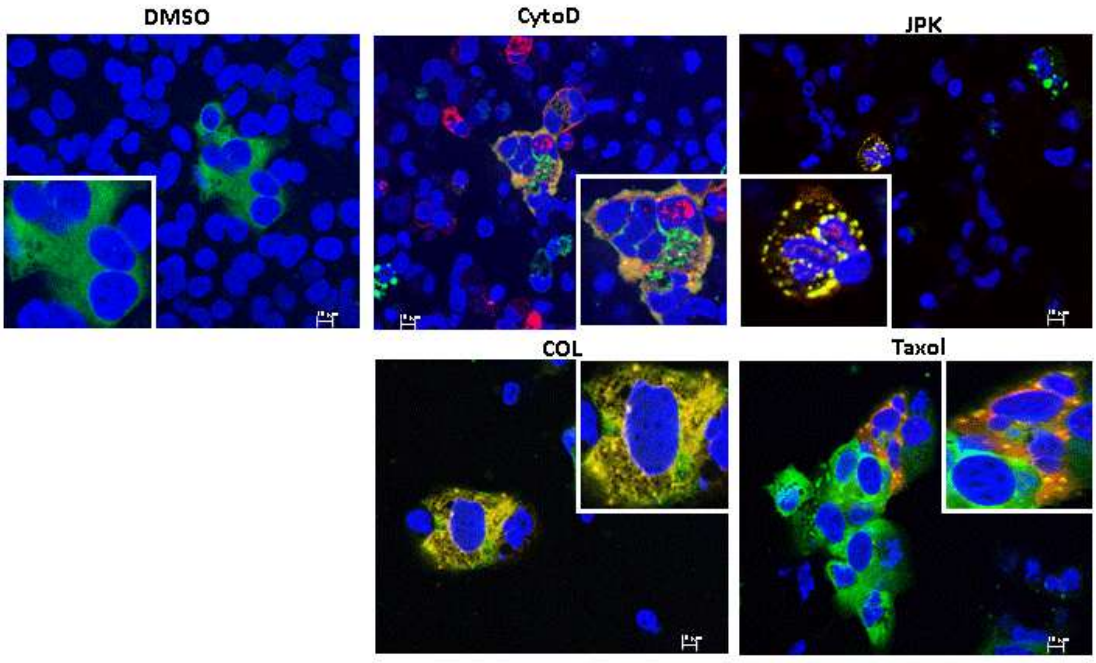

C red color represents GPx1 Norm, green color represents UPF1

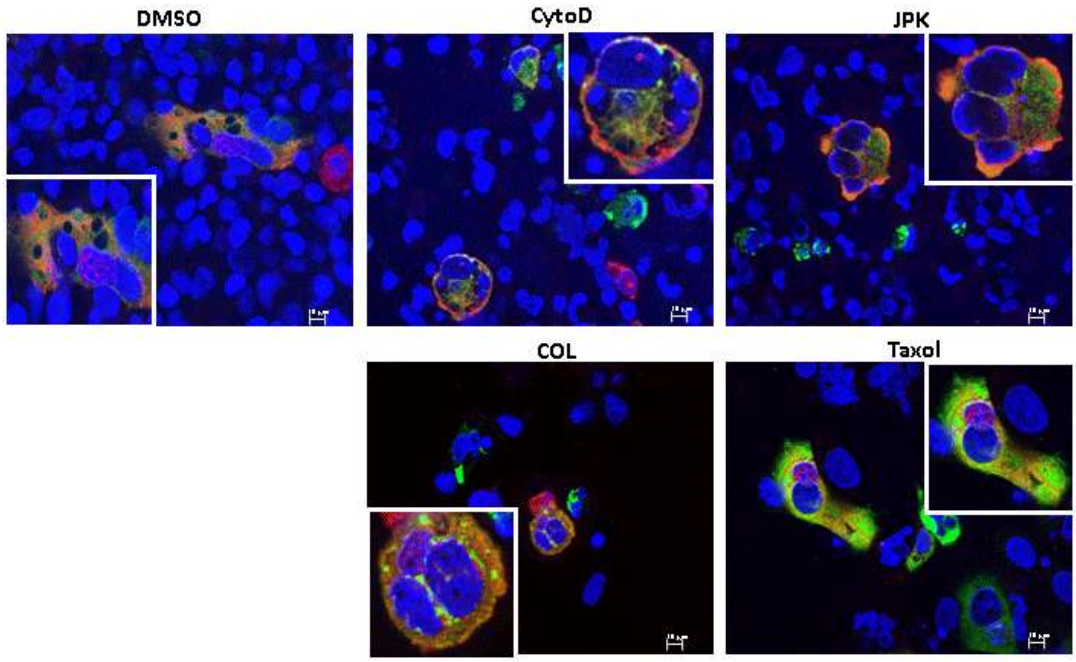

D red color represents GPx1 Ter, green color represents UPF1

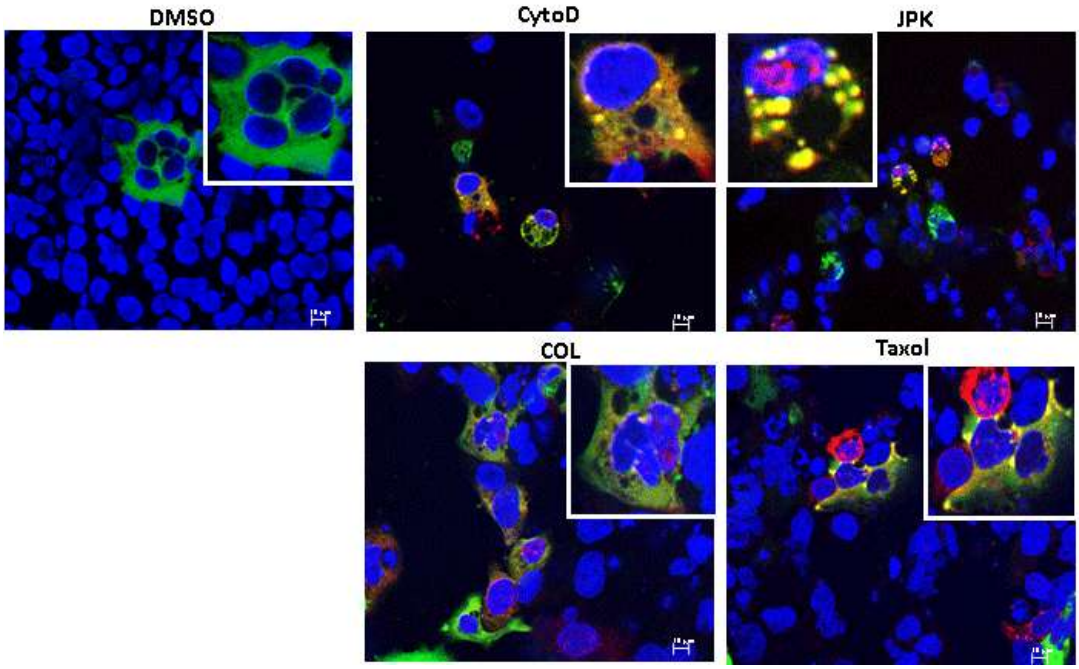

Figure 11: UPF1 colocolizes with NMD substrates after the treatment of cytoskeleton inhibitors in 6CFSMEo-cells

A red color represents Globin Norm or Ter, green color represents UPF3X

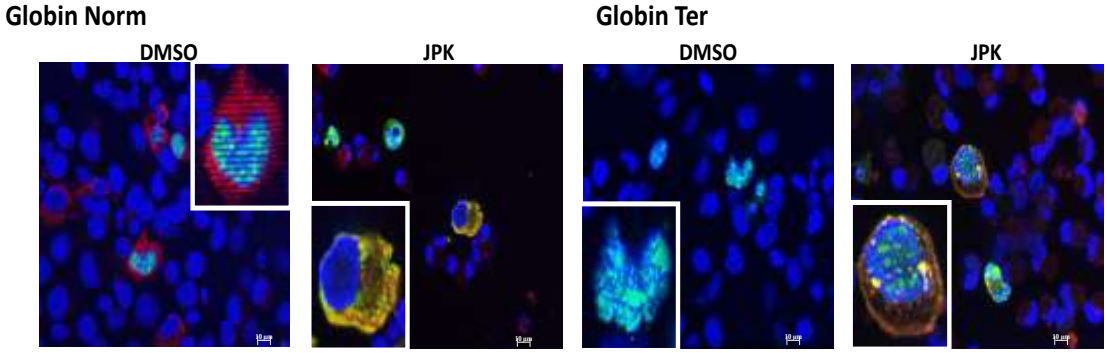

B red color represents GPx1 Norm or Ter, green color represents UPF3X

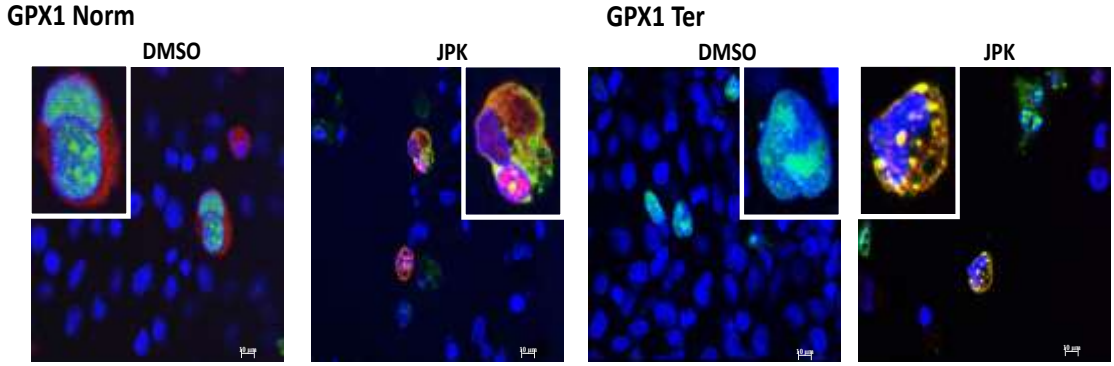

Figure 12: UPF3X colocolizes with NMD substrates in the presence of jasplakinolide in CFSMEo-cells

Figures 11-12: NMD factors colocolize with NMD substrates under cytoskeleton inhibitor treatment in 6CFSMEo-cells

6CFSMEo-cells were transfected with YFP-UPF1 (Figure11) or YFP-UPF3X (Figure12) and pCMV-Globin Norm (A) or 39Ter (B) or pCMV-GPx1 Norm (C) or 46Ter (D). Then cells were incubated respectively with DMSO, 1µM CytoD, 1µM JPK, 10µM COL or 1µM Taxol for 48 hours. Cells were fixed using formalin solution for 10 min at room temperature and permeabilized in 70% ethanol at 4°C for 1 hour. Cells were washed twice by 2xSSC and were incubated by prehybridization buffer for 1h at 37°C. Then cells were incubated with hybridization buffer (prehybridization buffer with Texas red-labeled probes) overnight at 37°C. Then Cells were washed by 2xSSC containing 10% formamide 2 times, 2xSSC+0.1% Triton X100 once, 1xSSC 2 times and finally incubated with Hoechst stain (blue) for 2 min at room temperature.

Since NMD factors do not colocolize with cytoskeleton when cytoskeleton is disorganized, I wanted to identify the nature of the foci that sequester them. Under other circumstances, NMD factors and NMD substrates can localize into a specific cytoplasmic foci called P-bodies (Durand, Cougot et al. 2007). My first hypothesis was that the cytoplasmic foci containing NMD susbtrates and NMD factors when

cytoskeleton is disorganized could be P-bodies. For that, I studied the localization of NMD factors (green) and P-bodies using a P-body marker (red) which is the decapping enzyme DCP1a (Anderson and Kedersha 2008) in 6CFSMEo-cells under cytoskeleton inhibitor treatment. Using the same experimental conditions as in the Figure 10, I found that in cytochalasin D or jasplakinolide treated cells, UPF1 (Figure 13A) partially concentrated in P-bodies, in contrast in colchicine or Taxol treated cells, UPF1 concentrated in P-bodies only. Concerning UPF3X (Figure 13B), this protein partially accumulated in P-bodies under jasplakinolide treatment only. To combine the results of Figure 13 and the results of Figures 11 and 12 which showed that NMD factors colocalized with NMD substrates under the cytoskeleton inhibitors treatment, I conclude that cytochalasin D and jasplakinolide induced only partially UPF1, UPF3X and NMD substrates to concentrate in P-bodies unlike the treatment by colchicine or taxol that leads to the accumulation of these molecules exclusively into P-bodies. Because western blot results demonstrated that cytochalasin D and japlakinolide can activate PTC-readthrough but colchicine and taxol can not, my hypothesis concerning the nature of the other cytoplasmic foci is that they could be the places where PTC readthrough occurs.

A UPF1

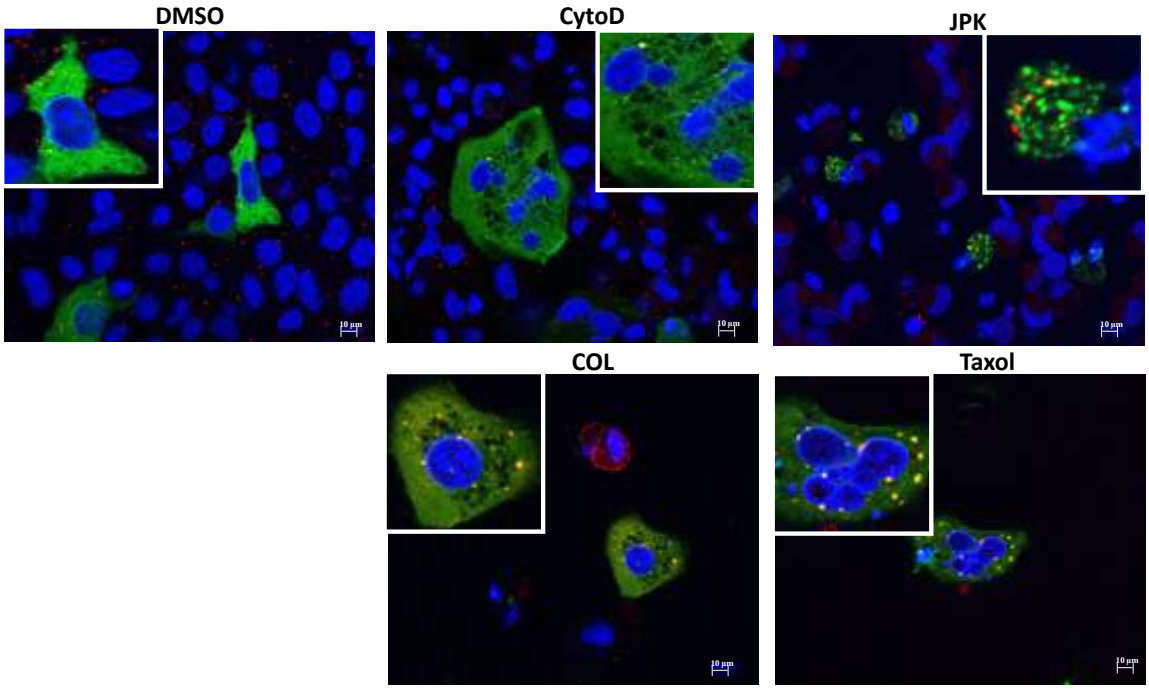

B UPF3X

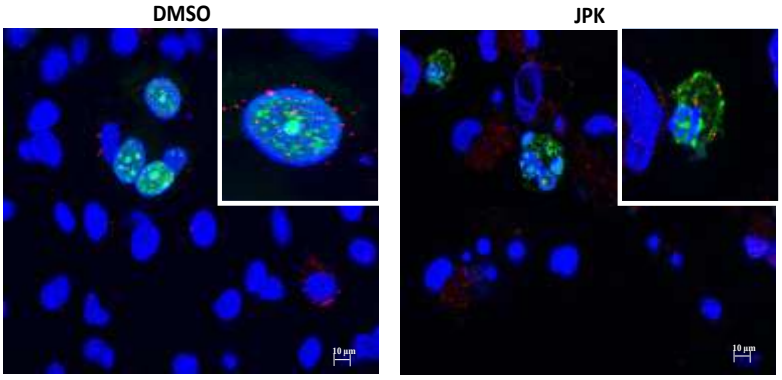

Figure 13: NMD factors partially or totally colocolize with P-bodies after the treatment of cytoskeleton inhibitors in 6CFSMEo-cells

6CFSMEo-cells transfected with YFP-UPF1 (A) or YFP-UPF3X (B) and pCMV GPx1 46Ter were incubated respectively with DMSO, 1µM CytoD, 1µM JPK, 10µM COL or 1 µM Taxol. 48 hour later, cells were fixed using formalin solution for 10 min at room temperature and permeabilized in 70% ethanol at 4°C for 1 hour. Cells were incubated sequentially with the primary antibodies (DCP1a) 1 hour at room temperature, washed three times with PBS, and incubated with anti-rabbit goat antibody Alexa Fluor 594 (red). Cells were washed three times with PBS and incubated with Hoechst stain (blue) for 2 min at room temperature.

Then the question of the identity of the unidentified granules where NMD factors and substrates concentrated was obsessing. If PTC readthrough occurs in these granules, translation factors have to be present in that structure. We then decided to study the protein composition of these granules starting by looking for the presence of proteins involved in translation. We first chose eukaryotic translation initiation factor 4E (eIF4E) which binds the 5’ cap structure of mRNA and indicates the steady-state round of translation. eIF4E can promote mRNAs to recruit other translation factors and plays an important role in mRNA translation (Scheper and Proud 2002). Here I checked whether the NMD substrate GPx1 Ter and eIF4E colocalize in cells treated with cytoskeleton inhibitors (Figure 14). I transfected 6CFSMEo- cells with pCMV-GPx1 46Ter and flag-UPF1 before treatment, and then detected GPx1 Ter mRNA by FISH probe and eIF4E using a specific anti-eIF4E antibody. In DMSO-treated cells, GPx1 Ter (red) was not found, which indicated that nonsense mutation -containing GPx1 mRNAs were degraded by NMD, and eIF4E was

distributed in the cytoplasm with some concentrations. Interestingly, under the four drugs treatment nonsense mutation-containing GPx1 mRNAs (red) were detected since NMD is inhibited and GPx1 Ter mRNAs colocalized with eIF4E. Since NMD factors (UPF1 or/and UPF3X) and NMD substrates can partially or totally colocalize with P-bodies, next step I checked whether eIF4E also localizes in P-bodies under the cytoskeleton inhibitors treatment.

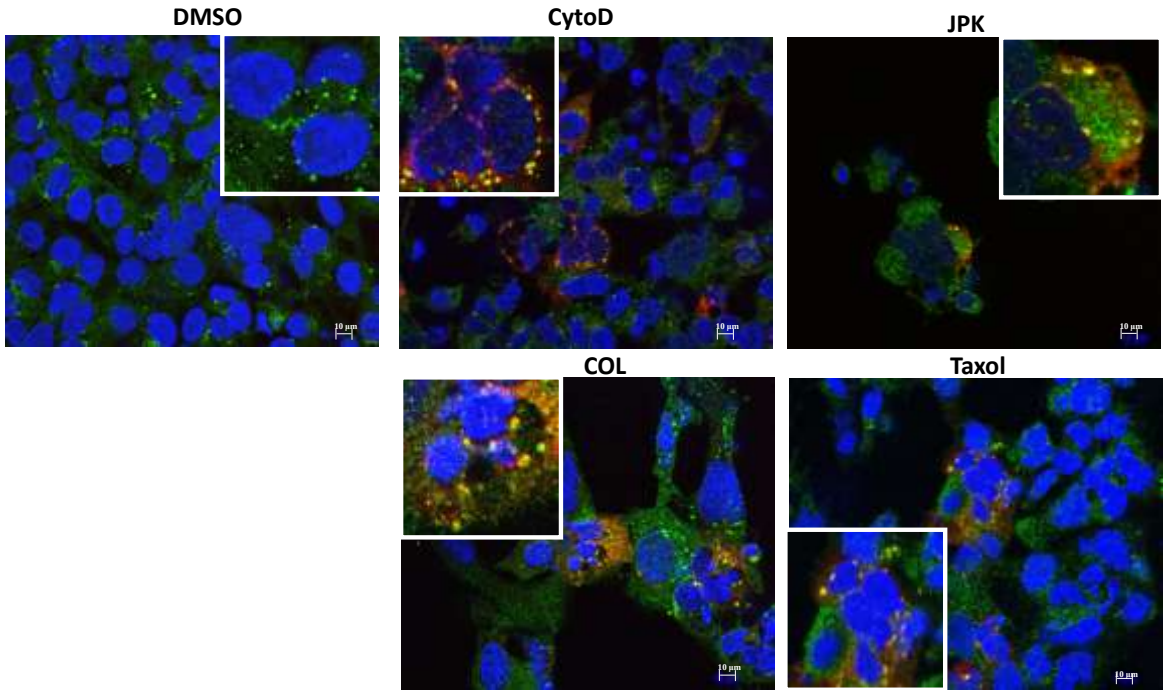

Figure 14: NMD substrates colocolize with eIF4E after the treatment of cytoskeleton inhibitors in 6CFSMEo-cells

6CFSMEo-cells transfected with flag-UPF1 and pCMV-GPx1 46Ter were incubated respectively with DMSO, 1µM CytoD, 1µM JPK, 10µM COL or 1 µM Taxol. 48 hours later cells were fixed using formalin solution for 10 min at room temperature and permeabilized in 70% ethanol at 4°C for 1 hour. Cells were fixed using formalin solution for 10 min at room temperature and permeabilized in 70% ethanol at 4°C for 1 hour. Cells were washed twice by 2xSSC and were incubated by prehybridization buffer for 1h at 37°C. Then cells were incubated with hybridization buffer (prehybridization buffer with Texas red-labeled probes) overnight at 37°C. Then Cells were washed by 2xSSC containing 10% formamide 2 times, 2xSSC+0.1% triton X100 once, 1xSSC 2 times; finally cells were incubated with the primary antibodies (eIF4E) 1 hour at room temperature, washed three times with PBS, and incubated with anti-rabbit goat antibody Alexa Fluor 488 (green). Cells were washed three times with PBS and incubated with Hoechst stain (blue) for 2 min at room temperature.

I transfected 6CFSMEo- cells with flag-UPF1 and the NMD substrate encoded by the plasmid pCMV-GPx1 46Ter. The four cytoskeleton inhibitors were then added to

the cell culture medium to treat the cells before to detect eIF4E and Dcp1a by the corresponding antibodies (Figure 15). In each samples, eIF4E was distributed in the cytoplasm and some aggregated in the cytoplasm. In DMSO-treated cells concentrated eIF4E colocalized whith Dcp1a as some studies have shown that eIF4E can accumulate in P-bodies and takes a key role in mRNP remodeling event (Andrei, Ingelfinger et al. 2005; Ferraiuolo, Basak et al. 2005). I found that in colchicine or taxol-treated cells all eIF4E cytoplasmic foci also colocalized with Dcp1a indicating that eIF4E is present in P-bodies. In contrast, cytochalasine D and jasplakinolide induce the cytoplasmic foci containing eIF4E to partially colocalize with Dcp1a suggesting that under these conditions, eIF4E localized into two different types of cytoplasmic foci. From results of the figures 13 to 15, I can conclude that microtubules inhibitors colchicine and taxol induce NMD factors (UPF1), NMD substrates and eIF4E to localize in P-bodies unlike in cytochalasine D or jasplakinolide-treated cells for which NMD factors (UPF1), NMD substrates and eIF4E partially localized in P-bodies and partially in other foci. The identity of the new type of cytoplasmic remains to be clarified.

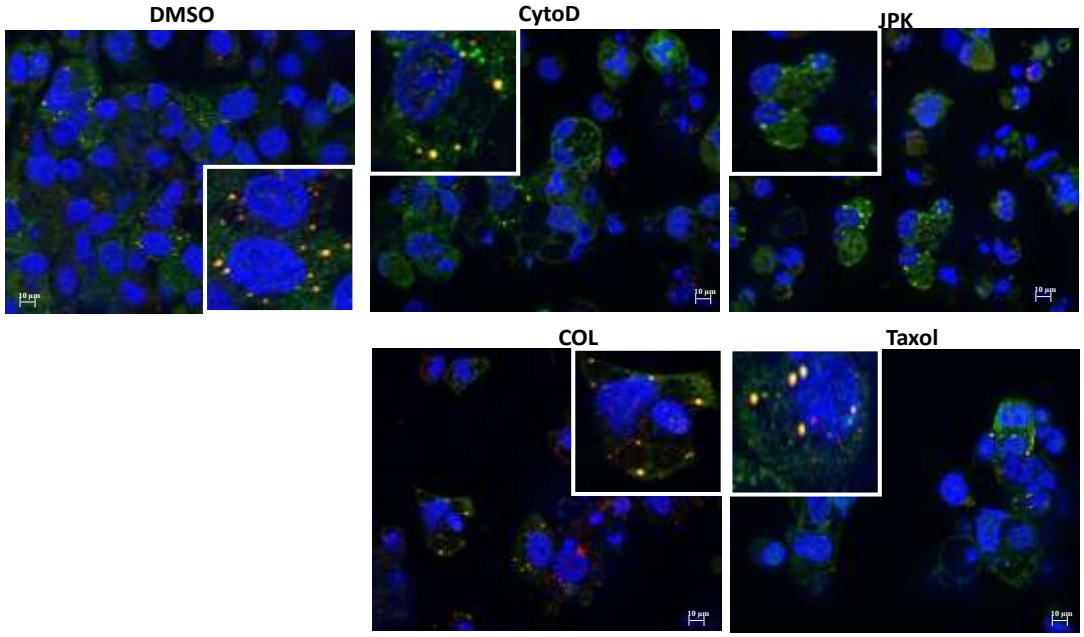

Figure 15: eIF4E partially or totally colocolize with P-bodies after the treatment by cytoskeleton inhibitors in 6CFSMEo-cells

6CFSMEo-cells transfected with flag-UPF1 (A) and pCMV-GPx1 46Ter were incubated respectively with DMSO, 1µM CytoD, 1µM JPK, 10µM COL or 1 µM Taxol. 48 hours later cells were fixed using formalin

solution for 10 min at room temperature and permeabilized in 70% ethanol at 4°C for 1 hour. Cells were incubated with the primary antibodies (DCP1a) (red) and eIF4E (green) hour at room temperature, washed three times with PBS, and incubated with anti-rabbit goat antibody Alexa Fluor 594 (red) and Alexa Fluor 488 (green). Cells were washed three times with PBS and incubated with Hoechst stain (blue) for 2 min at room temperature.

To further characterize the unidentified cytoplasmic foci present under cytochalasin D or jasplakinolide treatment, I studied the cellular distribution of ribosomes. For that, I analyzed the cellular location of the ribosomal protein L13 (RPL13) which is a component of the 60S subunit of ribosome (Kenmochi, Kawaguchi et al. 1998). Using the same method as for the Figure 13A, 48h after the DMSO or cytoskeleton inhibitors treatment, RPL13 was detected using a specific anti-RPL13 antibody. The cellular localization of UPF1 (in green) or RPL13 (in red) was observed under a fluorescence microscope (Figure 16). I found RPL13 was distributed in the cytoplasm with a granular aspect under DMSO as well as under the four cytoskeleton inhibitors treatment indicating that interfering with the cytoskeleton structure does not disturb the physiological cellular distribution of RPL13 (Tsai, Lee et al. 2012), even though UPF1 was concentrated in cytoplasmic foci as I previously observed. Since translation does not seem to occur in these foci, I needed to identify these structures by testing the presence of markers of other known cytoplasmic foci.

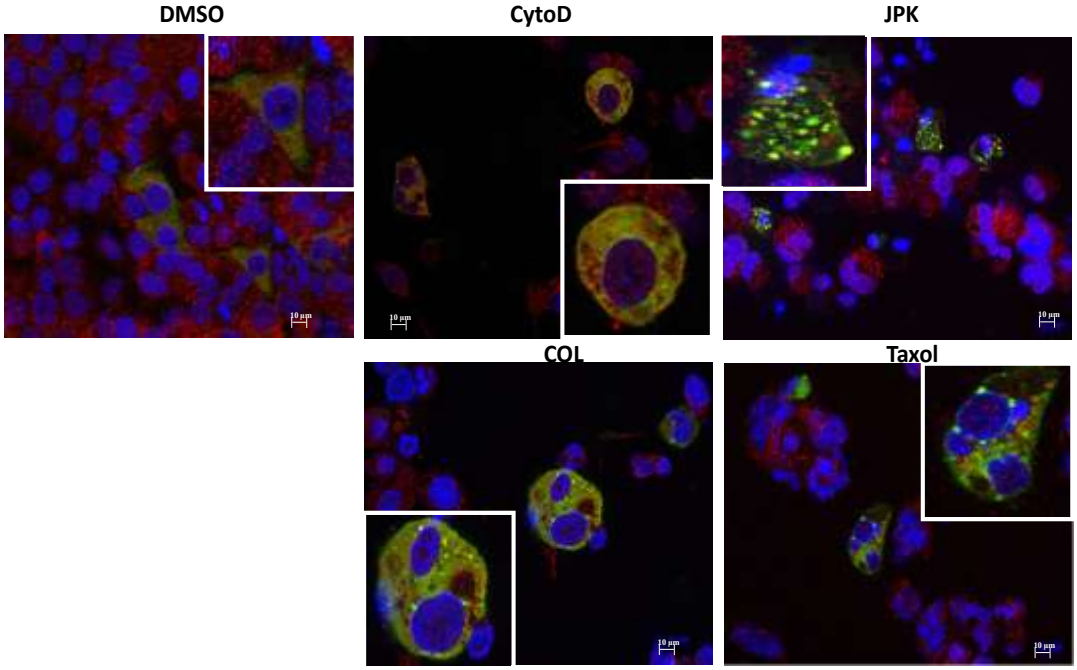

Figure 16: Cytoskeleton inhibitors do not affect the cellular location of ribosomes in 6CFSMEo-cells

6CFSMEo-cells transfected with YFP-UPF1 and pCMV-GPx1 46Ter were incubated respectively with DMSO, 1µM CytoD, 1µM JPK, 10µM COL or 1 µM Taxol. 48 hours later, cells were fixed using formalin solution for 10 min at room temperature and permeabilized in 70% ethanol at 4°C for 1 hour. Cells were incubated with the primary antibodies (anti-RPL13 antibody) 1 hour at room temperature, washed three times with PBS, and incubated with anti-rabbit goat antibody Alexa Fluor 594 (red). Cells were washed three times with PBS and incubated with Hoechst stain (blue) for 2 min at room temperature.

To further characterize the unknown cytoplasmic foci, I used markers of different cytoplasmic aggregates such as stress granules or autophagy vacuoles. To induce the formation of stress granules, I incubated my cells with 1.5mM of H2O2 for 4h and studied the stress granules marker eIF3β location (in red) (Figure 17). These conditions have been reported to induce stress granule formation (Brown, Roberts et al. 2011). Under these conditions, I was also able to observe stress granules which will allow me to determine whether the unknown cytoplasmic foci observed under cytoskeleton inhibitors treatment are stress granules or not. I found that the four drugs did not lead to the stress granule formation since I did not detect any colocalization between UPF1 and eIF3β. Recently Wengrod et al have demonstrated that NMD inhibition can activate autophagy (Wengrod, Martin et al.). Autophagy is a cell degradation system that occurs in response to nutrient starvation or reactive oxygen species and forms autophagosomes in the cells (Mizushima 2007). In order to test whether the unidentified cytoplasmic foci could be autophagosomes, I used LC3B (microtubule-associated protein 1 light chain 3β) which is a marker of autophagosomes (Tanida, Ueno et al. 2008). Using tag version of NMD factor and specific antibody raised against LC3B, I studied the cellular localization of NMD factors and LC3B protein (Figure 18). To determine whether my experimental conditions are adapted to the detection of autophagosomes, I treated cells with no serum medium for 24 hours which has been reported to induce autophagy (Delgado, Elmaoued et al. 2008). Figure 18 shows that autophagosomes were detected in serum-deprived cells unlike in the cytoskeleton treated cells in which no

autophagosomes were observed. These results exclude the possibility that our unknown foci are autophagosomes. Overall, my results demonstrate that the UPF1 or UPF3X cytoplasmic concentration observed in the presence of cytochalasin D and jasplakinolide are not P-bodies, stress granules or autophagosomes. Further experiments will be necessary to attempt to identify the nature of these cytoplasmic foci.

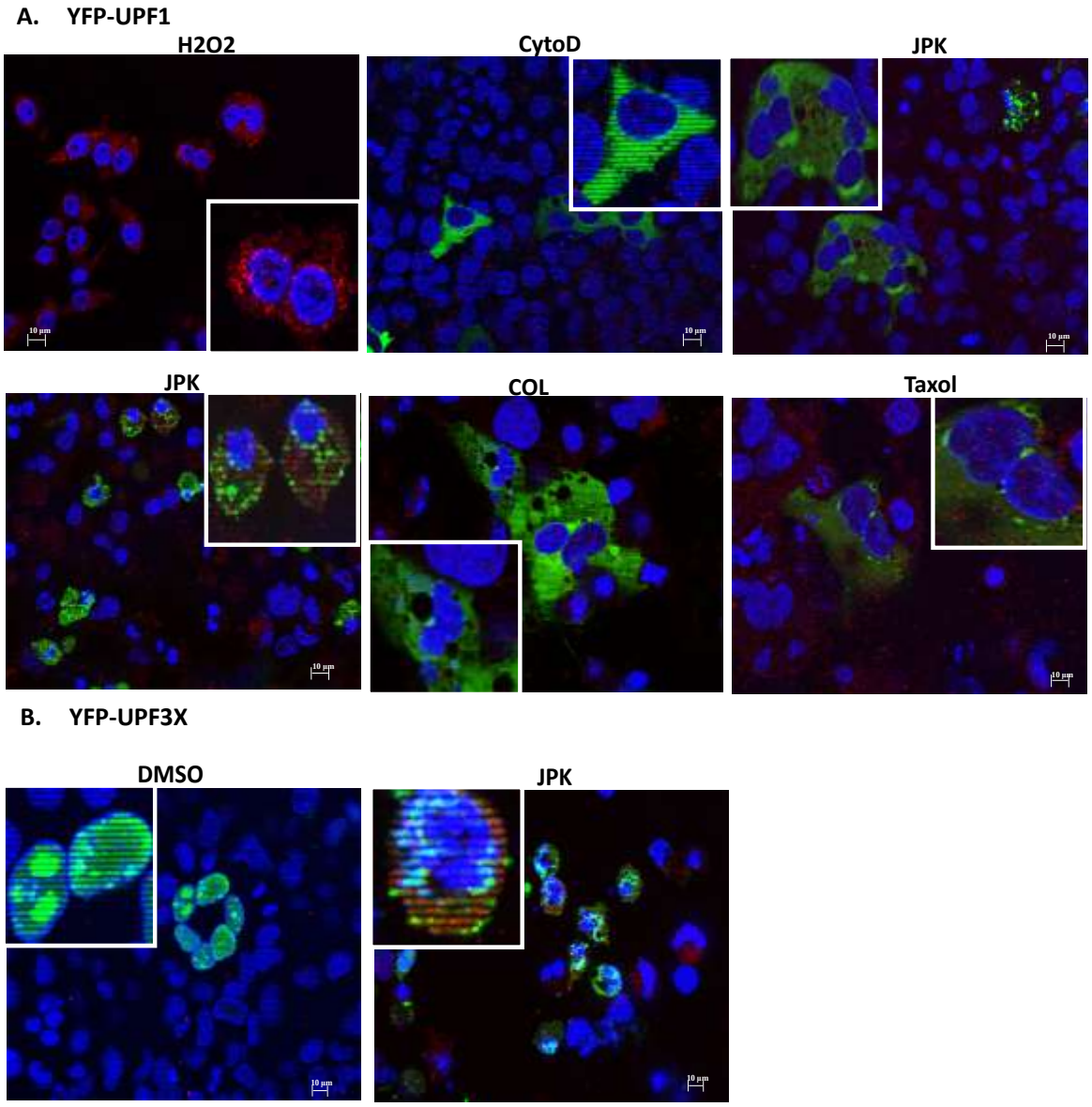

Figure 17: NMD factors do not colocolize with stress granules after the treatment of cytoskeleton inhibitors in 6CFSMEo-cells

6CFSMEo-cells transfected with YFP-UPF1 (A) or YFP-UPF3X (B) and one of NMD substrate pCMV-GPx1 46Ter were incubated respectively with DMSO, 1µM CytoD, 1µM JPK, 10µM COL or 1 µM Taxol for 48hours. 1.5mM H2O2 treated 6CFSMEo- cells for 4 hours as positive control. Cells were fixed using formalin solution for 10 min at room temperature and permeabilized in 70%

ethanol at 4°C for 1 hour. Cells were incubated with the primary antibodies (eIF3β) 1 hour at room temperature, washed three times with PBS, and incubated with anti-rabbit goat antibody Alexa Fluor 594 (red). Cells were washed three times with PBS and incubated with Hoechst stain (blue) for 2 min at room temperature.

A. YFP-UPF1

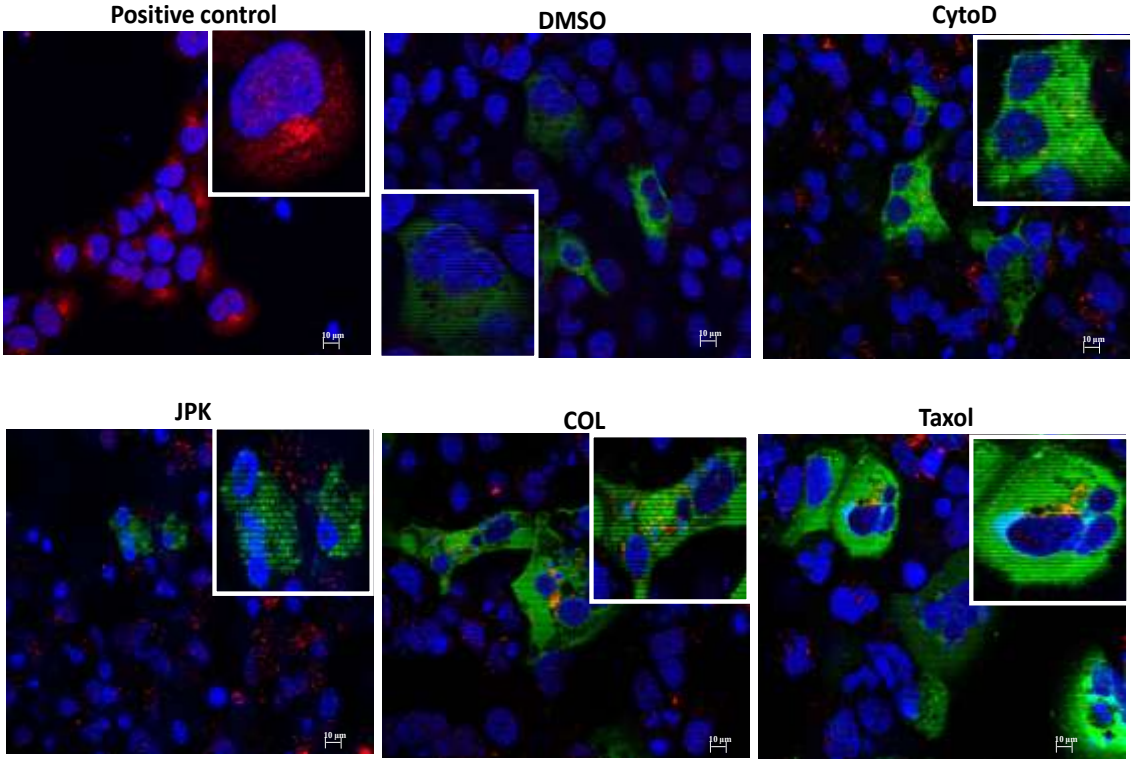

B. YFP-UPF3X

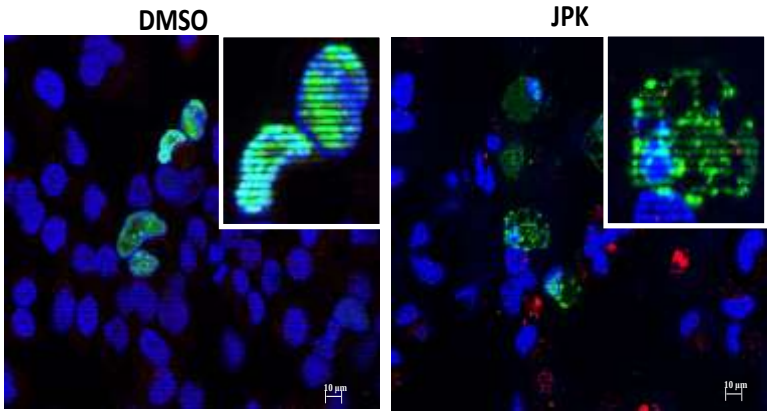

Figure 18: NMD factors do not colocolize with autophagosomes after the treatment of 6CFSMEo-cells with cytoskeleton inhibitors.

6CFSMEo-cells transfected with YFP-UPF1 (A) or YFP-UPF3X (B) and one of NMD substrate pCMV-globin Ter were incubated respectively with DMSO, 1µM CytoD, 1µM JPK, 10µM COL or 1 µM Taxol for 48 hours. 6CFSMEo-cells were incubated with no serum medium for 24 hours as positive control. Cells were fixed using formalin solution for 10 min at room temperature and permeabilized in 70% ethanol at 4°C for 1 hour. Cells were incubated with

the primary antibodies (LC3B) 1 hour at room temperature, washed three times with PBS, and incubated with anti-rabbit goat antibody Alexa Fluor 594 (red). Cells were washed three times with PBS and incubated with Hoechst stain (blue) for 2 min at room temperature.

Physical interaction is detected between cytoskeleton and NMD factors

In order to demonstrate the link between NMD and cytoskeleton by another approach than the microscopy, I focused my work on seeking a putative physical interaction between cytoskeleton components and NMD factors. To do that, I decided to perform immunoprecipitations of cytoskeleton components (actin or tubulin) and to analyze them for the presence of NMD factors. I treated 6CFSMEo- cells with DMSO, 1μM cytochalasin D, 1 μM jasplakinolide, 10μM colchicine or 1μM taxol for 48h and did immunoprecipitation using anti-actin or anti-tubulin antibody before to analyze them by western blot to check for the presence of NMD factors (Figure 19). In DMSO-treated cells, NMD factors UPF1, UPF2 and UPF3X can be detected in actin or tubulin antibody immunoprecipitation indicating that an interaction (direct or not) exists between the NMD complex and the cytoskeleton. Interestingly, we observed an almost complete abolition of the presence of NMD factors UPF1, UPF2 and UPF3X in actin or tubulin immunoprecipitation when cells were treated with one of the 4 cytoskeleton inhibitors. Surprisingly, jasplakinolide is the only one that can interfere with the interaction between tubulin and actin. My results suggest that the four cytoskeleton inhibitors might inhibit NMD by decreasing the interaction between NMD factors and cytoskeleton.

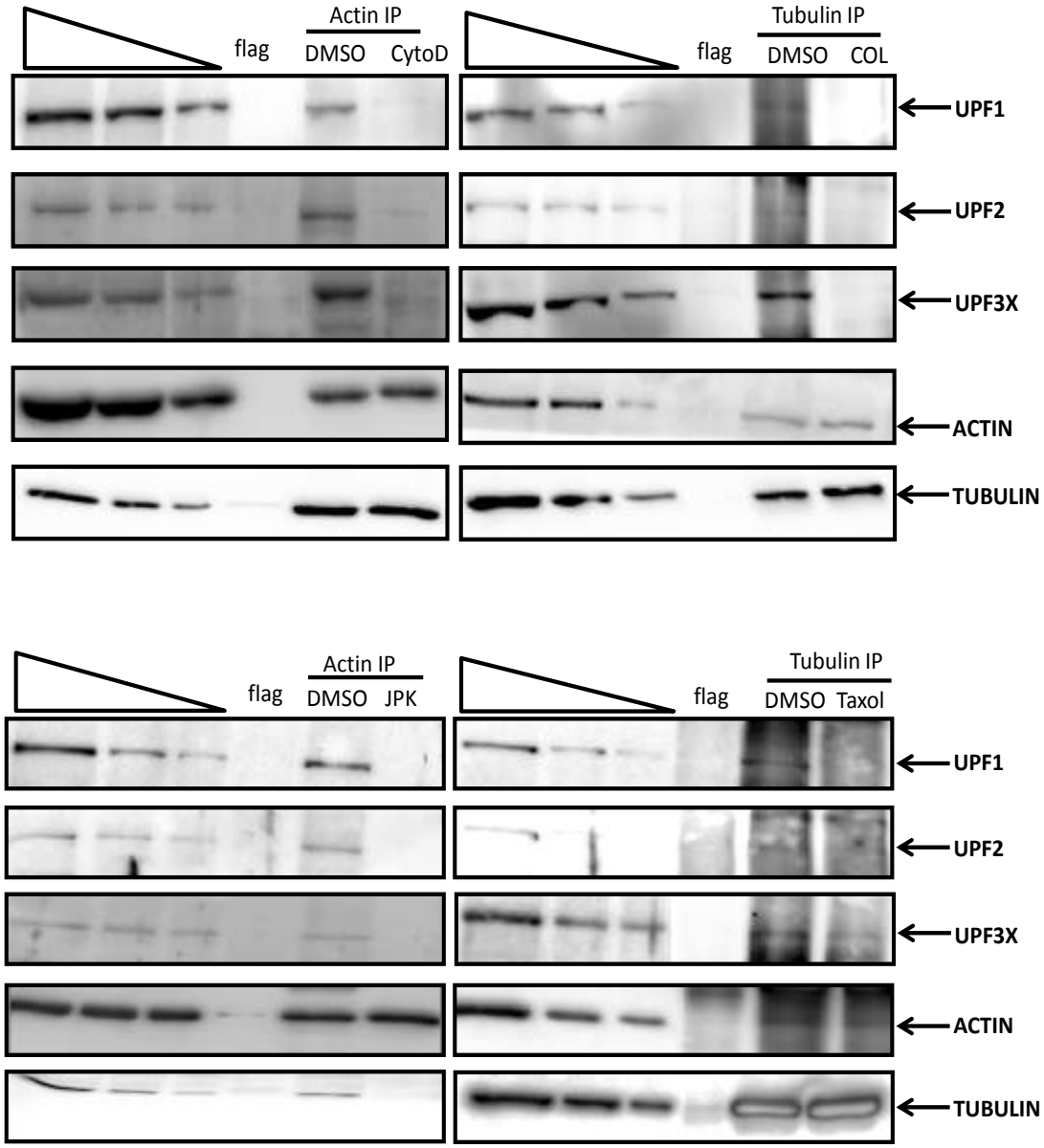

Figure 19: The interaction between NMD factors and cytoskeleton is disturbed in the presence of cytoskeleton inhibitors

6CFSMEo- cells were incubated respectively with DMSO, 1µM CytoD, 1µM JPK, 10µM COL or 1 µM Taxol for 48hours after, proteins were extracted to do immunoprecipitation by actin or tubulin antibody, flag antibody as negative control. Western blot was performed to analyze the presence of UPF1, UPF2, UPF3X, tubulin or actin protein. These results combine two independent experiments.

Discussion

NMD is an mRNA quality control mechanism that can distinguish and degrades PTC-containing mRNAs to prevent the production of toxic or nonfunctional truncated

proteins. Our lab and others have shown that PTC-containing mRNAs are targeted to cytoplasmic foci called P-bodies (Sheth and Parker 2006; Durand, Cougot et al. 2007). This statement suggests that a transport exists to bring PTC-containing mRNAs to the P-bodies. Since cytoskeleton is involved in some cell biological processes including intracellular transport (Rogers and Gelfand 2000; Fletcher and Mullins 2010), it makes sense to hypothesize that PTC-containing mRNAs are targeted to the P-bodies thanks to the cytoskeleton.

I first demonstrated a link between cytoskeleton and NMD pathway by measuring a decrease in the NMD efficiency when the integrity of the cytoskeleton is affected. For that, I used the transfected HeLa cells with a nonsense-containing mRNA or two cystic fibrosis cell lines called IB3 and 6CFSMEo- cells carrying an endogenous nonsense mutation-containing CFTR mRNA. To interfere with the structure of the cytoskeleton I chose two actin filaments inhibitors called cytochalasin D and jasplakinolide and two microtubules inhibitors named colchicine and taxol. My results show that the four cytoskeleton inhibitors can increase the level of nonsense-containing mRNAs and these effects of cytoskeleton inhibitors on NMD are not attributed to the increase of general transcription or general decrease of the translation (Figures 1, 2). I also excluded the possibility that apoptosis could be the reason of the NMD inhibition since these four drugs can not affect the expression of natural NMD substrates (Figure 4), not inhibit translation (Figure 6) and not induce apoptosis at least in IB3 and 6CFSMEo- cells (Figure 5).

Since these drugs can stabilize nonsense-containing mRNAs, the next question was to determine whether these stabilized nonsense-containing mRNAs can be translated into proteins and whether these drugs can also activate PTC readthrough. Molecules having the double properties to inhibit NMD and activate readthrough have been already reported (Correa-Cerro, Wassif et al. 2005; Gonzalez-Hilarion, Beghyn et al. 2012). Interestingly, actin filaments inhibitors cytochalasin D and jasplakinolide allow the synthesis of GPx1 truncated and full length protein in transfected HeLa cells (Figure7B). Both drugs were also capable of promoting the synthesis of the full length CFTR protein in IB3 or 6CFSMEo- cells (Figure 8). In

contrast, the microtubules inhibitors colchicine and taxol did not lead to the synthesis of either truncated or full-length proteins from PTC-containing mRNAs in these three cell lines. My results (Figure 9) show that under cytochalasin D or jasplakinolide treatment, CFTR protein is present on the cell membrane unlike under colchicine or taxol treatment since no CFTR protein is detected validating the western-blot results. These results further confirmed actin filaments inhibitors cytochalasin D or jasplakinolide can activate PTC readthrough. The above results demonstrate that actin filaments are not required for PTC readthrough. Surprisingly, cytochalasin D or jasplakinolide were not capable to induce readthrough from nonsense mutation-containing Globin mRNAs since truncated protein but not full length protein was observed by western-blot (Figure 7A). This could be the consequence of a readthrough-unadapted PTC environment since we know PTC-readthrough is highly dependent of the identity of the stop codon and the nucleotide context.

Next I wanted to understand how cytoskeleton inhibitors can inhibit NMD and why cytochalasin D and jasplakinolide can promote the synthesis of truncated or full-length proteins from nonsense mutation-containing mRNAs, but colchicine and taxol can not. For that I studied the cellular location of NMD factors (UPF1 and UPF3X) under the drugs treatment since these drugs can change the structure of cytoskeleton (Figure 3). I found that the four cytoskeleton inhibitors can induce UPF1 to aggregate in the cytoplasmic structures that exclude actin filaments or microtubules (Figure 10). I also observed that only actin filaments depolymerization inhibitor jasplakinolide induces UPF3X to concentrate in the cytoplasm. This result suggests actin filaments depolymerization is very important for the import of UPF3X into the nucleus. From the above microscopy results and the results of immunoprecipitation showing that the four drugs can decrease the presence of NMD factors (UPF1, UPF2 and UPF3X) in the actin or tubulin immunoprecipitation (Figure 19), I conclude that cytoskeleton inhibitors can interfere in the interactions between NMD factors and cytoskeleton and can induce UPF1 or/and UPF3X to accumulate in cytoplasm foci. In addition, the inhibition of NMD under cytoskeleton inhibitors

treatment is likely the result of a retention of UPF3X in the cytoplasm and a sequestration of NMD factors in some cytoplasmic foci.

Beside of UPF1 or/and UPF3X, I also demonstrated that NMD substrates (nonsense-containing Globin or GPx1 mRNAs) colocalized with UPF1 or UPF3X into the cytoplasmic foci (Figure 11 B, D and Figure 12). Interestingly, eIF4E, the cytoplasmic cap binding protein can also join these cytoplasmic foci (Figure 14). These cytoplasmic foci were identified as P-bodies in colchicine and taxol treated cells because UPF1 concentrations fully colocalized with the P-bodies marker DCP1a. It means that colchicine and taxol can cause NMD factor UPF1, NMD substrates and eIF4E to accumulate in P-bodies. It is possible that UPF1, NMD substrates and eIF4E are stalled in P-bodies and do not join the processing of translation, which could explain why under microtubule inhibitors colchicine or taxol treatment, the synthesis of proteins from nonsense mutation-containing mRNAs is not detected. There are some evidences to support this hypothesis. Disruption of microtubules can increase the formation of P-bodies and decrease the mobility of P-bodies and the component exchange beween P-bodies and stress granules (Sweet, Boyer et al. 2007; Aizer, Brody et al. 2008). In contrast, Marisa et al have shown that in MCF7 cells (a human breast cancer cell line) disruption of microtubules can decrease the component exchange between P-bodies and polysomes, stall hypoxia inducible factors 1α (HIF-1α) mRNAs in P-bodies and suppress the translation of HIF-1α (Carbonaro, O'Brate et al. 2011).

Only a portion of the cytoplasmic foci were P-bodies in cytochalasin D or jasplakinolide treated cells (Figures 13), which means that under cytochalasin D and jasplakinolide treatment NMD factors and substrates concentrate in two different foci (one is P-bodies, the other one still need to be identified). According to the protein results of Figures 7 and 8, actin filaments inhibitors cytochalasin D and jasplakinolide can activate PTC-readthrough but microtubules inhibitors colchicine and taxol can not. The first hypothesis concerning the identity of these cytoplasmic foci was the possibility that they would be the place where readthrough takes place. Unfortunatelly, I demonstrated that ribosomal protein L13 is not present in these

foci ruling out my first hypothesis (Figure 16). However I cannot exclude the possibility that the amount of ribosomes involved in readthrough is so low that the detection by microscopy is uncompatible. To identify the cytoplasmic foci formed by actin filaments inhibitors, I tested the possibility that they are stress granules or autophagosomes. For that, I used eIF3 β or LC3B to detect stress granules (Figure 17) and autophagosomes (Figure 18). The results showed that the four cytoskeleton inhibitors did not induce eIF3 β or LC3B protein to accumulate, which suggests cytoskeleton inhibitors did not form stress granules or autophagosomes. The identity of these cytoplasmic foci remains unclear and will need to be further characterized.

Overall my results show cytoskeleton inhibitors can decrease the interaction between NMD factors and cytoskeleton and can stall or partially stall NMD factors, NMD substrates in P-bodies to inhibit NMD. Actin filaments inhibitors can also promote PTC readthrough suggesting that actin filaments are not necessary for PTC readthrough (Figures 7 and 8). This is a very interesting point and we will need to understand the cytoskeleton specificity requirement in the readthrough process.

Some of the drugs that I used are already used in clinical treatments (colchicine or taxol for example). It would be interesting to determine whether their clinical efficacy is depending on the presence of PTC in genes involved in the pathology. To finish this project, I plan to further attempt to identify the nature of the cytoplasmic foci formed in cytochalasin D and jasplakinolide treated cells and check whether cytoskeleton inhibitors can also interfere with the function of other NMD factors (for example SMG5-7 proteins) since our team has shown that NMD inhibitor NMDI 1 can target SMG6, SMG7 to P-bodies with NMD substrates and exclude SMG5 from P-bodies (Durand, Cougot et al. 2007).

Materials and methods

Chemical molecules

Cytochalasin D (CytoD) and Jasplakinolide (JPK) were obtained from Enzo Life

Sciences. Colchicine (COL) was from Sigma and Taxol (Docetaxel) was obtained from Selleck Chemicals. Amlexanox was from Sequoia Research. Each molecule was dissolved in DMSO. The working concentration of CytoD, JPK or Taxol was 1µM and that of COL or amlexanox was 25µM.

Cell Culture

HeLa cells, stably transfected with the plasmids that encode either the pYFP-Globin 39Ter carrying a nonsense mutation at the position 39 or pYFP-GPx1 46Ter with a nonsense mutation at the position 46, were incubated in DMEM supplemented with 10% FBS and 1 U/ml ampicillin and 1U/ml of streptomycin. IB3 cells harboring a nonsense mutation on exon 20 of CFTR gene were grown in LHC-8 (without gentamicin) supplemented 10% FBS and 1 U/ml ampicillin and 1U/ml of streptomycin. 6CFSMEo- cells harboring a nonsense mutation on exon 1 of CFTR gene or 16HBE14o- cells which express wild type CFTR proteins were incubated in α-MEM supplemented 10% FBS, 1mM L-glutamine and 1 U/ml ampicillin and 1U/ml of streptomycin. Cells were incubated respectively with the molecules or DMSO as negative control for 24 hours or 48 hours at 37°c under 5% of CO_2.

RT-PCR analysis

RNAs were purified by RNazol (molecular research center, INC.). Reverse-transcription (RT) was performed using Superscript II (Life Technologies) and random hexamer for 2 hours at 42°C. Then specific cDNAs were amplified by radioactive PCR in the presence of dCTP (α^{33}P) (Perkin Elmer). PCR products were quantified by Personal Molecular Imager and QuantityOne quantification software (Bio-Rad) after a migration in a 5% acrylamide gel.

The list of primer sequences used in this study is:

Primers		Sequences
GAPDH	Sense	5’-CATTGACCTCAACTACATGG-3’
	Antisense	5’-GCCATGCCAGTGAGCTTCC-3’
Globin	Sense	5’-GGACGAGCTGTACAAGTATC-3’

	Antisense	5’-GGGTTTAGTGGTACTTGTGAGC-3’
GPX1	Sense	5’-GGACGAGCTGTACAAGTATC-3’
	Antisense	5’-CTTCTCACCATTCACCTCGCACTT-3’
CFTR	Sense	5’-GGCCAGAGGGTGGGCCTCTT-3’
	Antisense	5’-AGGAAACTGTTCTATCACAG-3’
SC35	Sense	5’-CCTCTTAAGAAAATGCTGCGGTCTC-3’
	Antisense	5’-ATCAGCCAAATCAGTTAAAATCTGC-3’
NAT9	Sense	5’-ATTGTGCTGGATGCCGAGA-3’
	Antisense	5’- ACCTAGCGTGGTCACTCCGTA-3’
TBL2	Sense	5’- GCAGTCATTTACCACATGC-3’
	Antisense	5’-TATTGTTTCTGCTTCTTGGAT-3’

Western blot analysis

Proteins were extracted in the following lysis buffer: 50mM Tris pH7, 20mM EDTA and 5% SDS. CFTR protein was analyzed by 7.5% SDS-PAGE. All the other proteins were migrated in the 10% SDS-PAGE gel. After migration, proteins were transferred to a nitrocellulose membrane and were incubated by the primary antibodies overnight at 4°C and were incubated with a secondary antibody (Jackson Immuno Research) at 4°C for 2h. Finally proteins were observed using SuperSignal West Femto Maximum Sensitivity Substrate (Pierce). The primary antibodies are antihuman CFTR C-terminus monoclonal antibody (clone 24-1) (R&D Systems), anti-GFP (G1544, Sigma) or anti-Ku80 (Epitomic).

CFTR detection at the cell membrane by micoscopy

6CFSMEo- cells were incubated on the 12mm slides coated by the coating solution (LHC basal medium+ 10mg/100ml BSA + 3mg/100ml vitrogen100 + 1mg/100ml human fibronectin) overnight at 37°C. The cells were treated by 1µM cytochalasin D, 1µM jasplakinolide, 10µM colchicine, 1µM taxol or DMSO. After 48h, cells were fixed by methanol at -20°C for 20min, washed by DPBS for 5 min, then permeabilized by 0.2% TritonX-100 for 20min at room temperature, and blocked by BSA before incubation of the primary antibody anti-CFTR overnight at 4°C. Cells were washed three times with 1% Tween-20 DBPS for 10 min each and were incubated with the Cy3-conjugated goat anti mouse IgG secondary antibody (Jackson immunoresearch)

for 1h at room temperature then washed three times with 1% Tween-20 DBPS for 10 min each, finally stained by Hoechst stain and observed under ZEISS ApoTome microscopy. 16HBE14o- cells were used as positive control.

Immunocytochemistry

6CFSMEo- cells were incubated on 12mm coated slides and were transfected with 250ng of plasmids YFP-UPF1 or YFP-UPF3X and pCMV-GPx1 46 Ter. 24h after transfection, cells were treated with 1µM cytochalasin D, 1µM jasplakinolide, 10µM colchicine, 1µM taxol or DMSO for 48h, then fixed with formalin for 10min at room temperature, washed with DPBS three times and permeabilized by 70% ethanol for 1h at 4°C. Cells were incubated with the primary antibodies (anti-actin (Abcam), anti-tubulin (Epitomics), anti-DCP1a (Sigma), anti-eIF4E (Santa Cruz), anti-eIF3β (Santa Cruz), or anti-LC3B (Novus)) for 1 hour at room temperature, washed three times with 0.05% Tween-20/PBS, and incubated with anti-rabbit goat antibody Alexa Fluor 594 (Invitrogen) for 1 hour at room temperature. Finally cells were incubated with Hoechst stain (blue) for 2 min at room temperature and detected under ZEISS ApoTome microscopy.

Fluorescence in situ hybridization (FISH) assays

6CFSMEo-cells were transfected with YFP-UPF1 or YFP-UPF3X and pCMV-Globin 39Ter or pCMV-GPX1 46Ter. Cells were incubated respectively with DMSO, 1µM CytoD, 1µM JPK, 10µM COL, 1µM Taxol for 48 hours. Cells were fixed using formalin solution for 10 min at room temperature and permeabilized in 70% ethanol at 4°C for 1 hour. Cells were washed twice by 2xSSC and were incubated by prehybridization buffer (125 µg/ml of tRNA, 500 µg/ml herring DNA, 2x SSC, 1% BSA, 10% dextran sulfate, 50% formamide,10 mM vanadyl ribonucleoside complexes) for 1h at 37°C. Then cells were incubated with hybridization buffer (prehybridization buffer with 0.1ng/ul Texas red-labeled probes (sequence: Globin 5’ CACTGAGTGAGCTGCA CTGTGACAAGCTGCACGTGGATCCTGAGAACTTC3’; GPx1 5’ CAGGCGCTTTCGCACCATCG ACATCGAACCCGATATAGAAGCCCTGCTGT 3’) overnight at 37°C. Then Cells were

washed by 2xSSC containing 10% formamide 2 times, 2xSSC+0.1% triton X100 once, 1xSSC 2 times and finally incubated with Hoechst stain (blue) for 2 min at room temperature.

Translation efficiency

6CFSMEo-Cells were incubated respectively with DMSO, 1µM cytochalasin D (CytoD), 1µM jasplakinolide (JPK), 10µM colchicine (COL), 1µM Taxol for 48 hours before harvesting cells or incubated with 200µg/ml cycloheximide (CHX) (as positive control) for 4h before harvesting cells. 1h before harvesting cells, 25µM L-azidohomoalaine (L-AHA) was added to the cell culture medium to be incorporated into newly synthesized proteins. Then cells were washed three times with PBS and lysed by lysis buffer on ice for 30min. Lysate was centrifuged and supernatant was collected. Following the manual of Click-iT Protein Analysis Detection Kits (Life Technologies), TAMRA molecule was bound to the L-AHA modified amino acid based on the chemoselective ligation between the azide of L-AHA and an alkyne of TAMRA in the Click-iT cell reaction buffer. Finally, TAMRA was detected and quantified by western-blot using a DNR MF-ChemiBIS 3, 2 (DNR) and Multi Gauge software (FUJIFILM). These results combine three independent experiments.

Immunoprecipitation

6CFSMEo- cells were lysed by the lysis buffer (1%TritonX-100,150mM NaCl, 10mMTris PH7.4, 1mM EDTA PH8.0, 1mM EGTA PH8.0, 0.2mM sodium orthovanadate, 0.5% NP-40,100 x cocktail). Protein G/A agarose beads incubated the cells extracts for 30min at 4°C to remove nonspecific interaction. Then cells extracts were incubated by mouse actin antibody (abcam) or rabbit tubulin antibody (EPITOMICS), after 2h at 4°C protein G/A agarose beads were added into the cells extracts for 2h at 4°C. Beads were washed three times by the lysis buffer. Finally 2x sample loading buffer eluted the beads, vortexed, centrifuged and collected the supernatant.

DISCUSSION AND PERSPECTIVES

About one-third of inherited genetic diseases are caused by PTCs and among these diseases approximately 10% of patients carry nonsense mutations (Frischmeyer and Dietz 1999; Mort, Ivanov et al. 2008). mRNAs containing nonsense mutations will be degraded by NMD to avoid the synthesis of deleterious or nonfunctional truncated proteins. There are several strategies to correct nonsense mutations. In our lab, we mainly study two of them: NMD inhibition and PTC-readthrough.

To find the new therapeutic tools to treat inherited genetic diseases resulting from nonsense mutations (for example, cystic fibrosis, Duchenne muscular dystrophy (DMD), hemophiliae,…), we developed screening systems to identify molecules which are capable of rescuing nonsense mutations. Our lab has already tested more than 30000 molecules and in the first project we found that amlexanox can not only inhibit NMD but also can activate PTC-readthrough to produce the synthesis of functional full length proteins in different cell lines with nonsense mutation containing mRNAs (Gonzalez-Hilarion, Beghyn et al. 2012). Since amlexanox is already a drug on the market used to treat mouth ulcers and some forms of asthmas, it will be a good candidate to be used as a therapeutic approach of genetic diseases caused by nonsense mutations. Although, the efficiency of CFTR expression rescue after amlexanox treatment is higher than with already known readthrough molecules such as G418 or PTC124, its efficacy remains very low. So our quest to find molecules with more specificity and/or more efficiency of NMD inhibition is still going on using our screening systems. After screening several small chemical libraries, we found some molecules related with apoptosis and some other with the cytoskeleton. We demonstrated that both can inhibit NMD. To further investigate the putative role of apoptosis or cytoskeleton in NMD, I took charge of the characterization of both selected molecules.

In the second project, I used apoptosis activator staurosporine to induce cell apoptosis and I found that during apoptosis NMD factors UPF1 and UPF2 can be cleaved by caspase 3 and caspase 7 to inhibit NMD. Because apoptosis is regulated by a series of signal cascades and among these signals, caspases play essential roles in apoptosis by cleaving the relevant proteins (Ashe and Berry 2003). I found that UPF1 and UPF2 are cleaved by caspase 3 and caspase 7 but I cannot exclude the possibility that other NMD factors are also targeted by caspases during apoptosis. For example, It has been shown that caspases can cleave translation initiation factors such as eIF4G, eIF4B, eIF3, eIF4E, etc (Clemens, Bushell et al. 2000). Among these proteins, eIF4G is involved in the pioneer round of translation forming a bridge between CBP80/20, the PABPC1/PABPN1 and other initiation factors. Deletion of eIF4G using viral proteases led to an inhibition of NMD (Lejeune, Ranganathan et al. 2004). As another example, Santoro et al have found that protein phosphatase 2A (PP2A) can be cleaved by caspase 3 during apoptosis (Santoro, Annand et al. 1998). In NMD pathway NMD factors SMG5/SMG7 complex or SMG6 can recruit PP2A to dephosphorylate UPF1 (Anders, Grimson et al. 2003; Chiu, Serin et al. 2003; Gatfield, Unterholzner et al. 2003). It is therefore expected that the cleavage of the PP2A results in the decrease of the dephosphorylation rate of UPF1 meaning an accumulation of hyperphosphorylated UPF1 which is known to inhibit NMD. The *release factor* eRF3 can also be cleaved by caspase3-mediated proteolysis and is degraded during apoptosis (Hashimoto, Hosoda et al. 2012). eRF3 binds eRF1 which interacts with ribosome, and eRF3 also connects to UPF1 to create a bridge between UPF1 and the ribosome. eRF3 plays an important role in forming SURF complex (Figure 11 in introduction), but when eRF3 is absent, SURF complex cannot be formed and NMD cannot be activated.

Cell death can occur via different pathways: apoptosis, necrosis, autophagy and some atypical cell death modalities (Kroemer, Galluzzi et al. 2009). The fact that we now clearly demonstrated that NMD is not required anymore during apoptosis raises the question whether NMD is still active during the other cell death pathways. Indeed, during necrosis a lot of DNAs and proteins are damaged and some specific

proteolytic pathways are activated like for example calcium-dependent cysteine proteases called calpains (Goll, Thompson et al. 2003; Han, Kim et al. 2008). Wengrod et al have shown that inhibiting NMD can activate autophagy (Wengrod, Martin et al. 2013), but it remains to determine whether during autophagy NMD is inhibited and by which mechanism. It would be interesting to study the efficiency of NMD during the other cell death pathways.

In the second project I also showed that UPF3X was not cleaved even though it contains several putative cleavage sites of caspases (Figure 1C and supplemental Figure S1 in the second project). It is possible that the cleavage site of caspases is selective or the cellular location of UPF3X which is almost exclusively in the nucleus protects it from being degraded by caspases unlike UPF1 or UPF2 that are mainly located in the cytoplasm (Serin, Gersappe et al. 2001; McStay, Salvesen et al. 2008).

In my third project, I found that destabilizing the cytoskeleton structure can decrease the interaction between NMD factors (UPF1, UPF2, and UPF3X) and cytoskeleton. Cytoskeleton inhibitors can induce NMD factors (UPF1 or/and UPF3X) and NMD substrates to concentrate in P-bodies or in other cytoplasmic foci. We hypothesized that the other cytoplasmic foci might be the place where PTC-readthrough takes place because actin filaments inhibitors (cytochalasin D and jasplakinolide) can activate PTC-readthrough and induced the formation of these cytoplasmic foci but in microtubules inhibitors (colchicine and taxol) treated cells, full length proteins were not produced and the new cytoplasmic foci were not observed (Figure 8 and Figure 13 in the third project). I attempted to identify these cytoplasmic foci and found that they are not P-bodies, stress granules or autophagosomes (Figures 13, 18-19 in the third project). They could be presented as P-body-like cytoplasmic foci. Translation of mRNAs consists of three stages: initiation, elongation and termination and every stage involves many proteins. Interestingly these cytoplasmic foci contain eIF4E which can promote the initiation of translation (Figures 15, 17 in the third project). To confirm the hypothesis that PTC-readthrough occurs in these cytoplasmic foci, I plan to look for the presence of elongation factors inside of these foci (for example elongation factor eIF5A, eEF1A, eEF1B, etc) (Abbott

and Proud 2004; Saini, Eyler et al. 2009).

Cytoskeleton is comprised of actin filaments, intermediate filaments and microtubules, and my study only focused on actin filaments and microtubules inhibitors. I demonstrated that actin filaments and microtubules play a role in NMD. However, I cannot exclude the possibility that intermediate filaments are also involved in NMD pathway. More experiments are required for this project. For example I will need to study the effect of intermediate filaments on NMD. I will also need to further characterize the new cytoplasmic foci and finally, I will have to determine which factors are responsible for the direct interaction between NMD factors and cytoskeleton components.

Overall results from my projects validated the screening results and allowed me to investigate in various fields of the cellular biology. For example, I am the first one to demonstrate that quality controls mechanisms such as NMD is inhibited during apoptosis. I also demonstrated that the inhibition of NMD induces the generation of caspase cleavage fragments with function as apoptosis activator and/or NMD inhibitor. The regulation of the expression of NMD factors during cell death is also very interesting because I showed that UPF1 and UPF2 are cleaved by caspases unlike UPF3X. These results raise the question of the function of UPF proteins in NMD and in other processings. The function of UPF2 in NMD is unknown but the fact that this protein has to be cleaved during apoptosis could suggest that this protein is involved in other pathways that have to be impaired for cell death progression. The study of NMD and cytoskeleton showed that NMD requires some specific cellular localizations and dynamic processing. Little is known about the journey followed by mRNPs subject to NMD from the nucleus to their degradation site except that a step has to occur in P-bodies (Durand, Cougot et al. 2007). My results bring some evidence that NMD requires some transport for NMD factors and substrates. If we succeed to characterize the new cytoplasmic foci, we might improve our knowledge in the different steps of NMD and/or readthrough mechanisms.

In my study I detected two special families of molecules (apoptosis inducers and cytoskeleton inhibitors) and compared the efficiencies of NMD inhibition and the

PTC-readthrough with amlexanox. I found that actin filaments inhibitors (cytochalasin D and jasplakinolide) not only inhibit NMD but also activate PTC-readthough and that microtubules inhibitors (colchicine and taxol) can increase the expression of nonsense-mutation containing mRNAs but not produce the synthesis of full length proteins (Figure 2, 8 in the third project). The efficiencies of these drugs are similar or higher than amlexanox. There are a number of studies on anti-tumor effect of cytochalasin D and jasplakinolide because they can induce apoptosis in many cell lines (Rubtsova, Kondratov et al. 1998; Neniskyte, Neher et al. 2011; Matsuki-Fukushima, Hashimoto et al. 2012). Now in the clinic, colchicine is already used to treat gout, and is an anti-inflammatory drug for many diseases (Cocco, Chu et al. 2010; van Echteld, Wechalekar et al. 2014). Taxol is used to treat various types of cancers (for example, lung, pancreatic, breast, ovarian cancer, etc) (Jordan and Wilson 2004). Although the molecules that I studied are toxic, some are already used in clinics to treat cancer in particular. Cancer treatment is highly variable from patients and by choosing more carefully the molecules used to induce apoptosis of the tumor cells, it might improve the efficiency of treatment depending on the mutations carried by the patient. For example, Taxol could be more adapted to the treatment of cancers involving a nonsense mutation in a tumor suppressor gene. In addition to affect the integrity of the cytoskeleton, cells from this type of patients might be even more sensitive to chemotherapy because the tumor suppressor gene will be re-expressed. Correction of nonsense mutation as a therapeutic approach then represents an example of personalized medicine.

The work that I did during my thesis follows completely the strategic development of our lab objectives which are to use inhibitors of NMD to propose new therapeutic approaches for genetic diseases caused by nonsense mutation and also to study the NMD mechanism and the readthrough processing thanks to these highly efficient molecular tools.

REFERENCES

A, H. F., B. van der Loo, et al. (2008). "Serological evidence for the association of Bartonella henselae infection with arrhythmogenic right ventricular cardiomyopathy." Clin Cardiol **31**(10): 469-71.

Abbott, C. M. and C. G. Proud (2004). "Translation factors: in sickness and in health." Trends Biochem Sci **29**(1): 25-31.

Abraham, R. T. (2001). "Cell cycle checkpoint signaling through the ATM and ATR kinases." Genes Dev **15**(17): 2177-96.

Abraham, R. T. (2004). "PI 3-kinase related kinases: 'big' players in stress-induced signaling pathways." DNA Repair (Amst) **3**(8-9): 883-7.

Adesnik, M. and J. E. Darnell (1972). "Biogenesis and characterization of histone messenger RNA in HeLa cells." J Mol Biol **67**(3): 397-406.

Adesnik, M., M. Salditt, et al. (1972). "Evidence that all messenger RNA molecules (except histone messenger RNA) contain Poly (A) sequences and that the Poly(A) has a nuclear function." J Mol Biol **71**(1): 21-30.

Aizer, A., Y. Brody, et al. (2008). "The dynamics of mammalian P body transport, assembly, and disassembly in vivo." Mol Biol Cell **19**(10): 4154-66.

Albinsson, S. and P. Hellstrand (2007). "Integration of signal pathways for stretch-dependent growth and differentiation in vascular smooth muscle." Am J Physiol Cell Physiol **293**(2): C772-82.

Alderuccio, F., E. K. Chan, et al. (1991). "Molecular characterization of an autoantigen of PM-Scl in the polymyositis/scleroderma overlap syndrome: a unique and complete human cDNA encoding an apparent 75-kD acidic protein of the nucleolar complex." J Exp Med **173**(4): 941-52.

Allmang, C., E. Petfalski, et al. (1999). "The yeast exosome and human PM-Scl are related complexes of 3' --> 5' exonucleases." Genes Dev **13**(16): 2148-58.

Alnemri, E. S., D. J. Livingston, et al. (1996). "Human ICE/CED-3 protease nomenclature." Cell **87**(2): 171.

Amrani, N., R. Ganesan, et al. (2004). "A faux 3'-UTR promotes aberrant termination and triggers nonsense-mediated mRNA decay." Nature **432**(7013): 112-8.

Amrani, N., M. S. Sachs, et al. (2006). "Early nonsense: mRNA decay solves a translational problem." Nat Rev Mol Cell Biol **7**(6): 415-25.

Anders, K. R., A. Grimson, et al. (2003). "SMG-5, required for C.elegans nonsense-mediated mRNA decay, associates with SMG-2 and protein phosphatase 2A." EMBO J **22**(3): 641-50.

Anderson, P. and N. Kedersha (2008). "Stress granules: the Tao of RNA triage." Trends Biochem Sci **33**(3): 141-50.

Andrei, M. A., D. Ingelfinger, et al. (2005). "A role for eIF4E and eIF4E-transporter in targeting mRNPs to mammalian processing bodies." RNA **11**(5): 717-27.

Apcher, S., C. Daskalogianni, et al. (2011). "Major source of antigenic peptides for the MHC class I pathway is produced during the pioneer round of mRNA translation." Proc Natl Acad Sci U S A **108**(28): 11572-7.

Applequist, S. E., M. Selg, et al. (1997). "Cloning and characterization of HUPF1, a human homolog of the Saccharomyces cerevisiae nonsense mRNA-reducing UPF1 protein." Nucleic Acids Res

25(4): 814-21.

Arribas-Layton, M., D. Wu, et al. (2013). "Structural and functional control of the eukaryotic mRNA decapping machinery." Biochim Biophys Acta **1829**(6-7): 580-9.

Ashe, P. C. and M. D. Berry (2003). "Apoptotic signaling cascades." Prog Neuropsychopharmacol Biol Psychiatry **27**(2): 199-214.

Avery, P., M. Vicente-Crespo, et al. "Drosophila Upf1 and Upf2 loss of function inhibits cell growth and causes animal death in a Upf3-independent manner." RNA **17**(4): 624-38.

Azzalin, C. M. and J. Lingner (2006). "The double life of UPF1 in RNA and DNA stability pathways." Cell Cycle **5**(14): 1496-8.

Azzalin, C. M. and J. Lingner (2006). "The human RNA surveillance factor UPF1 is required for S phase progression and genome stability." Curr Biol **16**(4): 433-9.

Badis, G., C. Saveanu, et al. (2004). "Targeted mRNA degradation by deadenylation-independent decapping." Mol Cell **15**(1): 5-15.

Ballut, L., B. Marchadier, et al. (2005). "The exon junction core complex is locked onto RNA by inhibition of eIF4AIII ATPase activity." Nat Struct Mol Biol **12**(10): 861-9.

Barbosa, C., I. Peixeiro, et al. (2013). "Gene expression regulation by upstream open reading frames and human disease." PLoS Genet **9**(8): e1003529.

Bedwell, D. M., A. Kaenjak, et al. (1997). "Suppression of a CFTR premature stop mutation in a bronchial epithelial cell line." Nat Med **3**(11): 1280-4.

Beelman, C. A. and R. Parker (1995). "Degradation of mRNA in eukaryotes." Cell **81**(2): 179-83.

Behm-Ansmant, I., D. Gatfield, et al. (2007). "A conserved role for cytoplasmic poly(A)-binding protein 1 (PABPC1) in nonsense-mediated mRNA decay." EMBO J **26**(6): 1591-601.

Behm-Ansmant, I., I. Kashima, et al. (2007). "mRNA quality control: an ancient machinery recognizes and degrades mRNAs with nonsense codons." FEBS Lett **581**(15): 2845-53.

Belgrader, P., J. Cheng, et al. (1993). "Evidence to implicate translation by ribosomes in the mechanism by which nonsense codons reduce the nuclear level of human triosephosphate isomerase mRNA." Proc Natl Acad Sci U S A **90**(2): 482-6.

Bentley, D. L. (2005). "Rules of engagement: co-transcriptional recruitment of pre-mRNA processing factors." Curr Opin Cell Biol **17**(3): 251-6.

Bentley, D. L. (2014). "Coupling mRNA processing with transcription in time and space." Nat Rev Genet **15**(3): 163-75.

Bhattacharyya, B., D. Panda, et al. (2008). "Anti-mitotic activity of colchicine and the structural basis for its interaction with tubulin." Med Res Rev **28**(1): 155-83.

Bhuvanagiri, M., A. M. Schlitter, et al. (2010). "NMD: RNA biology meets human genetic medicine." Biochem J **430**(3): 365-77.

Bicknell, A. A., C. Cenik, et al. (2012). "Introns in UTRs: why we should stop ignoring them." Bioessays **34**(12): 1025-34.

Bidou, L., I. Hatin, et al. (2004). "Premature stop codons involved in muscular dystrophies show a broad spectrum of readthrough efficiencies in response to gentamicin treatment." Gene Ther **11**(7): 619-27.

Black, D. L. (2003). "Mechanisms of alternative pre-messenger RNA splicing." Annu Rev Biochem **72**: 291-336.

Boll, W., J. S. Partin, et al. (1991). "Distinct pathways for basolateral targeting of membrane and secretory proteins in polarized epithelial cells." Proc Natl Acad Sci U S A **88**(19): 8592-6.

Bonetti, B., L. Fu, et al. (1995). "The efficiency of translation termination is determined by a synergistic interplay between upstream and downstream sequences in Saccharomyces cerevisiae." J Mol Biol **251**(3): 334-45.

Bonnet, A. and B. Palancade (2014). "Regulation of mRNA trafficking by nuclear pore complexes." Genes (Basel) **5**(3): 767-91.

Bono, F., J. Ebert, et al. (2004). "Molecular insights into the interaction of PYM with the Mago-Y14 core of the exon junction complex." EMBO Rep **5**(3): 304-10.

Bourgeois, C. F., F. Lejeune, et al. (2004). "Broad specificity of SR (serine/arginine) proteins in the regulation of alternative splicing of pre-messenger RNA." Prog Nucleic Acid Res Mol Biol **78**: 37-88.

Brown, J. A., T. L. Roberts, et al. (2011). "A novel role for hSMG-1 in stress granule formation." Mol Cell Biol **31**(22): 4417-29.

Brumbaugh, K. M., D. M. Otterness, et al. (2004). "The mRNA surveillance protein hSMG-1 functions in genotoxic stress response pathways in mammalian cells." Mol Cell **14**(5): 585-98.

Brumm, H., J. Muhlhaus, et al. "Rescue of Melanocortin 4 Receptor (MC4R) Nonsense Mutations by Aminoglycoside-Mediated Read-Through." Obesity (Silver Spring).

Buhler, M., A. Paillusson, et al. (2004). "Efficient downregulation of immunoglobulin mu mRNA with premature translation-termination codons requires the 5'-half of the VDJ exon." Nucleic Acids Res **32**(11): 3304-15.

Buhler, M., S. Steiner, et al. (2006). "EJC-independent degradation of nonsense immunoglobulin-mu mRNA depends on 3' UTR length." Nat Struct Mol Biol **13**(5): 462-4.

Burkard, K. T. and J. S. Butler (2000). "A nuclear 3'-5' exonuclease involved in mRNA degradation interacts with Poly(A) polymerase and the hnRNA protein Npl3p." Mol Cell Biol **20**(2): 604-16.

Butler, J. S. and P. Mitchell (2010). "Rrp6, Rrp47 and cofactors of the nuclear exosome." Adv Exp Med Biol **702**: 91-104.

Caamano, J., B. Ruggeri, et al. (1991). "Detection of p53 in primary lung tumors and nonsmall cell lung carcinoma cell lines." Am J Pathol **139**(4): 839-45.

Caceres, J. F., T. Misteli, et al. (1997). "Role of the modular domains of SR proteins in subnuclear localization and alternative splicing specificity." J Cell Biol **138**(2): 225-38.

Calero, G., K. F. Wilson, et al. (2002). "Structural basis of m7GpppG binding to the nuclear cap-binding protein complex." Nat Struct Biol **9**(12): 912-7.

Cao, D. and R. Parker (2003). "Computational modeling and experimental analysis of nonsense-mediated decay in yeast." Cell **113**(4): 533-45.

Carbonaro, M., A. O'Brate, et al. (2011). "Microtubule disruption targets HIF-1alpha mRNA to cytoplasmic P-bodies for translational repression." J Cell Biol **192**(1): 83-99.

Carstens, R. P., E. J. Wagner, et al. (2000). "An intronic splicing silencer causes skipping of the IIIb exon of fibroblast growth factor receptor 2 through involvement of polypyrimidine tract binding protein." Mol Cell Biol **20**(19): 7388-400.

Cartegni, L., S. L. Chew, et al. (2002). "Listening to silence and understanding nonsense: exonic mutations that affect splicing." Nat Rev Genet **3**(4): 285-98.

Carter, M. S., J. Doskow, et al. (1995). "A regulatory mechanism that detects premature nonsense codons in T-cell receptor transcripts in vivo is reversed by protein synthesis inhibitors in vitro." J Biol Chem **270**(48): 28995-9003.

Carter, M. S., S. Li, et al. (1996). "A splicing-dependent regulatory mechanism that detects translation

signals." EMBO J **15**(21): 5965-75.

Chakrabarti, S., F. Bonneau, et al. (2014). "Phospho-dependent and phospho-independent interactions of the helicase UPF1 with the NMD factors SMG5-SMG7 and SMG6." Nucleic Acids Res **42**(14): 9447-60.

Chakrabarti, S., U. Jayachandran, et al. (2011). "Molecular mechanisms for the RNA-dependent ATPase activity of Upf1 and its regulation by Upf2." Mol Cell **41**(6): 693-703.

Chan, W. K., A. D. Bhalla, et al. (2009). "A UPF3-mediated regulatory switch that maintains RNA surveillance." Nat Struct Mol Biol **16**(7): 747-53.

Chan, W. K., L. Huang, et al. (2007). "An alternative branch of the nonsense-mediated decay pathway." EMBO J **26**(7): 1820-30.

Chang, Y. F., J. S. Imam, et al. (2007). "The nonsense-mediated decay RNA surveillance pathway." Annu Rev Biochem **76**: 51-74.

Chaouch, S., V. Mouly, et al. (2009). "Immortalized skin fibroblasts expressing conditional MyoD as a renewable and reliable source of converted human muscle cells to assess therapeutic strategies for muscular dystrophies: validation of an exon-skipping approach to restore dystrophin in Duchenne muscular dystrophy cells." Hum Gene Ther **20**(7): 784-90.

Chapin, A., H. Hu, et al. (2014). "In vivo determination of direct targets of the nonsense-mediated decay pathway in Drosophila." G3 (Bethesda) **4**(3): 485-96.

Charlet, B. N., P. Logan, et al. (2002). "Dynamic antagonism between ETR-3 and PTB regulates cell type-specific alternative splicing." Mol Cell **9**(3): 649-58.

Chatr-Aryamontri, A., M. Angelini, et al. (2004). "Nonsense-mediated and nonstop decay of ribosomal protein S19 mRNA in Diamond-Blackfan anemia." Hum Mutat **24**(6): 526-33.

Chen, C. Y., R. Gherzi, et al. (2001). "AU binding proteins recruit the exosome to degrade ARE-containing mRNAs." Cell **107**(4): 451-64.

Chen, C. Y. and A. B. Shyu (2011). "Mechanisms of deadenylation-dependent decay." Wiley Interdiscip Rev RNA **2**(2): 167-83.

Cheng, J., P. Belgrader, et al. (1994). "Introns are cis effectors of the nonsense-codon-mediated reduction in nuclear mRNA abundance." Mol Cell Biol **14**(9): 6317-25.

Cheng, J. and L. E. Maquat (1993). "Nonsense codons can reduce the abundance of nuclear mRNA without affecting the abundance of pre-mRNA or the half-life of cytoplasmic mRNA." Mol Cell Biol **13**(3): 1892-902.

Cheng, Z., D. Muhlrad, et al. (2007). "Structural and functional insights into the human Upf1 helicase core." EMBO J **26**(1): 253-64.

Chester, A., A. Somasekaram, et al. (2003). "The apolipoprotein B mRNA editing complex performs a multifunctional cycle and suppresses nonsense-mediated decay." EMBO J **22**(15): 3971-82.

Chiu, S. Y., F. Lejeune, et al. (2004). "The pioneer translation initiation complex is functionally distinct from but structurally overlaps with the steady-state translation initiation complex." Genes Dev **18**(7): 745-54.

Chiu, S. Y., G. Serin, et al. (2003). "Characterization of human Smg5/7a: a protein with similarities to Caenorhabditis elegans SMG5 and SMG7 that functions in the dephosphorylation of Upf1." RNA **9**(1): 77-87.

Chlebowski, A., M. Lubas, et al. (2013). "RNA decay machines: the exosome." Biochim Biophys Acta **1829**(6-7): 552-60.

Clemens, M. J., M. Bushell, et al. (2000). "Translation initiation factor modifications and the regulation

of protein synthesis in apoptotic cells." Cell Death Differ **7**(7): 603-15.

Clerici, M., A. Deniaud, et al. "Structural and functional analysis of the three MIF4G domains of nonsense-mediated decay factor UPF2." Nucleic Acids Res **42**(4): 2673-86.

Clerici, M., A. Deniaud, et al. (2013). "Structural and functional analysis of the three MIF4G domains of nonsense-mediated decay factor UPF2." Nucleic Acids Res **42**(4): 2673-86.

Cocco, G., D. C. Chu, et al. (2010). "Colchicine in clinical medicine. A guide for internists." Eur J Intern Med **21**(6): 503-8.

Colgan, D. F. and J. L. Manley (1997). "Mechanism and regulation of mRNA polyadenylation." Genes Dev **11**(21): 2755-66.

Collart, M. A. and O. O. Panasenko (2012). "The Ccr4--not complex." Gene **492**(1): 42-53.

Conti, E. and E. Izaurralde (2005). "Nonsense-mediated mRNA decay: molecular insights and mechanistic variations across species." Curr Opin Cell Biol **17**(3): 316-25.

Correa-Cerro, L. S., C. A. Wassif, et al. (2005). "DHCR7 nonsense mutations and characterisation of mRNA nonsense mediated decay in Smith-Lemli-Opitz syndrome." J Med Genet **42**(4): 350-7.

Cozens, A. L., M. J. Yezzi, et al. (1992). "Characterization of immortal cystic fibrosis tracheobronchial gland epithelial cells." Proc Natl Acad Sci U S A **89**(11): 5171-5.

Cozens, A. L., M. J. Yezzi, et al. (1994). "CFTR expression and chloride secretion in polarized immortal human bronchial epithelial cells." Am J Respir Cell Mol Biol **10**(1): 38-47.

Crawford, G. E., J. A. Faulkner, et al. (2000). "Assembly of the dystrophin-associated protein complex does not require the dystrophin COOH-terminal domain." J Cell Biol **150**(6): 1399-410.

Cronstein, B. N., Y. Molad, et al. (1995). "Colchicine alters the quantitative and qualitative display of selectins on endothelial cells and neutrophils." J Clin Invest **96**(2): 994-1002.

Cui, Y., K. W. Hagan, et al. (1995). "Identification and characterization of genes that are required for the accelerated degradation of mRNAs containing a premature translational termination codon." Genes Dev **9**(4): 423-36.

Culbertson, M. R. and P. F. Leeds (2003). "Looking at mRNA decay pathways through the window of molecular evolution." Curr Opin Genet Dev **13**(2): 207-14.

da Paula, A. C., A. S. Ramalho, et al. (2005). "Characterization of novel airway submucosal gland cell models for cystic fibrosis studies." Cell Physiol Biochem **15**(6): 251-62.

Dahlberg, J. E., E. Lund, et al. (2003). "Nuclear translation: what is the evidence?" RNA **9**(1): 1-8.

Danckwardt, S., G. Neu-Yilik, et al. (2002). "Abnormally spliced beta-globin mRNAs: a single point mutation generates transcripts sensitive and insensitive to nonsense-mediated mRNA decay." Blood **99**(5): 1811-6.

Darmon, S. K. and C. S. Lutz (2012). "mRNA 3' end processing factors: a phylogenetic comparison." Comp Funct Genomics **2012**: 876893.

Das, S. and B. Das "mRNA quality control pathways in Saccharomyces cerevisiae." J Biosci **38**(3): 615-40.

Das, S. and B. Das (2013). "mRNA quality control pathways in Saccharomyces cerevisiae." J Biosci **38**(3): 615-40.

Delgado, M. A., R. A. Elmaoued, et al. (2008). "Toll-like receptors control autophagy." EMBO J **27**(7): 1110-21.

Doma, M. K. and R. Parker (2006). "Endonucleolytic cleavage of eukaryotic mRNAs with stalls in translation elongation." Nature **440**(7083): 561-4.

Dranchak, P. K., E. Di Pietro, et al. (2011). "Nonsense suppressor therapies rescue peroxisome lipid

metabolism and assembly in cells from patients with specific PEX gene mutations." J Cell Biochem.

Dreyfuss, G., V. N. Kim, et al. (2002). "Messenger-RNA-binding proteins and the messages they carry." Nat Rev Mol Cell Biol **3**(3): 195-205.

Du, M., X. Liu, et al. (2008). "PTC124 is an orally bioavailable compound that promotes suppression of the human CFTR-G542X nonsense allele in a CF mouse model." Proc Natl Acad Sci U S A **105**(6): 2064-9.

Durand, S., N. Cougot, et al. (2007). "Inhibition of nonsense-mediated mRNA decay (NMD) by a new chemical molecule reveals the dynamic of NMD factors in P-bodies." J Cell Biol **178**(7): 1145-60.

Durand, S. and J. Lykke-Andersen (2013). "Nonsense-mediated mRNA decay occurs during eIF4F-dependent translation in human cells." Nat Struct Mol Biol **20**(6): 702-9.

Eberle, A. B., S. Lykke-Andersen, et al. (2009). "SMG6 promotes endonucleolytic cleavage of nonsense mRNA in human cells." Nat Struct Mol Biol **16**(1): 49-55.

Eberle, A. B., L. Stalder, et al. (2008). "Posttranscriptional gene regulation by spatial rearrangement of the 3' untranslated region." PLoS Biol **6**(4): e92.

Eckmann, C. R., C. Rammelt, et al. (2011). "Control of poly(A) tail length." Wiley Interdiscip Rev RNA **2**(3): 348-61.

Edwalds-Gilbert, G., K. L. Veraldi, et al. (1997). "Alternative poly(A) site selection in complex transcription units: means to an end?" Nucleic Acids Res **25**(13): 2547-61.

el-Deiry, W. S., T. Tokino, et al. (1993). "WAF1, a potential mediator of p53 tumor suppression." Cell **75**(4): 817-25.

Elkon, R., A. P. Ugalde, et al. (2013). "Alternative cleavage and polyadenylation: extent, regulation and function." Nat Rev Genet **14**(7): 496-506.

Elmore, S. (2007). "Apoptosis: a review of programmed cell death." Toxicol Pathol **35**(4): 495-516.

Eulalio, A., I. Behm-Ansmant, et al. (2007). "P bodies: at the crossroads of post-transcriptional pathways." Nat Rev Mol Cell Biol **8**(1): 9-22.

Faustino, N. A. and T. A. Cooper (2003). "Pre-mRNA splicing and human disease." Genes Dev **17**(4): 419-37.

Feigenbutz, M., W. Garland, et al. (2013). "The exosome cofactor Rrp47 is critical for the stability and normal expression of its associated exoribonuclease Rrp6 in Saccharomyces cerevisiae." PLoS One **8**(11): e80752.

Ferraiuolo, M. A., S. Basak, et al. (2005). "A role for the eIF4E-binding protein 4E-T in P-body formation and mRNA decay." J Cell Biol **170**(6): 913-24.

Fiorini, F., M. Boudvillain, et al. (2013). "Tight intramolecular regulation of the human Upf1 helicase by its N- and C-terminal domains." Nucleic Acids Res **41**(4): 2404-15.

Fisette, J. F., J. Toutant, et al. (2010). "hnRNP A1 and hnRNP H can collaborate to modulate 5' splice site selection." RNA **16**(1): 228-38.

Flaherty, S. M., P. Fortes, et al. (1997). "Participation of the nuclear cap binding complex in pre-mRNA 3' processing." Proc Natl Acad Sci U S A **94**(22): 11893-8.

Fletcher, D. A. and R. D. Mullins (2010). "Cell mechanics and the cytoskeleton." Nature **463**(7280): 485-92.

Forch, P., O. Puig, et al. (2002). "The splicing regulator TIA-1 interacts with U1-C to promote U1 snRNP recruitment to 5' splice sites." EMBO J **21**(24): 6882-92.

Foveau, B., C. Leroy, et al. (2007). "Amplification of apoptosis through sequential caspase cleavage of the MET tyrosine kinase receptor." Cell Death Differ **14**(4): 752-64.

Franks, T. M., G. Singh, et al. (2010). "Upf1 ATPase-dependent mRNP disassembly is required for completion of nonsense- mediated mRNA decay." Cell **143**(6): 938-50.

Frejlich, E., J. Rudno-Rudzinska, et al. (2013). "Caspases and their role in gastric cancer." Adv Clin Exp Med **22**(4): 593-602.

Fribourg, S., D. Gatfield, et al. (2003). "A novel mode of RBD-protein recognition in the Y14-Mago complex." Nat Struct Biol **10**(6): 433-9.

Frischmeyer, P. A. and H. C. Dietz (1999). "Nonsense-mediated mRNA decay in health and disease." Hum Mol Genet **8**(10): 1893-900.

Frischmeyer, P. A., A. van Hoof, et al. (2002). "An mRNA surveillance mechanism that eliminates transcripts lacking termination codons." Science **295**(5563): 2258-61.

Fukuhara, N., J. Ebert, et al. (2005). "SMG7 is a 14-3-3-like adaptor in the nonsense-mediated mRNA decay pathway." Mol Cell **17**(4): 537-47.

Gaildrat, P., S. Krieger, et al. (2012). "Multiple sequence variants of BRCA2 exon 7 alter splicing regulation." J Med Genet **49**(10): 609-17.

Gaildrat, P., S. Krieger, et al. (2010). "The BRCA1 c.5434C->G (p.Pro1812Ala) variant induces a deleterious exon 23 skipping by affecting exonic splicing regulatory elements." J Med Genet **47**(6): 398-403.

Gallie, D. R. (1991). "The cap and poly(A) tail function synergistically to regulate mRNA translational efficiency." Genes Dev **5**(11): 2108-16.

Galluzzi, L., I. Vitale, et al. (2012). "Molecular definitions of cell death subroutines: recommendations of the Nomenclature Committee on Cell Death 2012." Cell Death Differ **19**(1): 107-20.

Gao, Q., B. Das, et al. (2005). "Cap-binding protein 1-mediated and eukaryotic translation initiation factor 4E-mediated pioneer rounds of translation in yeast." Proc Natl Acad Sci U S A **102**(12): 4258-63.

Garneau, N. L., J. Wilusz, et al. (2007). "The highways and byways of mRNA decay." Nat Rev Mol Cell Biol **8**(2): 113-26.

Gatfield, D., L. Unterholzner, et al. (2003). "Nonsense-mediated mRNA decay in Drosophila: at the intersection of the yeast and mammalian pathways." EMBO J **22**(15): 3960-70.

Gehring, N. H., J. B. Kunz, et al. (2005). "Exon-junction complex components specify distinct routes of nonsense-mediated mRNA decay with differential cofactor requirements." Mol Cell **20**(1): 65-75.

Gehring, N. H., S. Lamprinaki, et al. (2009). "Disassembly of exon junction complexes by PYM." Cell **137**(3): 536-48.

Geipel, U., I. Just, et al. (1990). "Inhibition of cytochalasin D-stimulated G-actin ATPase by ADP-ribosylation with Clostridium perfringens iota toxin." Biochem J **266**(2): 335-9.

Ghosh, A. and C. D. Lima (2010). "Enzymology of RNA cap synthesis." Wiley Interdiscip Rev RNA **1**(1): 152-72.

Ghosh, S. and A. Jacobson (2010). "RNA decay modulates gene expression and controls its fidelity." Wiley Interdiscip Rev RNA **1**(3): 351-61.

Goll, D. E., V. F. Thompson, et al. (2003). "The calpain system." Physiol Rev **83**(3): 731-801.

Gonatopoulos-Pournatzis, T. and V. H. Cowling (2014). "Cap-binding complex (CBC)." Biochem J **457**(2): 231-42.

Gonzalez-Hilarion, S., T. Beghyn, et al. (2012). "Rescue of nonsense mutations by amlexanox in human cells." Orphanet J Rare Dis **7**: 58.

Gonzalez, C. I., M. J. Ruiz-Echevarria, et al. (2000). "The yeast hnRNP-like protein Hrp1/Nab4 marks a transcript for nonsense-mediated mRNA decay." Mol Cell **5**(3): 489-99.

Goyenvalle, A., A. Babbs, et al. (2009). "Enhanced exon-skipping induced by U7 snRNA carrying a splicing silencer sequence: Promising tool for DMD therapy." Mol Ther **17**(7): 1234-40.

Graber, J. H., C. R. Cantor, et al. (1999). "In silico detection of control signals: mRNA 3'-end-processing sequences in diverse species." Proc Natl Acad Sci U S A **96**(24): 14055-60.

Gruenert, D. C., M. Willems, et al. (2004). "Established cell lines used in cystic fibrosis research." J Cyst Fibros **3 Suppl 2**: 191-6.

Gruter, P., C. Tabernero, et al. (1998). "TAP, the human homolog of Mex67p, mediates CTE-dependent RNA export from the nucleus." Mol Cell **1**(5): 649-59.

Gudikote, J. P. and M. F. Wilkinson (2002). "T-cell receptor sequences that elicit strong down-regulation of premature termination codon-bearing transcripts." EMBO J **21**(1-2): 125-34.

Gunnery, S. and M. B. Mathews (1995). "Functional mRNA can be generated by RNA polymerase III." Mol Cell Biol **15**(7): 3597-607.

Hamosh, A., B. J. Rosenstein, et al. (1992). "CFTR nonsense mutations G542X and W1282X associated with severe reduction of CFTR mRNA in nasal epithelial cells." Hum Mol Genet **1**(7): 542-4.

Han, S. I., Y. S. Kim, et al. (2008). "Role of apoptotic and necrotic cell death under physiologic conditions." BMB Rep **41**(1): 1-10.

Hashimoto, Y., N. Hosoda, et al. (2012). "Translation termination factor eRF3 is targeted for caspase-mediated proteolytic cleavage and degradation during DNA damage-induced apoptosis." Apoptosis **17**(12): 1287-99.

Hastings, M. L. and A. R. Krainer (2001). "Pre-mRNA splicing in the new millennium." Curr Opin Cell Biol **13**(3): 302-9.

He, F., X. Li, et al. (2003). "Genome-wide analysis of mRNAs regulated by the nonsense-mediated and 5' to 3' mRNA decay pathways in yeast." Mol Cell **12**(6): 1439-52.

Hedjran, F., J. M. Yeakley, et al. (1997). "Control of alternative pre-mRNA splicing by distributed pentameric repeats." Proc Natl Acad Sci U S A **94**(23): 12343-7.

Herold, A., M. Suyama, et al. (2000). "TAP (NXF1) belongs to a multigene family of putative RNA export factors with a conserved modular architecture." Mol Cell Biol **20**(23): 8996-9008.

Hodgkin, J., A. Papp, et al. (1989). "A new kind of informational suppression in the nematode Caenorhabditis elegans." Genetics **123**(2): 301-13.

Horiuchi, T. and T. Aigaki (2006). "Alternative trans-splicing: a novel mode of pre-mRNA processing." Biol Cell **98**(2): 135-40.

Hosoda, N., Y. K. Kim, et al. (2005). "CBP80 promotes interaction of Upf1 with Upf2 during nonsense-mediated mRNA decay in mammalian cells." Nat Struct Mol Biol **12**(10): 893-901.

Hossain, M. A., C. Chung, et al. (2013). "The yeast cap binding complex modulates transcription factor recruitment and establishes proper histone H3K36 trimethylation during active transcription." Mol Cell Biol **33**(4): 785-99.

Hua, Y., T. A. Vickers, et al. (2008). "Antisense masking of an hnRNP A1/A2 intronic splicing silencer corrects SMN2 splicing in transgenic mice." Am J Hum Genet **82**(4): 834-48.

Huh, G. S. and R. O. Hynes (1994). "Regulation of alternative pre-mRNA splicing by a novel repeated

hexanucleotide element." Genes Dev **8**(13): 1561-74.

Huntzinger, E., I. Kashima, et al. (2008). "SMG6 is the catalytic endonuclease that cleaves mRNAs containing nonsense codons in metazoan." RNA **14**(12): 2609-17.

Hwang, J., H. Sato, et al. (2010). "UPF1 association with the cap-binding protein, CBP80, promotes nonsense-mediated mRNA decay at two distinct steps." Mol Cell **39**(3): 396-409.

Imamachi, N., H. Tani, et al. "Up-frameshift protein 1 (UPF1): multitalented entertainer in RNA decay." Drug Discov Ther **6**(2): 55-61.

Imamachi, N., H. Tani, et al. (2012). "Up-frameshift protein 1 (UPF1): multitalented entertainer in RNA decay." Drug Discov Ther **6**(2): 55-61.

Inada, T. and H. Aiba (2005). "Translation of aberrant mRNAs lacking a termination codon or with a shortened 3'-UTR is repressed after initiation in yeast." EMBO J **24**(8): 1584-95.

Ishigaki, Y., X. Li, et al. (2001). "Evidence for a pioneer round of mRNA translation: mRNAs subject to nonsense-mediated decay in mammalian cells are bound by CBP80 and CBP20." Cell **106**(5): 607-17.

Isken, O., Y. K. Kim, et al. (2008). "Upf1 phosphorylation triggers translational repression during nonsense-mediated mRNA decay." Cell **133**(2): 314-27.

Isken, O. and L. E. Maquat (2007). "Quality control of eukaryotic mRNA: safeguarding cells from abnormal mRNA function." Genes Dev **21**(15): 1833-56.

Ivanov, P. V., N. H. Gehring, et al. (2008). "Interactions between UPF1, eRFs, PABP and the exon junction complex suggest an integrated model for mammalian NMD pathways." EMBO J **27**(5): 736-47.

Johnson, N. A., S. Sengupta, et al. (2004). "Endothelial cells preparing to die by apoptosis initiate a program of transcriptome and glycome regulation." FASEB J **18**(1): 188-90.

Jonas, S., O. Weichenrieder, et al. (2013). "An unusual arrangement of two 14-3-3-like domains in the SMG5-SMG7 heterodimer is required for efficient nonsense-mediated mRNA decay." Genes Dev **27**(2): 211-25.

Jordan, M. A. and L. Wilson (2004). "Microtubules as a target for anticancer drugs." Nat Rev Cancer **4**(4): 253-65.

Kanopka, A., O. Muhlemann, et al. (1996). "Inhibition by SR proteins of splicing of a regulated adenovirus pre-mRNA." Nature **381**(6582): 535-8.

Karam, R., J. Wengrod, et al. (2013). "Regulation of nonsense-mediated mRNA decay: implications for physiology and disease." Biochim Biophys Acta **1829**(6-7): 624-33.

Kashima, I., A. Yamashita, et al. (2006). "Binding of a novel SMG-1-Upf1-eRF1-eRF3 complex (SURF) to the exon junction complex triggers Upf1 phosphorylation and nonsense-mediated mRNA decay." Genes Dev **20**(3): 355-67.

Kataoka, N., M. D. Diem, et al. (2001). "Magoh, a human homolog of Drosophila mago nashi protein, is a component of the splicing-dependent exon-exon junction complex." EMBO J **20**(22): 6424-33.

Kaufer, N. F. and J. Potashkin (2000). "Analysis of the splicing machinery in fission yeast: a comparison with budding yeast and mammals." Nucleic Acids Res **28**(16): 3003-10.

Keeling, K. M., M. Du, et al. (2006). "Therapies of Nonsense-Associated Diseases." Nonsense-mediated mRNA Decay - Landes Bioscience **Editor : Lynne E. Maquat**: 121-136.

Kelly, S. M. and A. H. Corbett (2009). "Messenger RNA export from the nucleus: a series of molecular wardrobe changes." Traffic **10**(9): 1199-208.

Kenmochi, N., T. Kawaguchi, et al. (1998). "A map of 75 human ribosomal protein genes." Genome Res **8**(5): 509-23.

Kerekatte, V., B. D. Keiper, et al. (1999). "Cleavage of Poly(A)-binding protein by coxsackievirus 2A protease in vitro and in vivo: another mechanism for host protein synthesis shutoff?" J Virol **73**(1): 709-17.

Kerem, E., S. Hirawat, et al. (2008). "Effectiveness of PTC124 treatment of cystic fibrosis caused by nonsense mutations: a prospective phase II trial." Lancet **372**(9640): 719-27.

Keren, H., G. Lev-Maor, et al. (2010). "Alternative splicing and evolution: diversification, exon definition and function." Nat Rev Genet **11**(5): 345-55.

Kim, E., P. Ambroziak, et al. (1998). "A gene-targeted mouse model for familial hypobetalipoproteinemia. Low levels of apolipoprotein B mRNA in association with a nonsense mutation in exon 26 of the apolipoprotein B gene." J Biol Chem **273**(51): 33977-84.

Kim, V. N., J. Yong, et al. (2001). "The Y14 protein communicates to the cytoplasm the position of exon-exon junctions." EMBO J **20**(8): 2062-8.

King-Smith, C., P. A. Basciano, et al. (2001). "Effects of the actin-stabilizing drug, jasplakinolide, on pigment granule motility in isolated retinal pigment epithelial (RPE) cells of green sunfish, Lepomis cyanellus." Pigment Cell Res **14**(1): 14-22.

Klauer, A. A. and A. van Hoof (2012). "Degradation of mRNAs that lack a stop codon: a decade of nonstop progress." Wiley Interdiscip Rev RNA **3**(5): 649-60.

Klopfenstein, D. R., F. Kappeler, et al. (1998). "A novel direct interaction of endoplasmic reticulum with microtubules." EMBO J **17**(21): 6168-77.

Koh, J. Y., M. B. Wie, et al. (1995). "Staurosporine-induced neuronal apoptosis." Exp Neurol **135**(2): 153-9.

Kohler, A. and E. Hurt (2007). "Exporting RNA from the nucleus to the cytoplasm." Nat Rev Mol Cell Biol **8**(10): 761-73.

Kohtz, J. D., S. F. Jamison, et al. (1994). "Protein-protein interactions and 5'-splice-site recognition in mammalian mRNA precursors." Nature **368**(6467): 119-24.

Kong, J. and S. A. Liebhaber (2007). "A cell type-restricted mRNA surveillance pathway triggered by ribosome extension into the 3' untranslated region." Nat Struct Mol Biol **14**(7): 670-6.

Kopito, R. R. (1999). "Biosynthesis and degradation of CFTR." Physiol Rev **79**(1 Suppl): S167-73.

Krawczak, M., J. Reiss, et al. (1992). "The mutational spectrum of single base-pair substitutions in mRNA splice junctions of human genes: causes and consequences." Hum Genet **90**(1-2): 41-54.

Kroemer, G., L. Galluzzi, et al. (2009). "Classification of cell death: recommendations of the Nomenclature Committee on Cell Death 2009." Cell Death Differ **16**(1): 3-11.

Kuhn, U. and E. Wahle (2004). "Structure and function of poly(A) binding proteins." Biochim Biophys Acta **1678**(2-3): 67-84.

Kulkarni, M., S. Ozgur, et al. (2010). "On track with P-bodies." Biochem Soc Trans **38**(Pt 1): 242-51.

Kumar, G. R. and B. A. Glaunsinger (2010). "Nuclear import of cytoplasmic poly(A) binding protein restricts gene expression via hyperadenylation and nuclear retention of mRNA." Mol Cell Biol **30**(21): 4996-5008.

Kumar, G. R., L. Shum, et al. (2011). "Importin alpha-mediated nuclear import of cytoplasmic poly(A) binding protein occurs as a direct consequence of cytoplasmic mRNA depletion." Mol Cell Biol **31**(15): 3113-25.

Kunz, J. B., G. Neu-Yilik, et al. (2006). "Functions of hUpf3a and hUpf3b in nonsense-mediated mRNA decay and translation." RNA **12**(6): 1015-22.

Kuroyanagi, H. (2009). "Fox-1 family of RNA-binding proteins." Cell Mol Life Sci **66**(24): 3895-907.

Kuzmiak, H. A. and L. E. Maquat (2006). "Applying nonsense-mediated mRNA decay research to the clinic: progress and challenges." Trends Mol Med **12**(7): 306-16.

Labrador, M. and V. G. Corces (2003). "Extensive exon reshuffling over evolutionary time coupled to trans-splicing in Drosophila." Genome Res **13**(10): 2220-8.

Lareau, L. F., M. Inada, et al. (2007). "Unproductive splicing of SR genes associated with highly conserved and ultraconserved DNA elements." Nature **446**(7138): 926-9.

Lau, N. C., A. Kolkman, et al. (2009). "Human Ccr4-Not complexes contain variable deadenylase subunits." Biochem J **422**(3): 443-53.

Le Hir, H., E. Izaurralde, et al. (2000). "The spliceosome deposits multiple proteins 20-24 nucleotides upstream of mRNA exon-exon junctions." EMBO J **19**(24): 6860-9.

Le Hir, H., M. J. Moore, et al. (2000). "Pre-mRNA splicing alters mRNP composition: evidence for stable association of proteins at exon-exon junctions." Genes Dev **14**(9): 1098-108.

Le Marchand, Y., C. Patzelt, et al. (1974). "Evidence for a role of the microtubular system in the secretion of newly synthesized albumin and other proteins by the liver." J Clin Invest **53**(6): 1512-7.

Lee, C., M. Ferguson, et al. (1989). "Construction of the endoplasmic reticulum." J Cell Biol **109**(5): 2045-55.

Lefebvre, J., G. Muharram, et al. (2013). "Caspase-generated fragment of the Met receptor favors apoptosis via the intrinsic pathway independently of its tyrosine kinase activity." Cell Death Dis **4**: e871.

Lehner, B. and C. M. Sanderson (2004). "A protein interaction framework for human mRNA degradation." Genome Res **14**(7): 1315-23.

Lejeune, F., Y. Cavaloc, et al. (2001). "Alternative splicing of intron 3 of the serine/arginine-rich protein 9G8 gene. Identification of flanking exonic splicing enhancers and involvement of 9G8 as a trans-acting factor." J Biol Chem **276**(11): 7850-8.

Lejeune, F., Y. Ishigaki, et al. (2002). "The exon junction complex is detected on CBP80-bound but not eIF4E-bound mRNA in mammalian cells: dynamics of mRNP remodeling." EMBO J **21**(13): 3536-45.

Lejeune, F., X. Li, et al. (2003). "Nonsense-mediated mRNA decay in mammalian cells involves decapping, deadenylating, and exonucleolytic activities." Mol Cell **12**(3): 675-87.

Lejeune, F. and L. E. Maquat (2005). "Mechanistic links between nonsense-mediated mRNA decay and pre-mRNA splicing in mammalian cells." Curr Opin Cell Biol **17**(3): 309-15.

Lejeune, F., A. C. Ranganathan, et al. (2004). "eIF4G is required for the pioneer round of translation in mammalian cells." Nat Struct Mol Biol **11**(10): 992-1000.

Lenasi, T., B. M. Peterlin, et al. (2011). "Cap-binding protein complex links pre-mRNA capping to transcription elongation and alternative splicing through positive transcription elongation factor b (P-TEFb)." J Biol Chem **286**(26): 22758-68.

Lewis, B. P., R. E. Green, et al. (2003). "Evidence for the widespread coupling of alternative splicing and nonsense-mediated mRNA decay in humans." Proc Natl Acad Sci U S A **100**(1): 189-92.

Li, C., R. I. Lin, et al. (2003). "Nuclear Pnn/DRS protein binds to spliced mRNPs and participates in mRNA processing and export via interaction with RNPS1." Mol Cell Biol **23**(20): 7363-76.

Li, S. and M. F. Wilkinson (1998). "Nonsense surveillance in lymphocytes?" Immunity **8**(2): 135-41.

Li, Y. and M. Kiledjian (2010). "Regulation of mRNA decapping." Wiley Interdiscip Rev RNA **1**(2): 253-65.

Linde, L., S. Boelz, et al. (2007). "Nonsense-mediated mRNA decay affects nonsense transcript levels and governs response of cystic fibrosis patients to gentamicin." J Clin Invest **117**(3): 683-92.

Llorian, M., S. Schwartz, et al. (2010). "Position-dependent alternative splicing activity revealed by global profiling of alternative splicing events regulated by PTB." Nat Struct Mol Biol **17**(9): 1114-23.

Loh, B., S. Jonas, et al. (2013). "The SMG5-SMG7 heterodimer directly recruits the CCR4-NOT deadenylase complex to mRNAs containing nonsense codons via interaction with POP2." Genes Dev **27**(19): 2125-38.

Loughran, G., M. Y. Chou, et al. (2014). "Evidence of efficient stop codon readthrough in four mammalian genes." Nucleic Acids Res **42**(14): 8928-38.

Lubamba, B., B. Dhooghe, et al. (2012). "Cystic fibrosis: insight into CFTR pathophysiology and pharmacotherapy." Clin Biochem **45**(15): 1132-44.

Luo, M. L., Z. Zhou, et al. (2001). "Pre-mRNA splicing and mRNA export linked by direct interactions between UAP56 and Aly." Nature **413**(6856): 644-7.

Lykke-Andersen, J. (2002). "Identification of a human decapping complex associated with hUpf proteins in nonsense-mediated decay." Mol Cell Biol **22**(23): 8114-21.

Lykke-Andersen, J., M. D. Shu, et al. (2000). "Human Upf proteins target an mRNA for nonsense-mediated decay when bound downstream of a termination codon." Cell **103**(7): 1121-31.

Lykke-Andersen, J., M. D. Shu, et al. (2001). "Communication of the position of exon-exon junctions to the mRNA surveillance machinery by the protein RNPS1." Science **293**(5536): 1836-9.

Macdonald, P. (2001). "Diversity in translational regulation." Curr Opin Cell Biol **13**(3): 326-31.

Mangus, D. A., M. C. Evans, et al. (2004). "Positive and negative regulation of poly(A) nuclease." Mol Cell Biol **24**(12): 5521-33.

Mansoura, M. K., J. Biwersi, et al. (1999). "Fluorescent chloride indicators to assess the efficacy of CFTR cDNA delivery." Hum Gene Ther **10**(6): 861-75.

Maquat, L. E. (1995). "When cells stop making sense: effects of nonsense codons on RNA metabolism in vertebrate cells." RNA **1**(5): 453-65.

Maquat, L. E. (2002). "NASty effects on fibrillin pre-mRNA splicing: another case of ESE does it, but proposals for translation-dependent splice site choice live on." Genes Dev **16**(14): 1743-53.

Maquat, L. E. and C. Gong (2009). "Gene expression networks: competing mRNA decay pathways in mammalian cells." Biochem Soc Trans **37**(Pt 6): 1287-92.

Maquat, L. E., A. J. Kinniburgh, et al. (1981). "Unstable beta-globin mRNA in mRNA-deficient beta o thalassemia." Cell **27**(3 Pt 2): 543-53.

Marissen, W. E. and R. E. Lloyd (1998). "Eukaryotic translation initiation factor 4G is targeted for proteolytic cleavage by caspase 3 during inhibition of translation in apoptotic cells." Mol Cell Biol **18**(12): 7565-74.

Martin, L., A. Grigoryan, et al. (2014). "Identification and characterization of small molecules that inhibit nonsense mediated RNA decay and suppress nonsense p53 mutations." Cancer Res.

Martin, M. B., S. V. Angeloni, et al. (2004). "Regulation of estrogen receptor-alpha expression in MCF-7 cells by taxol." J Endocrinol **180**(3): 487-96.

Martineau, Y., M. C. Derry, et al. (2008). "Poly(A)-binding protein-interacting protein 1 binds to eukaryotic translation initiation factor 3 to stimulate translation." Mol Cell Biol **28**(21): 6658-67.

Martinez-Contreras, R., P. Cloutier, et al. (2007). "hnRNP proteins and splicing control." Adv Exp Med Biol **623**: 123-47.

Masse, I., L. Molin, et al. (2008). "A novel role for the SMG-1 kinase in lifespan and oxidative stress resistance in Caenorhabditis elegans." PLoS One **3**(10): e3354.

Matera, A. G. and Z. Wang (2014). "A day in the life of the spliceosome." Nat Rev Mol Cell Biol **15**(2): 108-21.

Matsuda, D., N. Hosoda, et al. (2007). "Failsafe nonsense-mediated mRNA decay does not detectably target eIF4E-bound mRNA." Nat Struct Mol Biol **14**(10): 974-9.

Matsuki-Fukushima, M., S. Hashimoto, et al. (2012). "The actin-specific reagent jasplakinolide induces apoptosis in primary rat parotid acinar cells." Arch Oral Biol **57**(5): 567-76.

McCracken, S., N. Fong, et al. (1997). "5'-Capping enzymes are targeted to pre-mRNA by binding to the phosphorylated carboxy-terminal domain of RNA polymerase II." Genes Dev **11**(24): 3306-18.

McCracken, S., M. Lambermon, et al. (2002). "SRm160 splicing coactivator promotes transcript 3'-end cleavage." Mol Cell Biol **22**(1): 148-60.

McIlwain, D. R., Q. Pan, et al. (2010). "Smg1 is required for embryogenesis and regulates diverse genes via alternative splicing coupled to nonsense-mediated mRNA decay." Proc Natl Acad Sci U S A **107**(27): 12186-91.

McStay, G. P., G. S. Salvesen, et al. (2008). "Overlapping cleavage motif selectivity of caspases: implications for analysis of apoptotic pathways." Cell Death Differ **15**(2): 322-31.

Medghalchi, S. M., P. A. Frischmeyer, et al. (2001). "Rent1, a trans-effector of nonsense-mediated mRNA decay, is essential for mammalian embryonic viability." Hum Mol Genet **10**(2): 99-105.

Mendell, J. T., C. M. ap Rhys, et al. (2002). "Separable roles for rent1/hUpf1 in altered splicing and decay of nonsense transcripts." Science **298**(5592): 419-22.

Mendell, J. T., N. A. Sharifi, et al. (2004). "Nonsense surveillance regulates expression of diverse classes of mammalian transcripts and mutes genomic noise." Nat Genet **36**(10): 1073-8.

Meng, W., Y. Dong, et al. (2009). "A clinical evaluation of amlexanox oral adhesive pellicles in the treatment of recurrent aphthous stomatitis and comparison with amlexanox oral tablets: a randomized, placebo controlled, blinded, multicenter clinical trial." Trials **10**: 30.

Metze, S., V. A. Herzog, et al. (2013). "Comparison of EJC-enhanced and EJC-independent NMD in human cells reveals two partially redundant degradation pathways." RNA **19**(10): 1432-48.

Mileusnic, R., C. L. Lancashire, et al. (2005). "Recalling an aversive experience by day-old chicks is not dependent on somatic protein synthesis." Learn Mem **12**(6): 615-9.

Millevoi, S. and S. Vagner (2010). "Molecular mechanisms of eukaryotic pre-mRNA 3' end processing regulation." Nucleic Acids Res **38**(9): 2757-74.

Mitchell, P. and D. Tollervey (2003). "An NMD pathway in yeast involving accelerated deadenylation and exosome-mediated 3'-->5' degradation." Mol Cell **11**(5): 1405-13.

Mizushima, N. (2007). "Autophagy: process and function." Genes Dev **21**(22): 2861-73.

Moriarty, P. M., C. C. Reddy, et al. (1998). "Selenium deficiency reduces the abundance of mRNA for Se-dependent glutathione peroxidase 1 by a UGA-dependent mechanism likely to be nonsense codon-mediated decay of cytoplasmic mRNA." Mol Cell Biol **18**(5): 2932-9.

Mort, M., D. Ivanov, et al. (2008). "A meta-analysis of nonsense mutations causing human genetic

disease." Hum Mutat **29**(8): 1037-47.

Mseka, T. and L. P. Cramer (2011). "Actin depolymerization-based force retracts the cell rear in polarizing and migrating cells." Curr Biol **21**(24): 2085-91.

Muhlemann, O., A. B. Eberle, et al. (2008). "Recognition and elimination of nonsense mRNA." Biochim Biophys Acta **1779**(9): 538-49.

Muhlrad, D. and R. Parker (1999). "Aberrant mRNAs with extended 3' UTRs are substrates for rapid degradation by mRNA surveillance." RNA **5**(10): 1299-307.

Muhlrad, D. and R. Parker (2005). "The yeast EDC1 mRNA undergoes deadenylation-independent decapping stimulated by Not2p, Not4p, and Not5p." EMBO J **24**(5): 1033-45.

Murphy, G. J., G. Mostoslavsky, et al. (2006). "Exogenous control of mammalian gene expression via modulation of translational termination." Nat Med **12**(9): 1093-9.

Nagarajan, V. K., C. I. Jones, et al. (2013). "XRN 5'-->3' exoribonucleases: structure, mechanisms and functions." Biochim Biophys Acta **1829**(6-7): 590-603.

Namy, O., I. Hatin, et al. (2001). "Impact of the six nucleotides downstream of the stop codon on translation termination." EMBO Rep **2**(9): 787-93.

Neniskyte, U., J. J. Neher, et al. (2011). "Neuronal death induced by nanomolar amyloid beta is mediated by primary phagocytosis of neurons by microglia." J Biol Chem **286**(46): 39904-13.

Neu-Yilik, G., B. Amthor, et al. (2011). "Mechanism of escape from nonsense-mediated mRNA decay of human beta-globin transcripts with nonsense mutations in the first exon." RNA **17**(5): 843-54.

Nguyen, J. T. and J. A. Wells (2003). "Direct activation of the apoptosis machinery as a mechanism to target cancer cells." Proc Natl Acad Sci U S A **100**(13): 7533-8.

Ni, J. Z., L. Grate, et al. (2007). "Ultraconserved elements are associated with homeostatic control of splicing regulators by alternative splicing and nonsense-mediated decay." Genes Dev **21**(6): 708-18.

Oh, J., J. Beckmann, et al. (2011). "Stimulation of the calcium-sensing receptor stabilizes the podocyte cytoskeleton, improves cell survival, and reduces toxin-induced glomerulosclerosis." Kidney Int **80**(5): 483-92.

Ohnishi, T., A. Yamashita, et al. (2003). "Phosphorylation of hUPF1 induces formation of mRNA surveillance complexes containing hSMG-5 and hSMG-7." Mol Cell **12**(5): 1187-200.

Okada-Katsuhata, Y., A. Yamashita, et al. (2012). "N- and C-terminal Upf1 phosphorylations create binding platforms for SMG-6 and SMG-5:SMG-7 during NMD." Nucleic Acids Res **40**(3): 1251-66.

Oliveira, V., W. J. Romanow, et al. (2008). "A protective role for the human SMG-1 kinase against tumor necrosis factor-alpha-induced apoptosis." J Biol Chem **283**(19): 13174-84.

Park, E. and L. E. Maquat "Staufen-mediated mRNA decay." Wiley Interdiscip Rev RNA **4**(4): 423-35.

Park, E. and L. E. Maquat (2013). "Staufen-mediated mRNA decay." Wiley Interdiscip Rev RNA **4**(4): 423-35.

Passos, D. O., M. K. Doma, et al. (2009). "Analysis of Dom34 and its function in no-go decay." Mol Biol Cell **20**(13): 3025-32.

Pastor, F., D. Kolonias, et al. (2010). "Induction of tumour immunity by targeted inhibition of nonsense-mediated mRNA decay." Nature **465**(7295): 227-30.

Peixeiro, I., A. Inacio, et al. (2011). "Interaction of PABPC1 with the translation initiation complex is critical to the NMD resistance of AUG-proximal nonsense mutations." Nucleic Acids Res **40**(3): 1160-73.

Perez-Ortin, J. E., P. Alepuz, et al. (2013). "Eukaryotic mRNA decay: methodologies, pathways, and links to other stages of gene expression." J Mol Biol **425**(20): 3750-75.

Perez, B., P. Rodriguez-Pombo, et al. (2012). "Readthrough strategies for therapeutic suppression of nonsense mutations in inherited metabolic disease." Mol Syndromol **3**(5): 230-6.

Perez Canadillas, J. M. and G. Varani (2003). "Recognition of GU-rich polyadenylation regulatory elements by human CstF-64 protein." EMBO J **22**(11): 2821-30.

Pohl, M., R. H. Bortfeldt, et al. (2013). "Alternative splicing of mutually exclusive exons--a review." Biosystems **114**(1): 31-8.

Pollard, T. D. (2003). "The cytoskeleton, cellular motility and the reductionist agenda." Nature **422**(6933): 741-5.

Popp, M. W. and L. E. Maquat (2014). "The dharma of nonsense-mediated mRNA decay in Mammalian cells." Mol Cells **37**(1): 1-8.

Qian, L., L. Theodor, et al. (1993). "T cell receptor-beta mRNA splicing: regulation of unusual splicing intermediates." Mol Cell Biol **13**(3): 1686-96.

Raijmakers, R., W. V. Egberts, et al. (2002). "Protein-protein interactions between human exosome components support the assembly of RNase PH-type subunits into a six-membered PNPase-like ring." J Mol Biol **323**(4): 653-63.

Ram, O. and G. Ast (2007). "SR proteins: a foot on the exon before the transition from intron to exon definition." Trends Genet **23**(1): 5-7.

Ramani, A. K., A. C. Nelson, et al. (2009). "High resolution transcriptome maps for wild-type and nonsense-mediated decay-defective Caenorhabditis elegans." Genome Biol **10**(9): R101.

Rebbapragada, I. and J. Lykke-Andersen (2009). "Execution of nonsense-mediated mRNA decay: what defines a substrate?" Curr Opin Cell Biol **21**(3): 394-402.

Rehwinkel, J., I. Letunic, et al. (2005). "Nonsense-mediated mRNA decay factors act in concert to regulate common mRNA targets." RNA **11**(10): 1530-44.

Rehwinkel, J., J. Raes, et al. (2006). "Nonsense-mediated mRNA decay: Target genes and functional diversification of effectors." Trends Biochem Sci **31**(11): 639-46.

Reimertz, C., D. Kogel, et al. (2003). "Gene expression during ER stress-induced apoptosis in neurons: induction of the BH3-only protein Bbc3/PUMA and activation of the mitochondrial apoptosis pathway." J Cell Biol **162**(4): 587-97.

Rittinger, K., J. Budman, et al. (1999). "Structural analysis of 14-3-3 phosphopeptide complexes identifies a dual role for the nuclear export signal of 14-3-3 in ligand binding." Mol Cell **4**(2): 153-66.

Rogers, S. L. and V. I. Gelfand (2000). "Membrane trafficking, organelle transport, and the cytoskeleton." Curr Opin Cell Biol **12**(1): 57-62.

Romao, L., A. Inacio, et al. (2000). "Nonsense mutations in the human beta-globin gene lead to unexpected levels of cytoplasmic mRNA accumulation." Blood **96**(8): 2895-901.

Roscigno, R. F. and M. A. Garcia-Blanco (1995). "SR proteins escort the U4/U6.U5 tri-snRNP to the spliceosome." RNA **1**(7): 692-706.

Rubtsova, S. N., R. V. Kondratov, et al. (1998). "Disruption of actin microfilaments by cytochalasin D leads to activation of p53." FEBS Lett **430**(3): 353-7.

Rufener, S. C. and O. Muhlemann (2013). "eIF4E-bound mRNPs are substrates for nonsense-mediated mRNA decay in mammalian cells." Nat Struct Mol Biol **20**(6): 710-7.

Ruiz-Echevarria, M. J. and S. W. Peltz (2000). "The RNA binding protein Pub1 modulates the stability of

transcripts containing upstream open reading frames." Cell **101**(7): 741-51.

Saijo, T., H. Kuriki, et al. (1985). "Inhibition by amoxanox (AA-673) of the immunologically, leukotriene D4- or platelet-activating factor-stimulated bronchoconstriction in guinea pigs and rats." Int Arch Allergy Appl Immunol **77**(3): 315-21.

Saijo, T., H. Kuriki, et al. (1985). "Mechanism of the action of amoxanox (AA-673), an orally active antiallergic agent." Int Arch Allergy Appl Immunol **78**(1): 43-50.

Saijo, T., H. Makino, et al. (1986). "The antiallergic agent amoxanox suppresses SRS-A generation by inhibiting lipoxygenase." Int Arch Allergy Appl Immunol **79**(3): 231-7.

Saini, P., D. E. Eyler, et al. (2009). "Hypusine-containing protein eIF5A promotes translation elongation." Nature **459**(7243): 118-21.

Saito, S., N. Hosoda, et al. (2013). "The Hbs1-Dom34 protein complex functions in non-stop mRNA decay in mammalian cells." J Biol Chem **288**(24): 17832-43.

Sakakibara, H. (1988). Japanese journal of clinical and experimental medicine **65**(9): 2960-66.

Sanford, J. R. and J. F. Caceres (2004). "Pre-mRNA splicing: life at the centre of the central dogma." J Cell Sci **117**(Pt 26): 6261-3.

Santoro, M. F., R. R. Annand, et al. (1998). "Regulation of protein phosphatase 2A activity by caspase-3 during apoptosis." J Biol Chem **273**(21): 13119-28.

Sato, H. and L. E. Maquat (2009). "Remodeling of the pioneer translation initiation complex involves translation and the karyopherin importin beta." Genes Dev **23**(21): 2537-50.

Sauman, I. and S. J. Berry (1993). "Cytochalasin-D treatment triggers premature apoptosis of insect ovarian follicle and nurse cells." Int J Dev Biol **37**(3): 441-50.

Schell, T., T. Kocher, et al. (2003). "Complexes between the nonsense-mediated mRNA decay pathway factor human upf1 (up-frameshift protein 1) and essential nonsense-mediated mRNA decay factors in HeLa cells." Biochem J **373**(Pt 3): 775-83.

Scheper, G. C. and C. G. Proud (2002). "Does phosphorylation of the cap-binding protein eIF4E play a role in translation initiation?" Eur J Biochem **269**(22): 5350-9.

Schmidt, K. and J. S. Butler (2013). "Nuclear RNA surveillance: role of TRAMP in controlling exosome specificity." Wiley Interdiscip Rev RNA **4**(2): 217-31.

Schneider, C., E. Leung, et al. (2009). "The N-terminal PIN domain of the exosome subunit Rrp44 harbors endonuclease activity and tethers Rrp44 to the yeast core exosome." Nucleic Acids Res **37**(4): 1127-40.

Schoenberg, D. R. (2011). "Mechanisms of endonuclease-mediated mRNA decay." Wiley Interdiscip Rev RNA **2**(4): 582-600.

Schweingruber, C., S. C. Rufener, et al. (2013). "Nonsense-mediated mRNA decay - mechanisms of substrate mRNA recognition and degradation in mammalian cells." Biochim Biophys Acta **1829**(6-7): 612-23.

Schwerk, C., J. Prasad, et al. (2003). "ASAP, a novel protein complex involved in RNA processing and apoptosis." Mol Cell Biol **23**(8): 2981-90.

Semlow, D. R. and J. P. Staley (2012). "Staying on message: ensuring fidelity in pre-mRNA splicing." Trends Biochem Sci **37**(7): 263-73.

Serin, G., A. Gersappe, et al. (2001). "Identification and characterization of human orthologues to Saccharomyces cerevisiae Upf2 protein and Upf3 protein (Caenorhabditis elegans SMG-4)." Mol Cell Biol **21**(1): 209-23.

Sharif, H. and E. Conti (2013). "Architecture of the Lsm1-7-Pat1 complex: a conserved assembly in

eukaryotic mRNA turnover." Cell Rep **5**(2): 283-91.

She, M., C. J. Decker, et al. (2008). "Structural basis of dcp2 recognition and activation by dcp1." Mol Cell **29**(3): 337-49.

Sheth, U. and R. Parker (2006). "Targeting of aberrant mRNAs to cytoplasmic processing bodies." Cell **125**(6): 1095-109.

Shi, Y. (2004). "Caspase activation, inhibition, and reactivation: a mechanistic view." Protein Sci **13**(8): 1979-87.

Silva, A. L., P. Ribeiro, et al. (2008). "Proximity of the poly(A)-binding protein to a premature termination codon inhibits mammalian nonsense-mediated mRNA decay." RNA **14**(3): 563-76.

Silva, A. L. and L. Romao (2009). "The mammalian nonsense-mediated mRNA decay pathway: to decay or not to decay! Which players make the decision?" FEBS Lett **583**(3): 499-505.

Singh, G., I. Rebbapragada, et al. (2008). "A competition between stimulators and antagonists of Upf complex recruitment governs human nonsense-mediated mRNA decay." PLoS Biol **6**(4): e111.

Spurdle, A. B., F. J. Couch, et al. (2008). "Prediction and assessment of splicing alterations: implications for clinical testing." Hum Mutat **29**(11): 1304-13.

Storey, J. D., J. Madeoy, et al. (2007). "Gene-expression variation within and among human populations." Am J Hum Genet **80**(3): 502-9.

Strambio-De-Castillia, C., M. Niepel, et al. (2010). "The nuclear pore complex: bridging nuclear transport and gene regulation." Nat Rev Mol Cell Biol **11**(7): 490-501.

Stroupe, M. E., T. O. Tange, et al. (2006). "The three-dimensional arcitecture of the EJC core." J Mol Biol **360**(4): 743-9.

Stutz, F., A. Bachi, et al. (2000). "REF, an evolutionary conserved family of hnRNP-like proteins, interacts with TAP/Mex67p and participates in mRNA nuclear export." RNA **6**(4): 638-50.

Stutz, F. and E. Izaurralde (2003). "The interplay of nuclear mRNP assembly, mRNA surveillance and export." Trends Cell Biol **13**(6): 319-27.

Sun, Q., T. Chen, et al. (2010). "Taxol induces paraptosis independent of both protein synthesis and MAPK pathway." J Cell Physiol **222**(2): 421-32.

Sun, X., X. Li, et al. (2001). "Nonsense-mediated decay of mRNA for the selenoprotein phospholipid hydroperoxide glutathione peroxidase is detectable in cultured cells but masked or inhibited in rat tissues." Mol Biol Cell **12**(4): 1009-17.

Sun, X., P. M. Moriarty, et al. (2000). "Nonsense-mediated decay of glutathione peroxidase 1 mRNA in the cytoplasm depends on intron position." EMBO J **19**(17): 4734-44.

Sureau, A., R. Gattoni, et al. (2001). "SC35 autoregulates its expression by promoting splicing events that destabilize its mRNAs." EMBO J **20**(7): 1785-96.

Susin, S. A., N. Zamzami, et al. (1996). "Bcl-2 inhibits the mitochondrial release of an apoptogenic protease." J Exp Med **184**(4): 1331-41.

Suzanne, M. and H. Steller (2013). "Shaping organisms with apoptosis." Cell Death Differ **20**(5): 669-75.

Sweet, T. J., B. Boyer, et al. (2007). "Microtubule disruption stimulates P-body formation." RNA **13**(4): 493-502.

Tange, T. O., T. Shibuya, et al. (2005). "Biochemical analysis of the EJC reveals two new factors and a stable tetrameric protein core." RNA **11**(12): 1869-83.

Tanida, I., T. Ueno, et al. (2008). "LC3 and Autophagy." Methods Mol Biol **445**: 77-88.

Thermann, R., G. Neu-Yilik, et al. (1998). "Binary specification of nonsense codons by splicing and cytoplasmic translation." EMBO J **17**(12): 3484-94.

Thoren, L. A., G. A. Norgaard, et al. (2010). "UPF2 is a critical regulator of liver development, function and regeneration." PLoS One **5**(7): e11650.

Thuret-Carnahan, J., J. L. Bossu, et al. (1985). "Effect of taxol on secretory cells: functional, morphological, and electrophysiological correlates." J Cell Biol **100**(6): 1863-74.

Tollner, T. L., S. A. Venners, et al. (2011). "A common mutation in the defensin DEFB126 causes impaired sperm function and subfertility." Sci Transl Med **3**(92): 92ra65.

Topisirovic, I., Y. V. Svitkin, et al. (2011). "Cap and cap-binding proteins in the control of gene expression." Wiley Interdiscip Rev RNA **2**(2): 277-98.

Torchet, C., C. Bousquet-Antonelli, et al. (2002). "Processing of 3'-extended read-through transcripts by the exosome can generate functional mRNAs." Mol Cell **9**(6): 1285-96.

Tork, S., I. Hatin, et al. (2004). "The major 5' determinant in stop codon read-through involves two adjacent adenines." Nucleic Acids Res **32**(2): 415-21.

Tousson, A., C. M. Fuller, et al. (1996). "Apical recruitment of CFTR in T-84 cells is dependent on cAMP and microtubules but not Ca2+ or microfilaments." J Cell Sci **109 (Pt 6)**: 1325-34.

Tsai, Y. J., H. I. Lee, et al. (2012). "Ribosome distribution in HeLa cells during the cell cycle." PLoS One **7**(3): e32820.

Unterholzner, L. and E. Izaurralde (2004). "SMG7 acts as a molecular link between mRNA surveillance and mRNA decay." Mol Cell **16**(4): 587-96.

Utter, C. J., S. A. Garcia, et al. (2011). "PolyA-specific ribonuclease (PARN-1) function in stage-specific mRNA turnover in Trypanosoma brucei." Eukaryot Cell **10**(9): 1230-40.

van Echteld, I., M. D. Wechalekar, et al. (2014). "Colchicine for acute gout." Cochrane Database Syst Rev **8**: CD006190.

van Hoof, A., P. A. Frischmeyer, et al. (2002). "Exosome-mediated recognition and degradation of mRNAs lacking a termination codon." Science **295**(5563): 2262-4.

Vanden Berghe, P., G. W. Hennig, et al. (2004). "Characteristics of intermittent mitochondrial transport in guinea pig enteric nerve fibers." Am J Physiol Gastrointest Liver Physiol **286**(4): G671-82.

Vasudevan, S. and S. W. Peltz (2003). "Nuclear mRNA surveillance." Curr Opin Cell Biol **15**(3): 332-7.

Viegas, M. H., N. H. Gehring, et al. (2007). "The abundance of RNPS1, a protein component of the exon junction complex, can determine the variability in efficiency of the Nonsense Mediated Decay pathway." Nucleic Acids Res **35**(13): 4542-51.

Wagner, E. J., A. P. Baraniak, et al. (2005). "Characterization of the intronic splicing silencers flanking FGFR2 exon IIIb." J Biol Chem **280**(14): 14017-27.

Wahl, M. C., C. L. Will, et al. (2009). "The spliceosome: design principles of a dynamic RNP machine." Cell **136**(4): 701-18.

Wang, D., J. Zavadil, et al. (2011). "Inhibition of nonsense-mediated RNA decay by the tumor microenvironment promotes tumorigenesis." Mol Cell Biol **31**(17): 3670-80.

Wang, J., J. P. Gudikote, et al. (2002). "Boundary-independent polar nonsense-mediated decay." EMBO Rep **3**(3): 274-9.

Wang, J., V. M. Vock, et al. (2002). "A quality control pathway that down-regulates aberrant T-cell receptor (TCR) transcripts by a mechanism requiring UPF2 and translation." J Biol Chem **277**(21): 18489-93.

Wang, W., K. Czaplinski, et al. (2001). "The role of Upf proteins in modulating the translation

read-through of nonsense-containing transcripts." EMBO J **20**(4): 880-90.

Wang, Y., X. Xiao, et al. (2013). "A complex network of factors with overlapping affinities represses splicing through intronic elements." Nat Struct Mol Biol **20**(1): 36-45.

Wee, L. J., T. W. Tan, et al. (2006). "SVM-based prediction of caspase substrate cleavage sites." BMC Bioinformatics **7 Suppl 5**: S14.

Welch, E. M., E. R. Barton, et al. (2007). "PTC124 targets genetic disorders caused by nonsense mutations." Nature **447**(7140): 87-91.

Wengrod, J., L. Martin, et al. "Inhibition of nonsense-mediated RNA decay activates autophagy." Mol Cell Biol **33**(11): 2128-35.

Wengrod, J., L. Martin, et al. (2013). "Inhibition of nonsense-mediated RNA decay activates autophagy." Mol Cell Biol **33**(11): 2128-35.

Wollerton, M. C., C. Gooding, et al. (2004). "Autoregulation of polypyrimidine tract binding protein by alternative splicing leading to nonsense-mediated decay." Mol Cell **13**(1): 91-100.

Yamaguchi, Y., A. Hayashi, et al. (2012). "L-MPZ, a novel isoform of myelin P0, is produced by stop codon readthrough." J Biol Chem **287**(21): 17765-76.

Yamashita, A. "Role of SMG-1-mediated Upf1 phosphorylation in mammalian nonsense-mediated mRNA decay." Genes Cells **18**(3): 161-75.

Yamashita, A. (2013). "Role of SMG-1-mediated Upf1 phosphorylation in mammalian nonsense-mediated mRNA decay." Genes Cells **18**(3): 161-75.

Yamashita, A., T. C. Chang, et al. (2005). "Concerted action of poly(A) nucleases and decapping enzyme in mammalian mRNA turnover." Nat Struct Mol Biol **12**(12): 1054-63.

Yamashita, A., N. Izumi, et al. (2009). "SMG-8 and SMG-9, two novel subunits of the SMG-1 complex, regulate remodeling of the mRNA surveillance complex during nonsense-mediated mRNA decay." Genes Dev **23**(9): 1091-105.

Yepiskoposyan, H., F. Aeschimann, et al. (2011). "Autoregulation of the nonsense-mediated mRNA decay pathway in human cells." RNA **17**(12): 2108-18.

Zenklusen, D., P. Vinciguerra, et al. (2002). "Stable mRNP formation and export require cotranscriptional recruitment of the mRNA export factors Yra1p and Sub2p by Hpr1p." Mol Cell Biol **22**(23): 8241-53.

Zhang, J. and L. E. Maquat (1997). "Evidence that translation reinitiation abrogates nonsense-mediated mRNA decay in mammalian cells." EMBO J **16**(4): 826-33.

Zhang, J., X. Sun, et al. (1998). "At least one intron is required for the nonsense-mediated decay of triosephosphate isomerase mRNA: a possible link between nuclear splicing and cytoplasmic translation." Mol Cell Biol **18**(9): 5272-83.

Zhang, J., X. Sun, et al. (1998). "Intron function in the nonsense-mediated decay of beta-globin mRNA: indications that pre-mRNA splicing in the nucleus can influence mRNA translation in the cytoplasm." RNA **4**(7): 801-15.

Zhang, S., M. J. Ruiz-Echevarria, et al. (1995). "Identification and characterization of a sequence motif involved in nonsense-mediated mRNA decay." Mol Cell Biol **15**(4): 2231-44.

Zhang, X. J., L. Yang, et al. (2002). "Induction of acetylcholinesterase expression during apoptosis in various cell types." Cell Death Differ **9**(8): 790-800.

Zwelling, L. A., E. Altschuler, et al. (1991). "N-(5,5-diacetoxypentyl)doxorubicin: a novel anthracycline producing DNA interstrand cross-linking and rapid endonucleolytic cleavage in human leukemia cells." Cancer Res **51**(24): 6704-7.